NSERC-CMIC FOOTPRINTS

Sundaralingam N, 2017, Vein pyrite composition as a potential vector for defining the Canadian Malartic footprint, BSc Thesis, Western U, ON, 58 p.

NSERC-CMIC Mineral Exploration Footprints Project Contribution 149.

canadamining innovationcouncil

NSERC CRSNG

Vein Pyrite Composition as a Potential Vector for Defining the Canadian Malartic Footprint

Neera Sundaralingam

Supervisors: Dr. Robert Linnen and Dr. Stéphane Perrouty

University of Western Ontario

B.Sc. Honours Thesis

Abstract

The main gold mineralization at the Canadian Malartic deposit is associated with disseminated pyrite or fine veinlets, which are related to the D_2 deformation event. The composition of the pyrite within the syn-D_2 veins may therefore record broad-scale fluid circulation, which ultimately can provide evidence for the origin of the deposit. This work focuses on the mineralogical and geochemical analysis of the veins and pyrite grains within them to ultimately determine whether pyrite grains define the Canadian Malartic footprint. Of the 2 vein generations recognized, one vein generation formed during D_2 and 3 sub-types contained pyrite, which were sampled for this study. Twenty-five samples were collected along two main transects leading away from the deposit. Five groups of primary vein mineralogy can be distinguished from petrographic analyses: group 1: Qz-Ab-Kfs-Cal-Bt, group 2: Qz-Ab-Kfs-Bt, group 3: Qz-Ab-Cal-Bt, group 4: Qz-Ab-Bt and group 5: Qtz-Cal-Bt. Vein mineralogy and structural characteristics closely resemble the main ore stage veins and are thus inferred to have formed during main gold mineralization. Along the transect to the south, pyrite is increasingly replaced by pyrrhotite, which can be interpreted as a result of the increasing metamorphic grade toward the south. Oscillatory zoning is observed within the pyrite grains in maps from electron probe microanalyses, which may reflect fluid evolution or fluid mixing. Multiple gold mineralization events may be inferred due to the presence of gold nanoparticles within the pyrite grains as well as within fractures of the grains. As and Au relationships infer that the vein pyrite grains are undersaturated with respect to gold, as the majority of the samples contain structural gold and are generally low in composition. Maximum gold contents within vein pyrite could be used as a weak vector to define the Canadian Malartic footprint as they decrease in gold concentration with increasing distance away from the deposit.

Acknowledgements

I am extremely grateful to my two supervisors, Dr. Robert Linnen and Dr. Stéphane Perrouty for their constant guidance and support during this project. Thank you both for providing me with advice and constructive criticism.

I would especially like to thank the members of the NSERC-CMIC Footprints project for giving me this opportunity to contribute to the project, including Cathryn Nadjiwon, Michael Lesher, Mark Hannington and Alan Galley.

I am grateful to the sponsors of the NSERC-CMIC Footprints project for supporting this project including Canadian Malartic. Thanks to François Bouchard and Marc Bardoux for their constructive comments.

Special thanks goes to Nicolas Piette-Lauzière and Nicolas Gaillard for their advices and feedback on this project as well.

I would also like to thank Marc Beauchamp at the University of Western Ontario for his help during EPMA analysis as well as Jean Claude Barrette at the University of Windsor for his assistance during LA ICP-MS analysis. Special thanks goes to Melissa Price and Iain Samson at the University of Windsor, for assisting me with Igor Pro and Iolite.

Lastly, I would like thank those who supported me during this entire project, including Marie Schell, my friends and of course, my family.

Table of Contents

List of Figures

List of Tables

List of Appendices

1 Introduction

1.1 Background

Canadian Malartic is the largest open pit gold mine in Canada, located within northern Quebec. This deposit lies southeast of the Abitibi greenstone belt, which is a prolific gold-bearing subprovince containing many gold camps along the Porcupine-Destor deformation zone as well as the Cadillac-Larder Lake deformation zone within it. This is a low grade high tonnage deposit with total proven and probable reserves currently standing at 10.7 Moz Au within 343.7 Mt, reaching a grade of 0.97 g/t Au found within this deposit (Belzile and Gignac, 2011). Gold was found in the Malartic area in 1923 and mining operations began largely underground (Wares and Burzynski, 2012). It was eventually converted into an open pit mine in 2009 (Wares and Burzynski, 2012). The mineralization of this deposit is either in disseminated grains within the alteration zone or in fine veins (Helt et al., 2014). In addition, Cartier and Parbec were gold camps that are located near the Canadian Malartic deposit and their locations are shown in Figure 3.

Pyrite is one of the most abundant sulphide minerals within the Earth's crust. It is important for ore deposit geochemistry as it is commonly associated with gold either as inclusions or structurally bound within the crystal lattice (Deditius et al. 2011). The geochemistry and structure of the pyrite grains can record the evolution of the fluid from which it precipitated, which would ultimately provide further explanation of the origin of this gold deposit.

1.2 Objectives and Scope

This research contributes to the Natural Sciences and Engineering Research Council (NSERC) and Canadian Mining Innovation Council (CMIC) Footprints project, which aims to contribute to the future of mineral exploration of concealed and deeply buried targets. This will be accomplished through understanding the geological, mineralogical, geochemical and geophysical parameters that define ore systems and their footprints (cmic-footprints.ca). This B.Sc. project aims to determine whether vein pyrite composition can define the Canadian Malartic footprint, which could ultimately be used as a tool for gold exploration. In order to do so, the objectives of this B.Sc. project are as follows:

a) To characterize veins containing pyrite within the footprint of the Canadian Malartic Mine, in the Pontiac meta-sedimentary host rock. This is to ensure the veins selected are related to the ore forming stage of the Canadian Malartic deposit.
b) To conduct mineralogical analyses of the veins and compare them with the mineralogy of the ore forming veins.
c) Conduct geochemical analyses of the veins to understand the fluids involved in its formation. These analyses will also determine the gold content within the vein pyrite in order to determine whether they define the footprint. These will also be compared with the pyrite disseminated within the meta-sedimentary host rocks in the deposit.

Vein generations and their structural settings were characterized during field work at the Canadian Malartic mine property at Malartic, Quebec; this was completed in the summer of 2016 as part of the NSERC-CMIC Footprints project. The mineralogy and geochemistry of veins were analysed using petrographic microscopes and an electron probe micro-analyzer (EPMA) in the Alan D. Edgar Laboratory at the University of Western Ontario from September 2016 to March 2017. The trace element compositions of pyrite were analysed by the laser ablation inductively coupled mass spectrometer (LA ICP-MS) at the University of Windsor in December 2016.

2 Tectonic Setting

2.1 Regional Geology

The Canadian Malartic deposit lies within the Pontiac subprovince, which is in the southeastern portion of the Superior province. The contact between the two subprovinces is defined as the Cadillac-Larder Lake deformation zone, which is a tectonic zone of steeply dipping major faults, trending approximately E-W (Helt et al., 2014).

2.1.1 The Abitibi Subprovince

The Abitibi subprovince is a greenstone belt that is composed of meta-volcanic-plutonic rocks and meta-sedimentary rocks. It was formed largely by two volcanic zones: an older volcanic zone to the north aged 2730 to 2710 Ma, and a younger volcanic zone to the south, aged 2705 to 2698 Ma (Card and Poulsen, 1998). The Porcupine-Destor Fault zone separates these two volcanic zones as seen in Figure 1 (Card and Poulsen, 1998).

U-Pb dating of zircon grains indicated the greenstone belt had formed between 2760 to 2750 Ma (Corfu, 1993). Major pre-orogenic magmatism occurred in 2720 to 2700 Ma and calc-alkaline plutons occurred later from 2694 Ma to 2690 Ma (Corfu et al., 1989; Corfu, 1993; Ayer et al. 2002; Helt et al., 2014) along with flyschoid sediment deposition from 2696 to 2687 Ma (Davis, 1992; Ayer et al., 2002; Helt et al., 2014). Timiskaming-type conglomerates and fluvial sandstones then deposited unconformably on top of the previous sequences as a result of uplift and erosion (Corfu et al., 1991; Davis, 1992; Corfu, 1993; Helt et al., 2014).

2.1.2 The Cadillac-Larder Lake Deformation Zone

The Cadillac-Larder Lake deformation zone separating two subprovinces hosts many gold camps including Kirkland Lake and Larder Lake camps in Ontario, as well as the Rouyn-Noranda, Cadillac, Malartic and Val d’Or camps in Quebec (Wares and Burzynski, 2012). At the point in which this deformation zone cuts through Malartic, it trends N320°E and further east it trends N280°E to N290°E, indicating the bifurcation of this fault zone (Gunning and Ambrose, 1940; Eakins, 1962). The lithostratigraphic group confined within this deformation zone is the Piché Group, which is composed of strongly deformed and altered mafic to ultramafic meta-volcanic rock (Wares and Burzynski, 2012).

2.1.3 The Pontiac Subprovince and Felsic Intrusions

The Pontiac subprovince south of the aforementioned deformation zone is largely composed of banded turbiditic greywacke, mudstone with some siltstone, ranging in bed thicknesses from about 1mm to 1m, forming approximately 2685 to 2682 Ma (Davis, 2002). The Pontiac subprovince is also intruded by porphyritic quartz monzodiorite to granodiorite intrusions formed approximately 2677 to 2678 Ma (Helt et al., 2014; De Souza et al., 2016). Their geometries vary, as they occur as sills, dykes, discontinuous lenses, as well as isolated stocks (Wares and Burzynski, 2012).

2.1.4 Lithostratographic Divisions of the Region

The main lithostratographic groups of the region reported by Wares and Burzynski (2012) are listed in order from north to south: The Malartic Groups composed of ultramafic volcanic rocks, the Kewagama Group is formed of greywacke, shale oxides facies iron formation and conglomerates. Additionally, the Blake River Group comprises predominately basalts, the Cadillac Group is mostly greywacke and polymictic conglomerates, the Piché Group is composed of talc-chlorite-carbonate schists, which represents strongly deformed and altered primary Mg-rich basalt and komatiitic volcanics. Finally, the group furthest south is the Pontiac meta-sedimentary rocks, which is the focus of this study.

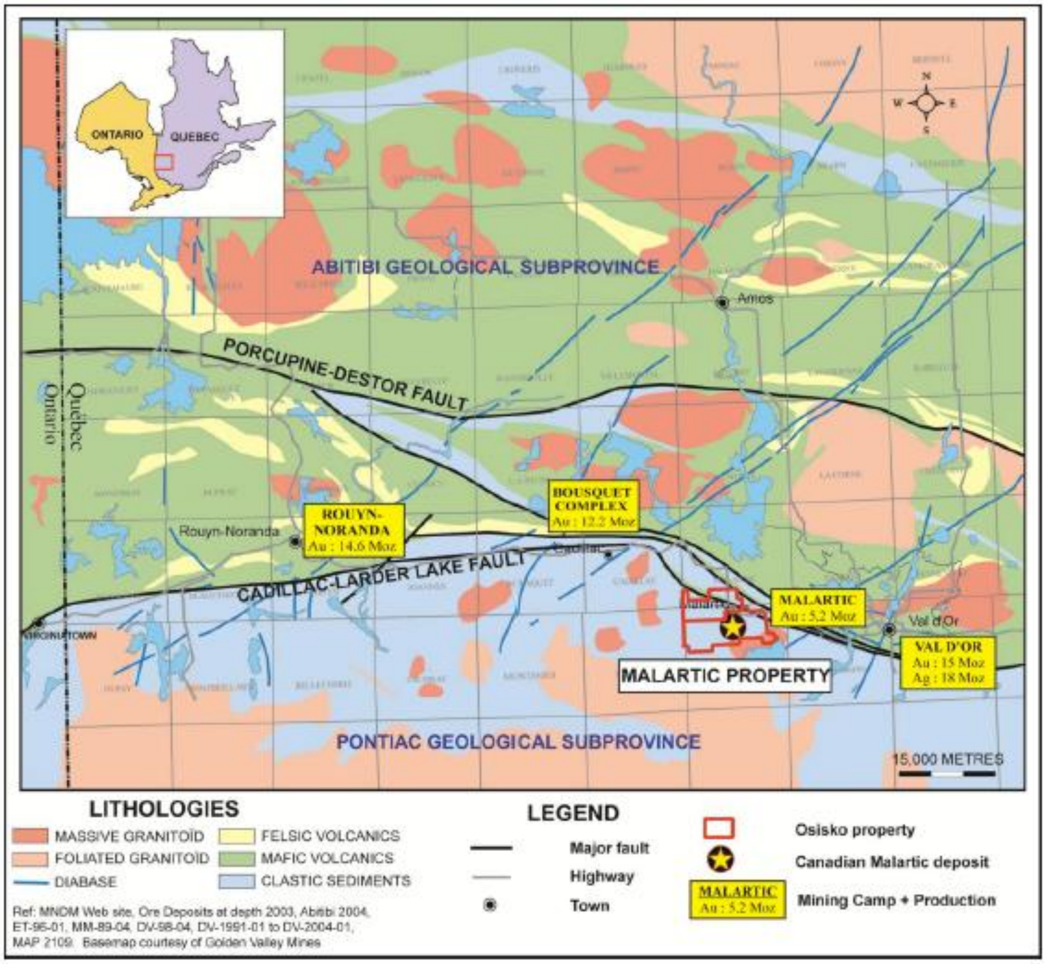

Fig. 1 Regional geology showing the Abitibi subprovince to the north, the Pontiac subprovince in the south as well as the two major tectonic zones, the Porcupine-Destor fault zone as well as the Cadillac-Larder Lake Tectonic zone and the Canadian Malartic deposit (Wares and Burskynski, 2012).

2.1.5 Metamorphism

Regional metamorphism occurred 2677 to 2643 Ma (Powell, 1995), resulting in a pattern of increasing grade towards the south. North of the Cadillac-Larder Lake deformation zone is comprised of a subgreenschist facies to upper greenschist within the Piché group as well as upper greenschist to amphibolite facies within the Pontiac group south of the Cadillac-Larder Lake deformation zone (Dimroth et al., 1983; Powell et al., 1995). There is also a notable line of constant metamorphic grade, called the garnet and staurolite isograd that occurs within the southern extremity of the Canadian Malartic deposit (Perrouty et al., 2017).

2.1.6 Deformation

This region underwent at least three deformation events (Derry, 1939). The first event, D1, occurred between 2687 to 2672 Ma, and is associated with tilting, folding and thrusting, leaving behind a rare and local pressure-solution S_1 cleavage (Sansfaçon and Hubert, 1990). The second event, D_2, occurred between 2680 (Sansfaçon and Hubert, 1990) and 2660 Ma (De Souza et al., 2016), and it involved N-S shortening (Robert, 2001). This event resulted in a more penetrative NW-SE pressure-solution S_2 cleavage, indicated by the alignment of biotite grains within the Pontiac meta-sedimentary rocks (Desrochers and Hubert, 1996). This event is also characterized by subvertical and subisoclinal F_2 folds with axial planes that trend NE. The last deformation event, D_3, followed D_2 but the ages are unknown. This event involved E-W shortening and generated small local kink folds (Desrochers and Hubert, 1996).

2.2 Local Geology

2.2.1 Deposit Limits

The northern limit of the Canadian Malartic deposit is defined by the Cadillac-Larder Lake deformation zone where the deposit lies within and immediately to the south of it (Figure 2) and the Sladen fault to the south of the deposit that trends E-W (Wares and Burzynski, 2012). The major rock units hosted within the Malartic deposit and footprint are the Piché meta-volcanic rocks, the Pontiac meta-sedimentary rocks and the monzodiorite intrusions (Wares and Burzynski, 2012). A third of the gold mineralization is hosted by the Piché group, the remaining gold mineralization lies south of the Cadillac-Larder Lake deformation zone where gold is hosted in the Pontiac meta-sedimentary rocks and in the felsic porphyritic intrusions (Wares and Burzynski, 2012).

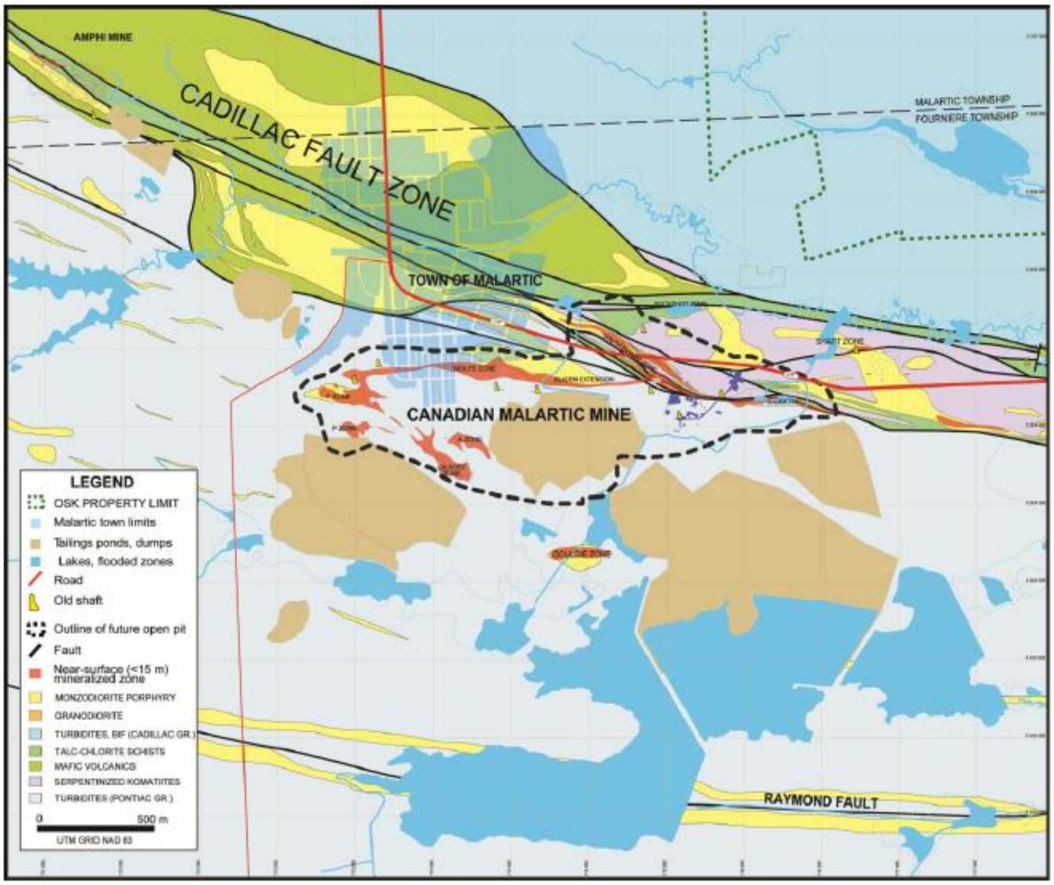

Fig. 2 Local Geology showing the Piché group, the Pontiac meta-sedimentary rock and felsic porphyritic intrusions in relation to Canadian Malartic deposit. (Wares and Burzynski, 2012).

2.2.2 Ore Characteristics

In the Canadian Malartic deposit, gold can be found largely as native gold and also as gold-silver-telluride minerals (Wares and Burzynski, 2012). It is found within two generations of thin and discontinuous veins, as well as finely disseminated grains in alteration zones around the main ore-stage veinlets (Helt et al., 2014). There is a strong association with gold mineralization and pyrite, and it is important to note that most of the gold grains associated with pyrite comprise approximately 49% of the native gold by volume (Helt et al., 2014). The ore is also associated with other phases as well including chalcopyrite, galena, sphalerite, molybdenite, hematite and Ag-Pb-Bi telluride minerals (Eakins, 1962; Sansfaçon and Hubert, 1990; Fallara et al., 2000; Helt et al., 2014; De Souza et al., 2015, 2016). Sericite, chlorite, rutile, celestite, barite are also minor phases that are associated with gold mineralization.

2.2.3 Alteration

Five types of alteration have been observed in the deposit. Carbonate alteration occurs throughout the deposit. Albitization occurs mostly within the meta-sedimentary rock and silicification occurs mostly within the intrusions (De Souza et al., 2015). Potassic alteration results in the prevalence of biotite and K-feldspar within the deposit and sulphidation occurs within the sedimentary and intrusive rocks (De Souza et al., 2015).

2.3 Previous Work

2.3.1 Pyrite Types

Previous work by Gao et al. (2015) observed five stages of pyrite within the meta-sedimentary host rock in the Canadian Malartic deposit, unlike this study, which focuses on vein pyrite within the Canadian Malartic footprint. Pyrite 1 formed pre-mineralization where there are high Co, As and Se contents as well as low Ni, Sb, Bi and Pb contents. Gao et al. (2015) interprets this type to have formed pre-mineralization and is likely diagenetic pyrite. Pyrite 2, 3 and 4 formed during gold mineralization and are enriched in Ag, Pb, Au and Bi and contain largely K-rich silicate inclusions, suggesting that they precipitated from a K-rich fluid. Pyrite 5 formed post-mineralization and contain high Co and Ni content and are low in other metals.

2.3.2 Vein Systems

A few studies have described the different vein systems within Malartic. Work by De Souza et al. (2015) described three types of veins. Vein 1 formed before the main ore forming stage and contains low gold values. Vein 2 formed during the main ore forming stage which have biotite at its selvages, and contain various amounts of quartz, calcite, biotite, microcline, albite, chlorite, pyrite and ankerite, as well as trace amounts of chalcopyrite, telluride minerals, gold and scheelite. These veins are interpreted to have formed syn-late D_2. Vein 3 is divided into three subtypes. V3b contains high values of gold, up to 42.3 ppm and V3c varies in gold content from 0.013 to 6.7 ppm with similar mineralogy of Vein 2 but also contain minor amounts of rutile, tourmaline, galena, native free gold and telluride minerals.

A more recent study by De Souza et al. (2016) reinforces the idea that mineralization is associated with the D_2 event. De Souza et al. (2016) observed that the ore zones are generally oriented NW-SE and E-W as they dominantly lie subparallel to S_2, which results from the D_2 event. These ore zones also trend subparallel to the east trending Sladen fault to the south of the deposit. De Souza et al. (2016) proposed that the D_2 deformation largely controlled gold mineralization at the Canadian Malartic deposit. Re-Os dating of molybdenite within high grade ore produced an age of 2664 ± 11 Ma (De Souza et al., 2016). This ore is thus considered to have formed syn-D2, which is dated between 2690 Ma (Sansfaçon and Hubert, 1990) and 2660 Ma (De Souza et al., 2016).

3 Methods

3.1 Mapping

Vein mapping was conducted on the Canadian Malartic property in order to classify veins based on mineralogy, timing and structural orientation. The structural controls observed in the field were: the sizes of veins, their orientations, cross cutting relationships with other veins as well as their relationship with the S2 foliation and thus the D2 event. Detailed descriptions of these outcrop observations are found within Appendix A. Twenty-five samples of veins containing pyrite grains were taken from the deposit, as well as proximal and distal to the deposit to understand whether the geochemical characteristics of the pyrite and vein vary in the Canadian Malartic deposit and footprint. In order to investigate vein pyrite variation in the footprint, the samples were taken parallel and perpendicular to metamorphic grade. Six samples were taken from the Canadian Malartic pit, and the remaining samples were taken along the two transects leading away from the deposit, seven samples trending NE-SW, which increased in metamorphic grade towards the south and twelve trending NW-SE, which were at a constant metamorphic grade (Figure 3). This study focused on the veins hosted by the Pontiac meta-sedimentary rocks, as they were the dominant host rock within the footprint as well as the Canadian Malartic deposit.

3.2 Geochemical and Mineralogical Analyses

3.2.1 Petrography

These samples were collected from outcrops along the two transects as well as drill cores. Twenty-five thin sections were prepared at Queen’s University. Detailed descriptions of the samples as well as their outcrops are located in within Appendix B and photos of hand samples are provided where available. Thin section images and the grains chosen for EPMA analysis as well as LA ICP-MS analysis are also within Appendix B. Petrographic analysis was conducted using both transmitted and reflected light in the Alan D. Edgar Laboratory at the University of Western Ontario. Detailed descriptions of the mineralogy, compositions of the veins, their selvages, alteration haloes and host rock are recorded in Appendix C.

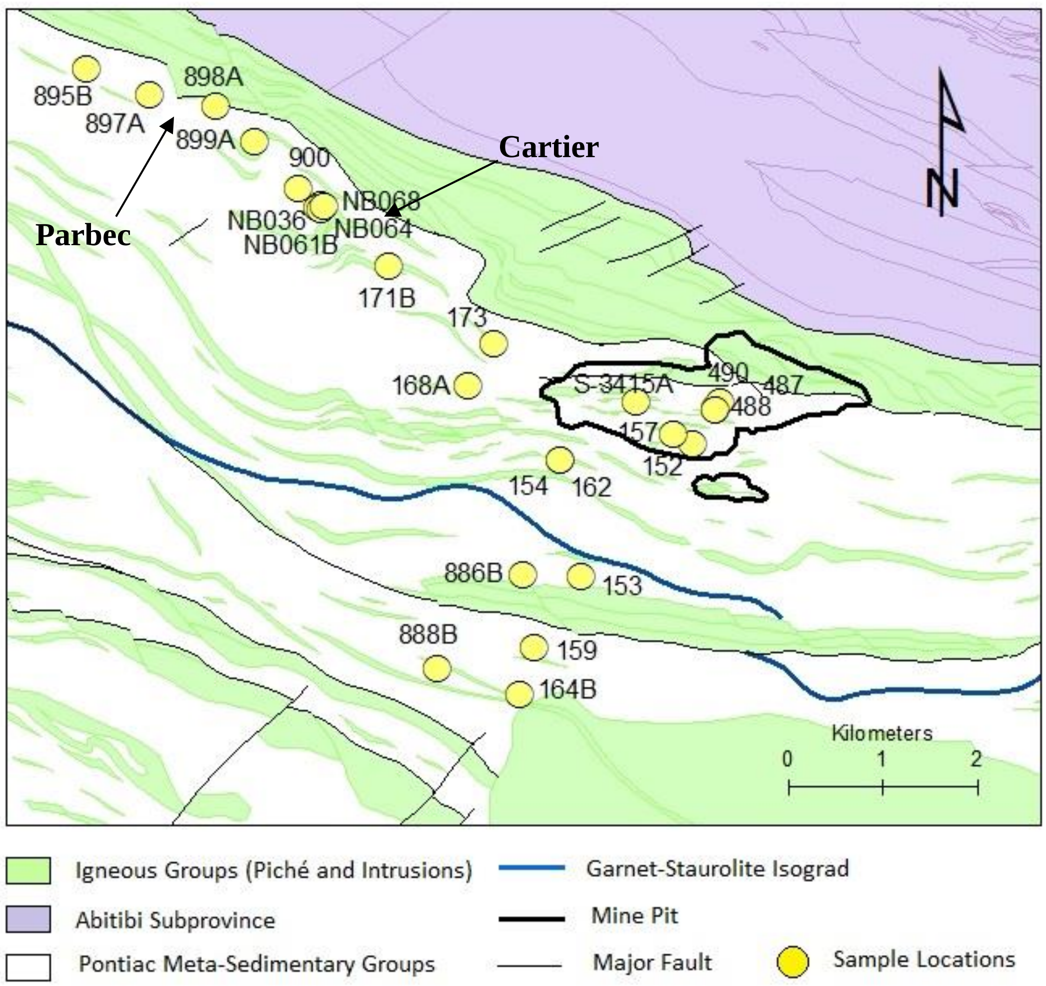

Fig. 3 Sample locations of veins along the NW-SE and NE-SW transects relative to the Canadian Malartic deposit. Figure is modified from Perrouty et al. (2017).

3.2.2 Electron Probe Micro-Analysis (EPMA)

Electron probe micro-analysis (EPMA) was used to obtain compositional information of the vein pyrite grains and to understand their variation within the Canadian Malartic footprint. Elemental analyses were conducted using wavelength-dispersive spectroscopy (WDS) as well as energy-dispersive spectroscopy (EDS). WDS Maps displaying elemental distribution throughout the pyrite grains were created to determine zoning patterns. Spot analyses were also conducted on 10 points of each pyrite grain within the sample in order verify general elemental distribution within the grain and points were taken from the outer edge leading into the core of the grain. Measuring elemental distributions will show if the fluid concentrations varied or were similar between samples, within a sample or between grains.

The electron beam conditions used to create the maps of pyrite grains are: 15 keV accelerating voltage, 50 nÅ probe current and a dwell time of 10 ms per pixel. The conditions for spot analysis in the pyrite grains are: A 15 keV accelerating voltage and a 50 nÅ and a spot size of 2 µm. The average percent errors for the elements analysed are located within Appendix D. Elemental standards and crystals used for EPMA analysis are also reported within Appendix D.

The elements analysed were (Cu), magnesium (Mg), arsenic (As), silicon (Si), lead (Pb), titanium (Ti), nickel (Ni), tungsten (W), cobalt (Co), iron (Fe), and sulphur (S). EPMA analyses measured mass percentages and error percentages for each element within pyrite. This data is found Appendix D as well. Mass percent averages of significant proportions of elements were calculated from each point and are also found within Appendix D.

Any negative mass percent values measured during EPMA analysis were adjusted to 0 as they represented values below background. Mass percent averages, minimums, maximums and ranges were then calculated for each grain and are reported in Appendix D.

3.2.3 Laser Ablation Inductively Coupled Plasma Mass Spectrometry (LA ICP-MS)

LA ICP-MS measured the trace element concentrations. This technique was mainly used to quantify gold content within the pyrite grains along the length of a grain. Up to two pyrite grains were selected from 17 representative samples to measure gold content along these traverses. The samples, grains and traverses used for analysis are listed in Appendix E. The grains were selected based on zoning characteristics as well as ensuring they contained few inclusions, as they would have interfered with this analysis.

The LA ICP-MS parameters of these traverses within this study were as follows: the laser output was at 35% with a pulse rate of 20 Hz and a spot size of 20 µm, which is the smallest size to provide the best resolution with reasonable detection limits. This was conducted at a traverse speed of 5 µm/s and laser pulse energy of 4.1mJ. Analyses were conducted in five batches with different run times, which increased with increasing grain sizes. Batch 1 contained samples 153, 3415A, and 152, which ran for 244 seconds per grain. Batch 2 contained samples NB036, 173, 899A and 157, which ran for 182 seconds. Batch 3 contained samples 168A, 895B, 897A and 898A, which ran for 146 seconds. Batch 4 contained samples 164B, 866B, 171B and 154, which ran for 153 seconds. Finally, batch 5 contained samples 900 and 159, which ran for 156 seconds. The following standards were used for the LA ICP-MS analysis: Nist610, which is a silicate glass, Po725, which is a synthetic pyrrhotite standard and Mass1, which is a synthetic polymetal sulphide standard. The concentrations of the elements Co, Ni, Se, Ag, Pb, Bi, As, Sb and Au were determined by analyzing the abundance of the following isotopes: Co59, Ni60, Se77, Se78 Au197, Ag107, Ag109, As75, Pb208, Bi209, Sb121 and Au 197. The majority of the Se and Ag concentrations measured using Se77 or Se78 and Ag107 or Ag109 were similar, within ± 40%. However, there is an isobaric Kr interference with Se78, and so Se abundances are based on Se77 values. There is also a Zn-argide interference with Ag107, so the Ag109 values were used to calculate Ag concentrations. These values were also compared with the vein pyrite compositions within the host rock of the deposit described by Gao et al. (2015), and especially to determine whether vein pyrite compositions define the Canadian Malartic deposit.

The laser counts the number of selected isotopes for each element with respect to time in seconds. In order to determine gold inclusions, figures of gold and sulphur counts were plotted against time. The sulphur counts represent the pyrite grain as broad curves. Gold measured at the same time as the broad sulphur curves are interpreted as structural gold within the pyrite. Any anomalously high peaks are interpreted as gold nanoinclusions within the pyrite grains, and can be confirmed when they occur simultaneously with silver since gold within this deposit is commonly associated with Ag-telluride minerals. These graphs (e.g. figure 4) were used to interpret where the inclusions are within each of the samples. These figures for each traverse, grain and sample are found within Appendix E.

When processing the data using the computer program Igor Pro with the Iolite extension, only certain parts of the peaks measured through LA ICP-MS were included in data processing. Figure 4 shows an example of the sulphur, gold, nickel and cobalt intensities with respect to time within sample 3415A traverse A3. The anomalously high peaks of gold, seen in the figure as the red peaks, were interpreted to be gold inclusions and were removed from analysis. The edges of the grains were also removed from analyses as these values could have been influenced by the area surrounding the grains. Figure 4 also shows the segments of the grains used for analysis indicated by the black boxes that are labeled with the sample's name. Images of all the segments of pyrite used for analyses are located within section F3 in Appendix F. Figures of sulphur, gold, nickel and cobalt intensities measured by LA ICP-MS with the segments chosen for each traverse is found in section F3 in Appendix F. Igor Pro and Iolite then processed the gold concentrations for each segment chosen along each traverse for each of the standards used, giving each segment three values for each element when applicable. For the pyrite samples, the data was processed using the molecular weight of iron within pyrite which is 46.55% and for any pyrrhotite grains analysed, the data was processed using the molecular weight of iron within pyrrhotite, which is 62.33 %. The data for each segment processed with each of the standards are displayed within Appendix G.

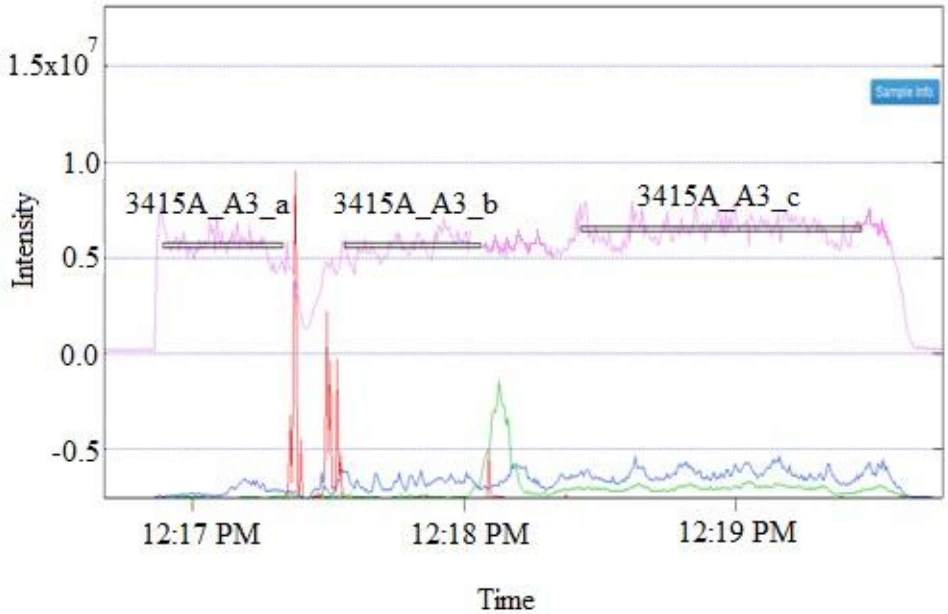

Fig. 4 Example of sulphur, gold, nickel and cobalt intensities measured through traverses within the pyrite grains of sample 3415A. Sections of traverse selected for analysis are indicated in black boxes labeled with the sample's name.

Average gold content in ppm for each sample could not be calculated as many of the segments analysed had concentrations below the detection limit. Since that value lies at some value between 0 ppm and the detection limit, the gold concentrations of those segments could not be quantified accurately. Thus, for the purpose of this study, maximum concentrations of gold for each sample within the three standards used were reported and an average limit of detection level was calculated for each sample. The level of detections reported were determined by taking an average of the level of detections for each sample within a standard and another average was taken of the three standards to determine an overall level of detection average for each sample. This same method was also conducted for the trace elements analysed with the addition of reporting minimum values. However, not all standards were applicable for each element and the standards that were applicable were used in determining maximum, minimum and level of detection concentrations.

4 Results

4.1 Vein Mapping

Two main types of vein generations were observed within the Canadian Malartic footprint within 55 outcrops. One of the vein generations formed after S_2 indicated by the alignment of biotite grains as these veins crosscut S_2 and lie at high angles to it. These veins are thus younger than D_2. Two vein sets were observed within this vein generation determined by their primary mineralogy, one had a main mineralogy of quartz and the other contained quartz and feldspar.

The other vein generation formed during $D_{2,}$ as they were influenced by the structural components that formed as a result of D_2. Eight vein sets were observed within this vein generation based on their mineralogy and their timing relationship with D2. Vein sets 1, 2 and 3 within this generation were sampled for this study as they contained pyrite and also formed during D_2. These veins had two different timing relationships with D_2. Vein type 1 crosscut S_1, which formed during D_1, but was still folded by F_2. Thus, this vein is older than D_1 and formed during D_2. This vein contained quartz, feldspar as well as pyrite and was also boudinaged at some outcrops. Only two samples were of this type, sample 159 and 888B. Vein set 2 and 3 were constrained within S_2, meaning the biotite grains wrapped around the veins that lay sub-parallel to S_2, and some were boudinaged as well. Vein set 2 was composed of quartz and pyrite and was also boudinaged at some locations. Three of the samples were of this type, samples 3415A, 897A and 900. The remaining samples fall under vein set 3 and contained 3 subsets, 3a, 3b, and 3c, which all contained quartz, feldspar and pyrite but had crosscutting relationships with each other, as 3a crosscut 3b, and 3b crosscut 3c.

The remaining vein sets of this generation were not sampled, as they did not contain pyrite. Vein sets 4, 5 and 6 had the same timing relationship with D_2 as vein set 1 but differed in its primary mineralogy of quartz, quartz and feldspar as well as quartz, feldspar and amphibole, respectively. Vein set 7 and 8 had the same timing relationship with D_2 as vein sets 2 and 3. Vein set 7 was composed of quartz and vein set 8 is composed of quartz and feldspar. Vein set 8 is also divided into three subtypes, 8a, 8b and 8c which crosscut each other as well, where 8a crosscut 8b and 8b crosscut 8c.

4.2 Mineralogy

While the sampled vein sets that were observed in outcrop scale had an observed mineralogy of quartz as well as quartz and feldspar, five groups of primary vein mineralogy can be distinguished from petrographic analyses. The groups are as follows and distribution of samples within these groups is displayed in Table 1:

Group 1: Quartz-Albite-K-feldspar-Calcite-Biotite

Group 2: Quartz-Albite-K-feldspar-Biotite

Group 3: Quartz-Albite-Calcite-Biotite

Group 4: Quartz-Albite-Biotite

Group 5: Quartz-Calcite-Biotite

The two samples of vein set 1 fell within group 4, vein set 3 samples all fell under group 5 and the remaining samples within vein set 2 fell under all of the groups. These primary vein mineralogy groups were well distributed throughout the pit and the two transects (Figure 5). Chlorite was present in nearly all samples and partly replaced biotite. An example of chlorite replacement of biotite is shown in Figure 6 where the darker biotite portion of the grain is replaced by chlorite as indicated by its lighter green colour.

Table 1. Primary vein mineralogy distribution within samples

Group 1	Group 2	Group 3	Group 4	Group 5
152	899A	162	159	3415A
157	NB036	168	888B	897A
487	488	NB064	171B	900
153	490	NB068	173	
164B		895B	NB061B	
154			898A	
886B				

The minor mineral composition is variable but may include chalcopyrite, galena, molybdenite, barite, rutile, ilmenite, titanite, apatite, muscovite, epidote, REE fluorocarbonate minerals, telluride minerals, scheelite and hornblende. Much like the primary vein mineralogy groups, these minor minerals are evenly distributed throughout the samples and are not specific to a location. Alteration haloes surround the veins and are characterized by bands of biotite at vein selvages and within the host rock. There is also disseminated pyrite as well as a reduced grain size within the host rock. An example of this alteration halo is also provided in Figure 6 where bands of biotite are present and run parallel to the veins and disseminated pyrite grains lay within a fine-grained host rock. Inclusions within the pyrite grains are largely composed of quartz, biotite, albite, k feldspar, chlorite, calcite, muscovite, chalcopyrite, telluride minerals, galena, molybdenite, REE flurorcarbonate minerals, epidote and apatite in variable proportions.

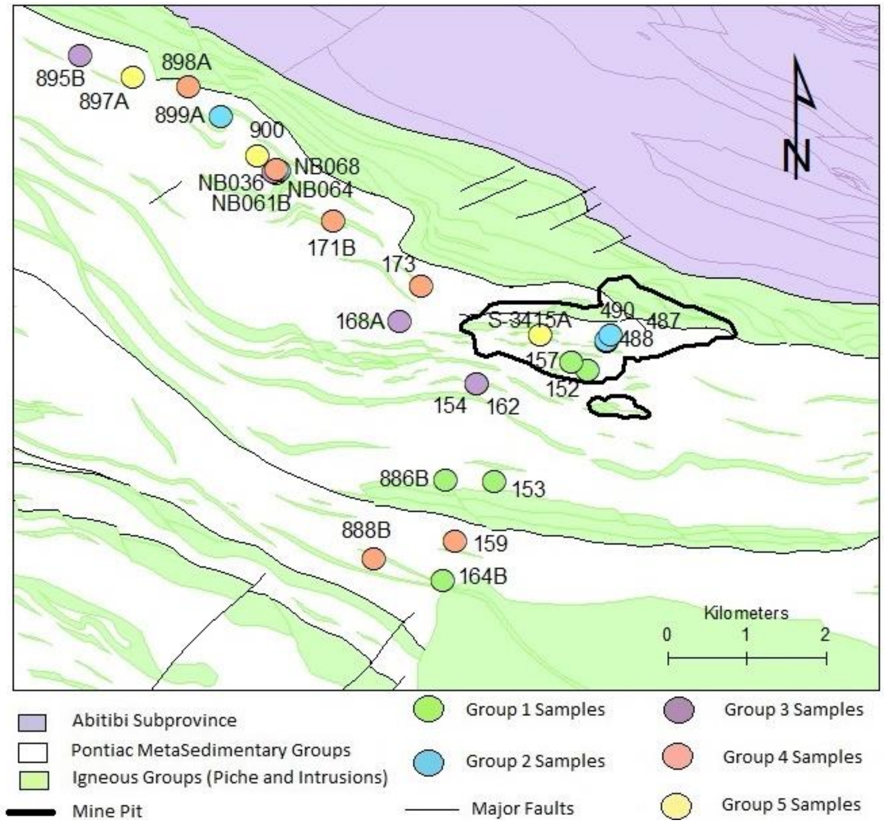

Fig. 5 Sample distribution of primary vein mineralogy groups. Figure is modified from Perrouty et al. (2017).

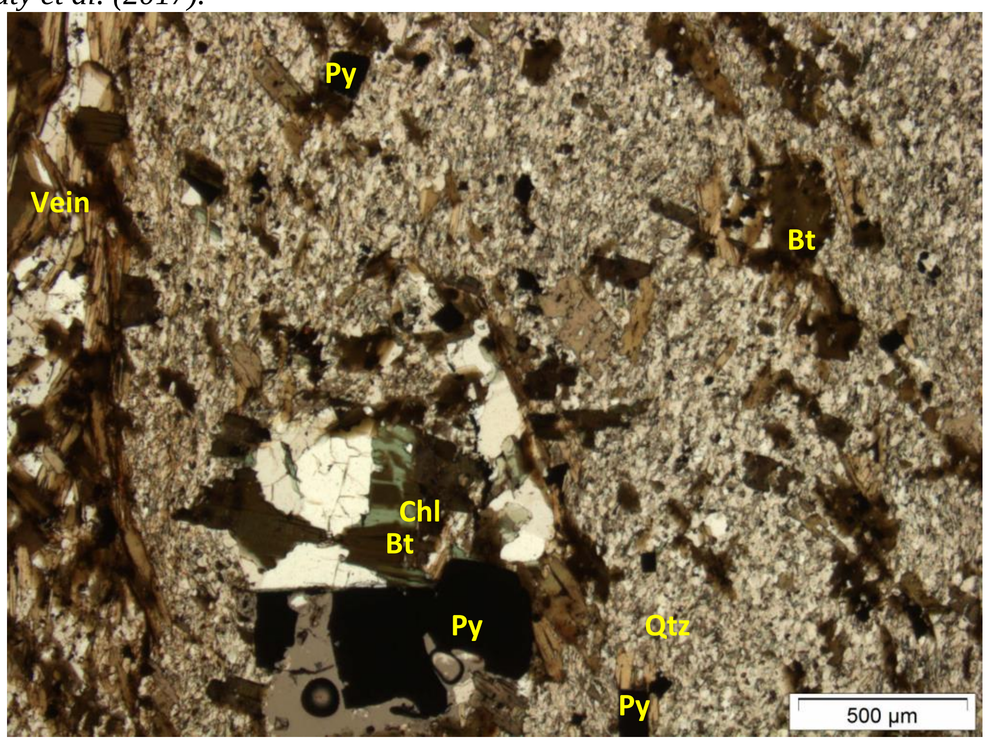

Fig. 6 Photomicrograph of 898A showing replacement texture and alteration halo.

Three sulphide mineral assemblages are observed within the samples and are displayed in Figure 7. Yellow symbols consist of pyrite grains, orange symbols consist of pyrite and pyrrhotite grains and red samples consist of pyrrhotite grains. The distribution of these three assemblages differ between the two transects as well. Yellow and orange samples are found along the E-W transect and display a random spatial distribution. Along the southern transect, pyrite is increasingly replaced by pyrrhotite as the sample dots are yellow towards the north, orange in the center and red towards the south. An example of this replacement texture is observed in Figure 8 within sample 749 taken from the Bravo zone on the Canadian Malartic property and its location is indicated in Figure 7. The pyrite grain in Figure 8 is replaced by pyrrhotite within the fractures of this grain as indicated by the light coloured mineral within the pyrite grain.

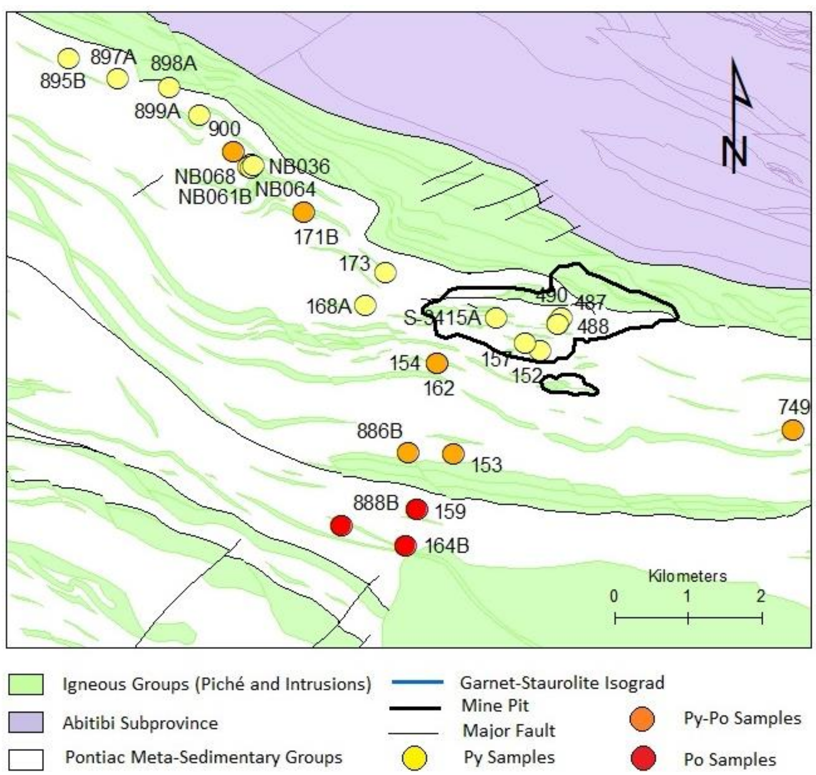

Fig. 7 Distribution of sulphide mineral assemblages and location of Sample 749 from the Bravo zone. Figure is modified from Perrouty et al. (2017).

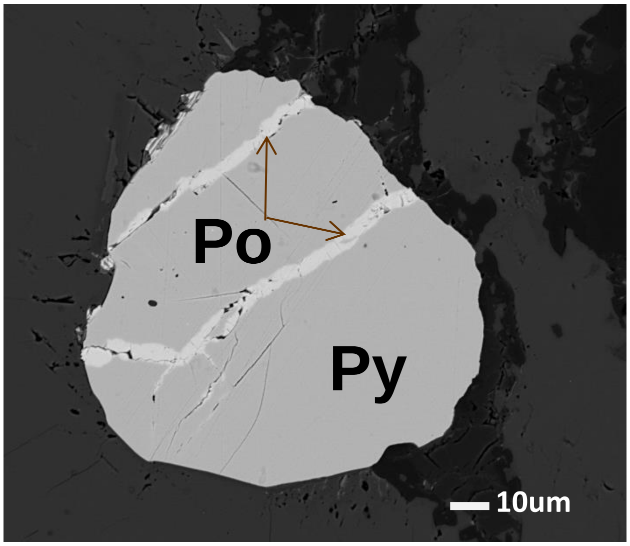

Fig. 8 Sample 749 from the Bravo zone. The darker pyrite grain is replaced by pyrrhotite within the fractures of the grain as indicated by the lighter colour.

4.3 Electron Probe Micro-Analysis

EPMA maps taken of pyrite grains from samples 153A and NB036 display an oscillatory zoning pattern. This pattern is shown in Figure 9a-d and is defined by concentric bands of differing nickel and cobalt content. Both grains show cores of pyrite that are enriched in cobalt and its outer edges are more enriched in nickel with the enrichment displayed in the brighter colours.

Due to the varied enrichment in both nickel and cobalt observed in the pyrite grains with oscillatory zoning, EPMA point data was also measured in pyrite grains with the remaining samples in order to record the differences in these elements. Points were taken from the edge of the grains towards the core of the grains, to record the difference in nickel and cobalt content.

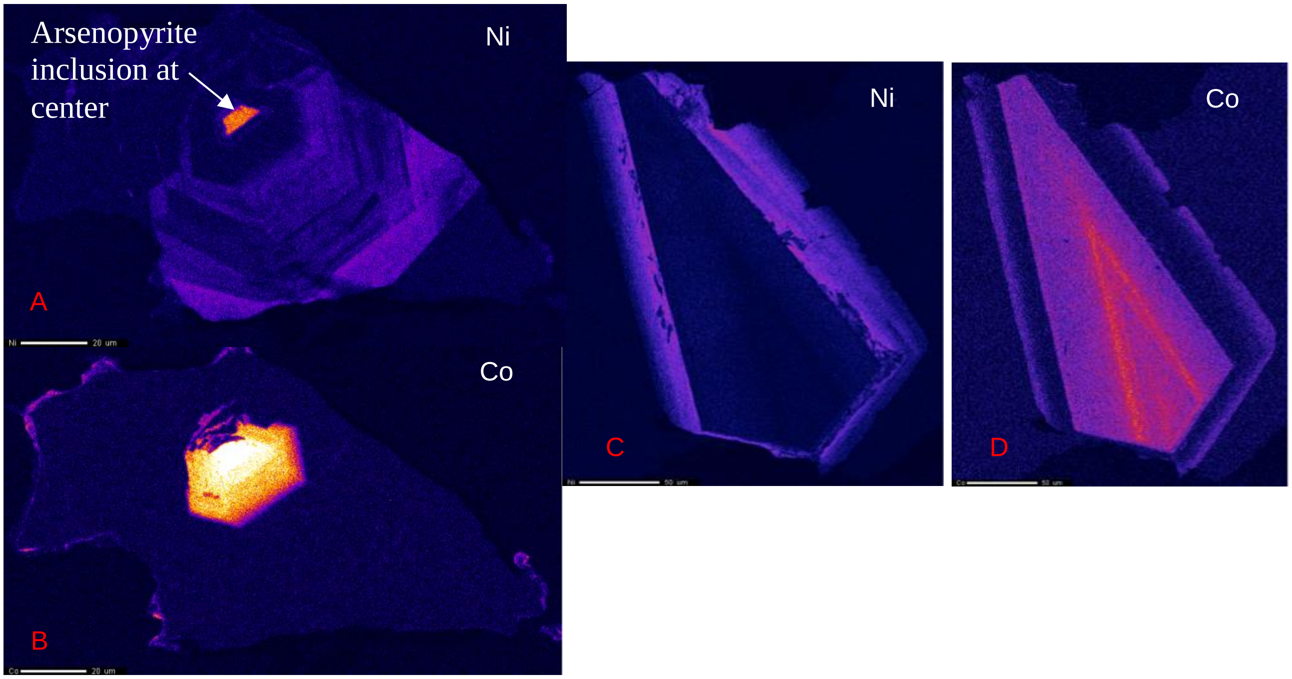

Fig. 9 EPMA maps of pyrite grains showing elemental distribution within. A: Ni distribution within sample 153A, grain C, B: Co distribution within sample 153A, grain C, C: Ni distribution within sample NB036, grain A, D: Co distribution within sample NB036, grain A. Brighter colours indicate enrichment of the element.

The mass percent values of nickel and cobalt in pyrite grains are displayed in Table 2 and Table 3, respectively. The remaining elements measured during EPMA point analysis did not show significant mass percentages within the pyrite grains and were thus not reported. Sample 153 varies in mass percent values of nickel from 0% in the core, which is in the periphery of the arsenopyrite inclusion in Figure 9a, to 3.69% at the edge of the pyrite grains. Mass percent values of cobalt for sample 153 varied from 24.80% in the core to 0.04% at the edge of the pyrite grain. Large ranges in mass percentages cobalt were also observed in sample 886B as well as 164B. The remaining samples did not display large ranges in cobalt and nickel enrichment, including the samples taken from the Canadian Malartic pit.

Table 2. Mass percent average, maximum, minimum and range of Nickel within each sample

Sample	Mass% Avg	Mass% min	Mass% max	Mass% range
168A Grain C	0.2	<LOD	0.8	0.8
3415A Grain A	0.03	0.01	0.1	0.05
153A Grain C	0.8	<LOD	3.7	3.7
886B Grain A	0.2	<LOD	0.9	0.9
NB036 Grain A	0.9	0.3	2.7	0.03
NB036 Grain B	0.01	<LOD	0.03	2.4
490 Grain A	0.01	<LOD	0.03	0.03
157 Grain A	0.02	<LOD	0.03	0.03
154 Grain A	0.03	<LOD	0.1	0.1
895B Grain A	0.01	<LOD	0.01	0.01
895B Grain B	0.01	0.01	0.04	0.04
164B Grain C	0.08	<LOD	0.2	0.2
162 Grain A	<LOD	<LOD	0.01	0.04

Table 3. Mass percent average, maximum, minimum and range of Cobalt within each sample

Sample	Mass% Avg	Mass% min	Mass% max	Mass% range
168A Grain C	0.06	0.04	0.2	0.1
3415A Grain A	0.07	0.03	0.2	0.1
153A Grain C	3.3	0.04	24.8	24.8
886B Grain A	0.4	0.05	2.2	2.1
NB036 Grain A	0.2	0.05	0.4	0.4
NB036 Grain B	1.1	0.09	1.9	1.9
490 Grain A	0.06	0.05	0.09	0.05
157 Grain A	0.2	0.04	0.6	0.5
154 Grain A	0.05	0.04	0.1	0.06
895B Grain A	0.07	0.05	0.1	0.04
895B Grain B	0.07	0.05	0.1	0.05
164B Grain C	0.9	0.01	2.8	2.8
162 Grain A	0.05	0.03	0.07	0.04

4.4 Laser Ablation Inductively Coupled Mass Spectrometry Analysis

4.4.1 Structural Gold Data

Gold maximum, minimum and level of detection concentrations are reported in ppm within Table 4. Significant values of gold were interpreted to be greater than 0.1 ppm.

These values were only found within the maximum values of 8 samples: 153, 3415A, 152, NB036, 157, 897A, 898A and 154. The highest concentrations of structural gold were within samples 152, 3415A, 157, 898A and NB036. For every sample, the minimum values of gold measured were below the detection limit, meaning that the minimum values were anywhere between 0 ppm to the detection limit concentration. 159 and 164B contained pyrrhotite and not pyrite; therefore the gold values in Table 4 for these samples represent structural gold within pyrrhotite grains. Also, for samples 164B, 900 and 159, the detection limits were anomalously high so this data was discarded.

Table 4. Maximum, minimum and limit of detection concentrations (in ppm) for Au

Sample	Au Max	Au Min	Au LOD
153	0.13	< LOD	0.06
3415A	0.28	< LOD	0.04
152	0.64	< LOD	0.06
NB036	0.63	< LOD	0.03
173	< LOD	< LOD	0.03
899A	< LOD	< LOD	0.02
157	0.34	< LOD	0.07
168A	0.08	< LOD	0.06
895B	0.04	< LOD	0.03
897A	0.11	< LOD	0.10
898A	0.37	< LOD	0.04
164B	< LOD	< LOD	0.34
886B	< LOD	< LOD	0.04
171B	< LOD	< LOD	0.05
154	0.17	< LOD	0.09
900	< LOD	< LOD	0.15
159	< LOD	< LOD	0.15

Gold concentrations as a function of distance from the deposit are displayed in Figure 10. The distance of each sample was measured from its distance from reference sample 488, which lay closest to the center of the pit. The green symbols indicate the maximum concentrations of gold that were assigned a numerical value. The red symbols indicate the limit of detection. The grey area underneath the red symbols indicate the region where the minimum concentrations of each grain lies, as they are all below the detection limit for each sample. Samples taken from the pit are labeled in green, samples taken from the N-S transect are labeled in red and samples taken from the E-W transect are labeled in blue. The gold concentrations within each segment measured for each sample are listed within Appendix F and the majority of the concentrations for each grain were below 0.1 ppm or below the detection limit.

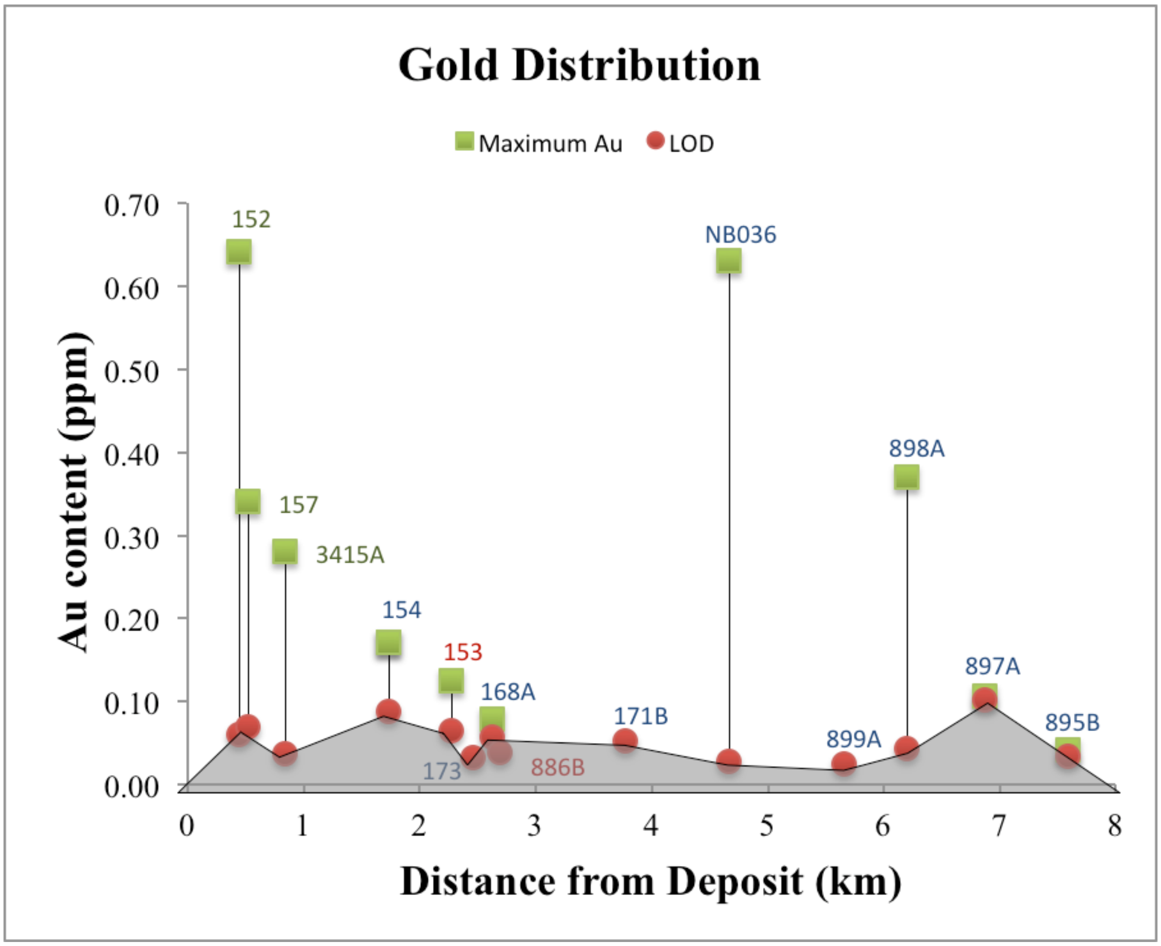

Fig. 10 Gold distribution within the samples as a function of distance from the deposit. Pit samples are labeled in green, samples taken from the N-S transect are labeled in red and samples taken from the E-W transect are labeled in blue.

4.4.2 Gold Inclusion Data

Gold inclusions were determined by looking at the intensities of sulphur gold and silver over time, i.e., spikes above background are considered to be inclusions. The full set of figures are found within Appendix F. Gold inclusions were found within 4 of the 17 samples analyzed and are 152, 3415A, 157 and 898A. 3 of these samples were taken from the Canadian Malartic pit and gold inclusions were found in multiple traverses within these grains. Sample 898A contained one gold inclusion within one of the traverses analysed.

Two types of gold inclusions are observed within the sample. The first type of inclusion exists within the fractures of the grains and these are observed in one of the inclusions from 3415A and the single inclusion within 898A. A gold inclusion lying within the fracture of the pyrite grain is displayed in Figure 11. In this figure, there is a drop in sulphur intensity, which is inferred to be a fracture within the pyrite grain and this occurs simultaneously with a sharp increase in gold content. The other type of gold inclusion occurs as nanoparticles within the pyrite grain and is found within the remainder of the observed gold inclusions. This is shown in Figure 12 where the sulphur intensity within the pyrite grain remains consistent with a simultaneous increase in gold intensity.

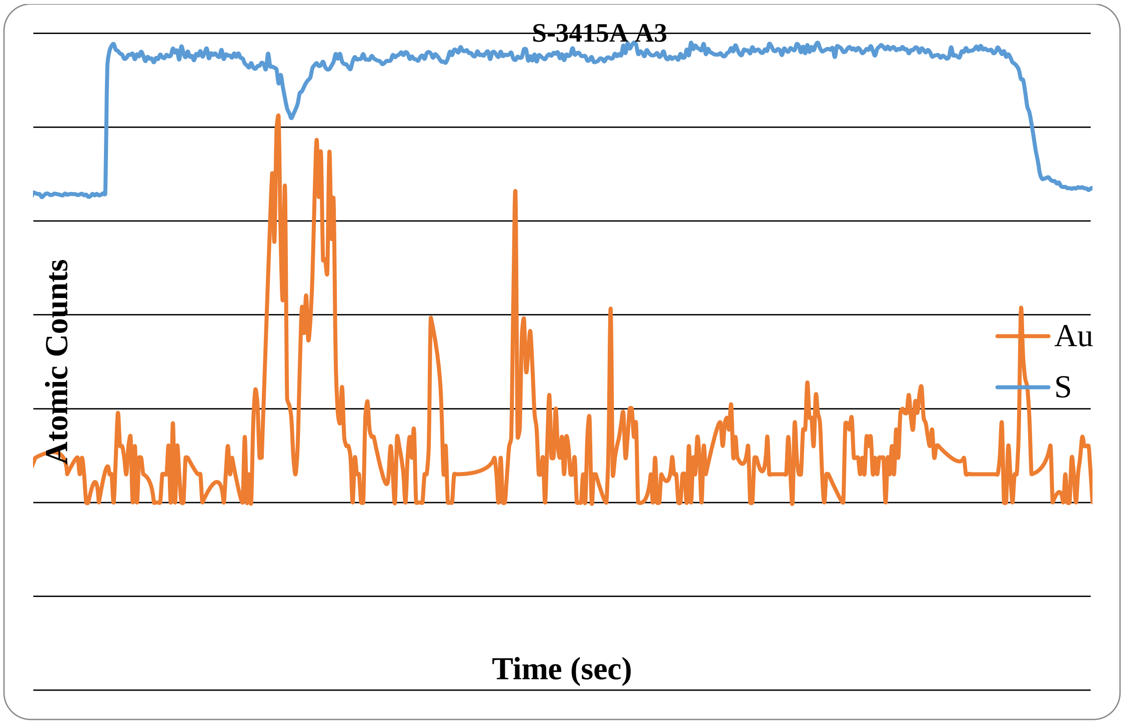

Fig. 11 Example of gold inclusion existing within the pyrite grain fracture along traverse A3 within sample 3415A.

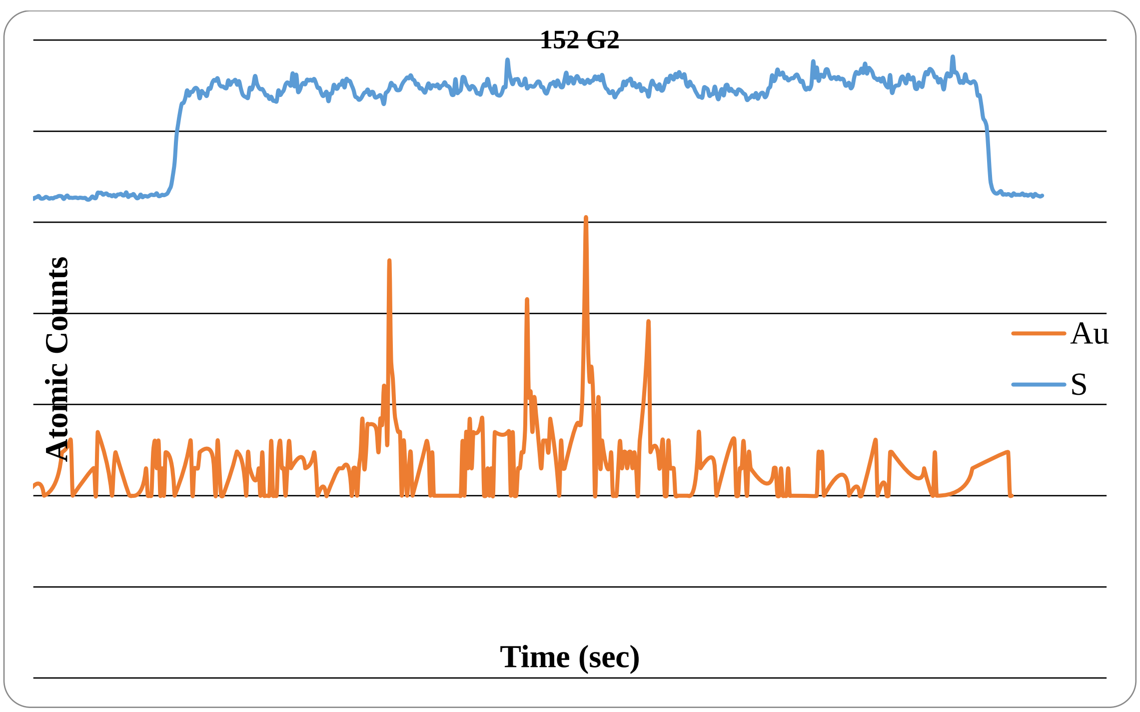

Fig. 12 Example of gold nanoparticle within the pyrite grain along traverse G2 in sample 152.

4.4.3 Other Trace Elements

Trace element maximum and minimum values as well as limits of detection are reported in ppm in Tables 5 to 9. These trace elements include Ni, Co, Se, Ag, As, Sb, Pb and Bi. While these values are reported in both maximum and minimum values, many grains contain concentrations of Ag, As, Se, Pb and Bi much greater than the level of detection as well as 0.1 ppm and are enriched in these trace elements. Generally, the samples also contain low values of Sb as the majority of the maximum values are below 0.1 ppm or below the detection limit.

Table 5. Maximum, minimum and limit of detection (LOD) concentrations in ppm of Co and Ni within vein pyrite samples

Sample	Co Max	Co Min	Co LOD	Ni Max	Ni Min	Ni LOD
153	8900	11	0.02	4390	15	0.3
3415A	735	43	0.02	691	177	0.2
152	370	42	0.03	765	84	0.3
NB036	17280	450	0.02	6670	4	0.1
173	2710	63	0.02	478	215	0.2
899A	340	82	0.02	1518	880	0.2
157	1910	5	0.06	318	24	0.5
168A	8.7	0.05	0.02	1518	880	0.2
895B	973	366	0.01	334	87	0.2
897A	37600	2900	0.03	7700	870	0.5
898A	405	64	0.01	770	138	0.2
164B	1161	325	0.2	1430	780	2.3
886B	680	57	0.02	272	92	0.2
171B	4910	27	0.03	1120	48	0.4
154	830	0.3	0.05	1020	97	0.5
900	6200	31	0.1	293	13	1.0
159	142	20	0.1	530	3	1.2

Table 6. Maximum, minimum and limit of detection (LOD) concentrations in ppm of Se and Ag within vein pyrite samples

Sample	Se Max	Se Min	Se LOD	Ag Max	Ag Min	Ag LOD
153	27	1	0.6	3	0.05	0.03
3415A	19	3	0.5	1	< LOD	0.02
152	28	15	0.8	2	0.04	0.03
NB036	50	19	0.4	469	< LOD	0.01
173	13	5	0.5	0.4	< LOD	0.02
899A	13	6	0.4	< LOD	< LOD	0.01
157	21	6	1.3	6	< LOD	0.05
168A	50	8	0.6	1	0.05	0.01
895B	6	4	0.4	0.01	< LOD	0.01
897A	102	39	1.2	110	4	0.02
898A	36	20	0.5	1	0.01	0.01
164B	49	21	5	6	< LOD	0.1
886B	13	5	0.4	0.1	< LOD	0.01
171B	23	5	0.7	0.04	< LOD	0.02
154	24	3	1	0.3	< LOD	0.03
900	47	3	2	0.04	< LOD	0.04
159	35	27	3	2	1	0.06

Table 7. Maximum, minimum and limit of detection (LOD) concentrations in ppm of Pb and Bi within vein pyrite samples

Sample	Pb Max	Pb Min	Pb LOD	Bi Max	Bi Min	Bi LOD
153	118	0.5	0.03	57	0.01	0.01
3415A	4	0.04	0.02	0.5	< LOD	0.01
152	63	0.3	0.03	9	< LOD	0.01
NB036	740	0.06	0.02	720	0.01	0.01
173	6	0.15	0.02	4	0.01	0.01
899A	0.5	< LOD	0.02	0.14	< LOD	0.01
157	7	0.2	0.05	38	0.1	0.01
168A	270	6	0.02	11	0.01	0.01
895B	0.07	0.02	0.01	0.03	< LOD	0.01
897A	7100	167	0.05	77	2	0.01
898A	8	1	0.02	33	0.1	0.01
164B	18	1	0.18	7	0.03	0.04
886B	37	2	0.01	1	0.01	0.01
171B	1	0.03	0.03	2	0.01	0.01
154	4	0.07	0.04	3	< LOD	0.01
900	39	< LOD	1.19	18	< LOD	0.02
159	22	1	0.07	28	0.08	0.02

Table 8. Maximum, minimum and limit of detection (LOD) concentrations in ppm of As and Sb within vein pyrite samples

Sample	As Max	As Min	As LOD	Sb Max	Sb Min	Sb LOD
153	2700	3	0.46	3	< LOD	0.07
3415A	33	1	0.29	0.05	< LOD	0.05
152	28	4	0.51	0.20	< LOD	0.08
NB036	4770	8	0.28	0.04	< LOD	0.04
173	11	1	0.32	0.03	< LOD	0.05
899A	411	117	0.24	< LOD	< LOD	0.04
157	33	1	0.92	0.07	< LOD	0.13
168A	2	< LOD	0.40	18	0.4	0.06
895B	2	1	0.26	< LOD	< LOD	0.03
897A	274	32	0.72	6	0.8	0.09
898A	920	135	0.30	0.2	< LOD	0.05
164B	4	< LOD	3.44	< LOD	< LOD	0.51
886B	100	7	0.34	3	0.1	0.04
171B	115	3	0.52	< LOD	< LOD	0.08
154	232	1	0.77	< LOD	< LOD	0.12
900	11	< LOD	1.39	< LOD	< LOD	0.24
159	4	< LOD	1.54	< LOD	< LOD	0.24

5 Discussion

5.1 Vein Mineralogy and Structural Relationships

While a few studies have been conducted on the veins within the deposit, studies of the veins within the footprint are limited. However, the veins observed within this study closely resemble the veins interpreted to have formed during the main ore mineralization stage in the deposit as described by both Helt et al. (2014) as well as De Souza et al. (2015).

Helt et al. (2014) reported the mineralogy observed within 3 main vein types within the Canadian Malartic deposit and are reported in Figure 13. V1 was associated with the pre-ore stage of gold mineralization, $V2_{main}$ formed during the main ore stage and $V2_{late}$ were late ore stage veins (Helt et al., 2014). Finally, V3 veins formed post-ore mineralization (Helt et al., 2014). The mineralogy of the veins observed within this study closely resembles that of the $V2_{main}$ veins. The $V2_{main}$ vein is the only type that contains pyrite, which is observed within all of the samples collected for this study. These $V2_{main}$ veins are also largely composed of plagioclase, quartz, k-feldspar, biotite, muscovite and ankerite (Helt et al., 2014). This primary mineralogy matched the minerals observed in the primary vein mineralogy of the samples within this study. However, these major minerals within the samples of this thesis occur in variable proportions and do not include ankerite. The minor mineralogy of these $V2_{main}$ veins is also very similar to the minor minerals found within the majority of samples in this study, which include, barite, scheelite, titanite, chalcopyrite, galena, molybdenite, and rutile (Helt et al., 2014). There is thus a strong similarity in both major and minor mineralogy of the veins sampled in this study with the $V2_{main}$ veins associated with the main stage of gold mineralization.

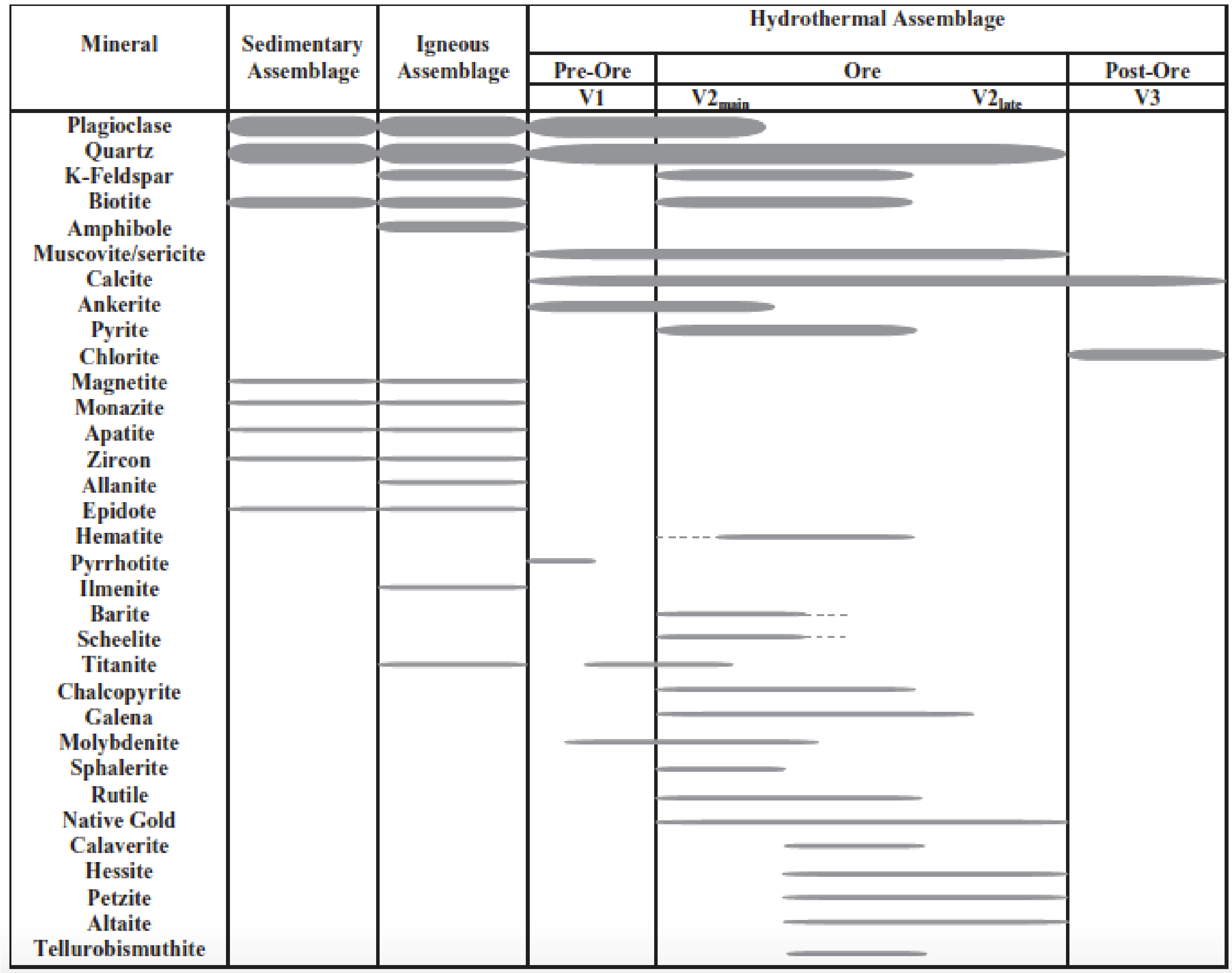

Fig. 13 Mineralogical assemblages of vein types in relation to different ore stages. Thicker lines denote a greater presence of the mineral, (Helt et al., 2014).

As previously mentioned, De Souza et al. (2015) also described 3 main vein types within the deposit and interpreted that the V2 veins in this study were also related to the main stage of gold mineralization. Much like the veins sampled in this study, the V2 veins described in De Souza et al. (2015) generally contained biotite selvages. These V2 veins also shared a similar mineralogy as the veins within this study as they were also composed of quartz, calcite, biotite, K-feldspar, albite, chlorite, and pyrite in variable proportions, but the veins in this study did not contain Fe-rich dolomite and ankerite observed within the V2 veins (De Souza et al., 2015). The V2 veins described by De

Souza et al. (2015) contained minor amounts of chalcopyrite, tellurides and scheelite, which are all observed within the samples of this study. However the veins in this study contained many more minor minerals. Unlike the V2main veins described by Helt et al. (2014) the minor mineralogy described in De Souza et al. (2015) did not match with the samples of this thesis as strongly as it only mentioned 3 minor minerals. However, the study by De Souza et al. (2015) agreed more strongly in its major mineralogy as each of the major minerals observed were present in variable proportions much like this study where five groups of primary vein mineralogy are observed.

The V2 veins were interpreted to have formed during syn-late D_2 as they were present as both deformed and undeformed filled fracture veins that lie subparallel to S_2, with some that were crenulated at high angles to S_2 (De Souza et al., 2016). Vein sets 2 and 3 that were classified in this study were constrained within S_2 and lie sub-parallel to it. They could thus be interpreted to be filled fracture veins as well, especially considering that some veins were even boudinaged along the S_2 direction. While the V2 veins described by De Souza et al. (2016) resemble the majority of the samples in this study in both mineralogy and structural relationships, the 2 samples of vein set 1 do not share the same structural relationship as they are folded by F_2 and do not lie sub parallel to S_2 nor are they crenulated.

A study within Cartier, a smaller region of the deposit's footprint, was one of the few investigations conducted on the vein systems within the Canadian Malartic footprint (Blacklock, 2015). Vein types A and B within this study resemble the veins observed in this study based on its structural relationship to S_2 and mineralogy. Vein type A had been observed to be tightly folded by D_2 much like samples 159 and 888B within this study, and the mineralogy of vein A matched these samples as well, which consisted of quartz, feldspar and biotite (Blacklock, 2015). Vein type B is generally oriented along S2 much like the remaining samples within this study but its mineralogy is similar to that of vein type A, which consisted of quartz, feldspar and biotite (Blacklock, 2015). This vein set matches the mineralogy and structural relationships of S_2 of the samples from primary mineralogy groups 2 and 4 within this study. The samples in this thesis do not resemble the mineralogy of vein sets A and B as strongly as they resemble the vein types of Helt et al. (2014) and De Souza et al. (2015) as they only share 3 major minerals. Blacklock (2015) inferred that these two vein sets formed before D_2 as they were deformed by the structural components that formed as a result of D_2, but it is more likely that these veins formed during the second deformation event as interpreted by De Souza et al. (2016) as well as this study where the veins formed either subparallel to S_2 as fracture-filling veins or perpendicular to S_2 as tension veins, which were then boudinaged along S_2 and folded by $F_{2.}$ Due to the general similarity in mineralogy and structural relationships of the veins sampled for this study with the veins studied in the deposit by both Helt et al. (2014) and De Souza et al. (2015, 2016), the veins within this thesis are inferred to have formed during the main stage of gold mineralization.

5.2 Oscillatory Zoning

The oscillatory zoning pattern observed in samples 153 and NB036 display a varying enrichment of nickel and cobalt. These pyrite grains could have formed as a result of two different processes. The first possibility is that the pyrite crystals grew from an evolving fluid. A study conducted by Schumacher et al. (1998), described oscillatory zoning within garnet, alternating between its calcium rich grossular component and its iron rich almandine component. Schumacher et al. (1998) attributed this zoning pattern to continuous reactions occurring during regional metamorphism, where there was complex growth and resorption of the garnet as a result of changing pressure and temperature conditions (Schumacher et al., 1998). So, small scale variations in regional metamorphism would result in variable P-T conditions that would favour differences in the rate of production of the mineral in different stages (Willner et al., 2001). A study conducted by Zacharias et al. (2016) agreed with this evolving fluid theory and attributed the oscillatory zoning pattern observed in pyrite grains indicated by its varying arsenic content to changes in arsenic activity of the fluid during pyrite precipitation or also in changing P-T conditions.

The second possibility is that the pyrite crystals precipitated from multiple fluids. A study conducted by Putnis et al. (1992) experimentally reproduced this compositional oscillatory zoning pattern in (Ba, Sr)SO_4 solid solutions grown by diffusion transport of Ba^{2+}, Sr^{2+} and SO_4^{2-} ions from $BaSO_4$ and $SrSO_4$ solutions. The crystals grew in non-equilibrium supersaturated conditions as nucleation of each zoned layer occurred when the supersaturation threshold of either solution was exceeded first (Putnis et al., 1998). This threshold required for nucleation and growth is strongly dependent on composition since the two solutions had large differences in solubility, resulting in concentration gradients that would preferentially nucleate one end member in supersaturated conditions over the other end member (Putnis et al., 1998). The concept of multiple fluids producing an oscillatory zoning pattern could explain how the pyrite grains had grown in this study with varying nickel and cobalt content as well.

Since the mineralogy and structural relationships of the veins sampled in this study closely resemble the veins associated with the main stage of gold mineralization, the genetic model of the Canadian Malartic deposit may explain the fluids involved in pyrite precipitation. Helt et al. (2014) inferred that gold mineralization occurred from an evolving fluid originating from exsolution of monzodioritic magma at mid crustal levels. This study suggests that as this fluid ascended to the surface, the host rock had undergone potassic alteration, carbonation and sulphidation as a result of H_2S loss in the fluid, increasing oxygen fugacity and also a drop in temperature. Analysis of the gold content within the pyrite could further suggest whether these samples are reflective of the deposit.

5.3 Trace Elements in Vein Pyrite

Gao et al. (2015) proposed 5 stages of host rock pyrite within the deposit based on their trace element composition and stages 1-4 seem to contain similar geochemical characteristics as the vein pyrite. As mentioned previously, stage 1 pyrite grains are enriched in Co, As, Se and are low in Ni, Sb, Bi and Pb. Stages 2 to 4 are enriched in Ag, Te, Pb, Au, and Bi. Stage 5 is enriched in Co and Ni but low in the other trace elements. The trace element compositions of the vein pyrite in this study share similarities with both stage 1 and stages 2-4 pyrite. Much like the stage 1 pyrite, the vein pyrite is enriched in Co, As and Se, however it is also enriched in Pb, Bi and mostly Ag as well which should have been low in stage 1 veins. The vein pyrite grains also resemble stages 2-4 pyrite as they are enriched in Pb, Bi, and largely Ag. However, unlike the pyrite grains of stages 2-4, the majority of the vein pyrite samples within the Canadian Malartic footprint are not enriched in Au in terms of gold incorporated within the lattice, as the majority of the segments measured contained low concentrations of gold. Since the vein pyrite share some similarities with both the stage 1 pyrite and the pyrite grains from stages 2-4, the vein pyrite could also be an intermediate between the two types, meaning they could have occurred between pre-mineralization and the main ore stage of mineralization. It could also suggest that different fluids were involved in the mineralization of host rock pyrite and the vein pyrite.

5.4 Gold concentrations

It would be inaccurate to base vein pyrite compositions on the minimum values measured within the grains as they all are not assigned numerical values and thus lay at some point between 0 ppm and the detection limit concentration. Since the gold concentrations of the majority of the segments measured lie below the detection limit or below 0.1 ppm, it can be inferred that these vein pyrite compositions generally contain values of gold that are not significant. This is also the case for the gold compositions of vein pyrrhotite grains within samples 159 and 164B, where both the maximum and minimum values of gold lie below the detection limit. Samples 898A and NB036 contain anomalously high maximum gold concentrations, but they are located within Parbec as well as Cartier and are inferred to contain high values since they are associated with gold mineralization zones. When looking solely at the maximum concentrations of gold within the rest of the samples, there is a general trend of decreasing gold content away from the deposit. This trend is observed within samples from both transects, suggesting that metamorphic grade does not influence gold concentrations. This relationship between the distance of the samples and their gold concentrations suggests that the vein pyrite grains are associated with the Canadian Malartic deposit as they increase in maximum gold content towards the deposit. This association could mean that maximum vein pyrite compositions of gold could be used as a weak vector to define the Canadian Malartic Footprint as it only accounts for maximum values of gold found within the pyrite grains.

While the vein and vein pyrite sampled for this study show an association with the Canadian Malartic deposit, the genetic model of the deposit described by Helt et al. (2014) may not be strongly supported. Helt et al. (2014) described that gold mineralization originated from an evolving fluid, however the gold inclusions observed within this study suggest that there may be at least two separate gold mineralization events where one fluid could have crystallized the pyrite grains and the nanoinclusions present within them as observed in samples 152, 3415A and 157. The other type of gold inclusions observed within the fracture of pyrite grains within sample 3415A and 898A suggest that a secondary fluid formed gold inclusions within the fractures afterwards.

5.5 Pyrite Saturation

Studies by Reich et al. (2005) and Deditius et al. (2014) explained the relationship between As and Au compositions within pyrite grains. Reich et al. (2005) determined that the maximum concentration of Au involved in the structure of pyrite is a function of As within the pyrite, meaning increasing amounts of As correlate with increasing amounts of Au. The relationship determined from this study is displayed in Figure 14. The line within the figure is the solubility limit of Au within pyrite determined by Reich et al. (2005) using the equation:

$$C_{Au} = C_{As} \times 0.02 + 4 \times 10^{-5}$$

This equation uses compositions of Au and As in mole percent and means that below the gold solubility limit, gold will be found within the pyrite grain in solid solution and crossing above the curve due to an increase in Au content or decrease in As content suggest that gold exists as nanoparticles within the pyrite. The opposite trend suggests that gold will exist within the pyrite structure. Deditius et al. (2014) examined this relationship introduced by Reich et al. (2005) and studied arsenic pyrite from multiple environments including orogenic deposits such as the Canadian Malartic deposit. The orogenic pyrite compositions in the study by Deditius et al. (2014) fall underneath the line in Figure 14, suggesting that these pyrite grains are controlled by a different solubility limit. Deditius et al. (2015) created a modified gold solubility limit for orogenic pyrite and is stated as the following equation:

$$C_{Au} = C_{As} \times 0.004 + 2 \times 10^{-7}$$

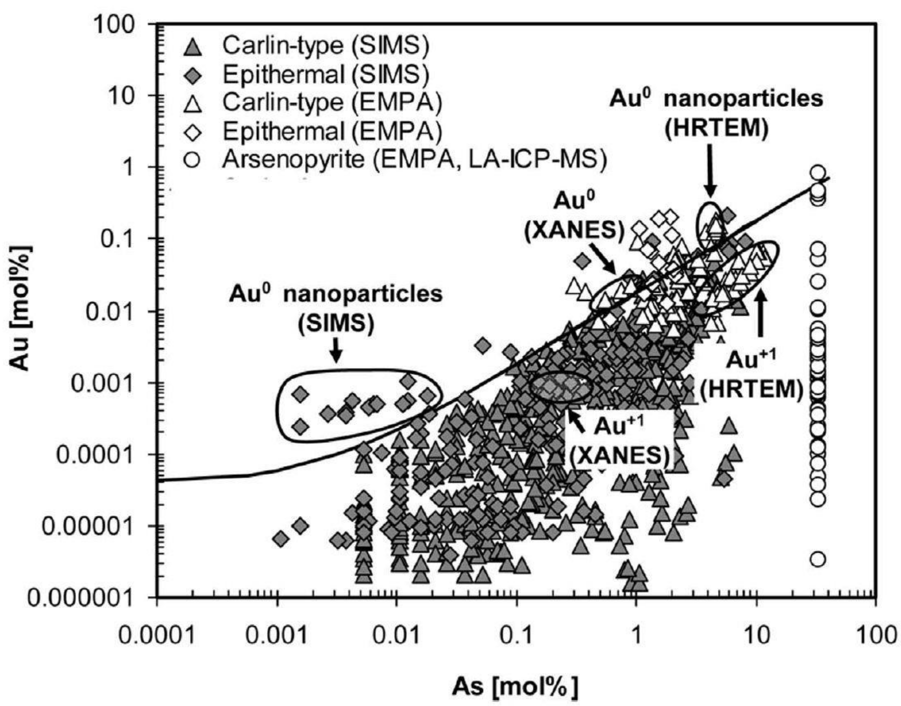

Fig. 14 Compositions of pyrite in Au-As space in mol%, showing the solid solubility limit of Au (Reich et al., 2005).

These two curves are plotted against the vein pyrite compositions within this study in Figure 15. The only samples that contained maximum values of gold that were assigned numerical values are plotted.

Similar to the results of Reich et al. (2005) and Deditius et al. (2014), the Au content within the vein pyrite grains appear to be a function of the As content as there appears to be an increase in gold with increasing As content. Samples 168A and 895B contain low As and Au concentrations and these concentrations increase for the rest of the samples. The vein pyrite compositions were also similar to the orogenic pyrite compositions from Deditius et al. (2014), as they all lie below the solubility limit determined by Reich et al. (2005) but the majority of the vein pyrite compositions also lie below the solubility limit determined by Deditius et al. (2014). The position of the vein pyrite compositions in relation to the gold solubility curves thus suggest that the vein pyrite grains are undersaturated with respect to gold. This relationship is supported by the vein pyrite compositions as the majority of samples do not contain inclusions. Samples 152, 3415A and 157 lie within and over the gold solubility limit of Deditius et al. (2014). These samples were from the pit and all contain gold inclusions, suggesting they are saturated or oversaturated with respect to gold. Sample 898A also contains a gold inclusion but lies further from the solubility curves. However, unlike the samples from the pit, which contained multiple inclusions only one gold inclusion was observed from the 4 traverses measured and may be considered negligible. Samples 168A and 895B were anomalies as they lie above the gold solubility limit but lack gold particles. This may be attributed to a maximum gold concentration at the detection limit.

These gold solubility limits are also temperature dependent as As and Au concentrations within pyrite decrease with increasing temperature, resulting in Au solubility within pyrite to decrease as well (Deditius et al., 2014). Since the Canadian Malartic deposit is orogenic and correspond well to the gold solubility limits of Deditius et al. (2014), these samples are higher temperature and have lower gold solubility limits within the grains, especially when compared to the pyrite compositions of Reich et al. (2005).

Thus the pyrite grains are undersaturated with respect to gold, resulting in the majority of the gold values to be interpreted as structural gold. The gold values below the curve of Deditius et al. (2014) lie further from the curve, which explains why the grains are generally low in gold content.

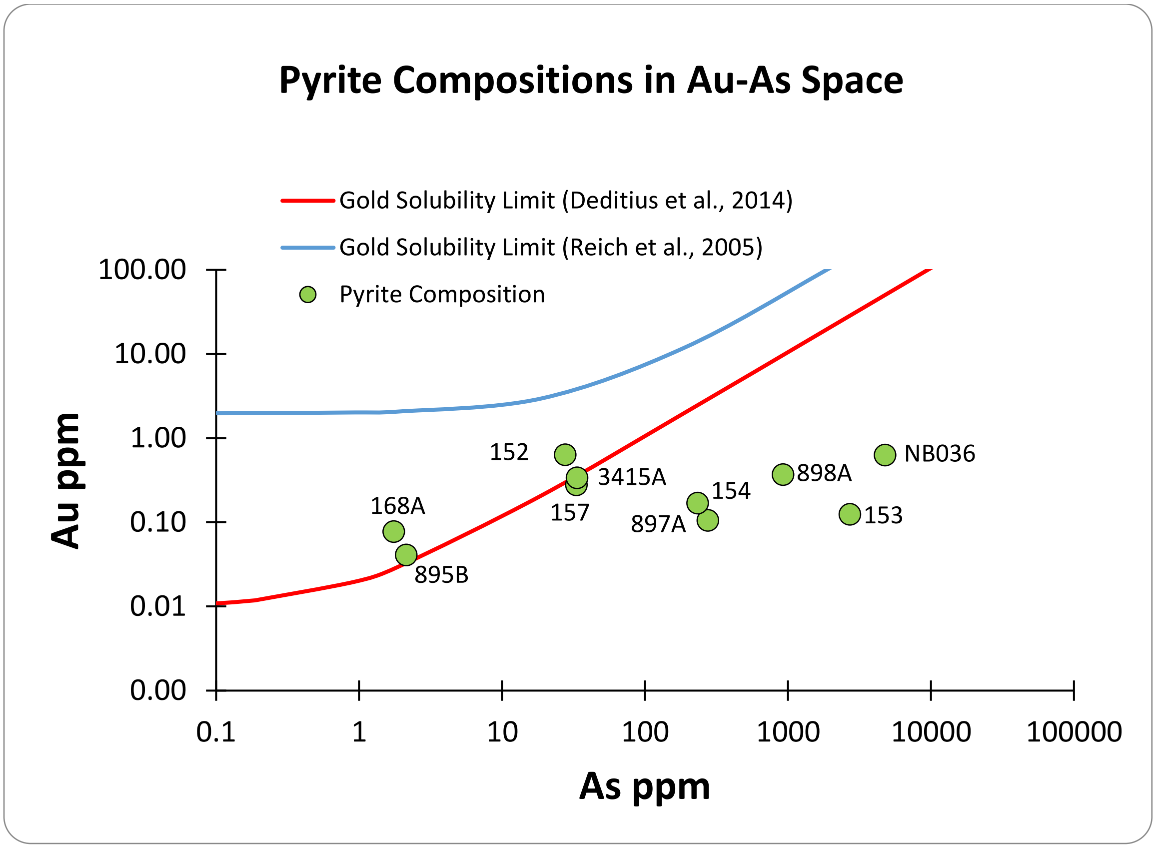

Fig. 15 Compositions of vein pyrite in ppm, the red curve represents the gold solubility limit determined by Reich et al. (2005) and the green curve represents the gold solubility limit determined by Deditius et al. (2014).

6 Conclusion

There is potential for vein pyrite compositions to be used as a vector to define the Canadian Malartic footprint. The mineralogy and structural characteristics of the veins sampled within this study closely can be inferred to have formed during the main stage of gold mineralization. The trace element concentrations of the vein pyrite surrounding the deposit do not closely reflect the trace element concentrations of the host rock pyrite grains in the footprint studied by Gao et al. (2015).

The oscillatory zoning pattern observed within the pyrite grains infer that the origin of the vein pyrite involve fluid mixing or fluid evolution.

Structural gold compositions within the vein pyrite are generally low, however when looking solely at the maximum gold compositions within the pyrite grains, there is a general decrease in maximum gold composition away from the deposit, and structural gold compositions within vein pyrite could thus be used as a weak vector to define the Canadian Malartic footprint. Multiple mineralization events may be inferred due to the presence of two types of gold inclusions within the vein pyrite grains.

The relationship between As and Au with respect to gold solubility within pyrite grains infer that the pyrite grains are undersaturated with respect to gold. This undersaturation is supported by the vein pyrite gold compositions as these pyrite grains generally contain low values of structural gold and the samples closest to the gold solubility curve are the only ones that contain gold inclusions.

7 Future Work

Vein pyrite compositions within the deposit must be characterized in more depth to understand vein pyrite variation within the deposit itself. Increased sampling will improve the understanding of the fluids involved as there would be stronger comparisons between the footprint vein pyrite and the deposit vein pyrite.

The two types of gold inclusions observed within the vein pyrite suggest multiple fluid events and future work could focus on an in-depth analysis of gold inclusions within the grains to understand the mineralization events involved.

More vein pyrite samples collected at higher densities would also be able to refine the suggestion that vein pyrite compositions can be used as a weak vector in defining the Canadian Malartic footprint. The relationship between distance and maximum gold content can be strengthened with an increased number of points that are more closely spaced.

8 References

Ayer, J.A., Thurston, P.C., Bateman, R., Dubé, B., Gibson, H.L., Hamilton, M.A., Hathway, B., Hocker, S.M., Houlé, M.G., Hudak, G., Ispolatov, V.O., Lafrance, B., Lesher, C.M., MacDonald, P.J., Péloquin, A.S., Piercey, S.J., Reed, L.E., and Thompson, P.H., 2005, Overview of results from the Greenstone Architecture Project: Discover Abitibi Initiative: Ontario Geological Survey Open File Report 6154, p. 146.

Belzile, E., and Gignac, L.P., 2011, Updated resource and reserve estimates for the Canadian Malartic project Malartic, Quebec: NI 43-101 Report, p. 261.

Blacklock, N., 2015, Vein characterization using structural controls and petrographic analysis at Cartier zone in the Canadian Malartic property at Malartic, Quebec: Unpublished B.Sc. honours thesis, Kingston, Canada, Queen's University, 58 p.

Card, K.D., and Poulsen, K.H., 1998, Geology and mineral deposits of the Superior province of the Canadian Shield, in Lucas, S.B., and St-Onge, M.R., ed., Geology of the Precambrian Superior and Grenville provinces: Geological Survey of Canada, Geology of Canada Series No. 7, p. 13–194.

Corfu, F., 1993, The evolution of the southern Abitibi greenstone belt in light of precise U-Pb geochronology: Economic Geology, v. 88, p. 132–1340.

Corfu, F., Jackson, S.L., and Sutcliffe, R.H., 1991, U-Pb ages and tectonic significance of late alkali magmatism and non-marine sedimentation, Timiskaming Group, southern Abitibi belt, Ontario: Canadian Journal of Earth Sciences, v. 28, p. 489–503.

Corfu F., Krough, T., Kwok, Y., and Jensen, L., 1989, U-Pb zircon geochronology in the southwestern Abitibi greenstone belt, Superior Province: Canadian Journal of Earth Sciences, v. 26, p. 1747–1763.

Davis, D.W., 1992, U-Pb dating of detrital zircon in sediments in the Pontiac and Abitibi subprovinces; preliminary results: Lithoprobe Report, v. 19, p. 33–35.

Davis, D.W., 2002, U-Pb geochronology of Archean metasedimentary rocks in the Pontiac and Abitibi Subprovinces, Quebec, Constraints on timing, provenance and regional tectonics: Precambrian Research, v. 115, p. 97–117.

Deditius, A.P., Utsunomiya, S., Reich, M., Kesler, S.E., Ewing, R.C., Hough, R., and Walshe, J., 2011, Trace metal nanoparticles in pyrite: Ore Geology Reviews, v. 42, p. 32–46.

Deditius, A.P., Reich, M., Kesler, S.E., Utsunomiya, S., Chryssoulis, S.L., Walshe, J., and Ewing, R.C., 2014, The coupled geochemistry of Au and As in pyrite from hydrothermal ore deposits: Geochemica et Cosmochimica. Acta, v.140, p. 644–670.

De Souza, S., Dubé, B., McNicoll, V.J., Dupuis, C., Mercier-Langevin, P., Creaser, R.A., and Kjarsgaard, I.M., 2015, Geology, hydrothermal alteration, and genesis of the world-class Canadian Malartic stockwork-disseminated Archean gold deposit, Abitibi, Quebec, In B. Dubé B., and Mercier-Langevin P., ed., Targeted Geoscience Initiative 4: Contributions to the Understanding of Precambrian Lode Gold Deposits and Implications for Exploration, Geological Survey of Canada, Open File 7852, p. 113–126.

De Souza, S., Dubé, B., McNicoll, V.J., Dupuis, C., Mercier-Langevin, P., Creaser, R.A., and Kjarsgaard, I.M., 2016, Geology and hydrothermal alteration of the world-class Canadian Malartic gold deposit, genesis of an Archean stockwork-disseminated gold deposit in the Abitibi greenstone belt, Quebec: Reviews in Economic Geology, v. 19, p. 1–000.

Derry, D.R., 1939, The geology of the Canadian Malartic gold mine, Quebec: Economic Geology, v. 34, p. 495–523.

Desrochers, J.P., and Hubert, C., 1996, Structural evolution and early accretion of the Archean Malartic composite block, southern Abitibi greenstone belt, Quebec, Canada: Canadian Journal of Earth Sciences, v. 33, p. 1556–1569.

Dimroth, E., Imreh, L., Goulet, N., and Rocheleau, M., 1983, Evolution of the south-central segment of the Archean Abitibi Belt, Quebec: Canadian Journal of Earth Sciences, v. 20, p. 1374–1388.

Eakins, P.R., 1962, Geological settings of the gold deposits of Malartic district, Abitibi east county, Québec: Department of Natural Resources, Geological Report 99, p. 155.

Fallara, F., Ross, P.S., and Sansfaçon, R., 2000, Caractérisation géochimique, pétrographique et structural, nouveau modèle métalloginique du camp minier de Malartic: Québec: Ministère des Ressources Naturelles, v. 2000–15, p. 155.

Gao, J.-F., Jackson, S.E., Dubé, B., Kontak, D.J., and De Souza, S., 2015, Genesis of the Canadian Malartic, Côté Gold, and Musselwhite gold deposits, in Insights from LA-ICP-MS element mapping of pyrite, in Dubé B. and Mercier-Langevin P., ed., Targeted Geoscience Initiative Contributions to the Understanding of Precambrian Lode Gold Deposits and Implications for Exploration: Geological Survey of Canada, Open File 7852, p. 157–175.

Gunning, J., and Ambrose, H., 1940, Malartic area, Quebec: Geological Survey of Canada Memoir 222, p. 142.

Helt, K., Williams-Jones, A., Clark, J., Wing, B., and Wares, R., 2014, Constraints on the genesis of the Archean oxidized, intrusion-related Canadian-Malartic gold deposit, Quebec, Canada: Economic Geology, v. 109, p. 713–735.

Perrouty, S., Gaillard, N., Piette-Lauziere, N., Mir, R., Bardoux, M., Olivo, G.R, Linnen, R.L., Bérube, C.L., Lypaczewski, P., Guilmette, C., and Feltrin, L., 2017, Structural setting for Canadian Malartic style of gold mineralization in the Pontiac Subprovince, south of the Cadillac Larder Lake Deformation Zone, Quebec, Canada: Ore Geology Reviews, v. 84, p. 185–201.

Powell, W.G., Carmichael., D.M., and Hodgson, C.J., 1995, Conditions and timing of metamorphism in the southern Abitibi greenstone belt, Quebec: Canadian Journal of Earth Sciences, v. 32, p. 787–805.

Putnis, A., Fernandez-Diaz, L., and Prieto, M., 1992, Experimentally produced oscillatory zoning in the (Ba,Sr)SO_4 solid solution: Nature, v. 358, p. 743–745.

Reich M., Kesler, S.E., Utsunomiya S., Palenik, C.S., Chryssoulis, S.L. and Ewing R.C., 2005, Solubility of gold in arsenian pyrite: Geochimica et Cosmochimica. Acta, v. 69, p. 2781–2796.

Robert., F., 2001, Syenite-associated disseminated gold deposits in the Abitibi greenstone belt, Canada: Mineralium Deposita, v. 36, p. 503–516.

Sansfaçon, R., 1986, The Malartic district, in Hubert, C., and Robert, F., eds., Canada-Mineralogical Association of Canada-Canadian Geophysical Union Joint Annual Meeting, Field Trip 14 Guidebook, Structure and gold, Rouyn to Val d'Or, Quebec, p. 27–41.

Sansfaçon, R., and Hubert, C., 1990, The Malartic Gold District, Abitibi greenstone belt, Québec: Geological setting, structure and timing of gold emplacement Barnat, East-Malartic, Canadian Malartic and Sladen Mines, in Rive, M., and Verpaelst, P., eds., The northwestern Quebec polymetallic belt: A summary of 60 years of mining exploration: Canadian Institute of Mining and Metallurgy, Special Volume 43, p. 221–235.

Schumacher, R., Rotzler, K., and Maresch, W.V., 1998, Subtle oscillatory zoning in garnet from regional metamorphic phyllites and mica schists, Western Erzgebirge, Germany: The Canadian Mineralogist, v. 37, p. 381–402.

Wares, R. and Burzynski, J., 2012, The Canadian Malartic Mine, Southern Abitibi belt, Quebec, Canada: Discovery and Development of an Archean Bulk-Tonnage Gold Deposit, Montreal: Osisko Mining Corporation.

Willner, A.P., Pawlig, S., Massonne, H.J., and Herve, F., 2001, Metamorphic evolution of spessartine quartzites (coticules) in the high-pressure, low-temperature complex at Bahia Mansa, Coastal Cordillera of South-Central Chile: The Canadian Mineralogist, v. 39, p. 1547–1569.

Zacharias, J., Fryda, J., Paterova, B., and Mihaljevic, M., 2016, Arsenopyrite and As-bearing pyrite from the Roudny deposit, Bohemian Massif: Mineralogical Magazine, v. 68, p. 31–46.

Appendix A: Outcrop Observations

Vein Mapping observations at outcrop locations

X Coordinate	Y Coordinate	Sediment	S2 Fol^{n}	Vein Count	Vein Type	Fol^{n} Rela^{n}	Mineralogy	Oxidation	VP in vein	Extra Info
712600	5335221	Small outcrop, sediment is light grey	310°, bedding at 262°	**75 cm outcrop** (<1mm=3) (1-5mm=3) (>5mm=0)	1	cut by foliation - older	granular quartz and feldspar with bands of amphibole within. There is also an alteration halo of feldspar and amphibole along the sides	Present	Yes	good for sampling, amphiboles are randomly oriented, slightly folded starting parallel to bedding then bends slightly towards 293°. A second vein is trends approx 318°
					2	cut by foliation - older	granular quartz and feldspar. More feldspar in this vein type	Present	Yes (black oxidized mineral)	slightly folded, trending generally towards 293°

							compared to 1.			
					3	cut by foliation - older	largely granular quartz, less feldspar	Present	Yes	trending generally towards 249°
					4	cut by foliation - older	unknown compositi on, thin veinlet	Oxidize d through out	No	trending 295°, need to see thin section for mineralogy
711469	5336037	sediment is light grey/grey brown to dark gery (due to biotite and fe oxidation), disseminate d pyrite throughout, even in areas with no veins	310°	**1.5 m outcrop** (<1mm= 4) (1- 5mm=1) (>5mm= 2)	1	cut by foliation - older	quartz and feldspar	Heavily Oxidize d	Yes. Associate d with disseminat ed pyrite surroundi ng	associated with disseminated pyrite, trending 297.

					2	cut by foliation - older	quartz and feldspar	Present	Yes. Associated with disseminated pyrite surrounding	veinlets cutting into 1 so younger than 1 but older than foliation. Associated with disseminated pyrite. Trending 352
					3	cut by foliation - older	granular quartz and feldspar	Present	Yes.	Probably not associated with the disseminated pyrite in the sediment. Veinlets are cut by 1 so older than 1. trending 202.
					4	cut by foliation - older	quartz and feldspar	Not visible	No.	very large vein but hard to tell composition and oxidation as the vein appears to sit "underneath" the sediment. Need saw to

										cut through and tell.
					5	cut by foliation - older	quartz and feldspar	Not visible	No	trending parallel to 1 (297°). Hard to tell composition and oxidation as the vein appears to sit "underneath" the sediment. Need saw to cut through and tell.
					6	cut by foliation - older	granular quartz	Present	No	trending 290°, boudinaged
711134	5336121	Small outcrop visible, weathered sediment, light grey	320°	**1.5 m outcrop** (<1mm= 2) (1-5mm=2) (>5mm= 2)	1	cut by foliation - older	largely feldspar with some granular quartz	In patches with the VP	Yes	sediment doesn’t have disseminated pyrite throughout but there is some surrounding

										this vein. Slightly folded and generally trending 275°
					2	cut by foliation - older	largely granular coarse grained quartz with feldspar.	In patches with the VP	Yes	some disseminated pyrite in sediment surrounding vein. Folded and "branches out" into 2 veins. Trending 350°
					3	cut by foliation - older	largely granular coarse grained quartz with feldspar.	few small patches of oxidatio n	No	zone of alteration surrounding the vein (dark brown and eroded on each side)
					4	cut by foliation - older	unknown compositi on, thin veinlet	Oxidize d through out	No	need to see in thin section for mineralogy. Trending approx 310°

710897	5336326	patchy visibility of outcrop due to vegetation	foliation changes between 320° to 350°	**1.5m outcrop** (<1mm=0) (1-5mm=1) (>5mm=2)	1	cut by foliation - older	granular quartz with feldspar	Oxidized throughout	No	folded, trending approximately 295° with bends at 258°
					2	cut by foliation - older	composed of granular quartz with feldspar along the sides of the vein (alteration halo?)	Present	No	also cut by 1 so older than 1 too. Very folded and experienced high strain. There is disseminated pyrite in the sediment surrounding this vein. One vein with hinge axis at 250°, other trending 220° to 250°

					3	cut by foliation - older	largely recrystallized quartz and some feldspar	Oxidized through out	Yes. Pyrite not visible in the smaller branches but still oxidized throughout.	good for sampling***large vein. Trending aprx 284° but "branching off" into 238° (other fractures along this plane so maybe vein was opened along this direction?
710756	5336535	small outcrop with few visible patches due to vegetation	foliation still ranges (from 309° to 350°)	**75cm outcrop** (<1mm=2) (1-5mm=2) (>5mm=0)	1	cut by foliation - older	granular quartz and some feldspar	No	No	
					2	cut by foliation - older	granular quartz with feldspar	Present	Yes. Disseminated pyrite also found in sediment surrounding vein	good sample*** very small and short. trending parallel to 1 but branches off into more

										veins towards 226°
710645	5336703	sediment is light grey/grey brown to dark grey (due to biotite and fe oxidation), beds are folded into a wavy pattern. Small outcrop with many veins with **disseminated pyrite** throughout with denser concentrations at approximat	308°	75 cm outcrop (<1mm=10) (1-5mm=1) (>5mm=0)	1	cut by foliation - older	unknown composition, thin veinlet	Heavily Oxidized	No	running almost perpendicular to foliation. Trending 225°. Most abundant vein type in outcrop. Should have pyrite due to disseminated pyrite surrounding it.

		ely the Northern and Southern end and doesn’t appear to correlate with a particular vein.								
					2	cut by foliation - older	quartz and feldspar	Heavily Oxidized	No	trending oblique to foliation 247°. Larger and denser pyrite in sediment around this vein (maybe linked together), harder to tell without looking in larger scale.

					3	cuts foliation - younger than foliation	granular quartz	No	No	parallel to bedding, trending 346°
					4	cut by foliation - older	thin veinlet, unknown compositi on	Heavily Oxidize d	No	densely oxidized in the sediment surrounding this vein. May contain pyrite du eot the associated disseminated pyrite. Trending 337°
					5	cut by foliation - older	unknown compositi on, thin veinlet	Heavily Oxidize d	No	may be linked to the surrounding disseminated pyrite in the sediment. Trending 307°

710645	5336703	outcrop is more continuous here than previous outcrop. Sediment is the same with disseminated pyrite in the sediment	303°	**1.5m outcrop** (<1mm=2) (1-5mm=3) (>5mm=1)	1	cut by foliation - older	granular quartz	patchy oxidation	Yes	Holes in vein from pyrite?, trending 242°. Large disseminated pyrite within the sediment.
					2	cut by foliation - older	granular quartz and feldspar	Present	Yes	thin veinlets, not as muct ruse throughout but have many oxidized sulphide grains. Disseminated pryite exist in the surrounding sediment as well.

					3	cuts foliation - younger than foliation	granular quartz	No	No	trending 296°, thin veinlets
					4	cut by foliation - older	quartz and feldspar	Present	Yes	parallel to foliation.
					5	cuts foliation - younger than foliation	quartz and feldspar	No	No	
710527	5336865	sediment is light grey, large outcrop. **Disseminated pyrite throughout**	310°	**1.5m outcrop** (<1mm=8) (1-5mm=5) (>5mm=1)	1	cuts foliation - younger than foliation	granular quartz	No	No	trending 325°
					2	cut by foliation - older	granular quartz and feldspar	Present	Yes	Holes in vein from pyrite?, parallel to 1. slightly folded
					3	cut by foliation - older	granular quartz	Present	Yes. LOTS.	trending 250°, pretty straight

					4	younger	quartz	No	No	trending 286°
710085	5337376	sediment is light grey and brown (due to fe oxidation) beds with some alternating between dark beds (inc biotite) are folded with hinge axis trending parallel to foliation. Disseminated pyrite found within sediment. Approximately 100 m from here is an outcrop where the pyrite crystals are growing	303°	**1.5m outcrop** (<1mm=0) (1-5mm=3) (>5mm=4)	1	cut by foliation - older. Cut by fractures along foliation.	granular quartz and feldspar	Present	Yes	most abundant. Trending 240°. Then refracts towards 226°. Some pyrite grains as large as 5mm.

		parallel to the foliation (elongated towards direction of foliation)								
					2	cut by foliation - older	quartz and feldspar	patchy oxidation	No, but there is disseminated pyrite in surrounding sediment	fewer disseminated pyrite in sediment compared to other veins. Trending parallel to 1.

					3	difficult to tell relationship with foliation	very white recrystallized quartz	little oxidation	No	parallel to 1 and 2
					4	cuts foliation - younger than foliation	granular quartz	No	No	parallel to foliation.
709671	5337739	sediment is light grey, large abundance of veins due to presence of late generation vein assemblage. Some disseminated pyrite present	range from 320°-340°	**75 cm outcrop** (<1mm=1) (1-5mm=0) (>5mm=1)	1	cut by foliation - older, folded along foliation.	recrystallized quartz and feldspar	Present	Yes. Disseminated pyrite also found in sediment surrounding vein	trending 332°, parallel to foliation (maybe same age?)
					2	difficult to tell relationship with foliation	quartz and feldspar. Appears to sit "underneat	No	No	parallel to 1

							h". Checked with chisel.			
					3	cut by foliation - older	granular quartz	Slightly oxidized	Yes	perpendicular to foliation. Trending 265°
					4	cut by foliation - older	unknown compositi on, thin veinlet, surroundin g part of vein sitting "underneat h"	Oxidize d through out	No	trending 219°
					5	cut by foliation - older	quartz and feldspar	super oxidized through out	Lots of VP	trending 243°
					6	cut by foliation - older	quartz and some feldspar. Seems to sit "underneat h"	Present	Lots of VP	trending 310°, folded slightly.

709157	5337863	sediment is light grey, late generation veins are present. Disseminated pyrite is present	313°	**150 cm outcrop** (<1mm=2) (1-5mm=2) (>5mm=3)	1	cut by foliation - older	granular quartz	Heavily Oxidized	Lots of VP, and disseminated pyrite in surrounding sediment	trending 298°, thin veinlet
					2	cut by foliation - older	too small to tell mineralogy	Heavily Oxidized	No, but there is disseminated pyrite in surrounding sediment	parallel to 1. thin veinlets, need thin section to tell
					3	cut by foliation - older	granular quartz in the center with feldspar along the sides	Present	Yes. Disseminated pyrite also found in sediment surrounding vein	trending 290°, boudinaged.
					4	cut by foliation - older	recrystallized quartz with little feldspar along the sides	Heavily Oxidized	1 or 2 VP grains	boudinaged, trending 303°

					5	cut by foliation - older	largely feldspar, some quartz	Present	Yes	very weathered vein, filled with holes (from pyrite?). Veins have thin veinlets "branching out" parallel to main vein. Trending 295°
					6	cut by foliation - older	quartz and feldspar	Heavily Oxidized	Yes	appears to "sit underneath the sediment", thin veinlet. Trending 280°
708613	5337700	light grey sediment, abundant late generation veins present	301°	**150 cm outcrop** (<1mm=4) (1-5mm=2) (>5mm=1)	1	cut by foliation - older	granular quartz, vitreous and coarse. Some feldspar	Present	No	thick vein, boudinaged slightly, trending 335°
					2	cut by foliation - older	granular quartz with feldspar at the edges	Heavily Oxidized	No	trending 300°

					3	cut by foliation - older	unknown compositi on, thin veinlet	Heavily Oxidize d	No	folded, hinge axis at 270°
708239	5337450	sediment is light grey, late generation veins are present	304°	**150 cm outcrop** (<1mm= 0) (1- 5mm=2) (>5mm= 1)	1	cut by foliation - older (maybe same age since it is also parallel to foliation ?)	granular quartz with some feldspar	Heavily Oxidize d	No	boudinaged parallel to foliation
					2	cut by foliation - older	largely feldspar, some quartz	patchy oxidatio n	No	less competent than 1. "branches out" into multiple parallel veins, many holes where pyrite could have been, trending 320°
					3	cut by foliation - older	granular quartz	Heavily Oxidize d	No	trending 315°

					4	cut by foliation - older	feldspar, amphiboles of random orientation within	some patches of oxidation	No	thick veins, folded with cross cutting late generation veins.. Trending 330°
					5	cut by foliation - older	granular quartz, alteration halo of feldspar around it,	Heavily Oxidized	No	oblique to previous veins,
					6	cut by foliation - older	unknown composition, thin veinlet	Heavily Oxidized	No, but there is disseminated pyrite in surrounding sediment	cuts into 5 so younger than 5. but still older than foliation. Surrounding the thin vein is a raised area making it seem like the rest of the vein sits "underneath"
					7	cut by foliation - older	granular quartz with thick feldspar	oxidized along the edges mostly	No	"branches out" slightly and boudinaged, trending 302°

							band on each side			
708074	5336923	sediment is light grey, patches of brown due to Fe oxidation.	316°	**75 cm outcrop** (<1mm=0) (1-5mm=0) (>5mm=1)	1	cut by foliation - older	largely feldspar, some quartz, with amphiboles of random orientation within the vein	No	No	thick vein, very folded, parallel to foliation
					2	cut by foliation - older	granular quartz and feldspar	Present	No	thin veins, parallel to foliation
					3	cut by foliation - older	recrystallized quartz with little feldspar and biotite within	patchy oxidation	Yes	folded, cuts into 1 so younger than 1 but older than foliation

707555	5337015	outcrop we went to with Bob saw folded veins with alteration halo with amphiboles	S2 foliati on is 315°, 2nd foliati on is 340° (can't tell which one came first)	**150 cm outcrop** (<1mm= 1) (1- 5mm=1) (>5mm= 2)	1	cut by foliation - older	granular quartz and feldspar with alteration halo of feldspar and amphibole (randomly oriented) along the sides	Oxidize d through out	No	folded with hinge axis parallel to second foliation
					2	cut by foliation - older	granular quartz and some feldspar	patchy oxidatio n	Yes	folded, trending 334°, thin

Appendix B: Sample Information

B1. Outcrop scale observations of the 25 samples collected. Available photos are provided.

Sample ID	Sample ID-Shortened	X	Y	Hand Sample	Location	Comments	Orientation
K388152	152	714730.1	5334147.8		Pit	In greywacke, 2 setting: vein A(py) // S2, subtle boudinage, syn D2, vein B cut vein A and S2, late D2, A:0.1-0.5 cm, B:0.2-1 cm, halo of disseminated pyrites	N/A

K388157	157	714519.3	5334250.1	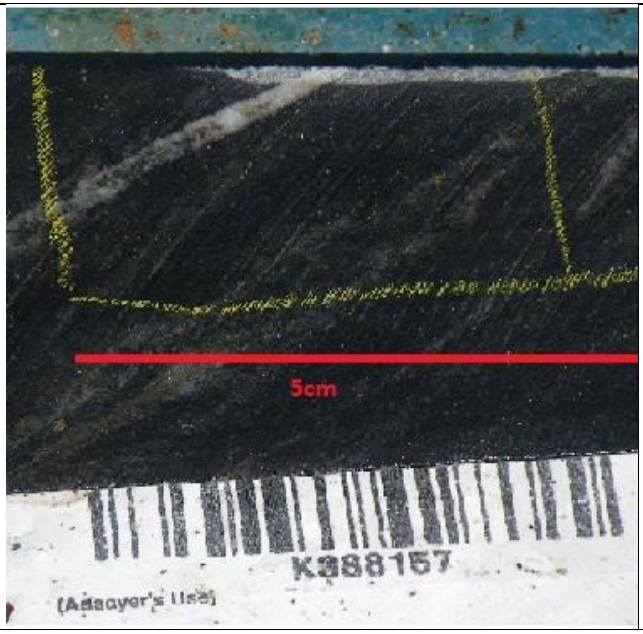	Pit	In greywacke, vein(py), subtle boudinage, syn D2, 0.1-0.5 cm, halo of disseminated pyrites	N/A

K389488	488	714969.8	5334523.6	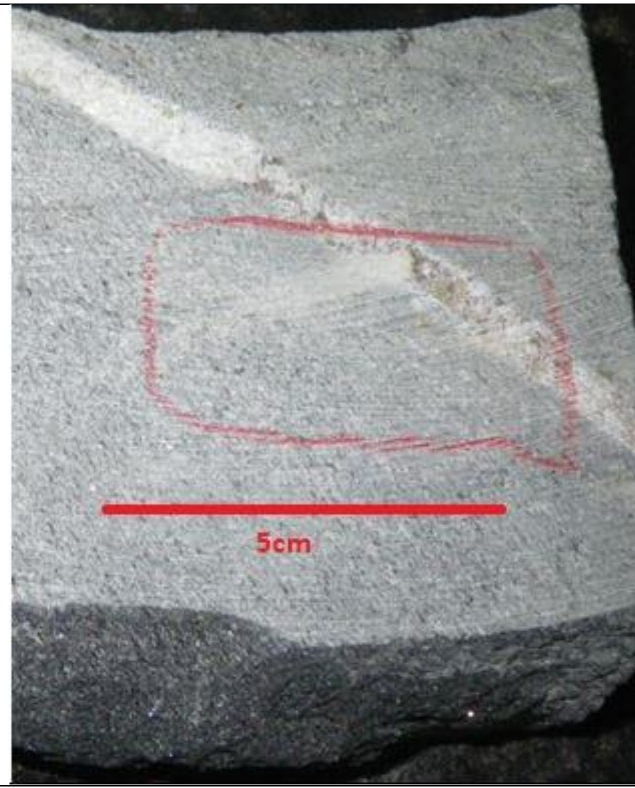	Pit	In greywacke, vein(py) // S2, subtle boudinage, syn D2, 0.1-1 cm, halo of disseminated py	185/75

K389490	490	715010.2	5334590.8	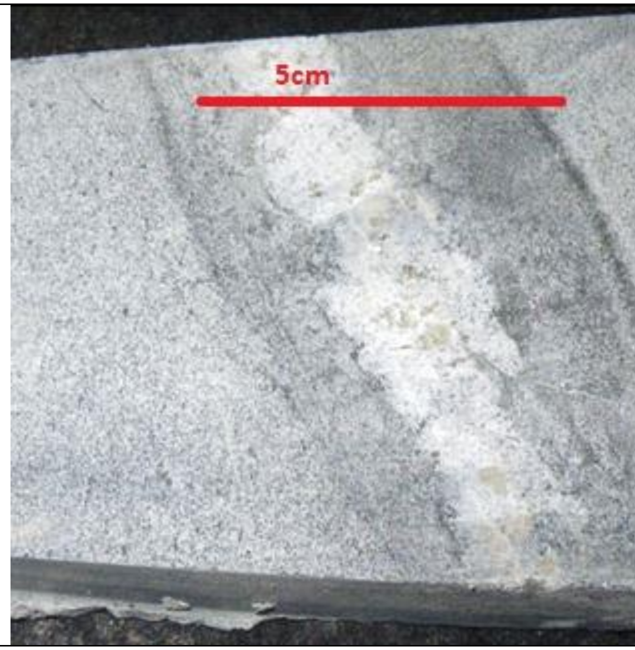	Pit	In greywacke, en echelon veins(py), syn D2, 1-2 cm, 2 cm biotite-rich halo	125/90
S-3415A	3415A	714127	5334590		Pit	In greywacke, vein(py) // S2, 0.1-2 cm, 2-3 cm alteration halo with disseminated pyrites	N/A

K389487	487	714970	5334504	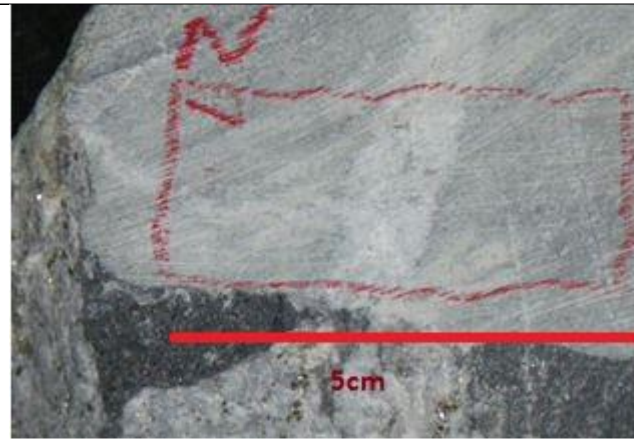	Pit	*In greywacke, vein(py) cutted by S2, 0.5-2 cm, subtle boudinage, early to syn D2, halo of disseminated py*	010/90
K388153	153	713549.8	5332747.4	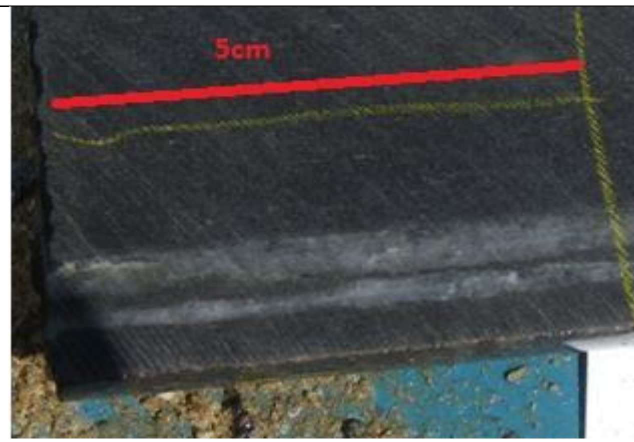	Transect NE-SW	In greywacke, S2 // vein(py), chlorite selvage, subtle boudinage, syn D2, 0.2-1 cm, halo of disseminated pyrites	Subvertical

K388154	154	713314.6	5333982.7	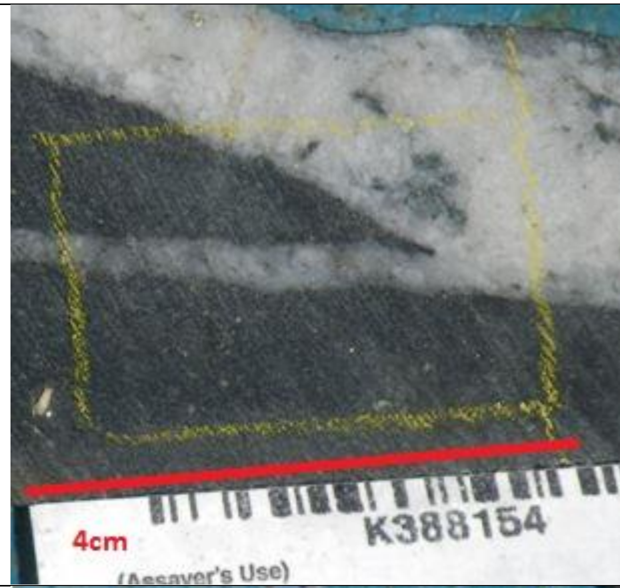	Transect NE-SW	In greywacke, vein(py) or POR, subtle boudinage, syn D2, 0.2-10 cm, halo of disseminated pyrites	N/A
K388159	159	713052.1	5331994.1	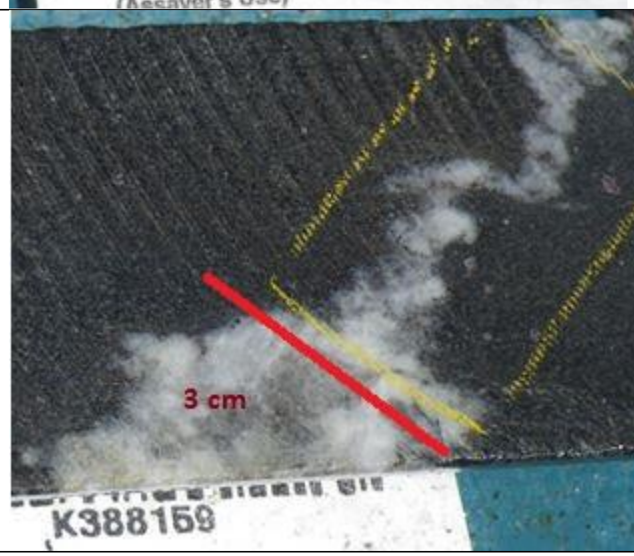	Transect NE-SW	*In garnet-bearing greywacke, vein(py) cutted by S2 and folded, early D2, 0.2-5 cm*	N/A

K388162	162	713314.6	5333982.7		Transect NE-SW	In greywacke, 2 setting: veinA(py) cutted by S2, subtle boudinage, syn D2, vein B // S2 cut vein A, late D2, A:0.5-2 cm, B:0.1-0.2 cm, halo of disseminated pyrites	N/A

K388164B	164B	712890.8	5331500.2		Transect NE-SW	*In garnet-bearing greywacke, vein(py) cutted by S2 and folded (isoclinnal), early D2, 0.2-1 cm*	Subvertical
K389886B	886B	712930	5332760	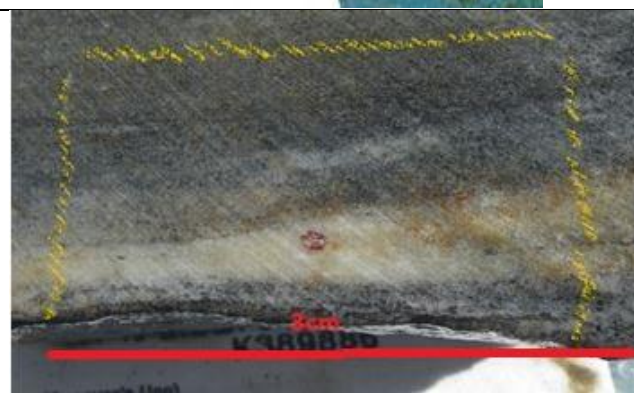	Transect NE-SW	In greywacke, vein(py), subtle boudinage, syn D2, 0.5-2 cm, halo of disseminated pyrites	125/90

K389888B	888B	712024	5331764	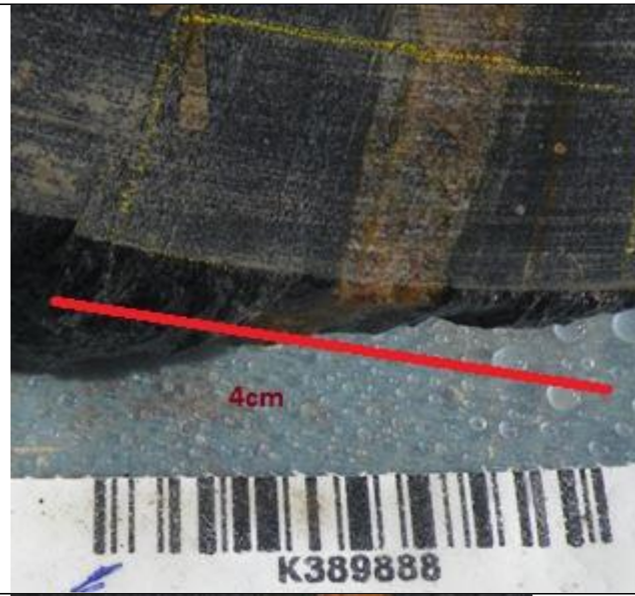	Transect NE-SW	In garnet-bearing greywacke, vein(py) cutted by S2, boudinage, syn D2, 0.5-1 cm	355/60
K388168A	168A	712350	5334770		Transect NW-SE	In greywacke, vein(py), boudinage, syn D2, 0.5-3 cm, halo of disseminated pyrites	130/90

K38817 1B	171B	711510	533604 3	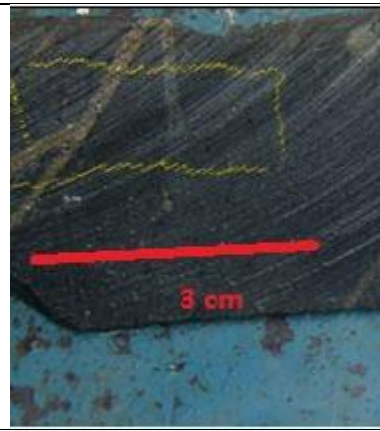	Transect NW-SE	In greywack e, vein(py), subtle boudinage , syn D2, 0.5-1 cm, halo of dissemina ted pyrites	160/90
K38817 3	173	712611	533522 2		Transect NW-SE	In greywack e, vein(py) // S2, subtle boudinage , syn D2, 0.5-1 cm, halo of dissemina ted pyrites	115/90
K38976 1	NB061 B	710780 .3	533669 5.6		Transect NW-SE	*In greywack e, conjugate veins(py) cutted by S2 and folded,*	140/90 180/90

						boudinage, early D2, 0.1-0.5 cm, pyrite with syn-D2 pressure shadows, halo of disseminated pyrites	
K389764	NB064	710752.5	5336651.1		Transect NW-SE	*In greywacke, "milky-white" vein(py), subtle boudinage, folded, early to syn D2, 0.5-200 cm, pyrrhotite in biotite-rich layers in greywackes*	N/A

K389768	NB068	710775.1	5336644.2		Transect NW-SE	In greywacke, 2 setting: vein A(py) cutted by S2, subtle boudinage, syn D2, vein B cut vein A and S2, late D2, A:0.1-0.5 cm, B:0.2-1 cm	A: 065/90 B: 130/25
K389835	NB036	710819.6	5336670.3		Transect NW-SE	In greywacke, vein(py), pyrite selvage, boudinage, syn D2, 0.5-1 cm, halo of disseminated pyrites	N/A

K389895B	895B	708294	5338132	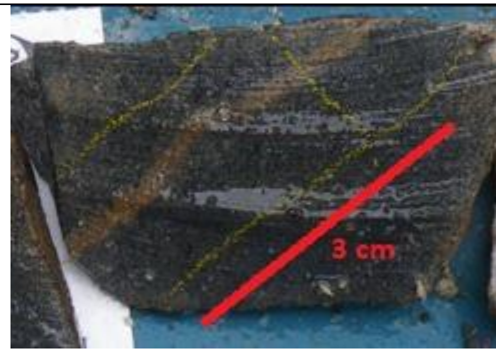	Transect NW-SE	In greywacke, vein(py) cutted by S2, subtle boudinage, syn D2, 0.2-1 cm, halo of disseminated pyrites	160/50
K389897A	897A	708958	5337858	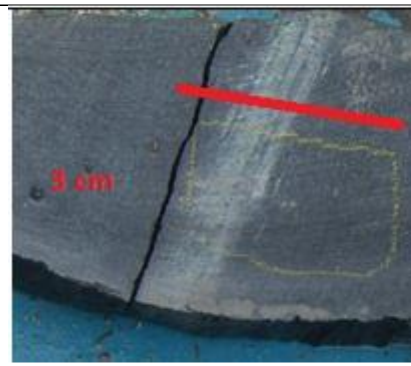	Transect NW-SE	In greywacke, vein(py) // S2, subtle boudinage, syn D2, 1-2 cm, chlorite, halo of disseminated pyrites	120/90

K389898A	898A	709668	5337738			Transect NW-SE	In greywacke, vein(py) // S2, syn D2, 0.1-0.2 cm, halo of disseminated pyrites	175/90
K389899A	899A	710077	5337361	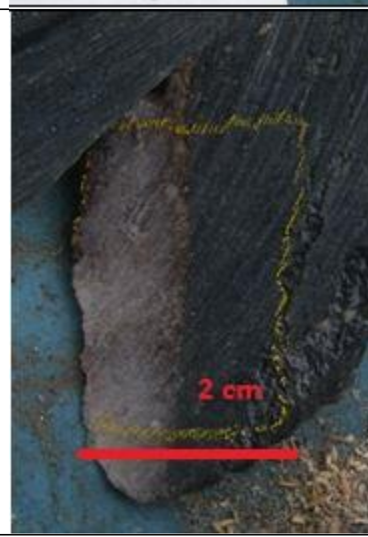		Transect NW-SE	In greywacke, vein(py) // S2, subtle boudinage, syn D2, 1-2 cm, halo of disseminated pyrites	120/90

K389900	900	710538	5336858	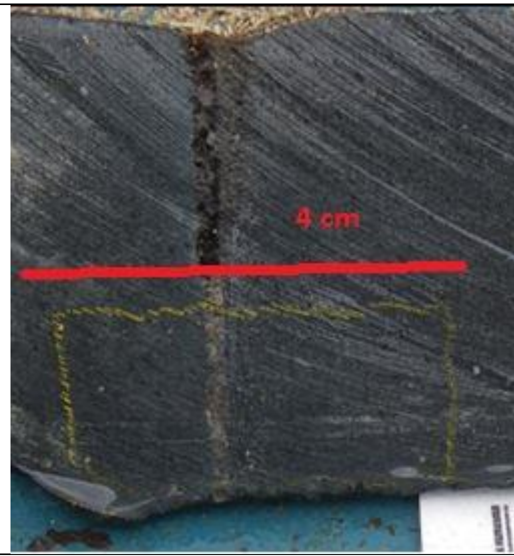	Transect NW-SE	In greywacke, vein(py) // S2, subtle boudinage, syn D2, 0.5-1 cm, halo of disseminated pyrites	125/90

B2. Thin section photos of the 25 samples collected. Grains chosen for EPMA and/or LA ICP-MS analyses are circled

Sample ID	Thin Section Photo
152	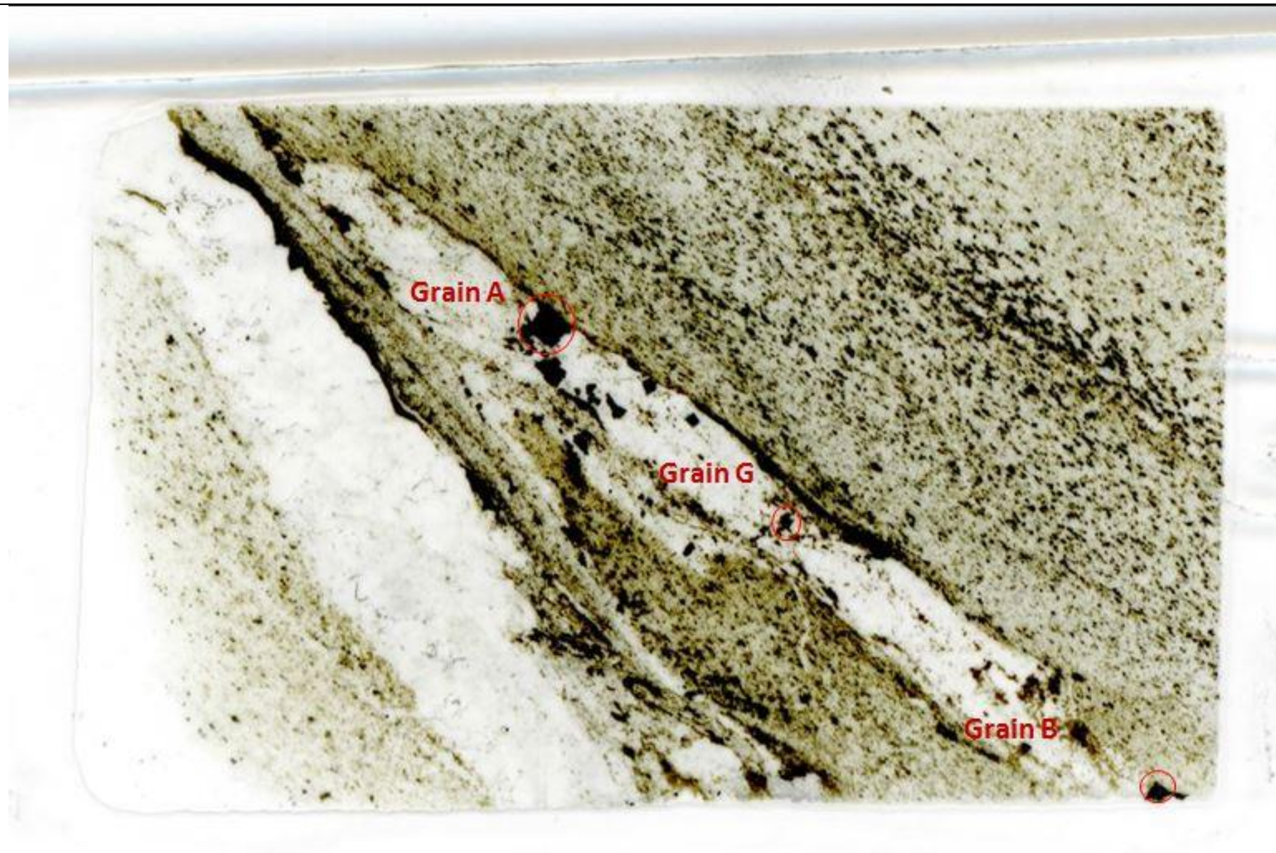

157	

488	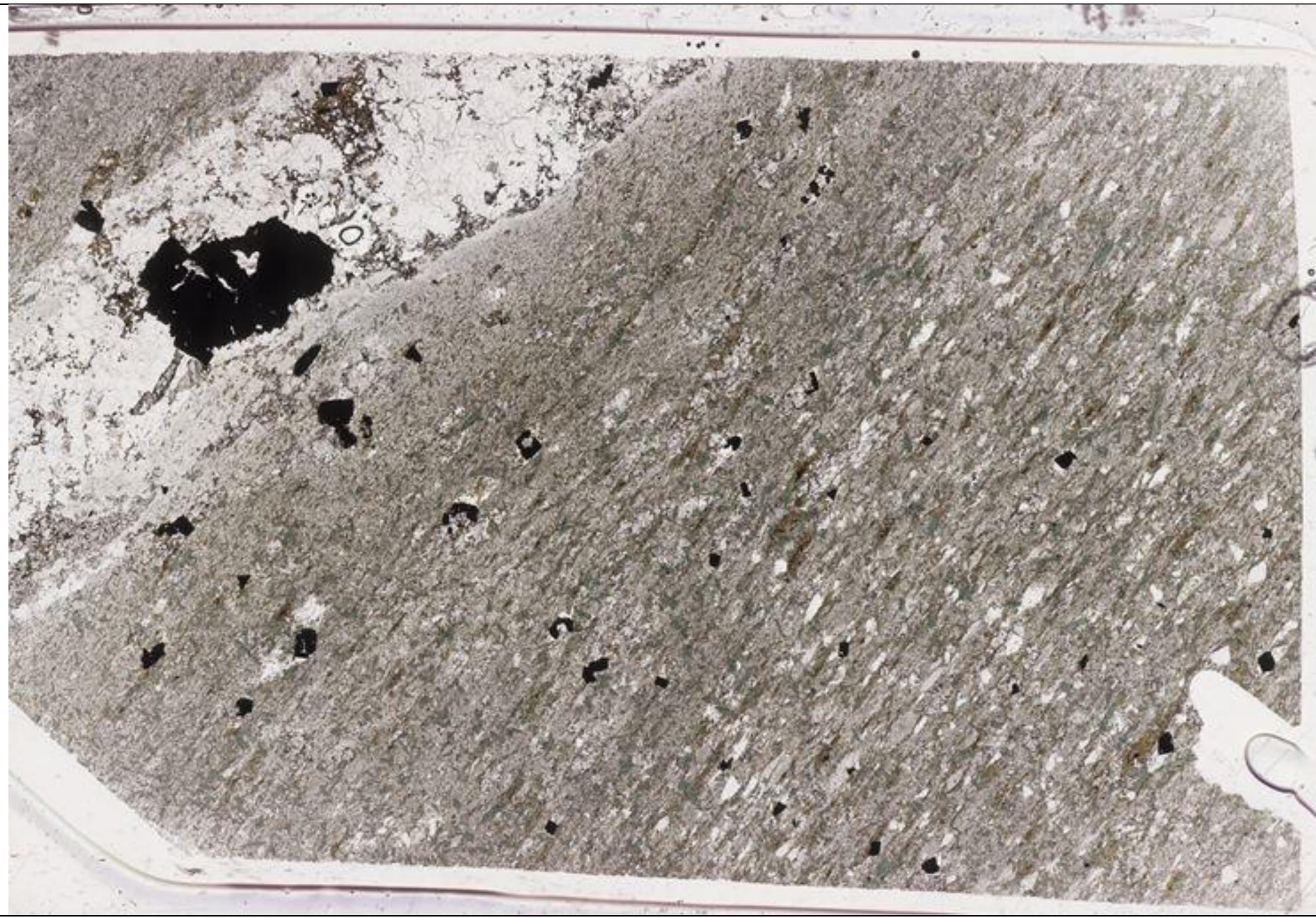

490	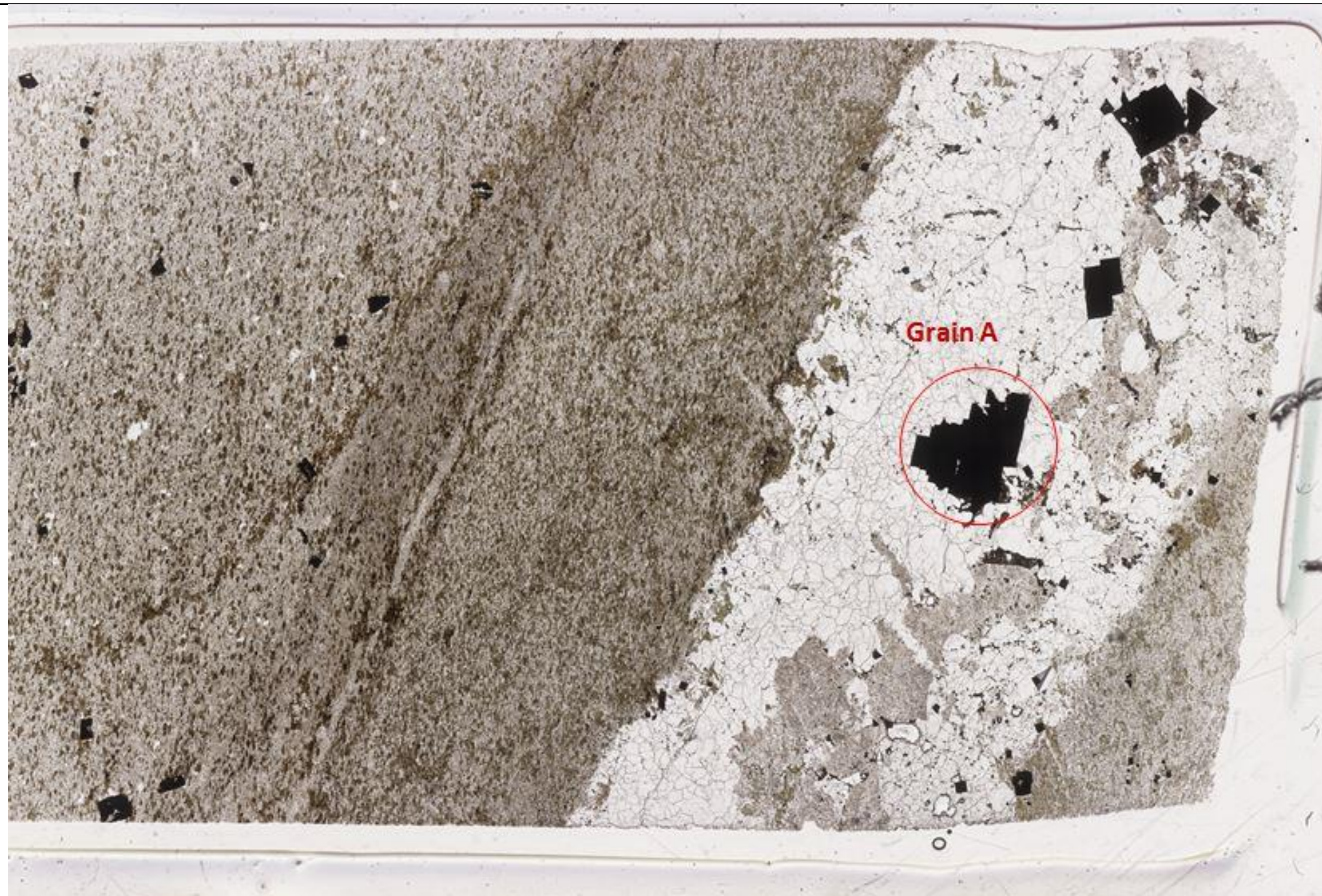

3415A	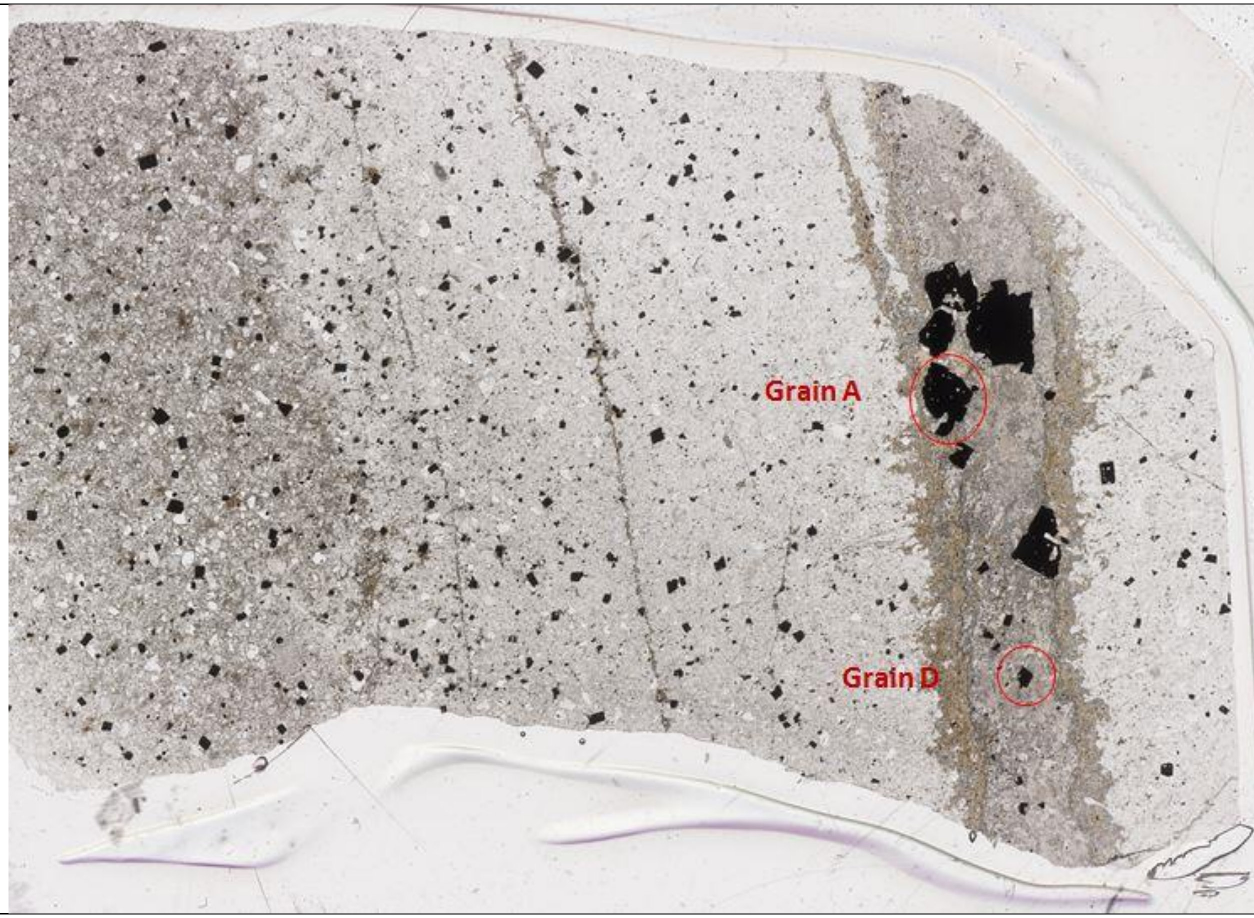

487	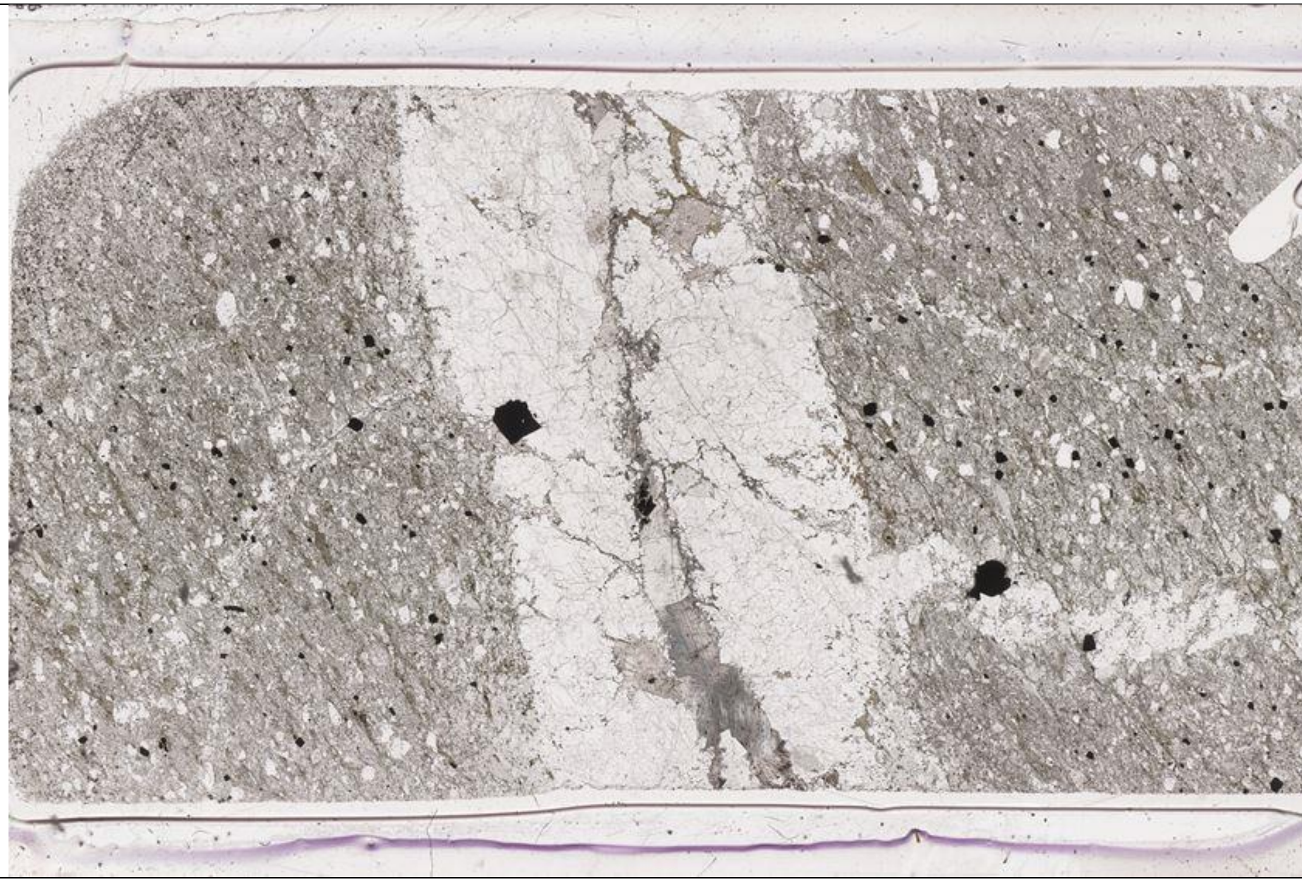

153	

154	

159	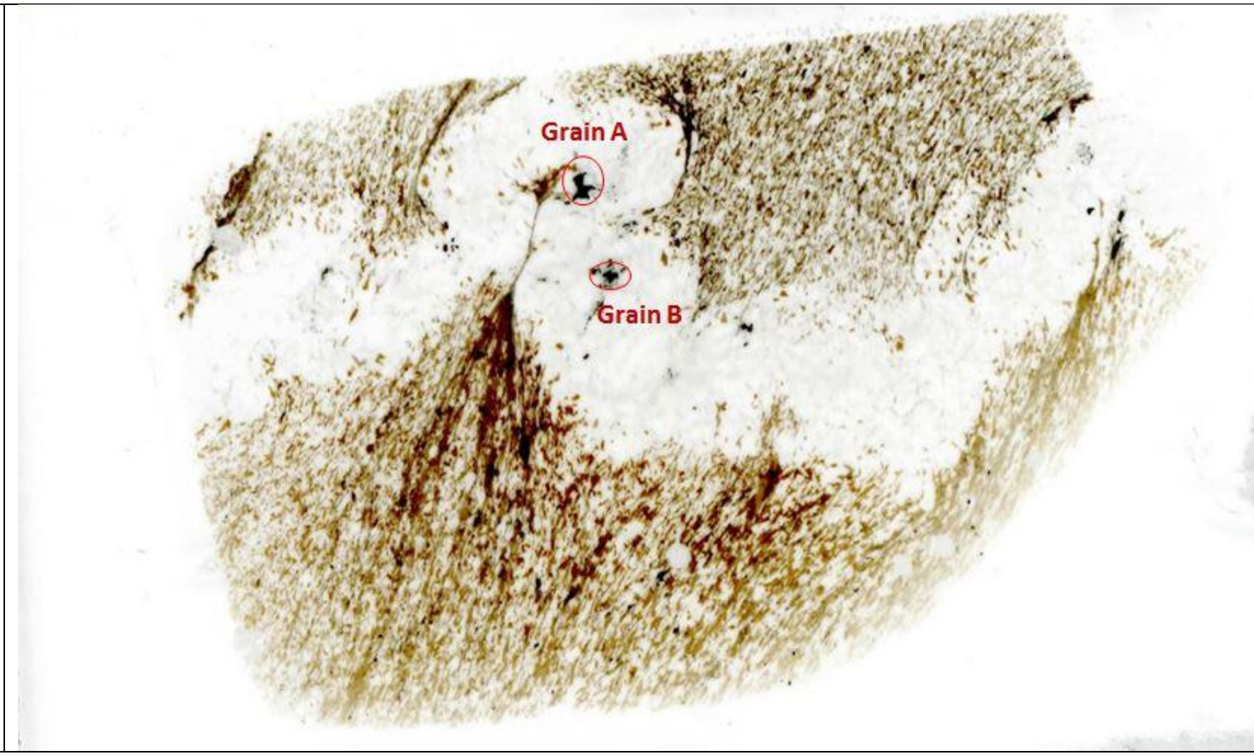

162	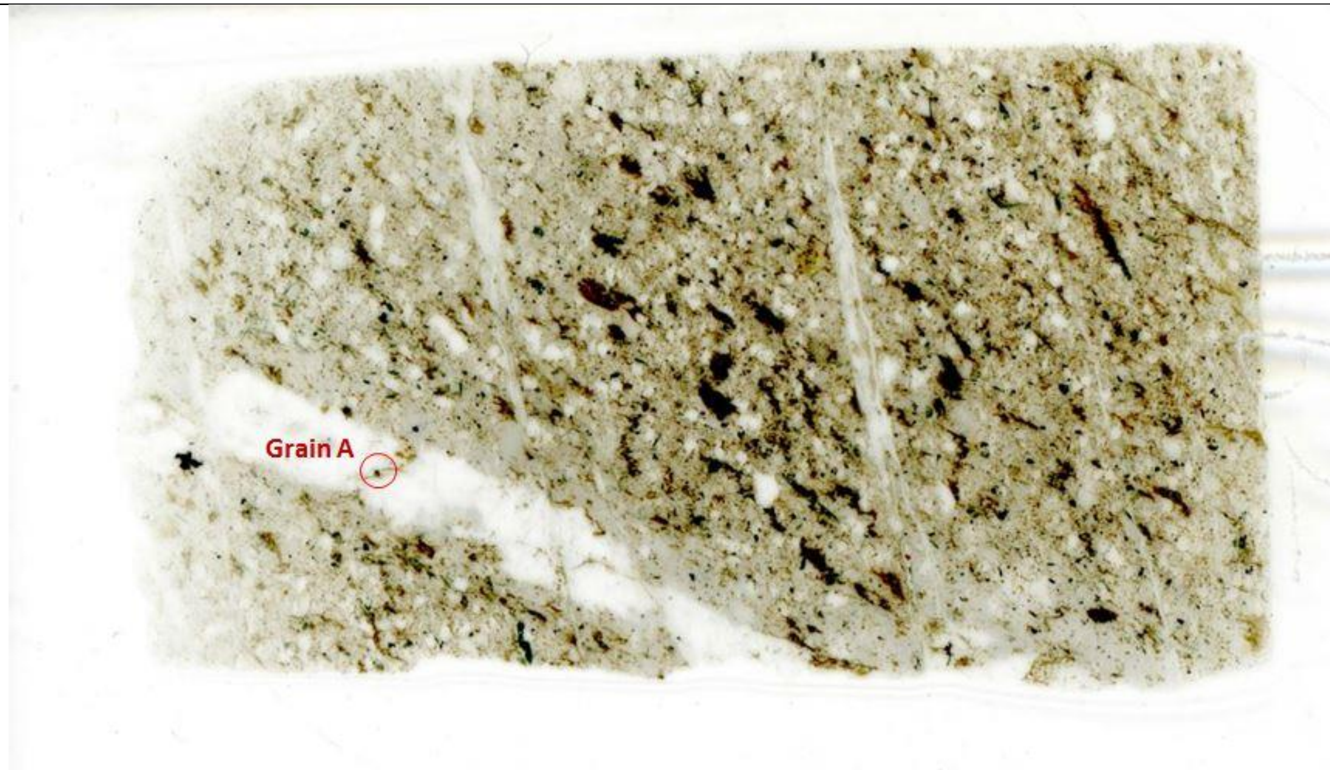

164B	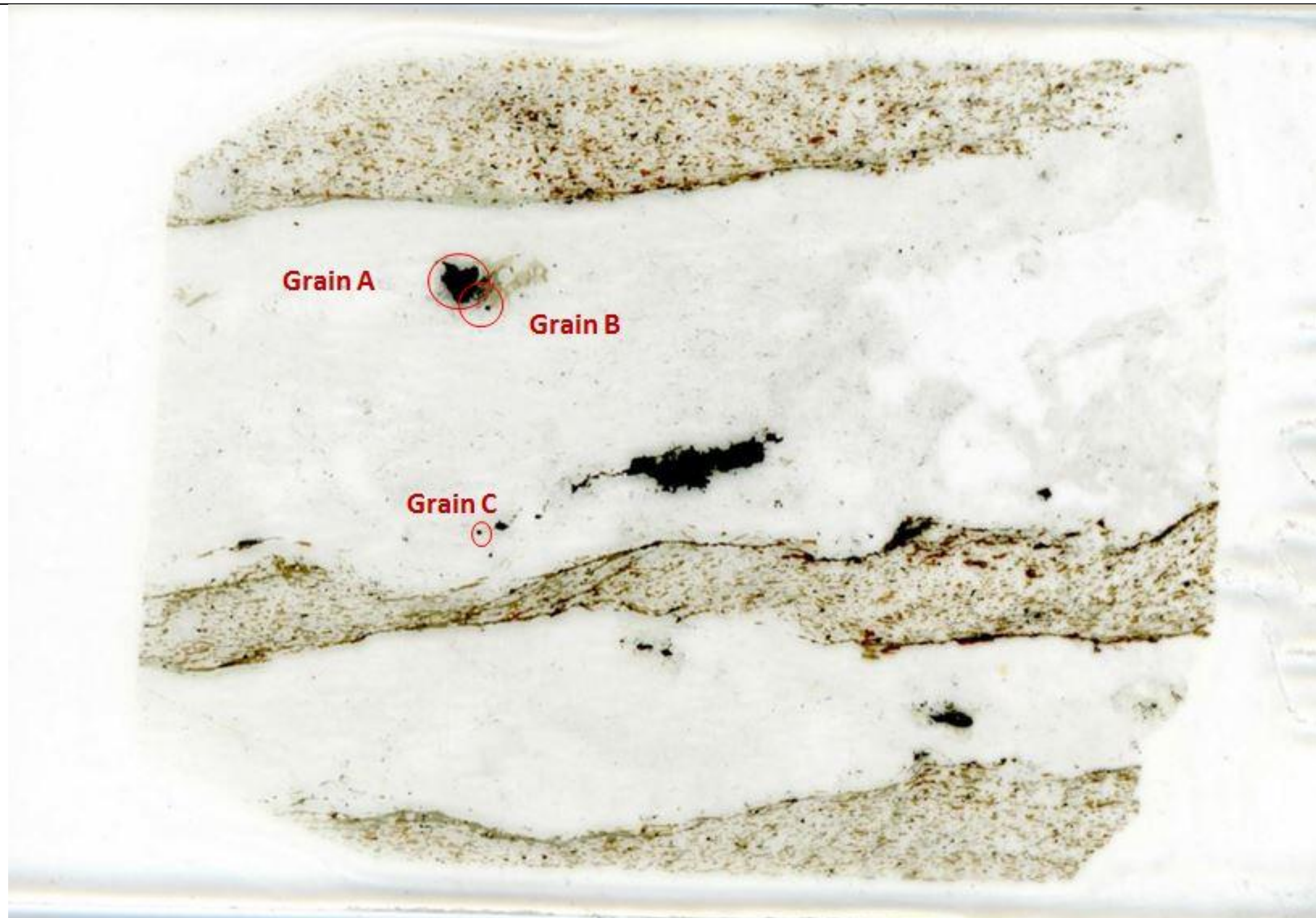

886B	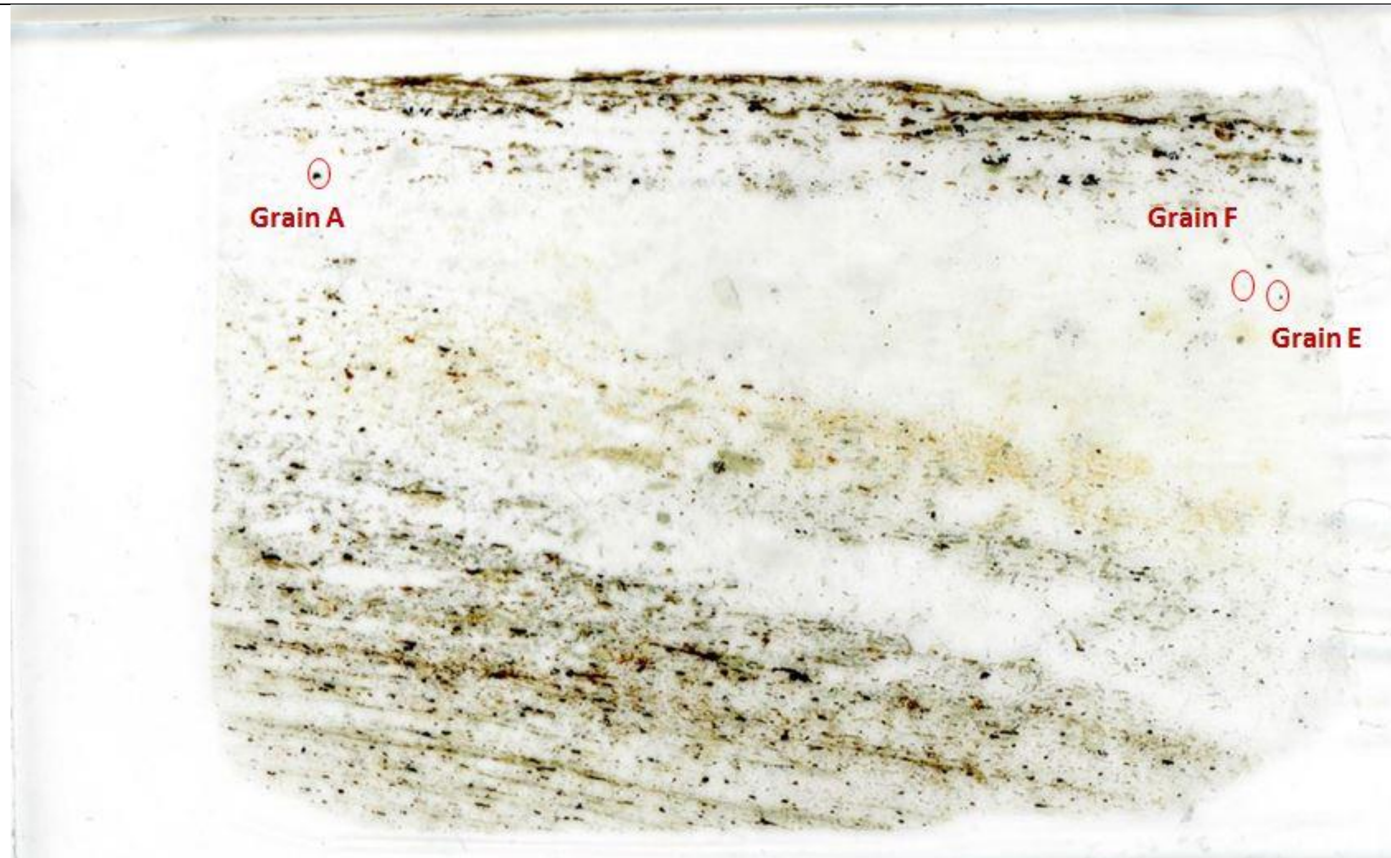

888B	

168A	

171B	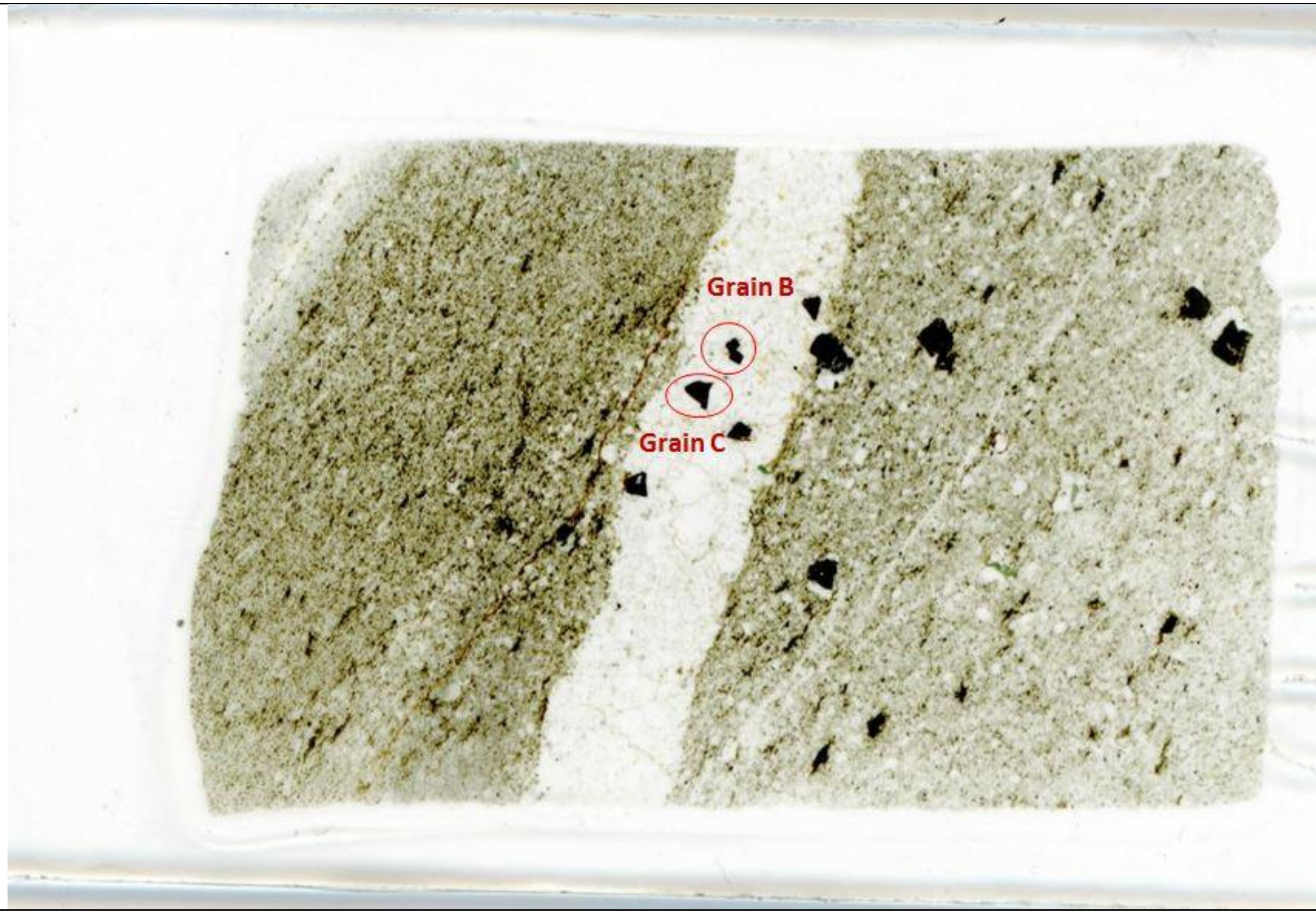

173	

NB061B	

NB064	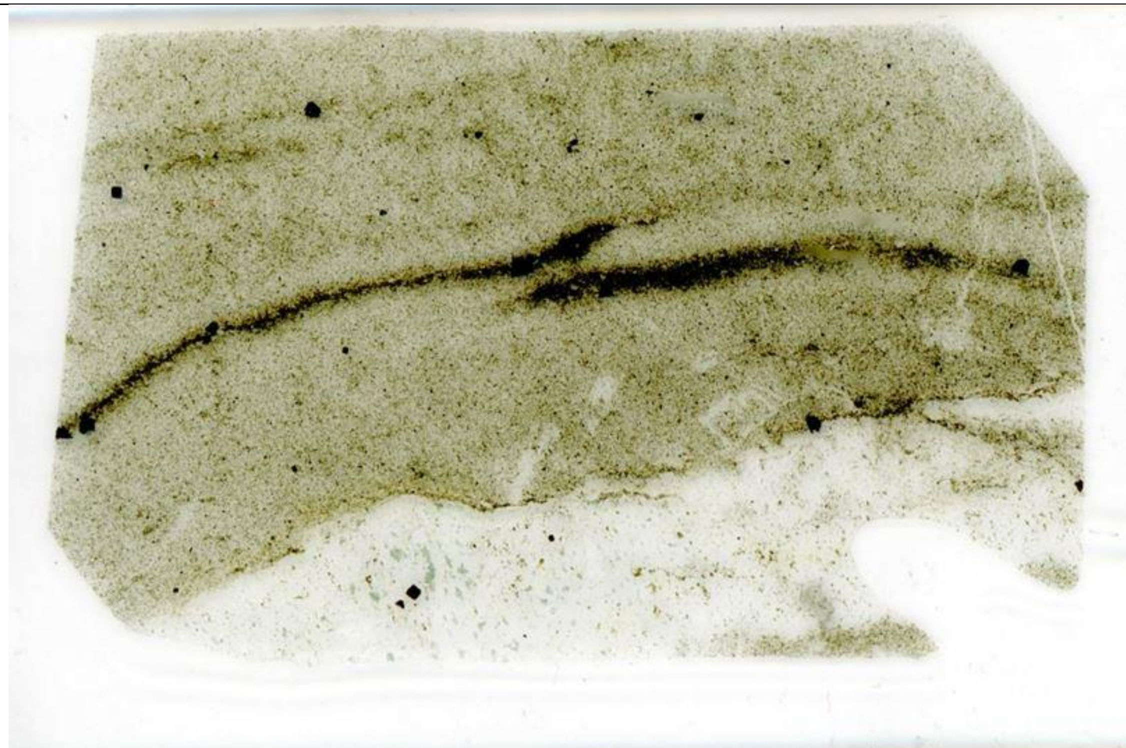

NB068	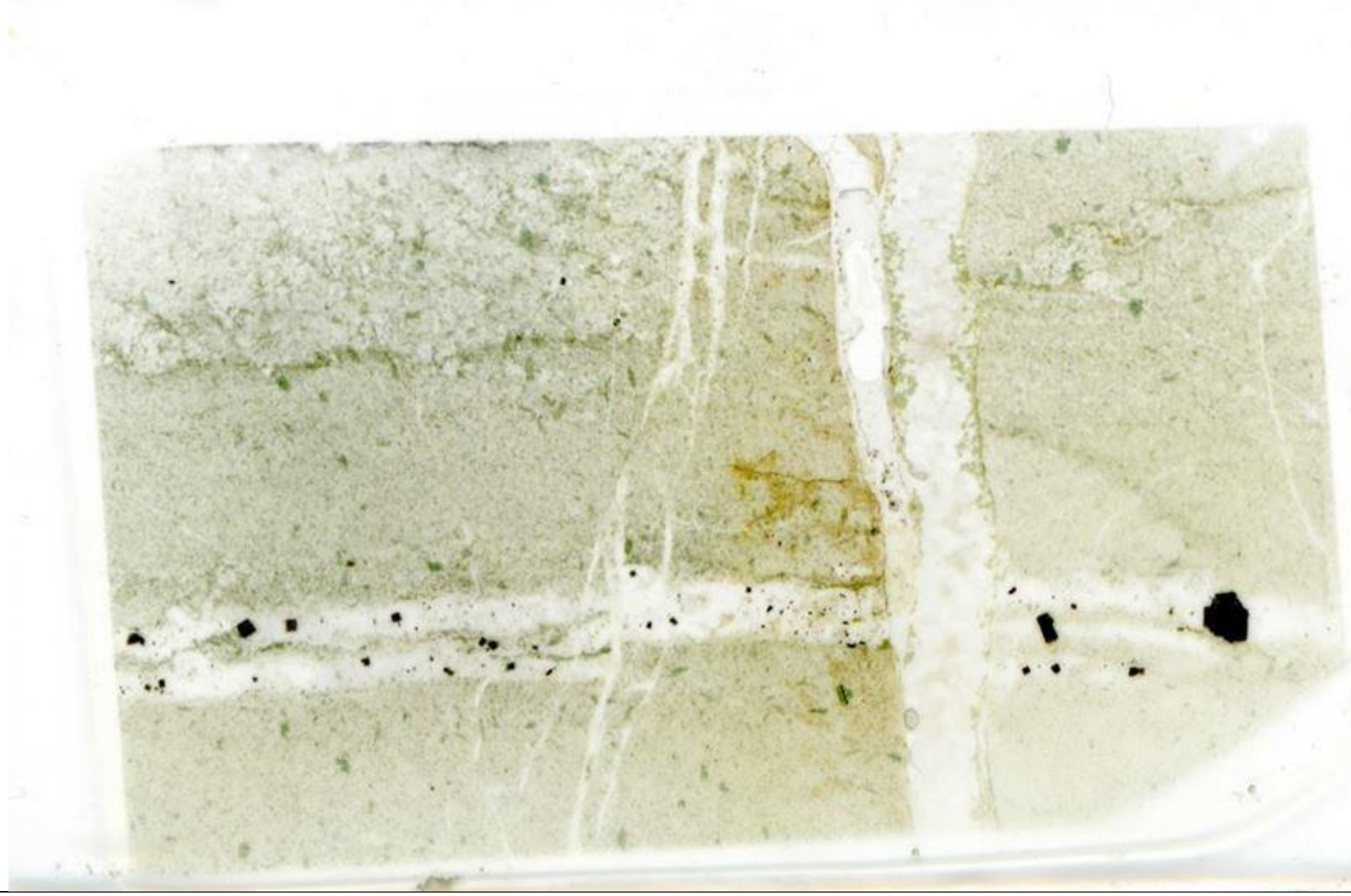

NB036	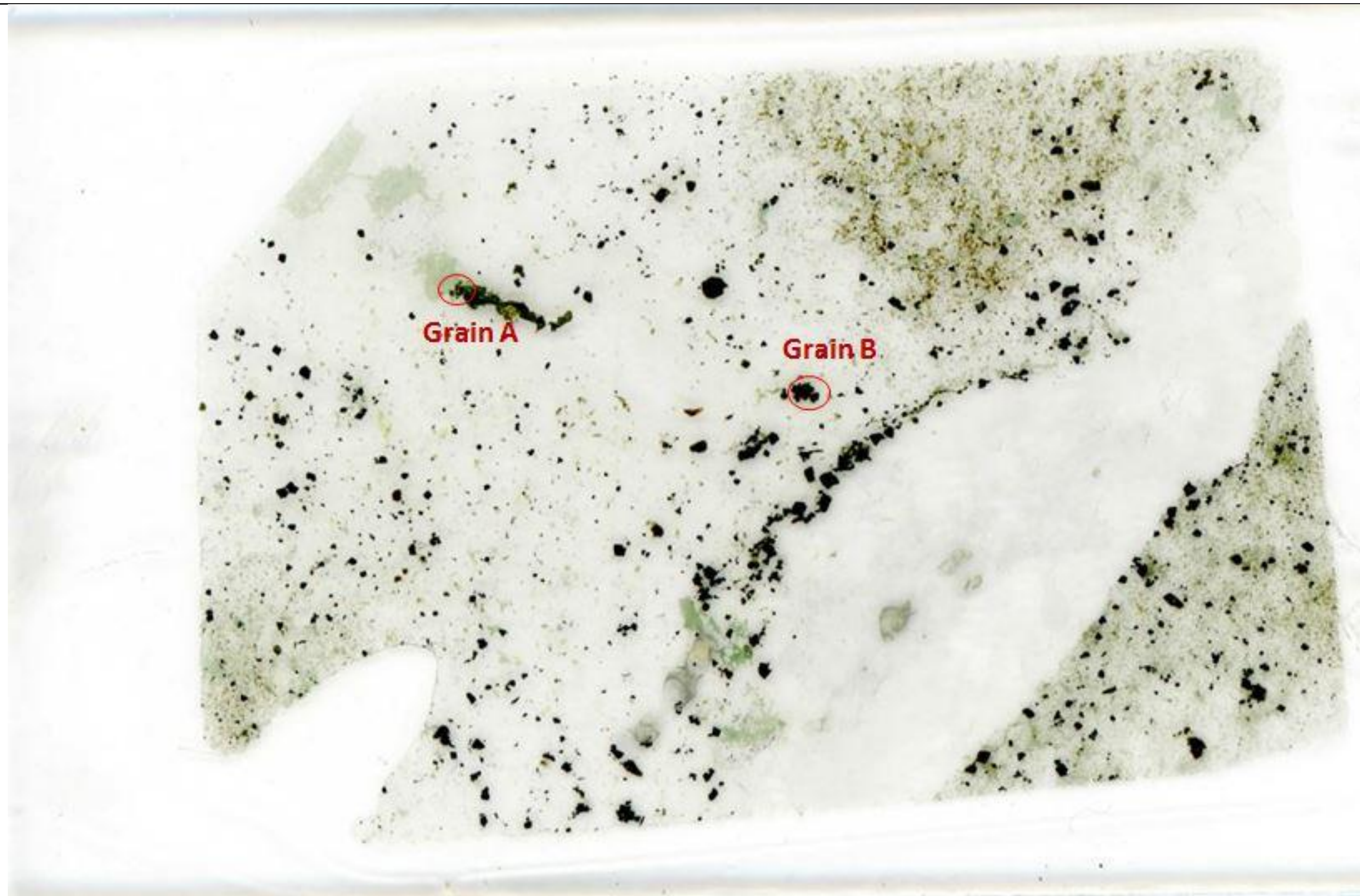

895B	

897A	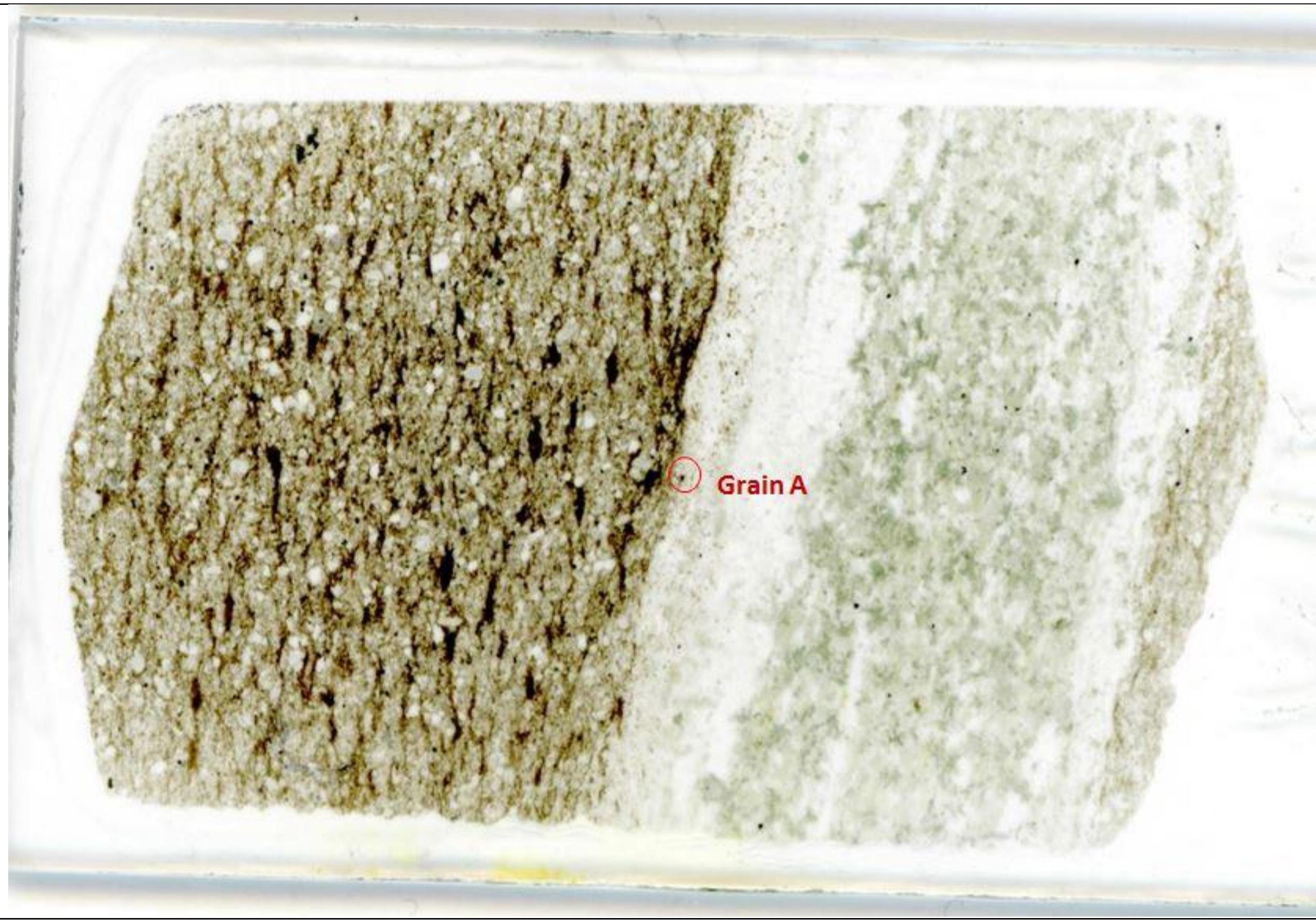

898A	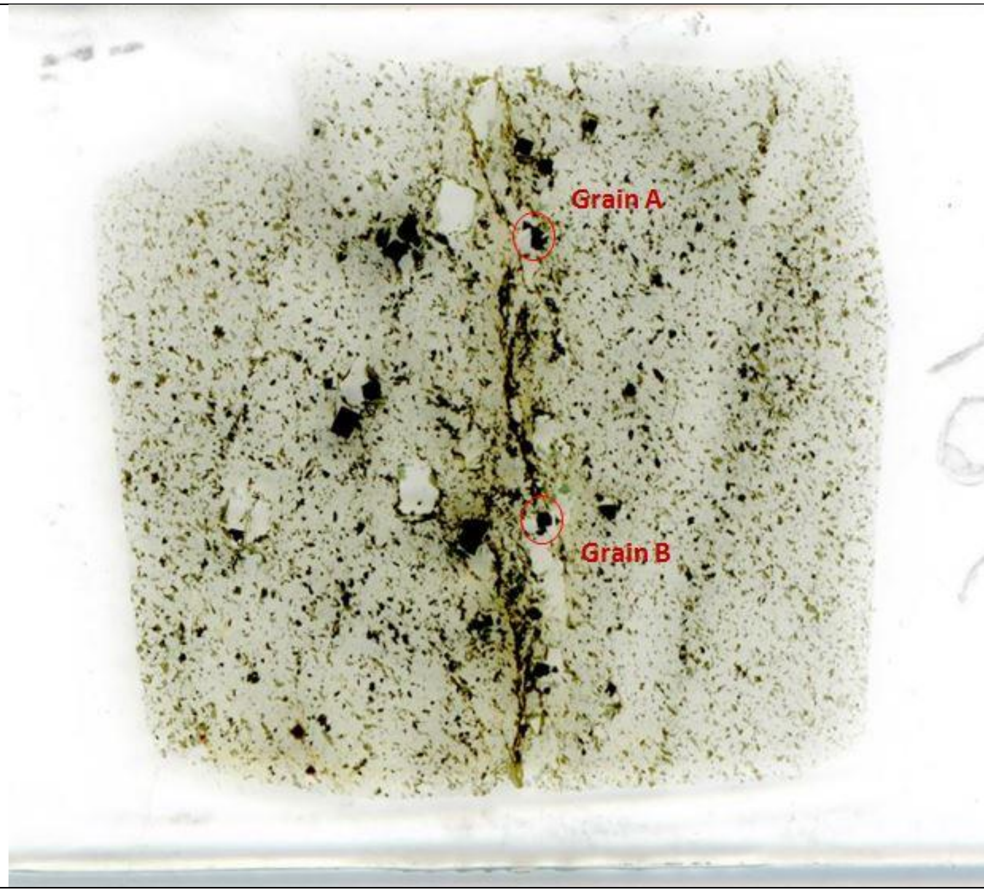

899A	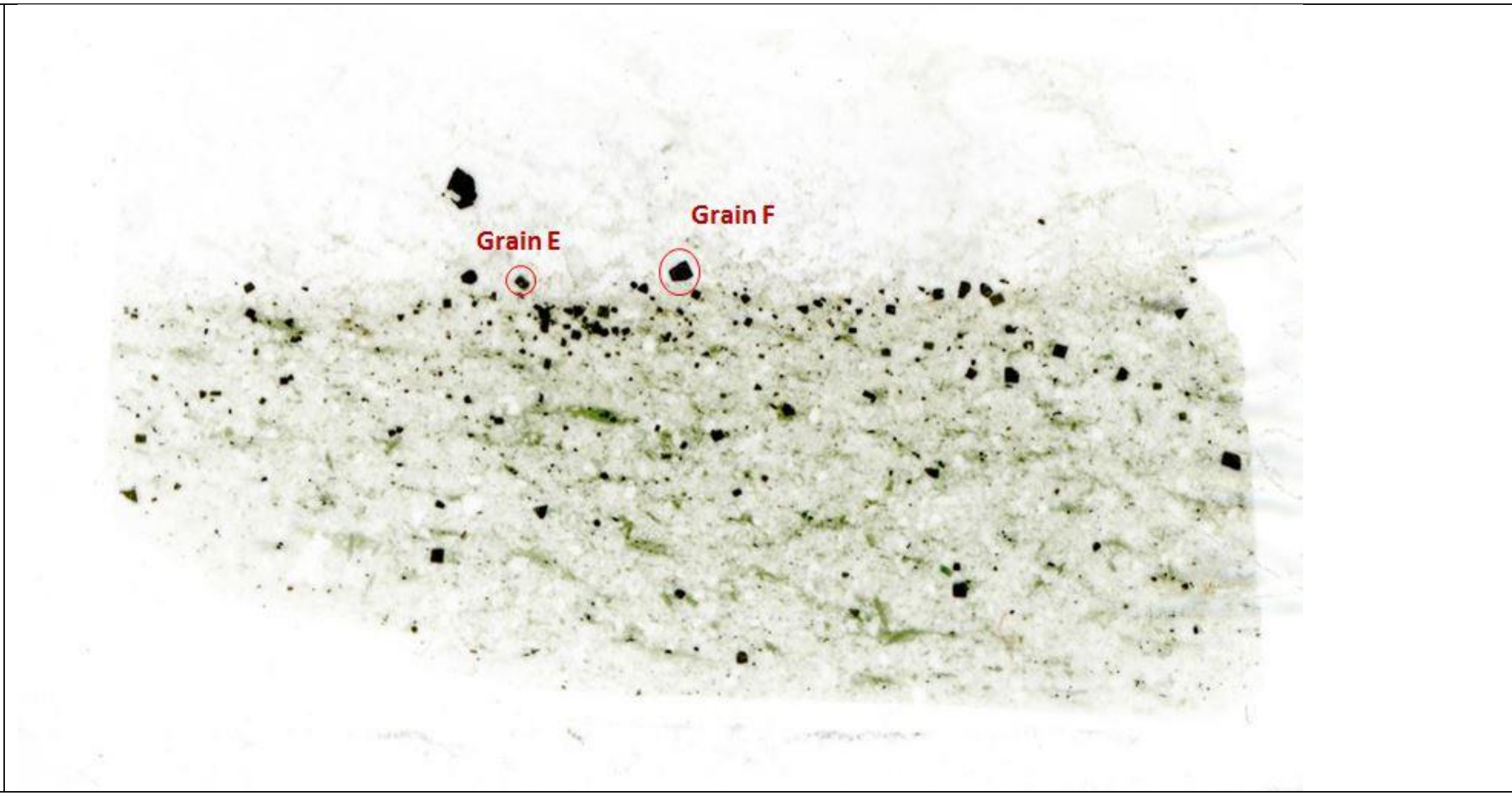

900	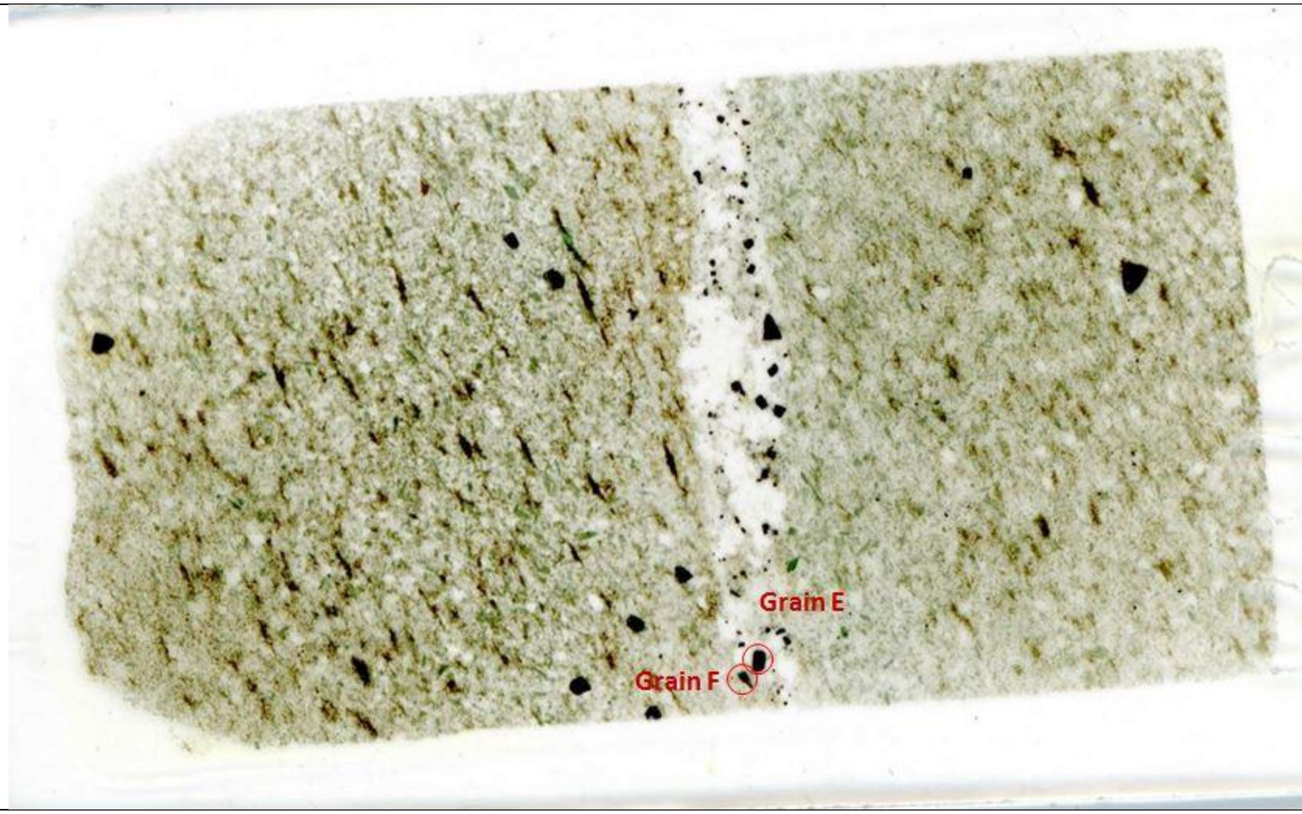

Appendix C: Petrography Observations

Slide 152 - Pit

General Observations:

Mineral	Grain size	Grain shape	Composition
Pyrite	500um-100um	Euhedral	15%
Biotite	200um to a few are microns in size	Subhedral to bladed	28%
Quartz	700um to submicron	Subhedral to anhedral	32%
Calcite-Dolomite?	Generally 200um-50um, to a few microns in size	Anhedral	4%
Albite	100um-50um	Anhedral	1%
K feldspar	100um – 50um	anhedral	Trace amount
Muscovite	Less than 20 um to submicron	Bladed	20%
Rutile	100um	Anhedral	Trace amount
Chalcopyrite	submicron	anhedral	Trace amount
Galena	A few microns to submicron	anhedral	Trace
REE phosphate - Monazite	A few microns	anhedral	Trace
Telluride mineral inclusion (Au, Ag and Ni)	A few microns	anhedral	trace
Scheelite	A few microns	anhedral	trace

- Orthoclase also contains fluid inclusions within
- Vein selvage has strong concentration of large grained biotite
  - Decrease in concentration of biotite away from vein also in grain size
- Disseminated pyrite grains are found within the host rock
- Pyrite grains are larger within the vein compared to the host rock and surrounding alteration assemblage
- Grains are euhedral
- Thick biotite rims along the vein selvages – higher concentration around the selvage and then decreases away from the vein
- Finer grained host rock (100um to submicron in size) with larger grains of pyrite and biotite.
- 2 directions of foliation. 1 direction of foliation is the majority of the slide. The other foliation appears to be associated with the youngest veins which cross cuts the dominant foliation of S2.

- The rutile grains can be found along the sides of the pyrite within the vein as well as alone within the vein
- Host rock changes. The host rock near the youngest thick vein contains more plagioclase and quartz. The host rock near the older thinner vein contains much finer material.
- Biotite grains are bladed to anhedral in the dominant (S2) foliation as they are cut and deformed slightly by the older foliation. The grains are more bladed and less anhedral in the younger foliation. The younger foliation's biotite grains are also larger (200um to submicron in size) whereas the older (S2) foliation associated biotite grains are more 100um to submicron in size.
- The biotite grains are very concentrated around the youngest vein's selvages as the younger foliation appears to overprint the existing dominant foliation. This becomes less concentrated away from the vein and the dominant foliation resumes.
- The quartz grains are very anhedral
- Muscovite within the host rock as well
- Thickest: Cuts dominant foliation – younger than dominant foliation.
    - Cuts into the mid-sized veins. Older than mid-sized veins.
    - The quartz grains vary in size but are generally much larger in this vein (approximately 700um) compared to the other veins which shows that it is less deformed (and younger) than the other veins. The grains have many fractures within each grain (From undergoing metamorphism?)
    - Largest vein has fewest pyrite grains (approximately 50um)
    - The second direction of foliation is associated with this vein. It only surrounds this particular vein's selvages. The biotite grains associated with this foliation are larger (some even 250um long) cut across the biotite grains associated with the dominant foliation.
    - Not a vein of interest
- Thinner vein vein: parallel to dominant foliation and the main vein of focus within this slide.
    - Contains the largest pyrite grains – 500um – generally 500-100um.
    - Vein of interest
    - Since this foliation is appears to be formed within the same event as this vein which is also associated with the largest pyrite grains, it appears that this foliation may be the S2 foliation. The other foliation is associated with the younger vein appears to carry very little pyrite so it appears that it may not be the vein of interest, nor the foliation of interest.
    - Pyrite grains contain quartz and biotite inclusions, these grains
    - These grains are more corroded – more marks along the surface

Thinner vein:

Mineral	Grain size	Grain shape	Composition
Pyrite	500um-100um	Euhedral	10%
Biotite	Generally 50um	Bladed to anhedral	15%
Quartz	Generally 200um-50um, a few are microns in size	Subhedral to anhedral	39%
Rutile	100um	Anhedral	trace
Albite	100um	anhedral	3%
K feldspar	50um	anhedral	1%
Calcite	Generally 200um-50um, to a few microns in size	Anhedral	30%
Iron oxide	50um to submicron	anhedral	2%
Chalcopyrite	A few microns in size	Anhedral	Trace amount
Galena	A few microns to submicron	anhedral	Trace
REE phosphate - Monazite	A few microns	anhedral	Trace
Telluride mineral inclusion (Au, Ag and Ni)	A few microns	anhedral	trace
Scheelite	A few microns	anhedral	trace
Muscovite	A few microns	anhedral	trace

- Pyrite grain inclusions:
    - Galena
    - Chalcopyrite
    - Biotite
    - K feldspar
    - Quartz
    - Monazite
    - Au-Ag Telluride mineral
    - Ni-Telluride
    - Albite
    - Muscovite
- There are iron oxide alterations along some of the sides of pyrite grains

Slide 157-Pit

General Observations:

Mineral	Grain size	Grain shape	Composition
Pyrite	500um to a few microns in size	Euhedral to anhedral	11%
Chalcopyrite	100um to submicron	Anhedral	1%
Quartz	200um to submicron	Anhedral	40%
Biotite	Generally less than 50um but can find 200um as well	Subhedral to bladed (finer grains are bladed)	30%
Chlorite	Less than 50um, very anhedral and fractured mostly seen in smaller fragments. Some grains around 100um	Anhedral	3%
Calcite Dolomite	700um to submicron (generally 100um to 50um)	Subhedral to anhedral	4%
Plagioclase	150um to 50um	anhedral	6%
K feldspar	150um to 50um	anhedral	5%
Rutile	A few microns	anhedral	Trace amount
Galena	A few microns	anhedral	Trace
Fluorocarbonates	A few microns	anhedral	Trace
Au-Ag Telluride mineral inclusion	A few microns	anhedral	Trace

- Overall one direction of foliation (S2) indicated by the direction of elongation of the biotite grains (the S2 foliation runs the width of the thin section slide)
- Biotite grains are finer here, generally 25um, but grains can also be 150um near veins and veinlets.
- Chlorite (pale green with lower than first order white extinction) is also along some of the veins.
- One main vein and many veinlets.
- Some grains of rutile within the vein

Vein:

- Parallel to foliation (biotite grains wrap around the vein's shape)
- This vein contains many large plagioclase grains (~500um) as well as quartz, calcite, and chlorite

- The grain boundaries within this vein are also difficult to tell as the grains are highly strained and are fractured into smaller pieces.

Vein:

Mineral	Grain size	Grain shape	Composition
Pyrite	500um to 100um, some are a few microns in size (fractured fragments surrounding main grains)	Anhedral	3%
Chalcopyrite	100um to submicron	Anhedral	2%
Quartz	Generally 200um-50um, a few are microns in size	Subhedral to anhedral	45%
Calcite	100um-50um, to a few microns in size	Anhedral	20%
Biotite	200 to 50um	Anhedral	15%
Albite	250um to 50um	Anhedral	10%
K feldspar	250um to 50um	anhedral	5%
Rutile	A few microns	anhedral	Trace amount
Galena	A few microns	anhedral	Trace
Fluorocarbonates	A few microns	anhedral	Trace
Au-Ag Telluride mineral inclusion	A few microns	anhedral	Trace

- Pyrite grain inclusions:
  - Au-Ag Telluride mineral
  - Chlorite
  - Quartz
  - REE Fluorocarbonate mineral
- The pyrite grains are associated with chalcopyrite.
- Large biotite grains and chlorite wrapping around the quartz and carbonate grains within the vein.
- Biotite normally fine grained along this slide but here they are coarse (approximately 200um to 50um)
- Chlorite between the pyrite grain fragments
- The pyrite grains have holes within the pyrite

Slide 3415A –Pit

General Observations:

Mineral	Grainsize	Grain shape	Composition
Pyrite	1mm to submicron, generally larger in the vein/veinlets	Euhedral to anhedral	10%
Plagioclase	100um to 25um	anhedral	10%
Quartz	100um to submicron	anhedral	35%
Biotite	250um to submicron	Subhedral to anhedral	18%
Chlorite	500um to submicorn	anhedral	4%
Calcite	500um to submicron	anhedral	10%
Muscovite	200um	subhedral	3%
Mg-rich baguette chlorite	~50um	bladed	2%
Chalcopyrite	A few microns	anhedral	Trace amounts (inclusions) within pyrite
Ag-Au telluride mineral	10-20um	anhedral	trace
Galena	2-40um	anhedral	trace
Albite	A few um	anhedral	trace
K feldspar	A few um	anhedral	trace
Rutile	A few microns	anhedral	trace
Titanite	A few microns	anhedral	trace
Zircon	A few microns	anhedral	trace
Iron oxide	submicron	anhedral	trace

- There is a thick accumulation (~500um thick) of large biotite grains at the vein selvage, just outside it reduced concentration – very little biotite until much further form the vein where the biotite tends to reappear
- The carbonate is only found within the vein within a host rock of predominantly quartz and biotite. Vein is parallel to foliation
- The biotite isn’t consistently dispersed along the thin section. The larger grains are more concentrated around the vein`s selvages The smaller grains are found within the host rock and are only a few microns to submicron in size.
- The pyrite grains are much larger within the vein but are finer within the host rock less than 80um.
- The vein selvages have coarser grained biotite compared to the host rock. Thick biotite rims mixed with patches of carbonate minerals in between,

Vein:

Mineral	Grainsize	Grain shape	Composition
Pyrite	1mm to 25um	Euhedral to anhedral	15%
Quartz	50um to submicron	anhedral	3%
Biotite	250um to submicron	Subhedral to anhedral	15%
Chlorite	500um to submicorn	anhedral	5%
Calcite	500um to submicron	anhedral	57%
Muscovite	200um	subhedral	3%
Mg-rich baguette chlorite	~50um	bladed	2%
Chalcopyrite	A few microns	anhedral	Trace amounts (inclusions) within pyrite
Ag-Au telluride mineral	10-20um	anhedral	trace
Galena	2-40um	anhedral	trace
Albite	A few um	anhedral	trace
K feldspar	A few um	anhedral	trace
Rutile	A few microns	anhedral	trace
Titanite	A few microns	anhedral	trace
Zircon	A few microns	anhedral	trace
Iron oxide	submicron	anhedral	trace

- Pyrite inclusions:
    - Chalcopyrite
    - Au-Ag Telluride mineral
    - Galena
    - K feldspar
    - Ag-Telluride mineral
    - Albite
    - Calcite
    - Quartz
    - Biotite
- High concentration of carbonate grains within the vein
- The biotite grains wrap around the veins, these grains very widely in size.
- The carbonate grains are highly anhedral
- There seems to be more of a bimodal distribution of quartz within the host rock as there are coarse quartz grains and a fine quartz matrix.

Slide 487 -Pit

Mineral	Grainsize	Grain shape	Composition
Pyrite	200um to submicron	Subhedral to Anhedral	7%
Chalcopyrite	50um to a few microns	Subhedral to Anhedral	Trace amount
Quartz	1mm to 50um	Subhedral to Anhedral	36%
Biotite	200um to submicron	Subhedral to Anhedral	25%
Carbonate	200um to submicron	Anhedral	10%
Rutile	50 um to submicron	Anhedral	2%
Chlorite	1mm to submicron	Anhedral	2%
Albite	200um to 50um	anhedral	2%
K feldspar	100-50um	Anhedral	1%
Muscovite	Generally a few microns to submicron, some are less than 20um	anhedral	15%
galena	A few microns	anhedral	trace
barite	A few microns	anhedral	trace

- Vein selvage has greater accumulation of large grained biotite but less concentrated overall in smaller grained biotite like the host rock
- Host rock is largely fined grained quartz, muscovite, carbonate and biotite. There are also larger quartz grains within which are approximately 1-2mm
    - Muscovite is highly birefringent with basal cleavage and not pleochroic
- The foliation runs along the width of the slide.
- The vein within the center is older than the foliation as the biotite veins of the foliation wrap around the sides of the vein.
    - The vein also branches out on either side.
- The veinlets in this thin section do not contain pyrite and are not a vein of interest

Veinlets:
- These veins contain no pyrite
- The veins are predominately carbonate with some smaller quartz grains
    - 70% carbonate
    - 25% quartz
    - 5% Chlorite along the veinlet selvages

Main Vein and branches:

Mineral	Grainsize	Grain shape	Composition
Pyrite	1mm and 100um	Anhedral and Euhedral	3%
Chalcopyrite	50um	Anhedral	Trace amount
Quartz	1mm to 50um	Subhedral	70%
Albite	200um to 50um	anhedral	2%
K feldspar	100-50um	Anhedral	1%
Biotite	100um to a few microns	Anhedral	5%
Carbonate	4mm to 50um	Anhedral	22%
galena	A few microns	anhedral	trace
barite	A few microns	anhedral	trace

- Pyrite inclusions:
    - Galena
    - Chalcopyrite
    - Quartz
    - Biotite
- There is one large pyrite within the vein and a smaller one approximately 100um in size

Slide 153-NE-SW Transect

General Observations:

Mineral	Grainsize	Grain shape	Composition
Pyrite	150um to submicron	Subhedral to anhedral	4%
Quartz	1mm to a few microns	Anhedral	39%
Pyrrhotite	500umm	anhedral	1%
Albite	100um to 1mm	anhedral	10%
K feldspar	50 um to 500um	anhedral	5%
Pentlandite	50um to a few microns	anhedral	Trace amount
Biotite	2mm to a few microns	Bladed to anhedral	27%
Chlorite	1mm to submicron	Anhedral	7%
Calcite	500um to submicron	Anhedral	5%
Rutile	50um to submicron	anhedral	trace
Chalcopyrite	submicron	anhedral	Trace amount
Iron oxide	250um to a few microns	anhedral	Trace amount
Galena	A few microns	anhedral	Trace
Bi-Co-telluride mineral	submicron	anhedral	Trace
Arsenopyrite	A fewmicrons	anhedral	trace
Molybdenite	A few microns	anhedral	trace

- Biotite grains at the vein selvage, within the vein and within the host rock proximal to the vein has altered into chlorite
- All biotite grains are a parallel. Assumed to be along the direction of foliation (S2), which runs down the length of the slide.
- The host rock in this thin section has undergone deformation. Not only are the biotite grains indicating the foliation direction but even the quartz grains in the host rock as the minerals are all elongated along this direction.
- It appears that the quartz within the host rock has recrystallized as there are bulges along the grain boundaries.
- The quartz grains within the vein do not appear to be heavily deformed along the foliation (larger grains, since it is quartz it probably requires much more to deform it like the biotite, carbonate and the smaller quartz grains). There are some deformed grains where the boundaries are a bit rough and fractured
- The carbonate grains appear to be deformed (grains seem to orient themselves along a line running along the foliation direction and they appear to be more anhedral in shape with rough and deformed grain boundaries)

- There is some chlorite along the vein selvages as well as within some of the host rock as an alteration product of biotite. Appear within zones of where biotite is concentrated or along the vein selvages.

Veins:

Mineral	Grainsize	Grain shape	Composition
Pyrite	150um to submicron	Subhedral to anhedral	2%
Quartz	1mm to a few microns, generally large	Anhedral	35%
Biotite	500um to a few microns	Bladed to anhedral	8%
Albite	100um to 1mm	anhedral	15%
K feldspar	50 um to 500um	anhedral	10%
Chlorite	Difficult to tell grain boundary	Anhedral	4%
Calcite-Dolomite	500um to submicron	Anhedral	15%
Rutile	50um to submicron	anhedral	1%
Chalcopyrite	submicron	anhedral	10
Iron oxide	250um to a few microns	anhedral	Trace amount
Galena	A few microns	anhedral	Trace
Bi-Co-telluride mineral	submicron	anhedral	Trace
Arsenopyrite	A fewmicrons	anhedral	trace
Molybdenite	A few microns	anhedral	trace

- Pyrite inclusions
  - Chalcopyrite
  - Arsenopyrite
  - Galena
  - Bi-Co Telluride mineral

Slide 164B NE-SW Transect

General Observations:

Mineral	Grainsize	Grain shape	Composition
Pyrrhotite	Less than 50um	anhedral	3%
Chalcopyrite	300um to submicron	Elongated (almost streak-like) and anhedral	1%
Garnet	1.5mm	anhedral	2%
Quartz	3mm to submicron	anhedral	10%
Biotite	2mm to a few microns in length	Bladed to anhedral	15%
Calcite	Less than 5o um to a few microns	anhedral	2%
Albite	50um to 1mm	Anhedral	43%
K feldspar	300um to 50um	Anhedral	15%
Apatite	200um	anhedral	1%
Epidote	50-250um	anhedral	1%
Muscovite	Generally 50um	Bladed to subhedral	1%
Chlorite	Less than 50um to submicron	anhedral	5%
Galena	A few microns	anhedral	Trace

- Large biotite grains accumulate along the vein selvage
    - Biotite alters to chlorite near the vein and within some of the host rock proximal to the vein
- Biotite grains are elongated along the direction of foliation. The grains are fairly long
- The host rock of this thin section seems to be similar to the host rock of the previous slide (153) where the quartz as well as the biotite are strained and elongated along the foliation direction.
- Greater amount of pyrite grains within the host rock than the veins but larger grains within the vein.

Veins:

Mineral	Grainsize	Grain shape	Composition
Pyrrhotite	3mm to submicron	anhedral	5%
Chalcopyrite	300um to submicron	Elongated (almost streak-like) and anhedral	1%
Quartz	3mm to submicron	anhedral	8%
Biotite	50um	Bladed to anhedral	trace
Calcite	A few microns	anhedral	3%
Albite	50um to 1mm	Anhedral	45%

K feldspar	300um to 50um	Anhedral	29%
Apatite	200um	anhedral	1%
Epidote	50-250um	anhedral	1%
Muscovite	Generally 50um	Bladed to subhedral	5%
Chlorite	50um	anhedral	1%
Galena	A few microns	anhedral	Trace

Slide 154-NE-SW Transect

General Observations:

Mineral	Grainsize	Grain shape	Composition
Pyrite	100um to 70um	Subhedral to anhedral	3%
Quartz	1mm to a few microns	Subhedral to anhedral	44%
Biotite	150um	Anhedral	17%
Muscovite	100um to submicron	anhedral or bladed	20%
Rutile	200um to a few microns	anhedral	Trace amount
Calcite	1mm to a few microns	anhedral	5%
Hornblende	100um	anhedral	Trace amount
Plagioclase	1mm to 100um	Anhedral	8%
K feldspar	1mm to 100um	Anhedral	3%
Microcline	500um to 100um	anhedral	Trace amount
Chalcopyrite	A few microns	anhedral	Trace amount
fluorocarbonate	A few microns	Anhedral	trace
Fluorite	A few microns	Anhedral	trace
Galena	A few microns	Anhedral	trace
Molybdenite	A few microns	Anhedral	trace

- The vein is older than foliation
    - Greater accumulation of biotite grains along vein selvage – no alteration zone
- The vein is within a fine grained host rock of quartz, muscovite and biotite
- More pyrite grains within the host rock and only a few are found within the veins. However the grains within the vein are larger compared to the host rock
- Some of the plagioclase and orthoclase contains many fluid inclusions
- Some of the quartz and orthoclase have muscovite and carbonate inclusions
- Green biotite found here –alteration product of biotite
- Mostly muscovite outside the rocks are also parallel to foliation (biotite alters into muscovite)
- The pyrite also contain biotite and rutile inclusions

Vein:

Mineral	Grainsize	Grain shape	Composition
Pyrite	100um to 70um	Subhedral to anhedral	2%
Quartz	1mm to a few microns	Subhedral to anhedral	45%
Biotite	150um	Anhedral	1%
Calcite	1mm to a few microns	anhedral	10%
Albite	1mm to 100um	Anhedral	25%
K feldspar	1mm to 100um	Anhedral	15%
Chalcopyrite	A few microns	anhedral	Trace amount
fluorocarbonate	A few microns	Anhedral	trace
Fluorite	A few microns	Anhedral	trace
Galena	A few microns	Anhedral	trace
Molybdenite	A few microns	Anhedral	trace

- Pyrite inclusions
    - Quartz
    - Biotite
    - Chalcopyrite
    - Albite

Slide 159-Transect NE-SW

General Observations:

Mineral	Grainsize	Grain shape	Composition
Pyrrhotite	1mm to a few microns	Subhedral to Anhedral	1%
Quartz	200um	Subhedral to anhedral	36%
Albite	200um-1mm	Anhedral	25%
Biotite	1.5mm to 100 generally, some are a few microns	Euhedral to subhedral	20%
Chlorite	1mm to 100um	Subhedral to anhedral	%15
Calcite	Less than 50 - submicron	anhedral	Trace amount
Garnet	1mm and 500um	Hexagonal and rounded	1%
Rutile	Less than 50 to a few microns	anhedral	2%
Epidote	A few microns	anhedral	trace

- Older than foliation – grains wrap around vein
- This thin section contains one folded vein in a host rock that is different than the host rocks of the other thin sections of this transect
    - Here it is largely quartz and biotite (some plagioclase). The quartz is not as fine grained as the previous slides and the biotite grains are longer as well.
- The folded vein appears to be older than the foliation as the biotite grains wrap around the vein
- Large round grains and hexagonal grains garnet grains within the sample
- The vein is largely plagioclase and quartz (45% and 50%) and biotite (5%) with some carbonate (trace amounts)
    - The grains within the veins are fractured
- Host rock appears to be recrystallized– bulge recrystallization
- All the sulphide minerals here are Pyrrhotite grains

Vein:

Mineral	Grainsize	Grain shape	Composition
Pyrrhotite	1mm to a few microns	Subhedral to Anhedral	5%
Quartz	200um	Subhedral to anhedral	56%
Albite	200um-1mm	Anhedral	30%
Biotite	1.5mm to 100 generally, some are a few microns	Euhedral to subhedral	5%
Chlorite	1mm to 100um	Subhedral to anhedral	3%
Calcite	Less than 50 - submicron	anhedral	Trace amount
Rutile	Less than 50 to a few microns	anhedral	1%
Epidote	A few microns	anhedral	trace

Slide 162 – NE-SW Transect

General Observations:

Mineral	Grainsize	Grain shape	Composition
Pyrite	200um to a few microns	anhedral	1%
Pyrrhotite	250um	anhedral	1%
Pentlandite	A few microns to submicron	anhedral	Trace
Quartz	500um and submicron	Anhedral	47%
Albite	500um to a few microns	anhedral	15%
K feldspar	250um to a few microns	anhedral	5%
Biotite	Largely a few microns but some approx. 250um	Euhedral to anhedral	17%
Hornblende	200um to a few microns	anhedral	10%
Epidote	150um to submicron	anhedral	1%
Calcite	1mm to 200um	anhedral	1%
Iron oxide	100um to submicron	anhedral	Trace amount
Muscovite	100um to 250um	anhedral	2%
Chlorite	A few microns to submicron	subhedral	Trace amount
Ni-Sulphide mineral	A few microns	anhedral	Trace amount
Chalcopyrite	A few microns	anhedral	trace

- There are two vein generations within the thin section.
    - The older one is cut by the foliation and the second set of veins
        - The older one also carries the pyrite grains
        - It is shifted as it is cut as well by the younger vein
    - The younger ones are veinlets that cut the main older vein as well as the foliation.
        - This vein generation is not of interest since it is younger than the foliation
- The host rock is fine grained and rich in quartz, feldspars and biotite
    - feldpars contains fluid inclusions, more of them within the host rock
    - Hornblende has fluid inclusions as well
    - Bimodal distribution of quartz grains
    - Greater hornblende concentration within the host rock compared to the vein.

Young Veinlets:

- These veinlets are composed of carbonate, quartz and muscovite

Main Vein:

Mineral	Grainsize	Grain shape	Composition
Pyrite	200um to a few microns	anhedral	1%
Pyrrhotite	250um	anhedral	1%
Pentlandite	A few microns to submicron	anhedral	Trace
Quartz	500um and submicron	Anhedral	66%
Albite	500um to a few microns	anhedral	20%
K feldspar	250um to a few microns	anhedral	5%
Biotite	Largely a few microns but some approx. 250um	Euhedral to anhedral	5%
Hornblende	200um to a few microns	anhedral	trace%
Iron oxide	100um to submicron	anhedral	Trace amount
Chlorite	A few microns to submicron	subhedral	1%
Ni-Sulphide mineral	A few microns	anhedral	Trace amount
Chalcopyrite	A few microns	anhedral	1%

- Iron oxide around the pyrite grains
- Ni-S inclusions in the pentlandite
- Grain B is almost all Pyrrhotite and some pentlandite interfingering growths almost. Orientation of pentlandite does not correlate with orientation
- Pyrite inclusions:
    - Biotite
    - Quartz
    - Chlorite

Slide 886B- NE-SW Transect

General Observations:

Mineral	Grainsize	Grain shape	Composition
Pyrite	1mm to a few microns	Anhedral to subhedral	2%
Pyrrhotite	Less than 50um	anhedral	1%
Quartz	1.5 mm to submicron	anhedral	20%
Albite	500um to 100um	Anhedral	35%
K feldspar	250um to 100um	anhedral	6%
Calcite	Less than 50um to a few microns	anhedral	5%
Biotite	2mm to 500um general, also a few microns to submicron	Subehdral to anhedral	12%
Epidote	Less than 50m to a few microns	anhedral	2%
Chlorite	2mm to 500um general, also a few microns to submicron	Subehdral to anhedral	10%
Muscovite	Less than 50m to a few microns	Anhedral to bladed	3%
Hornblende	500um	Subhedral to euhedral	3%
Chalcopyrite	A few microns	anhedral	Trace
Rutile/Titanite	20um	anhedral	trace
Sphalerite	2um	anhedral	trace
Apatite	100um to 50um	anhedral	1%
Molybdenite	A few microns	anhedral	trace

- Hole from pyrite visible (1.5mm, and Subhedral (orthogonal)) a single grain
- Pyrrhotite and Pyrite are both visible within this thin section
  - Majority of the large grains are Pyrrhotite and fewer grains of pyrite
  - The pyrite grains contain very few inclusions and are only a few microns large
- S2 runs along the length of the thin section
- Large amount of plagioclase within this thin section

Vein:

Mineral	Grainsize	Grain shape	Composition
Pyrite	1mm to submicorn	Anhedral to subhedral	4%
Pyrrhotite	Less than 50um	anhedral	1%

Quartz	1.5 mm to submicron	anhedral	10%
Albite	500um to 100um	Anhedral	50%
K feldspar	250um to 100um	anhedral	10%
Calcite	Less than 50um to a few microns	anhedral	8%
Biotite	2mm to 500um general, also a few microns to submicron	Subehdral to anhedral	5%
Epidote	Less than 50m to a few microns	anhedral	5%
Chlorite	2mm to 500um general, also a few microns to submicron	Subehdral to anhedral	4%
Muscovite	Less than 50m to a few microns	Anhedral to bladed	3%
Hornblende	500um	Subhedral to euhedral	5%
Chalcopyrite	A few microns	anhedral	Trace
Rutile/Titanite	20um	anhedral	trace
Sphalerite	2um	anhedral	trace
Apatite	100um to 50um	anhedral	1%
Molybdenite	A few microns	anhedral	trace

- Pyrite inclusions
    - Albite
    - quartz

Slide 888B- NE-SW Transect

General Observations:

Mineral	Grainsize	Grain shape	Composition
Pyrrhotite	Mostly around 100um-50um but one is 2mm and others are less than 50um to submicron	Anhedral	3%
Quartz	2mm to around 25um	anhedral	43%
Albite	1mm to 200um	anhedral	10%
Biotite	Generally 1mm to 200um, some are up to 3mm and some are also a few microns in length	Subhedral to anhedral	18%
Chlorite	500um to 250um	subhedral	2%
Staurolite	1.5mm to 700um	anhedral	2%
Rutile	Less than 100um to a few microns	anhedral	2%
Ilmenite	50um	anhedral	trace

- Majority of sulphide minerals are Pyrrhotite with small pyrite grains that are corroded
- En echelon vein with sigmoidal shape of biotite grains

Host Rock:

- Host rock is not as fine grained (a few microns to 100um here) as most of the host rocks along this transect. Mostly quartz and biotite
- Some host rock quartz grains have biotite inclusions within. Host rock quartz grains are recrystallized

Vein:

- The main vein within the thin section appears to be older or the same age as the foliation – the biotite grains wrap around the vein
- The vein is folded with hinge of folds parallel to S2
- Large quartz and albite grains within the vein (2mm to 500um, some are closer to 100um)
- Contains Staurolite within the vein – high relief, low birefringence, colourless to yellow pleochroic.

Mineral	Grainsize	Grain shape	Composition
Pyrrhotite	Mostly around 100um-50um but one is 2mm and others are less than 50um to submicron	Anhedral	15%
Quartz	2mm to around 25um	anhedral	41%
Iron oxide	submicron	anhedral	2%
Albite	1mm to 200um	anhedral	20%
Biotite	Generally 1mm to 200um, some are up to 3mm and some are also a few microns in length	Subhedral to anhedral	20%
Chlorite	500um to 250um	subhedral	1%
Rutile	Less than 100um to a few microns	anhedral	1%

Slide 168A – NW-SE Transect

General Observations:

Mineral	Grainsize	Grain shape	Composition
Pyrite	1mm to a few microns	anhedral	2%
Quartz	4mm to 100um	anhedral	30%
Albite	1mm to 100um	anhedral	12%
K feldspar	200um to 50um	anhedral	5%
Biotite	Generally 400um to 100um, some are closer to 800um others are much smaller and a few microns to submicron	Bladed euhedral to anhedral	27%
Apatite	1.5mm and 2mm	Anhedral and euhedral	3%
Muscovite	Generally 400um to 100um, some are closer to 800um others are much smaller and a few microns to submicron	Bladed euhedral to anhedral	15%
Chlorite	2mm to 50um	Subhedral anhedral	3%
Ilmenite	50-250um	anhedral	3%
Galena	A few microns	anhedral	trace
Chalcopyrite	A few microns	anhedral	trace

- The foliation generally runs across the length of the slide
- There is one main vein within
- Apatite within the vein
    - Unknown high relief, low birefringence, parallel extinction, colourless in PPL

Host Rock:

- It appears that biotite and portions of host rock are cutting into portions of the vein
    - Host rock contains portions of finer grained quartz, biotite and some plagioclase

Vein:

- Quartz and Albite grains are very large – 4mm to 1mm and fractured

Mineral	Grainsize	Grain shape	Composition
Pyrite	1mm to a few microns	anhedral	2%
Quartz	4mm to 100um	anhedral	60%
Albite	1mm to 100um	anhedral	15%
K feldspar	200um to 50um	anhedral	5%
Biotite	Generally 400um to 100um, some are closer to 800um others are much smaller and a few microns to submicron	Bladed euhedral to anhedral	5%
Apatite	1.5mm and 2mm	Anhedral and euhedral	5%
Ilmenite	50-250um	anhedral	5%
Chlorite	2mm to 50um	Subhedral anhedral	3%
Galena	A few microns	anhedral	trace
Chalcopyrite	A few microns	anhedral	trace

- Pyrite inclusion
  - Galena
  - Chalcopyrite
  - Chlorite
  - K feldspar
  - Albite
  - Quartz

Slide 171B – NW-SE Transect

General Observations:

Mineral	Grainsize	Grain shape	Composition
Pyrite	2mm to 1mm mostly, some are around 100um to submicron	Anhedral	4%
Pyrrhotite	100um	anhedral	1%
Iron oxide	submicron	anhedral	1%
Quartz	1mm to submicron	Anhedral	52%
Albite	500um to 250um	anhedral	3%
Muscovite	100um	Bladed to subhedral	Trace amounts in vein
Biotite	100um to submicron	Anhedral to bladed	40%
Chlorite	400 to a few microns	anhedral	Trace amount
Rutile	Less than 50um to a few microns	Anhedral	2%
Epidote	50um to a few microns	anhedral	Trace
Barite	A few microns	Anhedral	trace
Galena	A few microns	Anhedral	trace

- Biotite alters to chlorite within the vein, at the vein selvage and within host rock proximal to vein
- Accumulation of larger biotite grains at vein selvage
- There are two veins within the thin section, both are parallel to foliation
- One is a veinlet near the top composed entirely of quartz but it contains no pyrite to examine- won`t be a vein of interest
- The second vein is a thick vein
    - The pyrite grains within this thin section and vein are altered in the edges into iron oxide
- The majority of the pyrite grains are within the vein which is unusual for most of these samples since the host rock tends to have a greater concentration of but smaller pyrite grains.
- Here it appears to be exclusively within the vein

Vein:

Mineral	Grainsize	Grain shape	Composition
Pyrite	2mm to 1mm mostly, some are around 100um to submicron	Anhedral	8%
Pyrrhotite	100um	anhedral	1%
Iron oxide	submicron	anhedral	1%
Quartz	1mm to submicron	Anhedral	83%
Albite	500um to 250um	anhedral	5%
Biotite	100um to submicron	Anhedral to bladed	1%
Rutile	Less than 50um to a few microns	Anhedral	2%
Barite	A few microns	Anhedral	trace
Epidote	50um to a few microns	anhedral	Trace
Galena	A few microns	Anhedral	trace

- Quartz grain size of veins is larger than host rock (1mm-100um)
- Pyrite inclusions
    - Quartz
    - Chalcopyrite
    - Biotite
    - Epidote
    - Galena

Slide 173 – NW-SE Transect

General Observations:

Mineral	Grainsize	Grain shape	Composition
Pyrite	1mm to a few microns in size	anhedral	3%
Iron oxide	submicron	anhedral	2%
Chalcopyrite	500um to a few microns	anhedral	1%
Rutile	A few microns in size	Anhedral to bladed	Trace amount
Quartz	1.5mm	anhedral	42%
Albite	500um	anhedral	4%
Epidote	800um to 100um, some are a few microns in size	anhedral	3%
Biotite	Generally 1.5mm to 100um, some are a few microns to submicron within the host rock matrix	Subhedral to anhedral	32%
Chlorite	300um to 50um	Anhedral	3%
Hornblende	1.5mm to 100um generally, some a few microns to submicron within the host rock	Anhedral to subhedral	10%
Anhydrite	A few microns	Anhedral	trace
Barite	A few microns	Anhedral	trace
Galena	A few microns	Anhedral	trace
Titanite	A few microns	Anhedral	trace

- Epidote found within the vein as well as along right outside the vein selvage.
  - Green to pink in PPL
- High concentration of amphiboles cutting to vein at multiple directions
  - Large biotite grains at vein selvage but lower concentration in host rock proximal to vein compared to distal
- Bimodal quartz grain size within the host rock.
  - Almost all biotite grains run parallel to foliation
  - The hornblende is also mostly parallel to foliation
    - Some of the grains seem to cut through the biotite grains
- There are much more and larger biotite and hornblende grains in the host rock further from the veins compared to proximal to the veins
- Foliation runs approximately along the width of the thin section

- It appears that all the veins within this thin section are older than foliation as biotite grains wrap around the vein as well as cut into the vein
    - These veins are all parallel to foliation
- Pyrite is altered in edges into iron oxide

Veins:

Mineral	Grainsize	Grain shape	Composition
Pyrite	1mm to a few microns in size	anhedral	5%
Iron oxide	submicron	anhedral	3%
Chalcopyrite	500um to a few microns	anhedral	1%
Rutile	A few microns in size	Anhedral to bladed	Trace amount
Quartz	1.5mm	anhedral	69%
Albite	500um	anhedral	2%
Epidote	800um to 100um, some are a few microns in size	anhedral	5%
Biotite	Generally 1.5mm to 100um, some are a few microns to submicron within the host rock matrix	Subhedral to anhedral	2%
Chlorite	300um to 50um	Anhedral	3%
Hornblende	1.5mm to 100um generally, some a few microns to submicron within the host rock	Anhedral to subhedral	10%
Anhydrite	A few microns	Anhedral	trace
Barite	A few microns	Anhedral	trace
Galena	A few microns	Anhedral	trace
Titanite	A few microns	Anhedral	trace

- Pyrite inclusions
    - Quartz, Anhydrite, Barite, Galena, Titanite, Epidote, Chalcopyrite

Slide NB061B – NW-SE Transection

General Observations:

Mineral	Grainsize	Grain shape	Composition
Pyrite	Generally 250um, the ones in the vein are 1mm – 500um	Euhedral to subhedral	2%
Iron oxide	Submicron	anhedral	Trace amount
Chalcopyrite	Generally 100-50um	Subhedral	1%
Epidote	Less than 50um to a few microns	anhedral	15%
Quartz	800um to submicron	anhedral	42%
Albite	1mm	Anhedral	1%
Chlorite	100um and smaller, to submicron, some can be up to 1mm	Anhedral, some subhedral	35%
Biotite	100um and smaller, to submicron, some can be up to 1mm	subhedral	3%
Rutile	100um to 150um	Anhedral	1%
titanite	A few microns	anhedral	trace
apatite	250um to a few microns	anhedral	trace
Ilmenite	A few microns	anhedral	trace
Barite	A few microns	anhedral	trace

- It appears that both veins are older than the foliation within the slide
- There is vein with smaller quartz grains (generally 100um) which is cut by foliation where biotite grains cut across the width of the vein
    - Contains no pyrite
    - Not a vein of interest
- The larger one which contains large pyrite grains (1mm-500um) contains larger grains of quartz (800 to 100um) and is also cut by foliation where biotite grains cut into the vein
- Pyrite grains here are altered into iron oxide
- Pyrite grains contain quartz and biotite inclusions
    - Biotite grains wrap around the grains – older than foliation
- Rutile is found within the vein but also near the vein selvage as there are blades of rutile almost running parallel to foliation

Mineral	Grainsize	Grain shape	Composition
Pyrite	Generally 250um, the ones in the vein are 1mm – 500um	Euhedral to subhedral	20%
Iron oxide	Submicron	anhedral	Trace amount
Chalcopyrite	Generally 100-50um	Subhedral	1%
Epidote	Less than 50um to a few microns	anhedral	1%
Quartz	800um to submicron	anhedral	55%
Albite	1mm	Anhedral	5%
Chlorite	100um and smaller, to submicron, some can be up to 1mm	Anhedral, some subhedral	15%
Rutile	100um to 150um	Anhedral	1%
titanite	A few microns	anhedral	trace
apatite	250um to a few microns	anhedral	2%
Ilmenite	A few microns	anhedral	trace
Barite	A few microns	anhedral	trace

- Pyrite inclusion
    - Ilmenite
    - Epidote,
    - Apatite
    - Albite
    - Quartz

Slide NB064 – NW-SE Transect

General Observations:

Mineral	Grainsize	Grain shape	Composition
Pyrite			2%
Quartz	200um to a few microns (majority fine)	anhedral	40%
Albite	500um to 100um	Anhedral	8%
K feldspar	500um to 100um	anhedral	2%
Epidote	250 to a few microns	anhedral	1%
Biotite	100um to submicron	Anhedral to bladed	42%
Chlorite	300um to submicorn	anhedral	3%
Rutile	100um and to a few microns generally, grains in the biotite bands are 800um	Generally anhedral to bladed, large grains are subhedral	2%
Chalcopyrite	A few microns	Subhedral	Trace amount
Iron oxide	submicron	anhedral	Trace amount

- Greater concentration of biotite at vein selvage
- There are two directions of biotite elongation here.
- The dominant one is parallel to the vein within the thin section as the biotite grain run parallel to the vein along the selvage and a bit further into the host rock.
- The minor direction is where biotite grains grow over and cut the existing biotite.
- Overall biotite grains appear to be smaller than most -100um and smaller
- There are also high concentrations of biotite within bands in the thin section.
    - These bands are closer to the vein
- The quartz grains are not as fine grained as most of the quartz within the host rock. (50um to a few microns in size)
- Rutile found
    - Within the host rock – the rutile is found as blades within the host rock in multiple directions of elongation

Vein:

Mineral	Grainsize	Grain shape	Composition
Pyrite			2%
Quartz	200um to a few microns (majority fine)	anhedral	25%
Albite	500um to 100um	Anhedral	25%
K feldspar	500um to 100um	anhedral	8%
Biotite	100um to submicron	Anhedral to bladed	30%
Chlorite	300um to submicorn	anhedral	8%
Rutile	100um and to a few microns generally, grains in the biotite bands are 800um	Generally anhedral to bladed, large grains are subhedral	2%
Chalcopyrite	A few microns	Subhedral	Trace amount
Iron oxide	submicron	anhedral	Trace amount

- Pyrite inclusions
    - Muscovite
    - Epidote
    - Quartz

Slide NB068 – NW-SE Transect

General Observations:

Mineral	Grainsize	Grain shape	Composition
Pyrite	250um to a few microns	Subhedral to anhedral	2%
Iron oxide	submicron	anhedral	Trace amount
Hornblende	A few microns in size	Subhedral to anhedral (initially euhedral due to shadow and alteration)	1%
Albite	1mm to 500um	anhedral	10%
K feldspar	500um to 250um	anhedral	5%
Quartz	400um to a few microns	anhedral	35%
Muscovite	Less than 50um to submicron	Anhedral or bladed	15%
Chlorite	Most are a few microns to submicron, some are 200-100um	Anhedral to subhedral	25%
Biotite	200um to a few microns	anhedral	Trace amount
Rutile	Less than 50um to a few microns in size	Anhedral or bladed	4%
Chalcopyrite	A few microns in size	anhedral	3%
Fluorocarbonate	100um to a few microns	anhedral	trace
galena	A few microns	anhedral	trace
Titanite	A few microns	anhedral	trace
Ilmenite	A few microns	anhedral	trace
barite	A few microns	anhedral	trace

- Greater concentration of large grained chlorite proximal to vein and at vein selvage
- Biotite grains concentrated at vein selvage
- Foliation runs down the length of the slide
- Two vein generations within this slide
    - One is younger than the foliation –cross cuts foliation, host rock and older vein
        - Contains quartz and plagioclase
        - Not a vein of interest
    - Older vein is parallel to foliation and appears to be of similar age

- Euhedral pyrite grain - (grain shadow infilled with pyrite)

Vein:

Mineral	Grainsize	Grain shape	Composition
Pyrite	250um to a few microns	Subhedral to anhedral	20%
Iron oxide	submicron	anhedral	Trace amount
Albite	1mm to 500um	anhedral	15%
K feldspar	500um to 250um	anhedral	5%
Quartz	400um to a few microns	anhedral	40%
Chlorite	Most are a few microns to submicron, some are 200-100um	Anhedral to subhedral	20%
Chalcopyrite	A few microns in size	anhedral	trace
Fluorocarbonate	100um to a few microns	anhedral	trace
galena	A few microns	anhedral	trace
Titanite	A few microns	anhedral	trace
Ilmenite	A few microns	anhedral	trace
barite	A few microns	anhedral	trace

- Pyrite inclusion
    - Chalcopyrite
    - Chlorite
    - Titanite
    - Ilmenite
    - Barite

Slide 895B – NW-SE Transect

General Observations:

Mineral	Grainsize	Grain shape	Composition
Pyrite	2mm to 100um	Euhedral to anhedral	4%
Quartz	1.5mm to a few microns	anhedral	36%
Albite	500umto 100um	anhedral	15%
K feldspar	250um to 100um	anhedral	5%
Epidote	70um to submicron	anhedral	8%
Iron oxide	submicron	anhedral	Trace amount
Biotite	1mm to 100um generally, some are a few microns	Bladed to anhedral	30%
Ilmenite	150um to submicron	Anhedral	2%
Barite	A few microns	anhedral	trace

- There is one vein within the thin section. It is older than the foliation as it cuts through the vein
- The pyrite grains appeared to be initially euhedral, but the grains are altered into iron oxide
- Host rock has two bimodal quartz grain distribution (200um to a few microns) with larger biotite grains and rutile
- Biotite concentrated at vein selvages
- Disseminated pyrite within the host rock

Vein:

Mineral	Grainsize	Grain shape	Composition
Pyrite	2mm to 100um	Euhedral to anhedral	15%
Quartz	1.5mm to a few microns	anhedral	40%
Albite	500umto 100um	anhedral	20%
K feldspar	250um to 100um	anhedral	5%
Iron oxide	submicron	anhedral	10%
Biotite	1mm to 100um generally, some are a few microns	Bladed to anhedral	10%
Barite	A few microns	anhedral	trace

- Pyrite inclusions: quartz, barite, calcite

Slide 899A – NW-SE Transect

General Observations:

Mineral	Grainsize	Grain shape	Composition
Pyrite	1mm to 50um	Subhedral to anhedral	8%
Iron oxide	submicron	anhedral	2%
Quartz	2mm to submicron	Anhedral	25%
Calcite	1mm to submicron	anhedral	5%
Albite	400um to a few microns	anhedral	17%
Chalcopyrite	100um	Anhedral	Trace amount
Chlorite	400um to submicron	Anhedral to subhedral	25%
Biotite	100um to submicron	anhedral	3%
Hornblende	1mm to a 50um	anhedral	15%
Apatite	100um	anhedral	trace
Xenotime	A few microns	anhedral	trace
molybdenite	A few microns	anhedral	trace
Muscovite	A few microns	anhedral	trace
Galena	A few microns	anhedral	trace
titanite	A few microns	anhedral	trace
Pyrrhotite	A few microns	anhedral	trace

- Vein selvage and host rock area proximal to vein has greater concentration of larger grained biotite
- Foliation runs approximately along the length of the slide
- Host rock bimodal distribution with quartz (400um to submicron)
- Hornblende is more concentrated distal to the vein

Vein:

Mineral	Grainsize	Grain shape	Composition
Pyrite	1mm to 50um	Subhedral to anhedral	2%
Iron oxide	submicron	anhedral	2%
Quartz	2mm to submicron	Anhedral	55%
Calcite	1mm to submicron	anhedral	20%
Albite	400um to a few microns	anhedral	20%
Chalcopyrite	100um	Anhedral	Trace amount
Chlorite	400um to submicron	Anhedral to subhedral	trace
Biotite	100um to submicron	anhedral	1%
Apatite	100um	anhedral	trace
Xenotime	A few microns	anhedral	trace
molybdenite	A few microns	anhedral	trace
Muscovite	A few microns	anhedral	trace
Galena	A few microns	anhedral	trace
titanite	A few microns	anhedral	trace
Pyrrhotite	A few microns	anhedral	trace

- Pyrite inclusion:
    - Galena
    - Chlorite
    - Quartz
    - Chalcopyrite
    - titanite

Slide 900 – NW-SE Transect

General Observations:

Mineral	Grainsize	Grain shape	Composition
Pyrite	1mm to a few microns	Subhedral to anhedral	3%
Iron oxide	submicron	anhedral	1%
Pyrrhotite	200um	anhedral	1%
Quartz	2mm to a few microns	Anhedral	36%
Calcite	2mm to submicron	Anhedral	5%
Epidote	100um to submicron	Anhedral	3%
Biotite	1mm to a few microns	Subhedral to anhedral	30%
Chalcopyrite	A few microns	Anhedral (v)	Trace
Chlorite	300um	anhedral	Trace amount
Rutile	100um to submicron	Anhedral	2%
Hornblende	1mm to a few microns	Subhedral to anhedral	20%
Barite	A few microns	Anhedral (v)	Trace

- Host rock contains epidote grains
- There is one vein within the thin section – older than foliation and cut by foliation
- Biotite parallel to foliation
- Host rock bimodal distribution grain size - 300um to submicron
- All the pyrite grains are altered into iron oxide
    - Even host rock has corroded and altered pyrite
    - Rutile is also found within the host rock – can be from altered pyrite
- Pyrite grains are concentrated within the vein and less within the host rock – also smaller in the host rock
    - Different from majority of other thin sections

Vein:

Mineral	Grainsize	Grain shape	Composition
Pyrite	1mm to a 10um	Subhedral to anhedral	20%
Pyrrhotite	200um	anhedral	1%
Iron oxide	submicron	anhedral	1%
Quartz	2mm to a few microns	Anhedral	44%
Calcite	2mm to submicron	Anhedral	35%
Biotite	A few microns	anhedral	trace
Chalcopyrite	A few microns	anhedral	Trace
Barite	A few microns	Anhedral (v)	Trace

- Pyrite inclusions
    - Chalcopyrite
    - Quartz
    - Pyrrhotite

Slide 898A – NW-SE Transect

Mineral	Grainsize	Grain shape	Composition
Pyrite	2mm to a few microns	Euhedral to anhedral	8%
Quartz	1mm to submicron	Anhedral	35%
Muscovite	Less than 50um to submicron	Bladed to anhedral	10%
Albite	50 to 100um	anhedral	5%
Epidote	A few microns to submicron	anhedral	5%
Biotite	800um to submicron	Subhedral to anhedral	30%
Chlorite	300um to submicron	anhedral	8%
Apatite	50um	anhedral	trace
Barite	A few microns	anhedral	trace
Titanite	A few microns	anhedral	trace
Zircon	A few microns	anhedral	trace

- Epidote found in host rock and vein
- High concentration of large grained biotite at vein selvage
- Biotite alters into chlorite at vein selvage and proximal to vein in host rock

Host Rock:

- The foliations approximately along the width of the thin section
    - This is indicated by the finer biotite and muscovite grains within the host rock
        - May the large amount of muscovite present within the finer grains within the host rock are formed from altered biotite
- Bimodal distribution of biotite within the rock (200 to 100um vs 50-25um)
    - Fine grained biotite all are parallel to direction of foliation
    - Large grains are not parallel, they go in multiple directions
- Composed of biotite (bimodal), muscovite (fine grained), quartz (fine grained), and rutile (fine grained and anhedral

Vein:

Mineral	Grainsize	Grain shape	Composition
Pyrite	2mm to a few microns	Euhedral to anhedral	20%
Quartz	1mm to submicron	Anhedral	40%
Albite	50 to 100um	anhedral	15%
Biotite	800um to submicron	Subhedral to anhedral	10%
Chlorite	300um to submicron	anhedral	15%
Apatite	50um	anhedral	trace
Barite	A few microns	anhedral	trace
Titanite	A few microns	anhedral	trace
Zircon	A few microns	anhedral	trace

- Pyrite inclusions
    - Barite
    - Apatite
    - Titanite
    - Quartz
- The vein is deformed and fragmented by a deformation event associated with the larger grained biotite. These grains cut into the veins as well as wrap around it as well as the pyrite grains
    - These biotite grains also face multiple directions and appear to form in "clusters"
- It appears that the foliation occurs after the formation and fragmentation of the veins
    - All the fine biotite grains deviate in direction proximal to the vein and wrap around the vein.
    - Unlike the large biotite grains, the finer ones all are consistently facing one direction and do not form clusters
    - The fine biotite grains also shift in direction between the larger biotite grains as well – indicating that it is younger than the larger biotite as well as the vein
    - This foliation is also associated with the fine grained muscovite as they all also trend along that direction
- Square shaped holes within the thin section – may have carried pyrite which had fallen out

Slide 897A – NW-SE Transect

Mineral	Grainsize	Grain shape	Composition
Pyrite	500um to a few microns	anhedral	2%
Pyrrhotite	50um	anhedral	trace
Pentlandite	10um	anhedral	trace
Iron oxide	submicron	anhedral	Trace amount
Chalcopyrite	A few microns in size	Anhedral	Trace amount
Calcite	1mm to submicron	anhedral	3%
Quartz	800um to submicron	anhedral	46%
Epidote	100um to submicron	anhedral	15%
Biotite	1.3mm to submicron	Subhedral to anhedral	24%
Rutile	100 to submicron	anhedral	1%
Actinolite-tremolite	250um to a few microns	acicular	5%
Chlorite	250um to a few microns	anhedral	3%
Ilmenite	A few microns	anhedral	trace
Scheelite	250um to a few microns	anhedral	1%

Host Rock:

- The host rock also contains carbonate and augite on top of the biotite and quartz
- Larger quartz grains approximately 250um contain inclusions of muscovite, biotite and fluid inclusions
- Bimodal distribution of quartz 400um to submicron

Vein:

- Vein also contains carbonate
- Pyrite here has small grains
    - 100um approximately to a few microns
    - Altered into iron oxide
- Actinolite-tremolite and epidote in large proportions compared to the rest of the samples
- very few pyrite grains within this vein, mostly near the edge of the veins
- biotite grains are concentrated at the vein selvages
- Disseminated pyrite grains within the host rock

Mineral	Grainsize	Grain shape	Composition
Pyrite	500um to a few microns	anhedral	2%
Pyrrhotite	50um	anhedral	trace
Pentlandite	10um	anhedral	trace
Iron oxide	submicron	anhedral	Trace amount
Chalcopyrite	A few microns in size	Anhedral	Trace amount
Calcite	1mm to submicron	anhedral	8%
Quartz	800um to submicron	anhedral	36%
Epidote	100um to submicron	anhedral	25%
Biotite	1.3mm to submicron	Subhedral to anhedral	4%
Rutile	100 to submicron	anhedral	1%
Actinolite-tremolite	250um to a few microns	acicular	20%
Chlorite	250um to a few microns	anhedral	3%
Ilmenite	A few microns	anhedral	trace
Scheelite	250um to a few microns	anhedral	1%

- Pyrite inclusions
    - Epidote
    - Quartz

Slide NB036 – NW-SE Transect

Mineral	Grainsize	Grain shape	Composition
Pyrite	500um to a few microns	anhedral	2%
Quartz	2mm to submicron	anhedral	20%
Albite			19%
Calcite	3mm to submicron	anhedral	15%
Chalcopyrite	3mm	anhedral	2%
Muscovite	A few microns to submicorn	Anhedral or bladed	3%
Epidote	200um to submicron	anhedral	4%
Biotite	150 to submicron	Anhedral to subhedral	10%
Ilmenite	700um to a few microns	Some euhedral and subhedral, mostly anhedral	10%
Chlorite	800um to submicron	Acicular or anhedral	15%
Galena	A few microns	Anhedral	trace
Apatite	A few microns	Anhedral	trace
Titanite	A few microns	Anhedral	Trace

- Two veins perpendicular to each other
    - The main vein is parallel to foliation
- The smaller vein containing pyrite and rutile and is perpendicular and cross cuts foliation
        - The chlorite grains at the vein selvage wrap around the vein
        - Younger vein and foliation – chlorite/biotite and rutile grains at the vein selvage at some locations
- Majority of biotite has altered into chlorite

Vein:

Mineral	Grainsize	Grain shape	Composition
Pyrite	500um to a few microns	anhedral	1%
Quartz	2mm to submicron	anhedral	5%
Albite			60%
Calcite	3mm to submicron	anhedral	18%
Chalcopyrite	3mm	anhedral	3%
Muscovite	A few microns to submicorn	Anhedral or bladed	1%
Epidote	200um to submicron	anhedral	5%
Ilmenite	700um to a few microns	Some euhedral and subhedral, mostly anhedral	3%
Chlorite	800um to submicron	Acicular or anhedral	4%
Galena	A few microns	Anhedral (i)	trace
Apatite	A few microns	Anhedral (i)	trace
Titanite	A few microns	Anhedral (v)	Trace

- Pyrite inclusion
    - Galena
    - Quartz
    - Apatite

Slide 488 – Pit

Mineral	Grainsize	Grain shape	Composition
Pyrite	4mm to a few microns	Subhedral to anhedral	10%
Calcite-Dolomite	2mm to a few microns	anhedral	10%
Iron oxide	submicron	Anhedral	5%
Hornblende	1mm to a few microns	Subhedral to anhedral	15%
Epidote	300um to a few microns	anhedral	3%
Biotite	1mm to submicron	Subhedral to anhedral	25%
Albite	600um to submicron	anhedral	3%
Quartz	600um to submicron	anhedral	30%
Chalcopyrite	50um to a few microns	anhedral	Trace amount
Bornite	A few microns to submicron	Anhedral	Trace amount
Unknown mineral of U, Ti, Pb, Sr, Cr and Fe	A few microns	anhedral	Trace amount
Galena	A few microns to submicron	anhedral	Trace amount

- Vein here is parallel to foliation
- Usually find accumulation at vein selvage with large biotite grains, not found here
    - Here they contain higher concentrations of carbonates and a zone of fine grained quartz (with some submicron biotite grains, 100-50um carbonates and a few large quartz grains)
    - This region, as well as some of the host rock distal to the vein, do not contain arfvedsonite or even large grains of biotite.
- Iron oxide is found within the vein as well as within the host rock just outside the proximal zone of host rock to the vein
- Epidote found within the host rock
- Edges of pyrite associated with chalcopyrite

Vein:

Mineral	Grainsize	Grain shape	Composition
Pyrite	4mm to a few microns	Subhedral to anhedral	20%
Calcite-Dolomite	2mm to a few microns	anhedral	15%
Iron oxide	submicron	Anhedral	10%
Biotite	A few microns	Subhedral to anhedral	5%
Albite	600um to submicron	anhedral	10%
Quartz	600um to submicron	anhedral	40%
Chalcopyrite	50um to a few microns	anhedral	Trace amount
Bornite	A few microns to submicron	Anhedral	Trace amount
Unknown mineral of U, Ti, Pb, Sr, Cr and Fe	A few microns	anhedral	Trace amount
Galena	A few microns to submicron	anhedral	Trace amount

- Bornite inclusions within iron oxide surrounding grain A
- Pyrite inclusions
    - Epidote
    - Chalcopyrite
    - Galena
    - Bornite
    - biotite

Slide 490 – Pit

Thin section:

Mineral	Grainsize	Grain shape	Composition
Pyrite	3mm to a few microns	Euhedral to anhedral	5%
Iron oxide	Submicron	anhedral	2%
Biotite	500um to a few microns		39%
Chlorite	100um to a few microns	anhedral	3%
Quartz	1.5mm to submicron	anhedral	40%
Albite	2mm to 0.250um	anhedral	10%
Calcite	100um	Anhedral	trace
Monazite	A few microns	anhedral	trace
Fluorocarbonate	A few microns	anhedral	trace
Galena	A few microns	anhedral	trace
Muscovite	A few microns	subhedral	1%

- Vein is subparallel to foliation running diagonally across the slide and biotite grains wrap approximately around the vein
- There is a greater concentration of biotite for most of the host rock, the most distal regions are less concentrated in biotite
- The vein selvages are concentrated in larger biotite grains at some areas, in others they are more concentrated in fine grained quartz
- There are a few biotite grains as well as chlorite – alteration product of biotite within the vein. They aren't elongated along any direction in particular – multiple directions

Vein:

Mineral	Grainsize	Grain shape	Composition
Pyrite	3mm to a few microns	Euhedral to anhedral	10%
Iron oxide	Submicron	anhedral	5%
Biotite	500um to a few microns	Euhedral to anhedral	4%
Chlorite	100um to a few microns	anhedral	10%
Quartz	1.5mm to submicron	anhedral	39%
Albite	2mm to 0.250um	anhedral	30%
Calcite	100um	Anhedral	1%
Muscovite	A few microns	subhedral	1%
Monazite	A few microns	anhedral	trace

Fluorocarbonate	A few microns	anhedral	trace
Galena	A few microns	anhedral	trace

- Pyrite :
  - Biotite and quartz inclusion
  - Cpy inclusion
  - Galena inclusion
  - Albite inclusion
- Fluorocarbonate within the vein
- Galena along the sides of pyrite

Appendix D: EPMA Analysis

D1. Average error percent for each element during EPMA analysis

Element	Average Error %
Cu	653
Mg	726
As	443
Si	230
Pb	88
Ti	1127
Ni	540
W	1028
Co	42
S	622
Fe	0

D2. Elemental standards and crystals used for pyrite grains for EPMA. Fe and S are measured with Energy Dispersive Spectrometer.

Element	Crystals	Compound	Standard
Cu	TAP	Copper Metal	Astimex MetM25-44 standard block
Mg	TAP	Hornblende	Smithsonian USNM 143965
As	TAP	Gallium Arsenide	Astimex MetM25-44 standard block
Pb	PETj	Lead metal	Astimex MetM25-44 standard block
Ti	PETj	Rutile	Unknown origin
Ni	LIFH	Nickel metal	Astimex MetM25-44 standard block
W	LIFL	Tungsten metal	Astimex MetM25-44 standard block
Co	LIFL	Cobalt metal	Astimex MetM25-44 standard block
Fe, S	EDS	Pyrite	Astimex MinM25-53 standard block

D3. EPMA mass percent measurement for each element in pyrite grains

Comment	Cu (Mass%)	Mg (Mass%)	As (Mass%)	Si (Mass%)	Pb (Mass%)	Ti (Mass%)	Ni (Mass%)	W (Mass%)	Co (Mass%)	Fe (Mass%)	S (Mass%)	Total (Mass%)
168A-GrainC-01	0.02	0.02	0.02	0.04	0.12	0.01	0.78	0.06	0.15	45.1	52.8	99.1
168A-GrainC-02	0.03	0.08	0.02	0.01	0.06	0.01	0.01	0.03	0.06	46.3	53.1	99.5
168A-GrainC-03	0.08	0.06	0.04	0.01	0.09	<LOD	0.012	<LOD	0.035	46.16	52.98	99.317
168A-GrainC-04	<LOD	0.008	0.029	0.013	0.144	0	0.006	0.072	0.056	46.226	53.047	99.505
168A-GrainC-05	0.001	<LOD	0.012	0.015	0.135	0.003	<LOD	0.178	0.059	46.136	53.274	99.802
168A-GrainC-06	0.018	<LOD	0.001	0.02	0.126	0.002	0.001	0.123	0.066	46.144	53.085	99.581
168A-GrainC-07	<LOD	0.009	0.042	0.008	0.191	<LOD	<LOD	0.053	0.037	46.406	53.357	100.043
168A-GrainC-08	<LOD	0.006	0.019	0.013	0.126	0.038	0.797	0.066	0.053	45.288	53.095	99.481
168A-GrainC-09	<LOD	0.015	0.035	0.109	0.142	<LOD	0.032	0.028	0.044	45.557	52.187	98.104
168A-GrainC-10	0.029	0	0.03	0.005	<LOD	<LOD	0.073	0.047	0.043	46.126	53.266	99.802
3415A-GrainA-01	<LOD	0.004	0.007	0.008	0.205	0.008	0.016	0.03	0.084	45.992	52.792	99.114
3415A-GrainA-02	0.067	0.002	0.033	0.007	0.201	0.004	0.063	<LOD	0.166	45.719	52.89	99.143
3415A-GrainA-03	0.05	0.001	0.022	0.011	0.142	0.006	0.022	0.015	0.032	46.129	53.005	99.435

3415A-GrainA-04	<LOD	<LOD	0.011	0.005	0.091	<LOD	0.009	0.025	0.042	46.191	52.85	99.184
3415A-GrainA-05	0.003	<LOD	<LOD	0.005	0.136	0.004	0.025	<LOD	0.033	45.989	52.914	99.073
3415A-GrainA-06	0.006	0.007	0.009	0.011	0.117	<LOD	0.016	0.085	0.056	46.173	53.108	99.585
3415A-GrainA-07	0.044	<LOD	0.015	0.01	0.133	0.009	0.028	0.125	0.16	46.091	53.093	99.705
3415A-GrainA-08	<LOD	0.001	0.02	0.008	0.147	<LOD	0.018	0.084	0.059	46.077	53.114	99.478
3415A-GrainA-09	<LOD	0.006	0.027	<LOD	0.127	<LOD	0.015	0.171	0.065	46.181	53.131	99.7
3415A-GrainA-10	<LOD	0.001	0.011	<LOD	0.12	0.001	0.06	<LOD	0.044	46.84	53.602	100.541
153A-GrainC-01	<LOD	<LOD	41.74	0.028	0.239	0.004	3.685	0.078	24.798	8.602	22.815	100.831
153A-GrainC-02	<LOD	<LOD	1.642	0.009	0.185	<LOD	0.359	<LOD	2.04	43.81	51.572	98.63
153A-GrainC-03	<LOD	<LOD	0.016	0.013	0.129	0.007	0	0.063	6.046	40.587	52.806	99.652
153A-GrainC-04	0.03	<LOD	0.014	0.006	0.152	0.008	0.569	<LOD	0.047	45.8	53.099	99.679
153A-GrainC-05	0.008	-0.008	0.008	0.017	0.136	0.003	0.41	<LOD	0.044	46.13	53.16	99.843
153A-GrainC-06	<LOD	<LOD	0.574	0.015	0.166	0	1.07	<LOD	0.083	45.031	52.402	99.194
153A-GrainC-07	0.026	<LOD	0.209	0.015	0.204	<LOD	1.361	0.082	0.057	44.794	53.051	99.78
153A-GrainC-08	<LOD	<LOD	0.018	0.012	0.167	0.013	0.146	<LOD	0.053	46.168	53.028	99.071

153A-GrainC-09	<LOD	0.006	0.017	0.029	0.129	<LOD	-<LOD	<LOD	0.043	46.5	53.119	99.77
153A-GrainC-10	-<LOD	0.002	0.146	0.054	0.104	<LOD	<LOD	0.122	0.052	46.001	53.095	99.507
886B-GrainA-01	0.039	0.004	0.018	0.011	0.183	0	0.014	0.145	1.208	45.368	53.068	100.058
886B-GrainA-02	<LOD	0	0.006	0.014	0.074	<LOD	0.02	0.145	2.196	44.169	53.169	99.777
886B-GrainA-03	0.009	<LOD	0.007	0.015	0.092	<LOD	0.272	<LOD	0.062	60.278	38.593	99.303
886B-GrainA-04	<LOD	<LOD	0.016	0.005	0.117	0.008	0.006	0.049	0.054	62.906	36.246	99.366
886B-GrainA-05	<LOD	0.002	0.043	0.015	0.125	<LOD	0.132	0.002	0.062	61.969	36.942	99.272
886B-GrainA-06	<LOD	0.011	0.023	0.014	0.145	<LOD	0.301	0.196	0.064	60.381	38.512	99.596
886B-GrainA-07	<LOD	<LOD	0.022	0.01	0.041	<LOD	0.325	<LOD	0.059	60.236	38.35	98.863
886B-GrainA-08	<LOD	0.001	0.03	0.016	0.097	<LOD	<LOD	0.014	0.066	62.583	36.281	99.026
886B-GrainA-09	<LOD	0.002	0.041	0.021	0.095	<LOD	0.008	0.267	0.082	62.649	36.189	99.27
886B-GrainA-10	0.002	<LOD	0.03	0.092	0.071	<LOD	0.875	<LOD	0.076	59.074	38.315	98.417
NB036-GrainB-01	<LOD	<LOD	0.804	0.009	0.165	0.002	0.296	0.041	1.87	44.406	52.688	100.208
NB036-GrainB-02	0.071	<LOD	0.797	0.008	0.139	<LOD	0.266	<LOD	2.012	44.032	52.725	99.884
NB036-GrainB-03	0.09	<LOD	0.494	0.01	0.132	<LOD	0.549	0.028	1.283	44.793	52.972	100.325

NB036-GrainB-04	0.094	<LOD	0.409	0.003	0.115	<LOD	0.638	<LOD	1.032	44.819	53.054	100.053
NB036-GrainB-05	<LOD	<LOD	0.027	0.011	0.208	0	2.702	0.084	0.091	43.748	53.336	100.157
NB036-GrainB-06	0.039	<LOD	0.079	0.013	0.157	0.009	1.117	<LOD	0.515	44.647	53.319	99.801
NB036-GrainA-01	<LOD	0.008	0.069	0.015	0.007	<LOD	0.027	0.059	0.053	68.105	0	68.29
NB036-GrainA-02	<LOD	<LOD	0.047	0.015	0.017	<LOD	0.007	0.068	0.076	68.065	0	68.265
NB036-GrainA-03	<LOD	0.002	0.028	0.009	0.179	<LOD	0.01	<LOD	0.081	46.345	53.163	99.753
NB036-GrainA-04	0.029	0.001	0.01	0.002	0.184	<LOD	0.028	0.058	0.461	45.845	53.125	99.732
NB036-GrainA-05	0.01	0.002	0.009	0.001	0.147	<LOD	<LOD	0.121	0.055	45.905	53.245	99.485
NB036-GrainA-06	0.021	<LOD	<LOD	<LOD	0.168	<LOD	<LOD	0.022	0.39	46.16	53.356	100.1
NB036-GrainA-07	0.069	0.003	0.008	0.002	0.107	<LOD	<LOD	0.066	0.103	46.395	53.288	100.017
NB036-GrainA-08	0.082	<LOD	0.004	0.01	0.149	0.006	0.005	<LOD	0.074	46.731	53.497	100.532
490-GrainA-01	0.072	0.003	0.021	0.001	0.22	0.011	0.03	0.038	0.089	46.213	53.023	99.721
490-GrainA-02	0.037	<LOD	0.017	0.006	0.17	<LOD	0.009	0.141	0.071	46.44	53.494	100.377
490-GrainA-03	<LOD	0.006	0.022	0.007	0.081	<LOD	0.021	<LOD	0.062	46.479	53.248	99.814
490-GrainA-04	<LOD	0.005	0.036	<LOD	0.155	0.002	0.016	0.006	0.04	46.424	53.409	100.075

490-GrainA-05	0.01	0.005	0.004	<LOD	0.177	<LOD	<LOD	<LOD	0.037	46.206	53.275	99.551
490-GrainA-06	0.003	0	0.029	0.008	0.14	<LOD	0.007	0.049	0.049	46.439	53.3	100.023
490-GrainA-07	0.018	<LOD	0.036	<LOD	0.1	0.005	0.002	0.415	0.044	46.141	53.342	100.099
490-GrainA-08	<LOD	0.004	0.013	0.003	0.056	<LOD	0.025	0.02	0.071	42.944	0.066	43.124
157-GrainA-01	0.002	<LOD	0.031	0.002	0.186	<LOD	0.033	<LOD	0.184	46.006	53.17	99.495
157-GrainA-02	0.02	<LOD	0.042	<LOD	0.117	<LOD	0.025	<LOD	0.212	45.997	53.057	99.32
157-GrainA-03	<LOD	0.002	0.009	0.001	0.139	<LOD	0.001	<LOD	0.284	45.952	53.086	99.358
157-GrainA-04	<LOD	0.003	0.006	0.003	0.164	0.001	<LOD	0.058	0.038	46.094	53.237	99.583
157-GrainA-05	0.009	<LOD	0.02	0.005	0.163	<LOD	0.02	0.098	0.038	46.354	53.167	99.863
157-GrainA-06	<LOD	0.002	0.007	0.007	0.13	<LOD	0.017	0.068	0.04	46.473	53.261	99.959
157-GrainA-07	0.029	0.006	0.021	0	0.136	0.004	0.001	<LOD	0.066	46.257	53.114	99.487
157-GrainA-08	<LOD	<LOD	0.056	0.01	0.17	0.012	0.019	0.194	0.566	45.956	53.11	100.012
154-GrainA-01	0	0.002	0.011	0.009	0.158	0.002	0.022	0.125	0.045	45.862	53.123	99.359
154-GrainA-02	0.018	0.007	0.03	<LOD	0.188	0.009	0.046	0.107	0.066	46.078	52.973	99.521
154-GrainA-03	0.031	<LOD	0.02	0.006	0.147	0.008	0.01	0.03	0.039	46.307	53.035	99.63

154-GrainA-04	<LOD	<LOD	0.015	0.001	0.156	<LOD	<LOD	<LOD	0.058	46.09	52.663	97.542
154-GrainA-05	<LOD	<LOD	0.012	0.002	0.125	0.001	0.027	0.121	0.049	46.151	53.114	99.573
154-GrainA-06	0.087	0.002	0.023	0.011	0.125	0.005	0.107	<LOD	0.043	45.923	52.943	99.192
154-GrainA-07	<LOD	<LOD	0.025	0.009	0.09	<LOD	0.021	<LOD	0.095	45.976	52.989	98.61
154-GrainA-08	<LOD	<LOD	0.018	<LOD	0.064	<LOD	0.022	0.085	0.044	46.109	53.147	99.46
154-GrainA-09	0.048	0.006	0.009	0	0.143	<LOD	0.038	0.765	0.043	45.885	53.321	100.242
154-GrainA-10	0.081	<LOD	0.028	<LOD	0.175	0.005	0.02	0.087	0.052	46.034	53.084	99.556
895B-GrainA-01	<LOD	<LOD	0.023	0.007	0.155	0.011	0.013	<LOD	0.084	46.498	53.058	98.639
895B-GrainA-02	<LOD	0	0.014	0.006	0.168	0.003	0.008	0.021	0.08	46.549	53.309	100.133
895B-GrainA-03	<LOD	0	0.022	0.007	0.153	0.01	0.005	0.064	0.049	46.587	53.3	100.187
895B-GrainA-04	0.004	<LOD	0.003	0.014	0.186	<LOD	0.004	<LOD	0.077	46.5	53.401	100.117
895B-GrainB-01	0.082	<LOD	0	<LOD	0.119	<LOD	<LOD	<LOD	0.061	46.301	53.154	99.643
895B-GrainB-02	<LOD	0.005	0.019	0.855	0.116	0	<LOD	0.017	0.053	48.727	27.562	77.279
895B-GrainB-03	<LOD	<LOD	0.016	0.006	0.167	0.001	0.011	<LOD	0.075	46.247	53.265	99.699
895B-GrainB-04	<LOD	0.006	0.018	<LOD	0.195	<LOD	0	0.058	0.077	46.224	53.25	99.815

895B-GrainB-05	0.065	<LOD	0.046	<LOD	0.194	<LOD	0.034	0.07	0.074	46.31	53.268	100.037
895B-GrainB-06	0.028	<LOD	0.028	<LOD	0.143	0.012	0.02	0.12	0.059	46.391	53.316	100.109
895B-GrainB-07	<LOD	<LOD	0.022	0.003	0.12	0	0.035	0.073	0.105	60.44	38.344	99.112
164B-GrainC-01	<LOD	0.001	0.035	0.006	0.177	0.001	0.105	0.115	0.195	46.08	53.068	99.685
164B-GrainC-02	<LOD	<LOD	<LOD	39.015	<LOD	0.008	0.002	<LOD	0.012	0.292	0.085	38.437
164B-GrainC-03	<LOD	0	0.006	0.013	0.174	<LOD	0.007	0.027	2.539	43.961	53.235	99.931
164B-GrainC-04	0.037	<LOD	0	0.011	0.146	0.002	<LOD	<LOD	2.74	43.484	53.001	99.043
164B-GrainC-05	<LOD	<LOD	0.022	0.012	0.102	<LOD	<LOD	<LOD	2.8	43.438	53.052	99.336
164B-GrainC-06	0.01	<LOD	0	0.015	0.178	<LOD	0.122	0.14	0.063	60.409	38.465	99.379
164B-GrainC-07	<LOD	0.006	0.03	0.006	0.128	<LOD	0.136	0.068	0.065	60.498	38.443	99.284
164B-GrainC-08	0.009	0.003	0.011	0.009	0.158	<LOD	0.141	<LOD	0.064	60.021	38.509	98.845
164B-GrainC-09	<LOD	<LOD	0.005	0.01	0.116	<LOD	0.147	0.112	0.065	60.505	38.563	99.461
164B-GrainC-10	<LOD	<LOD	0.031	0.015	0.095	<LOD	0.158	<LOD	0.07	60.41	38.405	99.019
162-GrainA-01	0.011	0	0.018	0.028	0.19	0.014	0.005	0.05	0.047	45.778	53.244	99.385
162-GrainA-02	<LOD	<LOD	0.037	0.015	0.141	<LOD	<LOD	0.096	0.044	45.788	53.04	99.093

162-GrainA-03	0.043	0.007	<LOD	0.014	0.18	0.001	<LOD	<LOD	0.056	45.833	52.971	98.969
162-GrainA-04	0.05	0.005	0.004	0.012	0.16	0.003	0.011	0.07	0.042	45.776	52.925	99.058
162-GrainA-05	0.025	0.001	0.006	0.003	0.223	<LOD	<LOD	0.11	0.054	45.709	52.859	98.976
162-GrainA-06	<LOD	0.006	0.012	0.007	0.16	<LOD	<LOD	<LOD	0.026	45.874	52.834	98.76
162-GrainA-07	<LOD	0.002	0.009	0.055	0.176	<LOD	0.122	<LOD	0.069	45.458	52.746	98.566

D.4 EPMA error percent measurement for each element in pyrite grains

Comment	Cu (Error%)	Mg (Error%)	As (Error%)	Si (Error%)	Pb (Error%)	Ti (Error%)	Ni (Error%)	W (Error%)	Co (Error%)	W (Error%)	Fe (Error%)	Total (Error%)
168A-GrainC-01	300	300	222.98	31.58	73.39	185.1	5.65	1202.71	18.99	441.6	0	2782
168A-GrainC-02	300	196.61	159.07	81.04	141.44	300	2502.61	351.45	42.5	7781.14	0	11855.86
168A-GrainC-03	135.73	244.8	76.53	101.42	103.45	300	260.97	300	77.18	300	0	1900.08
168A-GrainC-04	300	182.48	128.35	83.9	67.62	300	508.85	294.89	48.05	294.86	0	2209
168A-Grai	7753.3	300	315.68	74.7	70.8	826.16	300	1073.83	46.17	228.15	0	10988.79

nC-05												
168A-GrainC-06	642.17	300	6068.16	57.53	79.14	892.4	2808.84	139.72	41.03	300	0	11328.99
168A-GrainC-07	300	178.46	88.18	147.41	51.3	300	300	263.73	73.26	774.27	0	2476.61
168A-GrainC-08	300	252.73	195.54	85.21	77.82	58.57	5.6	429.31	50.92	300	0	1755.7
168A-GrainC-09	300	100.76	103.18	11.96	65.74	300	100.34	786.41	60.86	751.66	0	2580.91
168A-GrainC-10	402.83	300	121.66	216.62	51.21	300	46.14	282.79	63.34	300	0	2084.59
3415A-GrainA-01	300	342.17	511.46	144.04	44.42	253.59	199.68	619.86	32.46	300	0	2747.68
3415A-GrainA-02	171.37	891.67	110.72	170.33	47.46	581.52	52.14	300	17.38	3007.31	0	5349.9
3415A-GrainA-03	233.78	2418.88	166.21	102.71	68.04	331.26	141.73	952.95	83.27	300	0	4798.83
3415A-Grai	300	300	329.57	228.22	106.79	300	333.52	1085.59	65.79	834.34	0	3883.82

nA-04												
3415A-GrainA-05	3593.9	300	300	220.77	66.91	569.46	130.34	300	81.77	300	0	5863.15
3415A-GrainA-06	1872.32	208.13	387.19	100.36	82.26	300	202.73	153.98	47.73	2524.71	0	5879.41
3415A-GrainA-07	256.61	300	247.7	111.81	70.79	226.58	114.53	104.72	18.47	300	0	1751.21
3415A-GrainA-08	300	1077.28	177.07	139.54	64.66	300	180.3	351.8	45.47	246.48	0	2882.6
3415A-GrainA-09	300	246.75	135.38	300	75.71	300	214.68	253.7	41.81	300	0	2168.03
3415A-GrainA-10	300	1459.79	329.92	300	82.21	3489.87	54.93	300	60.63	296.08	0	6673.43
153A-GrainC-01	300	300	0.71	52.59	46.12	501.71	1.94	190.94	0.69	476.58	0	1871.28
153A-GrainC-02	300	300	4.32	129.76	50.26	300	10.54	300	2.79	181.25	0	1578.92
153A-Grai	300	300	234.2	89.78	73.9	284.16	21132.39	248.6	1.51	429.3	0	23093.84

nC-03												
153A-GrainC-04	376.84	300	259.87	189.83	62.46	247.15	7.29	300	57.19	300	0	2100.63
153A-GrainC-05	1559.31	300	447.43	67.1	70.27	743.2	9.51	300	60.11	300	0	3856.93
153A-GrainC-06	300	300	8.99	74.71	57.95	4997.39	4.5	300	33.65	300	0	6377.19
153A-GrainC-07	458.5	300	19.65	74.4	45.64	300	3.82	196.75	47.37	317.52	0	1763.65
153A-GrainC-08	300	300	203.25	98.34	58.23	159.48	23.6	300	50.39	297.93	0	1791.22
153A-GrainC-09	300	258.76	209.74	39.36	74.65	300	300	300	62.94	300	0	2145.45
153A-GrainC-10	300	661.85	27.6	22.66	94.5	300	300	289.38	51.56	174.11	0	2221.66
886B-GrainA-01	288.42	351.12	204.52	100.91	54.04	14351.28	232.12	436.85	3.9	175.45	0	16198.61
886B-Grai	300	3554.28	605.11	82.53	127.59	300	156.14	118.51	2.68	300	0	5546.84

nA-02												
886B-GrainA-03	1499.65	300	545.37	82.61	105.19	300	13.77	300	44.48	300	0	3491.07
886B-GrainA-04	300	300	248.46	235.15	81.46	274.05	506.35	371.07	51.22	300	0	2667.76
886B-GrainA-05	300	1089.36	91.41	82.6	73.71	300	26.11	5588.11	44.98	300	0	7896.28
886B-GrainA-06	300	157.24	168.31	84.57	63.08	300	12.37	3664.57	43.54	400.21	0	5193.89
886B-GrainA-07	300	300	182.96	122.95	238.39	300	11.79	300	46.64	948.67	0	2751.4
886B-GrainA-08	300	1746.8	134.83	76.77	96.25	300	300	1124.87	41.88	1906.18	0	6027.58
886B-GrainA-09	300	692.25	95.17	59.43	98.93	300	413.4	2962.36	34.02	300	0	5255.56
886B-GrainA-10	6027.21	300	129.85	14.43	137.77	300	5.22	300	36.84	215.59	0	7466.91
NB036-Grai	300	300	7.04	125.52	57.53	1088.1	12.75	329.4	2.94	2232.43	0	4455.71

nB-01												
NB036-GrainB-02	165.26	300	7.03	133.95	68.7	300	13.73	300	2.81	300	0	1591.48
NB036-GrainB-03	129.62	300	9.86	117.91	73.75	300	7.49	892.94	3.74	300	0	2135.31
NB036-GrainB-04	130.11	300	11.79	368.75	85.81	300	6.55	300	4.32	300	0	1807.33
NB036-GrainB-05	300	300	140.13	103.66	46.32	24052.7	2.43	159.23	30.94	300	0	25435.41
NB036-GrainB-06	315.1	300	47.48	90.17	62.55	234.76	4.35	300	7.05	300	0	1661.46
NB036-GrainA-01	300	232.59	62.73	81.43	1107.6	300	112.62	390.54	47.94	300	0	2935.45
NB036-GrainA-02	300	300	91.1	81.37	481.28	300	450.24	233.93	33.03	300	0	2570.95
NB036-GrainA-03	300	944.28	131.21	127.49	54.88	300	311.81	300	33.07	622.65	0	3125.39
NB036-Grai	405.66	1389.78	385.19	465.88	52.13	300	113.45	237.7	7.65	901.05	0	4258.49

nA-04												
NB036-GrainA-05	1230.2	804.4	405.73	2034.6	63.9	300	300	268.09	49.77	172.9	0	5629.59
NB036-GrainA-06	563.23	300	300	300	59.17	300	300	1398.58	8.64	957.48	0	4487.1
NB036-GrainA-07	169.29	550.79	453.44	666.65	91.78	300	300	868.64	26.83	300	0	3727.42
NB036-GrainA-08	142	300	1031.82	117.69	65.49	383.65	624.83	300	37.48	991.79	0	3994.75
490-GrainA-01	163.9	565.76	173.06	755.32	43.35	196.57	108.48	549.64	31.3	566.52	0	3153.9
490-GrainA-02	312.94	300	208.83	184.01	56.36	300	349.43	323.1	38.71	300	0	2373.38
490-GrainA-03	300	268.87	166.87	154.82	121.74	300	152.66	300	43.11	300	0	2108.07
490-GrainA-04	300	339.9	97.21	300	62.06	1121.98	194.96	2224.89	67.93	300	0	5008.93
490-GrainA-05	1145.85	285.18	826.13	300	52.61	300	300	300	72.9	270.72	0	3853.39
490-GrainA-06	3539.55	13590.13	127.23	132.74	70.1	300	450.23	281.35	54.29	300	0	18845.62

490-GrainA-07	654.74	300	100.6	300	97.04	422.87	1520.16	3389.28	62.52	300	0	7147.21
490-GrainA-08	300	401.01	305.65	383.77	123.66	300	106.67	567.5	31.6	1734.9	0	4254.76
157-GrainA-01	6258.26	300	117.21	581.13	50.9	300	99.72	300	16.09	300	0	8323.31
157-GrainA-02	562.16	300	86.46	300	83.83	300	125.97	300	14.27	606.39	0	2679.08
157-GrainA-03	300	702.48	407.77	894.43	67.93	300	4658.47	300	11.16	495.85	0	8138.09
157-GrainA-04	300	439.85	592.55	339.58	58.85	3223.86	300	227.29	69.96	300	0	5851.94
157-GrainA-05	1263.77	300	184.65	220.43	61.35	300	160.13	475.87	70.27	300	0	3336.47
157-GrainA-06	300	750.5	545.13	171.66	74.15	300	191.87	191.87	66.51	3248.81	0	5840.5
157-GrainA-07	398.48	259.4	179.4	300	71.48	484.52	5387.86	300	40.69	143.71	0	7565.54
157-GrainA-08	300	300	65.25	112.63	56.3	172.66	164.24	153.55	6.5	106.7	0	1437.83
154-GrainA-01	300	678.37	317.85	124.06	61.09	1032.39	147.54	105.95	59.01	853.36	0	3679.62
154-Grai	646.1	208.32	121.15	300	51.07	232.79	70.92	174.74	40.33	211.77	0	2057.19

nA-02												
154-GrainA-03	381.57	300	183.47	189.81	66.32	277.36	328.8	571.43	69.08	824.73	0	3192.57
154-GrainA-04	300	300	245.29	1052.81	62.96	300	300	300	46.85	300	0	3207.91
154-GrainA-05	300	300	325	748.16	78.29	3625.33	119.43	312.57	55.4	179	0	6043.18
154-GrainA-06	135.88	813.92	156.88	102.59	77.17	461.83	31.47	300	62.4	300	0	2442.14
154-GrainA-07	300	300	147.5	129.7	110.02	300	152.3	300	30.09	300	0	2069.61
154-GrainA-08	300	300	211.09	300	157.23	300	146.14	204.39	61.42	300	0	2280.27
154-GrainA-09	246.19	255.48	410.09	2339.16	66.89	300	86.35	55268.84	62.11	758.95	0	59794.06
154-GrainA-10	143.4	300	131.67	300	54.63	391.43	162.12	498.68	52.04	255.27	0	2289.24
895B-GrainA-01	300	300	162.1	166.31	60.84	195.54	240.03	300	32.77	213.64	0	1971.23
895B-GrainA-02	300	4368.24	275.41	195.66	57.59	636.31	387.71	802.59	35.64	1166.83	0	8225.98
895B-	300	7503.85	161.2	168.91	63.08	218.02	682.86	203.77	55.76	300	0	9657.45

GrainA-03												
895B-GrainA-04	2719.14	300	1490.89	80.96	53.56	300	736.17	300	36.4	381.26	0	6398.38
895B-GrainB-01	144.11	300	300	300	82.81	300	300	300	44.15	1068.54	0	3139.61
895B-GrainB-02	300	283.04	197.04	2.64	74.57	16776.28	300	734.95	48.17	300	0	19016.69
895B-GrainB-03	300	300	228.13	179.58	58.23	1947.1	276.28	300	36.73	1470.93	0	5096.98
895B-GrainB-04	300	276.02	203.23	300	50.36	300	300	239.49	34.61	300	0	2303.71
895B-GrainB-05	179.97	300	79.46	300	49.4	300	95.58	215.83	37.69	447.94	0	2005.87
895B-GrainB-06	421.56	300	133.81	300	67.13	171.23	164.18	112.42	46.22	688.35	0	2404.9
895B-GrainB-07	300	300	178.03	472.6	79.94	11605.15	93.89	256.91	27.08	300	0	13613.6
164B-Grai	300	1355.77	104.28	189.05	55.5	1787.6	32.01	350.55	15.44	300	0	4490.2

nC-01												
164B-GrainC-02	300	300	300	0.3	300	209.06	1024.1	300	152.75	182.15	0	3068.36
164B-GrainC-03	300	4067.09	686.35	90.93	54.4	300	481.47	1240.26	2.46	300	0	7522.96
164B-GrainC-04	316.34	300	7495.35	103.96	65.89	878.05	300	300	2.35	300	0	10061.94
164B-GrainC-05	300	300	166.31	94.66	94.53	300	300	300	2.32	300	0	2157.82
164B-GrainC-06	1285.47	300	7899.77	82.82	53.29	300	27.74	149.51	43.73	153.77	0	10296.1
164B-GrainC-07	300	305.38	131.27	206.12	72.59	300	25.72	340.72	42.95	314.12	0	2038.87
164B-GrainC-08	1428.74	533.63	351.9	137.2	60.7	300	24.9	300	43.89	300	0	3480.96
164B-GrainC-09	300	300	737.25	124.3	83.71	300	23.89	120.89	42.27	300	0	2332.31
164B-Grai	300	300	123.13	80.51	99.56	300	22.27	300	40.28	300	0	1865.75

nC-10												
162-GrainA-01	1013.38	300	203.27	41.39	50.01	153.21	699.3	265.39	57.6	1507.73	0	4291.28
162-GrainA-02	300	300	97.46	78.07	69.14	300	300	136.77	61.69	300	0	1943.13
162-GrainA-03	269.73	207.63	300	80.57	52.64	1809.56	300	300	47.05	300	0	3667.18
162-GrainA-04	224.87	296.25	920.32	91.36	60.81	694.86	286.03	189.1	64.43	1149.66	0	3977.69
162-GrainA-05	473.57	2029.62	636.34	404.19	44.65	300	300	119.25	49.26	300	0	4656.88
162-GrainA-06	300	265.93	321.97	171.51	59.6	300	300	300	102.07	344.19	0	2465.27
162-GrainA-07	300	653.02	431.28	22.15	56.18	300	27.81	300	38.6	3655.03	0	5784.07

D.5. Mass% averages, minimums, maximums and rages for cobalt in pyrite

Sample	Co(Mass %)	Co Mass % avg	Co Mass % Min	Co Mass % Max	Range
168A Grain C	0.156	0.16	0.03	0.15	0.12
	0.063				
	0.035				
	0.056				
	0.059				
	0.066				
	0.037				
	0.053				
	0.044				
	0.043				

3415A Grain A	0.084	0.07	0.03	0.17	0.13
	0.166				
	0.032				
	0.042				
	0.033				
	0.056				
	0.16				
	0.059				
	0.065				
	0.044				
153A Grain C	24.798	3.3	0.04	24.8	24.8
	2.04				
	6.046				
	0.047				
	0.044				
	0.083				
	0.057				
	0.053				
	0.043				
	0.052				
886B Grain A	1.208	0.4	0.05	2.2	2.1
	2.196				
	0.062				
	0.054				
	0.062				
	0.064				
	0.059				
	0.066				
	0.082				
	0.076				
NB036 Grain B	1.87	1.1	0.1	2.0	1.9
	2.012				
	1.283				
	1.032				
	0.091				
	0.515				
NB036 Grain A	0.053	0.2	0.05	0.5	0.4
	0.076				
	0.081				
	0.461				
	0.055				

	0.39				
	0.103				
	0.074				
490 Grain A	0.089	0.06	0.04	0.09	0.05
	0.071				
	0.062				
	0.04				
	0.037				
	0.049				
	0.044				
	0.071				
157 Grain A	0.184	0.18	0.04	0.6	0.5
	0.212				
	0.284				
	0.038				
	0.038				
	0.04				
	0.066				
	0.566				
154-GrainA-01	0.045	0.05	0.04	0.1	0.06
	0.066				
	0.039				
	0.058				
	0.049				
	0.043				
	0.095				
	0.044				
	0.043				
	0.052				
895B Grain A	0.084	0.07	0.05	0.08	0.03
	0.08				
	0.049				
	0.077				
895B Grain B	0.061	0.08	0.05	0.1	0.05
	0.053				
	0.075				
	0.077				
	0.074				
	0.059				
	0.105				
	0.195	0.9	0.01	2.8	2.8

164B Grain C	0.012				
	2.539				
	2.74				
	2.8				
	0.063				
	0.065				
	0.064				
	0.065				
	0.07				
162 Grain A	0.047	0.048	0.026	0.069	0.043
	0.044				
	0.056				
	0.042				
	0.054				
	0.026				
	0.069				

D.6 Mass% averages, minimums, maximums and rages for nickel in pyrite

Sample	Ni(Mass%)	Ni(Mass%)	Ni Mass % avg	Min	Max	Range
168A Grain C	0.778	0.778	0.2	<LOD	0.8	0.8
	0.001	0.001				
	0.012	0.012				
	0.006	0.006				
	-0.005	<LOD				
	0.001	0.001				
	-0.01	<LOD				
	0.797	0.797				
	0.032	0.032				
	0.073	0.073				
3415A Grain A	0.016	0.016	0.02	0.01	0.06	0.05
	0.063	0.063				
	0.022	0.022				
	0.009	0.009				
	0.025	0.025				
	0.016	0.016				
	0.028	0.028				
	0.018	0.018				
	0.015	0.015				

	0.06	0.06				
153A Grain C	3.685	3.685	0.8	<LOD	3.7	3.7
	0.359	0.359				
	-0.512	<LOD				
	0.569	0.569				
	0.41	0.41				
	1.07	1.07				
	1.361	1.361				
	0.146	0.146				
	-0.017	<LOD				
	-0.021	<LOD				
886B Grain A	0.014	0.014	0.2	<LOD	0.9	0.9
	0.02	0.02				
	0.272	0.272				
	0.006	0.006				
	0.132	0.132				
	0.301	0.301				
	0.325	0.325				
	-0.015	<LOD				
	0.008	0.008				
	0.875	0.875				
NB036 Grain B	0.296	0.296	0.9	0.3	2.7	2.4
	0.266	0.266				
	0.549	0.549				
	0.638	0.638				
	2.702	2.702				
	1.117	1.117				
NB036 Grain A	0.027	0.027	0.03	<LOD	0.02	0.03
	0.007	0.007				
	0.01	0.01				
	0.028	0.028				
	-0.007	<LOD				
	-0.004	<LOD				
	-0.014	<LOD				
	0.005	0.005				
490 Grain A	0.03	0.03	0.01	<LOD	0.03	0.03
	0.009	0.009				
	0.021	0.021				
	0.016	0.016				
	-0.003	<LOD				
	0.007	0.007				

	0.002	0.002				
	0.025	0.025				
157 Grain A	0.033	0.033	0.02	<LOD	0.03	0.03
	0.025	0.025				
	0.001	0.001				
	-0.019	<LOD				
	0.02	0.02				
	0.017	0.017				
	0.001	0.001				
	0.019	0.019				
154-GrainA-01	0.022	0.022	0.03	<LOD	0.1	0.1
	0.046	0.046				
	0.01	0.01				
	-0.001	<LOD				
	0.027	0.027				
	0.107	0.107				
	0.021	0.021				
	0.022	0.022				
	0.038	0.038				
	0.02	0.02				
895B Grain A	0.013	0.013	0.01	<LOD	0.01	0.01
	0.008	0.008				
	0.005	0.005				
	0.004	0.004				
895B Grain B	-0.008	<LOD	0.01	<LOD	0.03	0.03
	-0.017	<LOD				
	0.011	0.011				
	0	0				
	0.034	0.034				
	0.02	0.02				
	0.035	0.035				
164B Grain C	0.105	0.105	0.08	<LOD	0.16	0.16
	0.002	0.002				
	0.007	0.007				
	-0.011	<LOD				
	-0.007	<LOD				
	0.122	0.122				
	0.136	0.136				
	0.141	0.141				
	0.147	0.147				
	0.158	0.158				

162 Grain A	0.005	0.005	0.05	<LOD	0.01	0.01
	-0.002	<LOD				
	-0.002	<LOD				
	0.011	0.011				
	-0.007	<LOD				
	-0.002	<LOD				
	-0.122	<LOD				

Appendix E

E.1 Samples, grains and traverses measured during LA ICP-MS analysis

Sample	Grain	Traverse
153	C & B	C, B1, B2
S-3415A	A & D	A1, A2, A3, D1, D2
152	A, G & B	A, G1, G2, B1, B2
NB036	A & B	B1, B2, A
173	A & B	B1, B2, A1, A2
899A	E & F	E1, E2, F1, F2
157	A & C	A1, A2, C1, C2
168A	C & D	D1, D2, D3, C1, C2
895B	E & F	F1, F2, E1, E2, E3
897A	A	A1, A2, A3
898A	A & B	A1, A2, B1, B3
164B	A & B	A1, A2, A3, A4, B1, B2
886B	E & F	E, F
171B	C & B	C1, C2, B1, B2
154	A & B	A1, A2, B1, B2, B3
900	E & F	E1, E2, F1, F2
159	A & B	A1, A2, A3, B1, B2

E2. Atomic counts of S, Au, Ag107 and Ag109. Gold inclusions are indicated by anomalously high peaks of gold with simultaneously high peaks of silver.

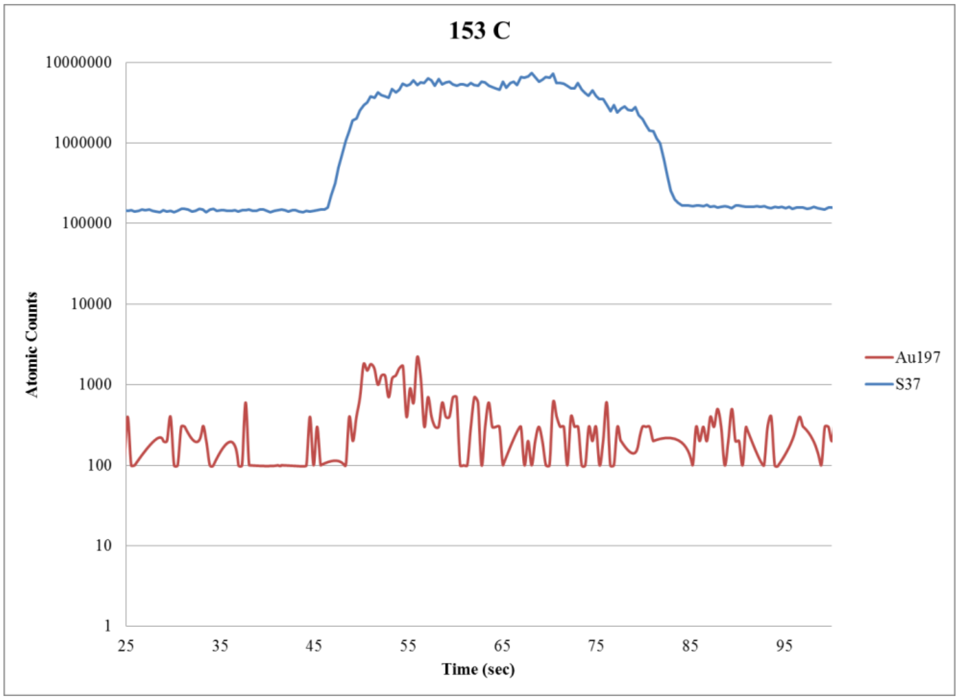

No anomalously high peaks, so no gold inclusions.

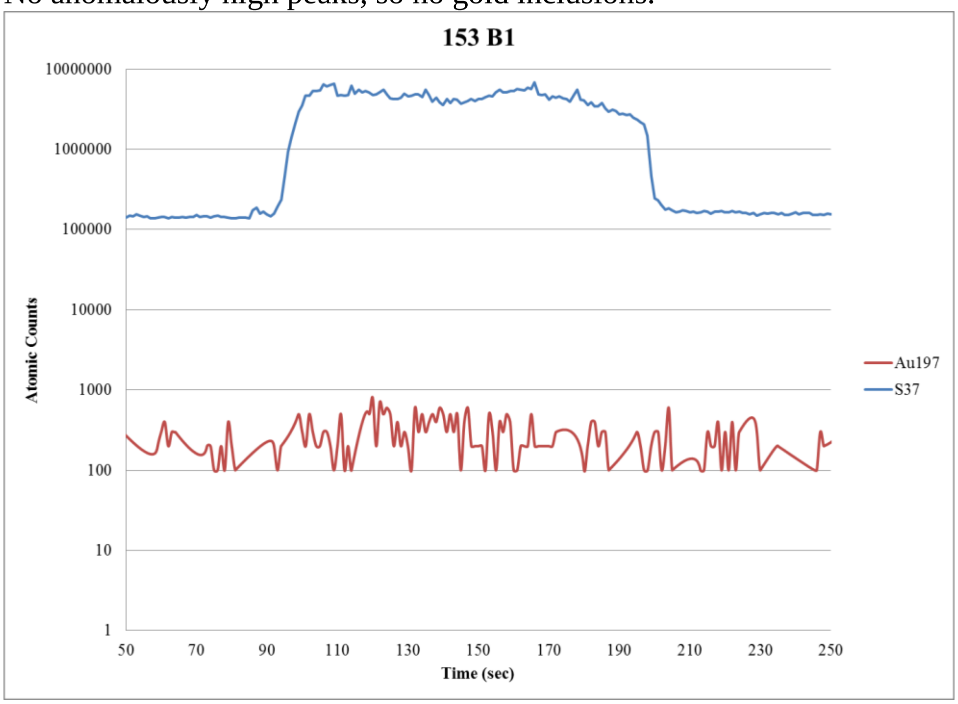

No anomalously high peaks, so no gold inclusions.

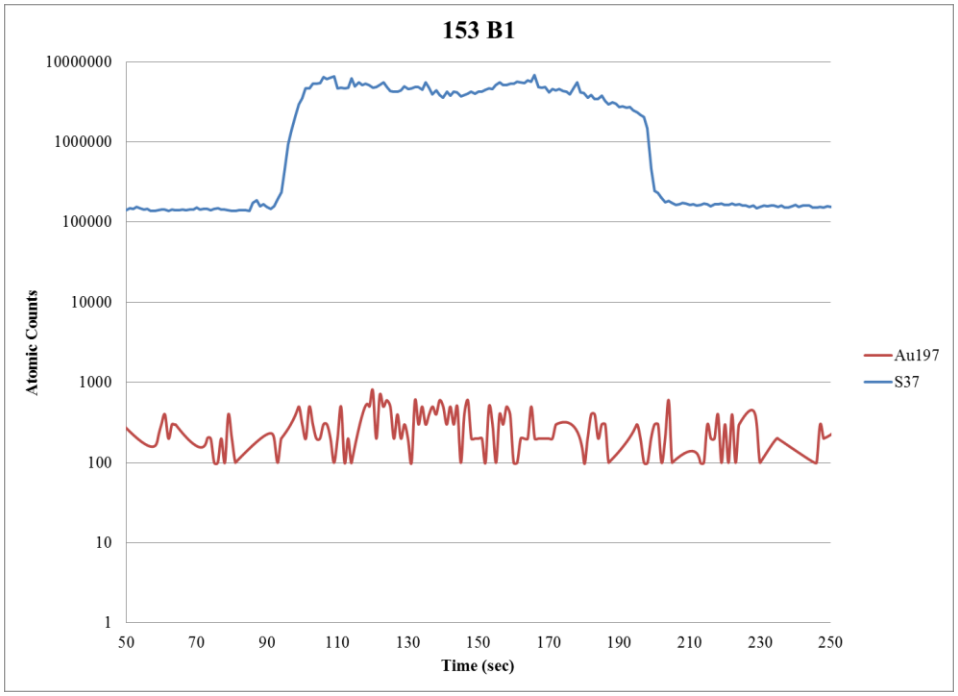

No anomalously high peaks, so no gold inclusions.

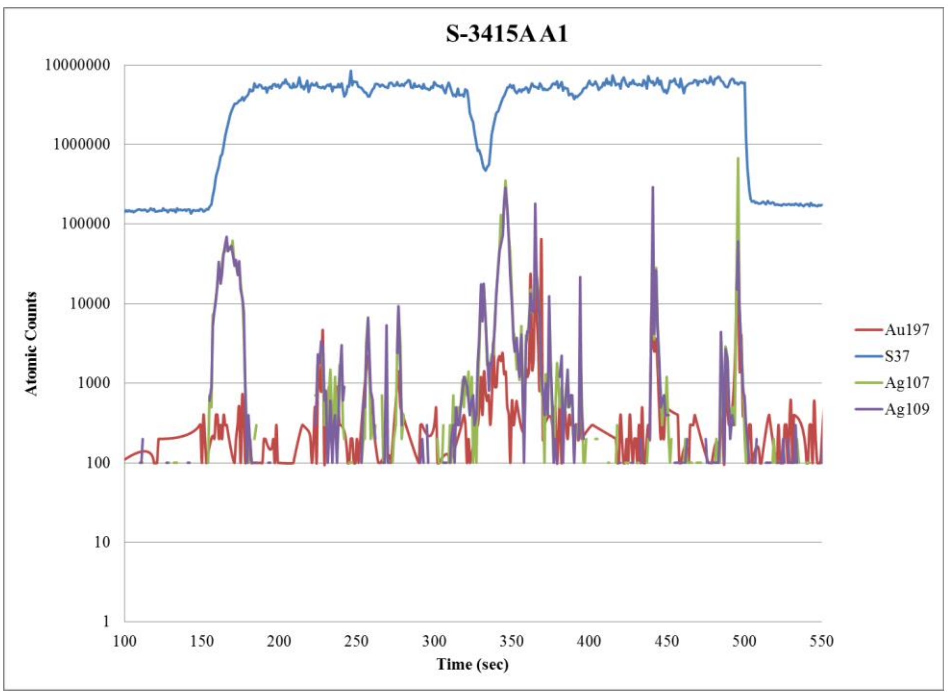

Inclusions found within S-3415 A1 with the high peaks of gold and silver at approximately 350 seconds and 500 seconds.

No anomalously high peaks, so no gold inclusions.

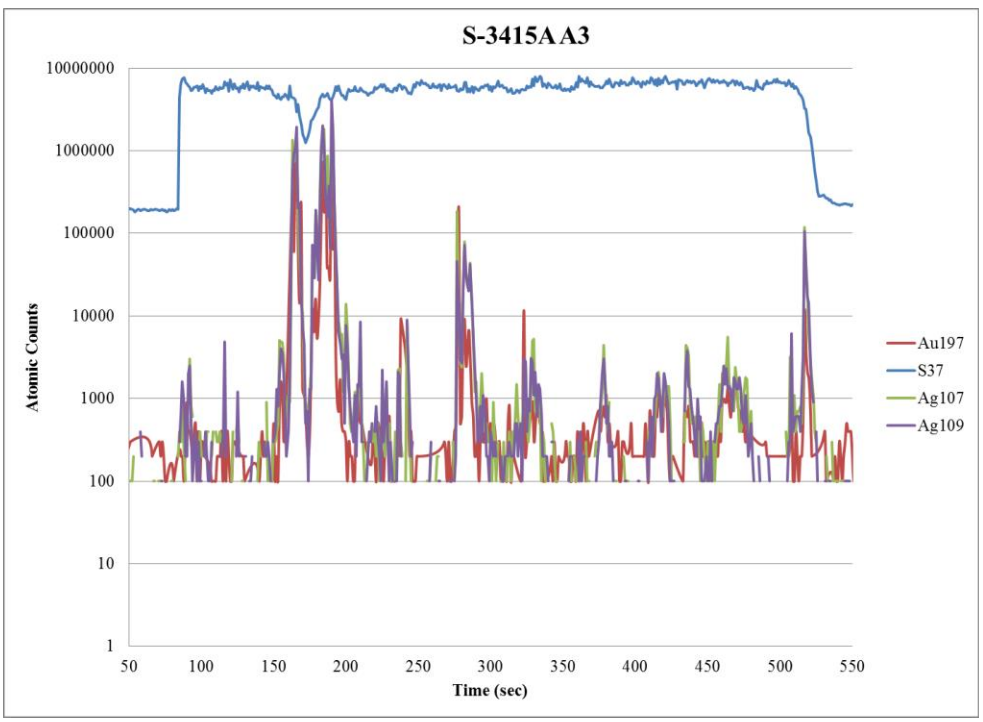

Inclusions found within S-3415 A3 with the high peaks of gold and silver at approximately 175 seconds and 300 seconds.

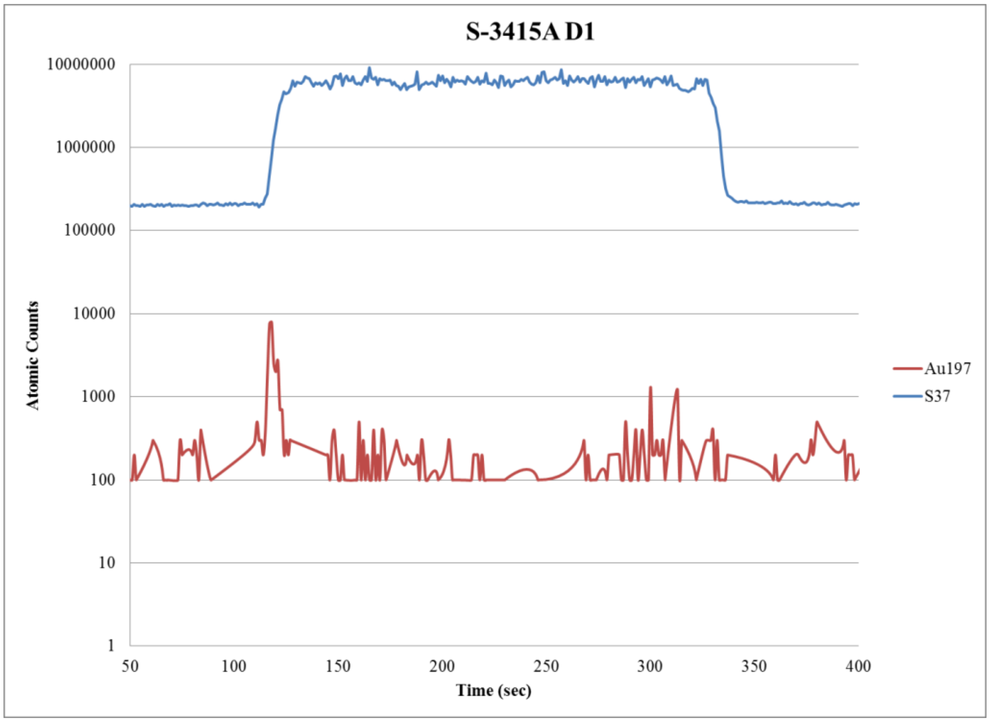

No anomalously high peaks, so no gold inclusions.

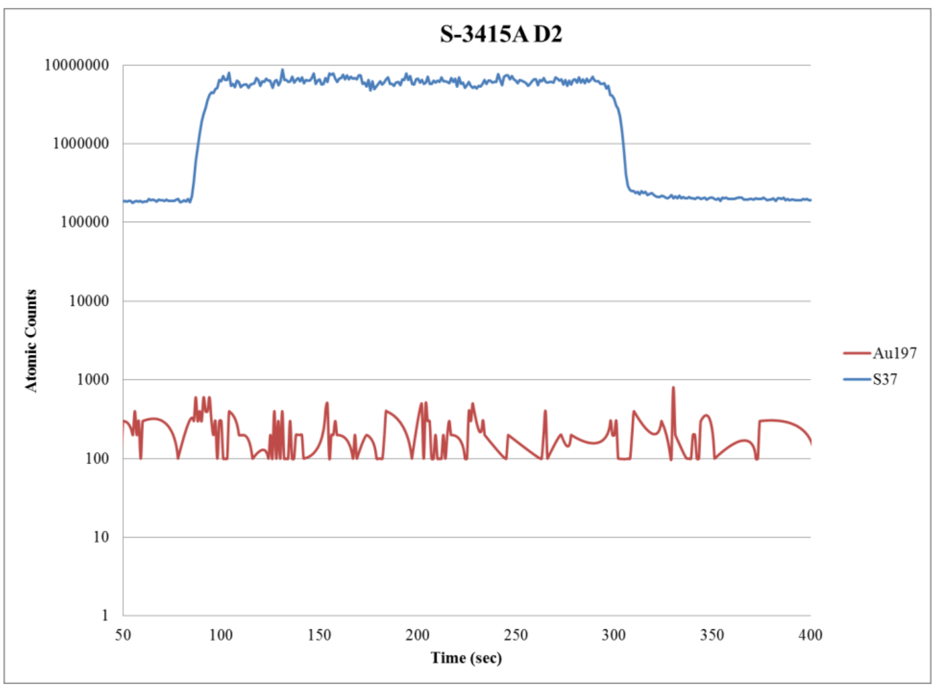

No anomalously high peaks, so no gold inclusions.

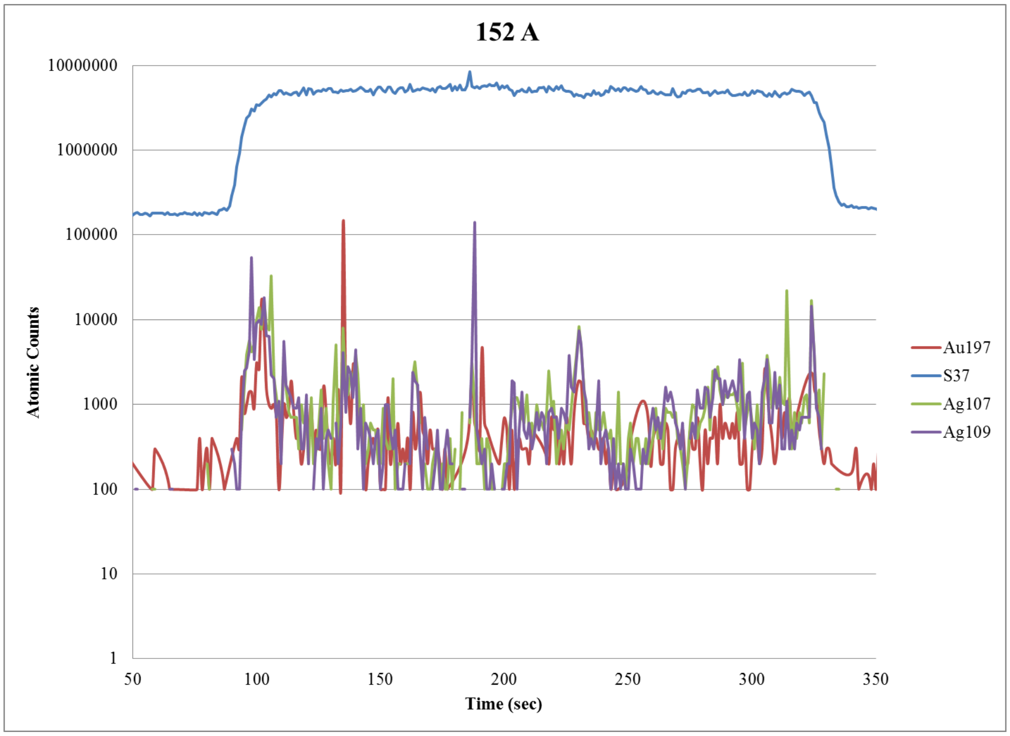

Inclusions found within 152 A with the high peaks of gold and silver at approximately 140 seconds and 200 seconds.

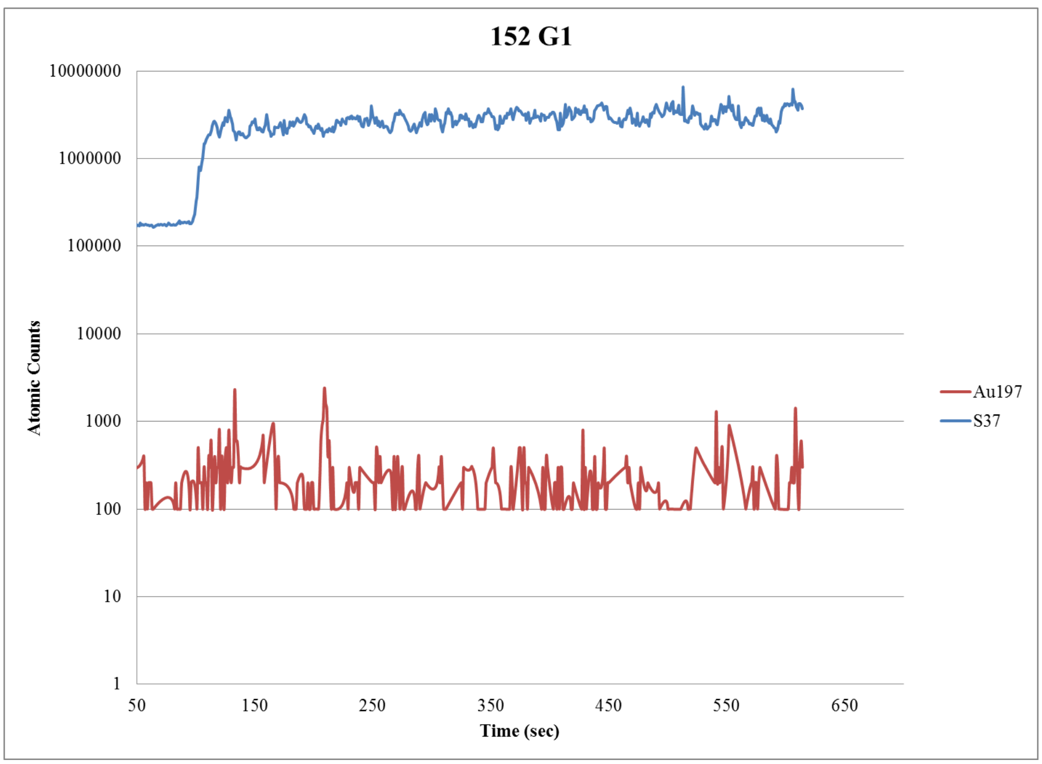

No anomalously high peaks, so no gold inclusions.

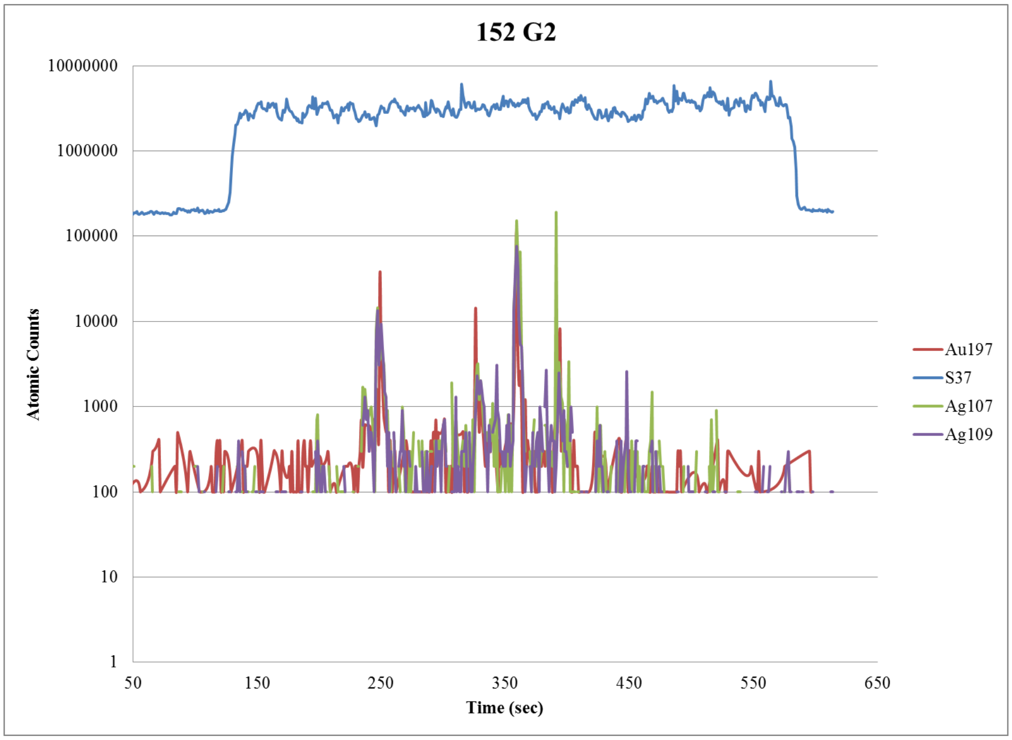

Inclusions found within 152 G2 with the high peaks of gold and silver at approximately 250 seconds and 350 seconds.

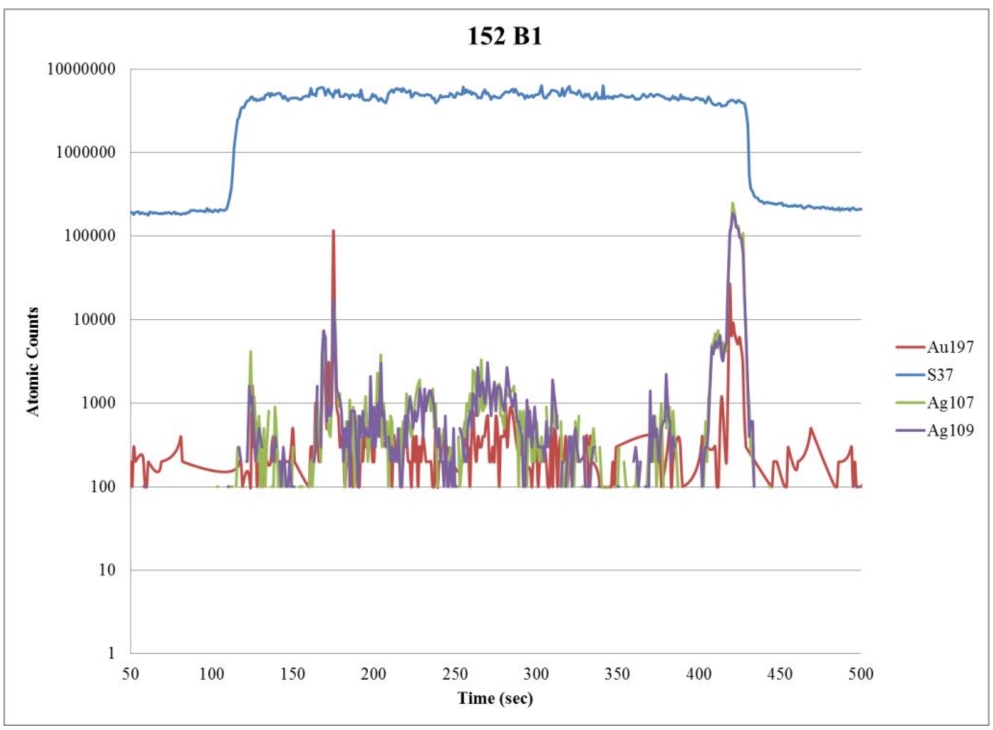

Inclusions found within 152 B1 with the high peaks of gold and silver at approximately 175 seconds and 425 seconds.

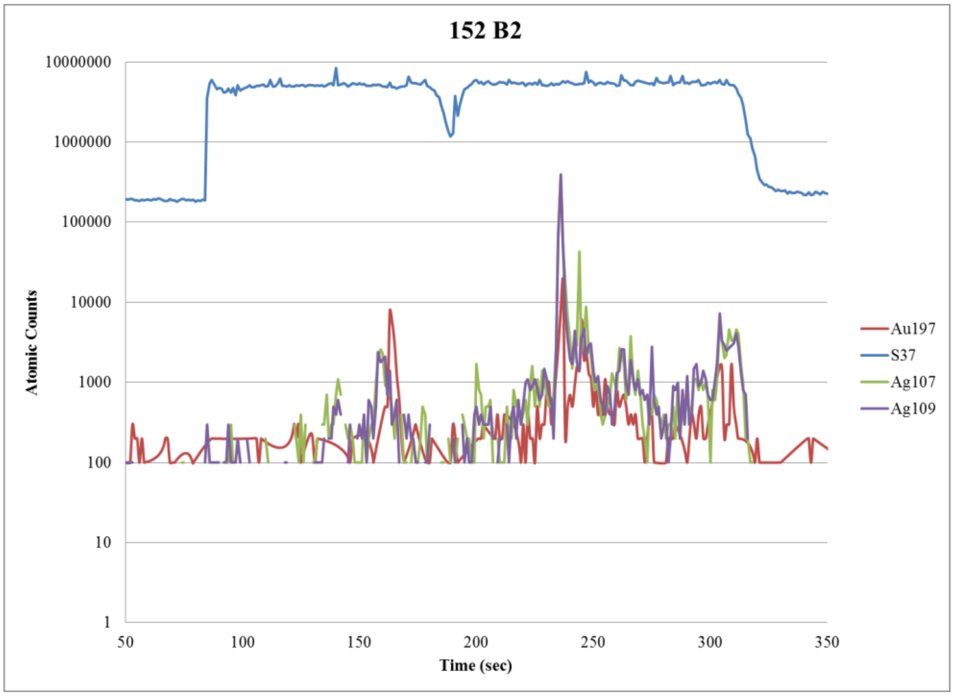

Inclusion found within 152 B2 with the high peak of gold and silver at approximately 250 seconds.

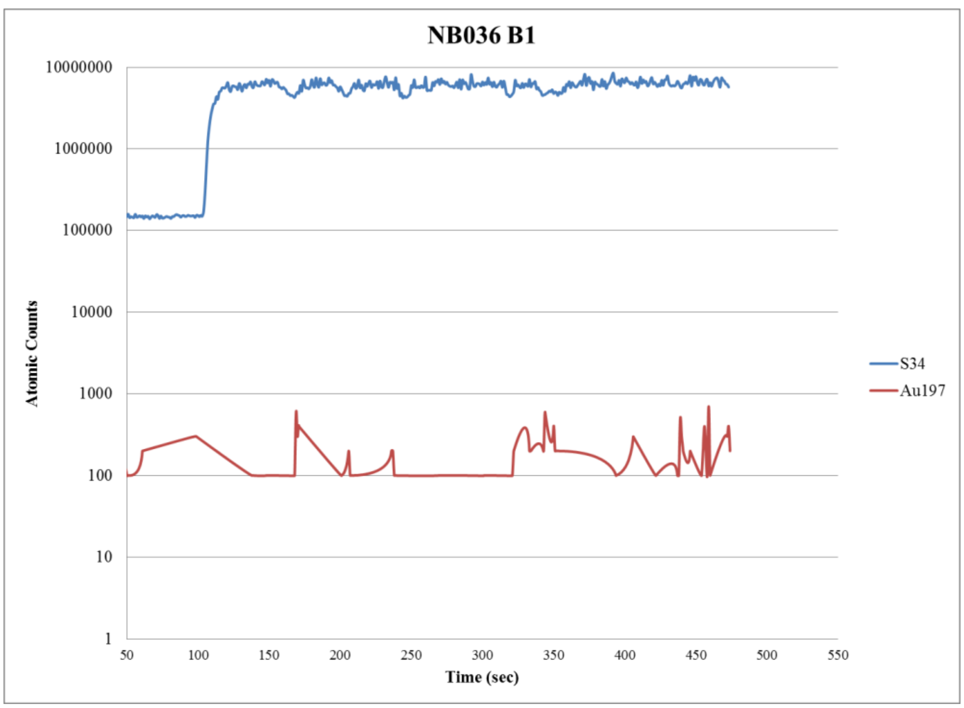

No anomalously high peaks, so no gold inclusions.

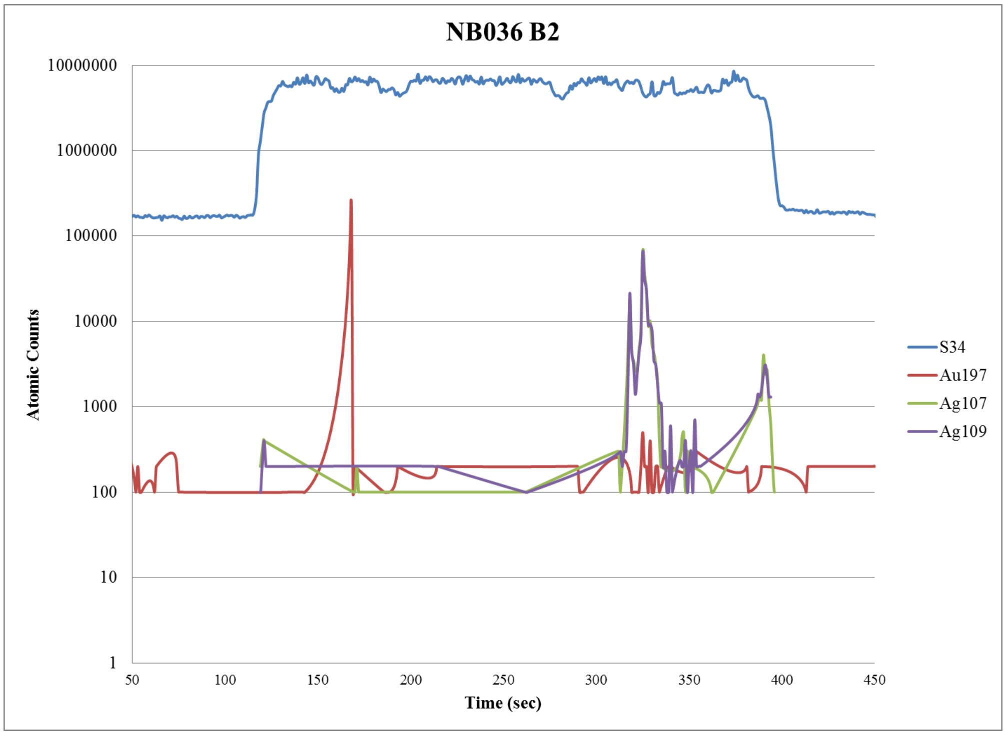

No inclusion within NB036 B2 as it is just one anomalously high point that does not show a simultaneously high peak with silver.

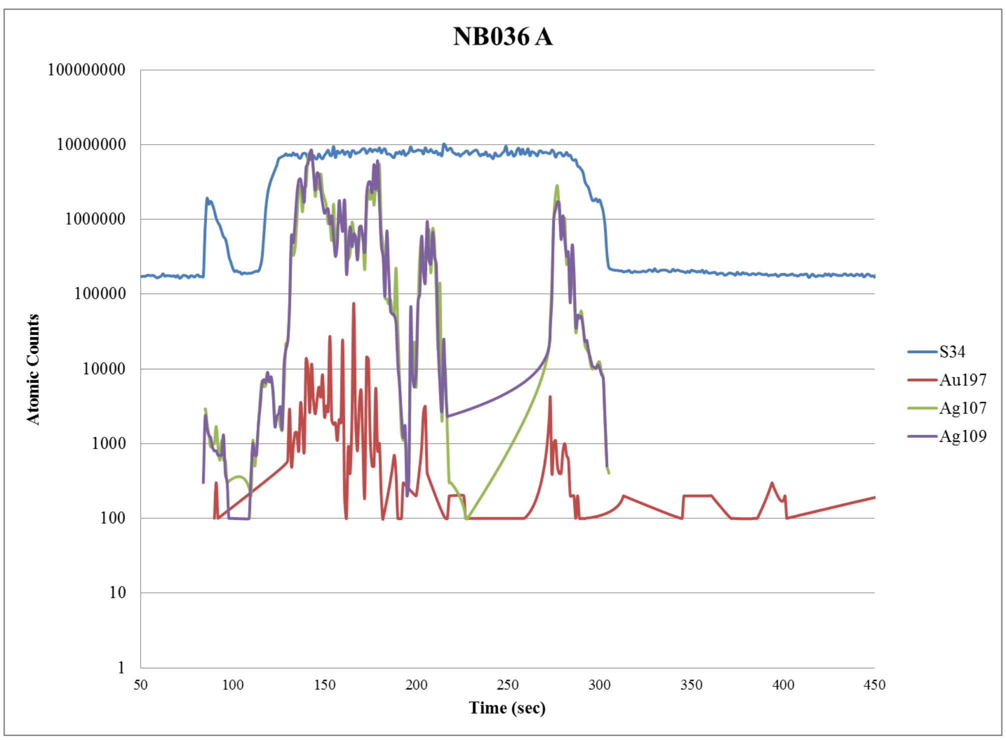

No inclusion within NB036 A the high gold values are broad and suggest they are structural gold within pyrite grain.

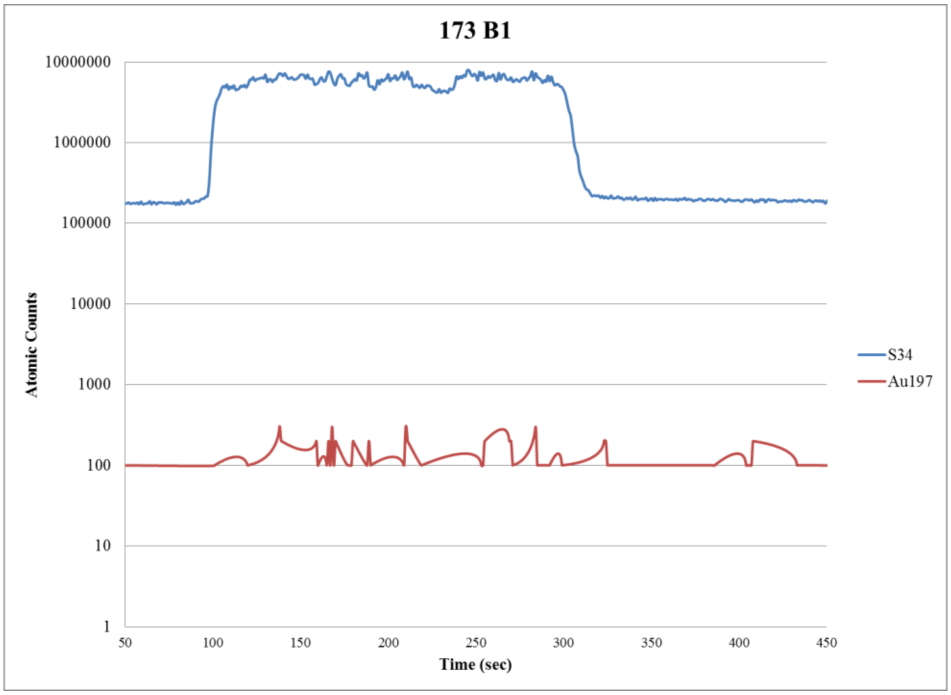

No anomalously high peaks, so no gold inclusions.

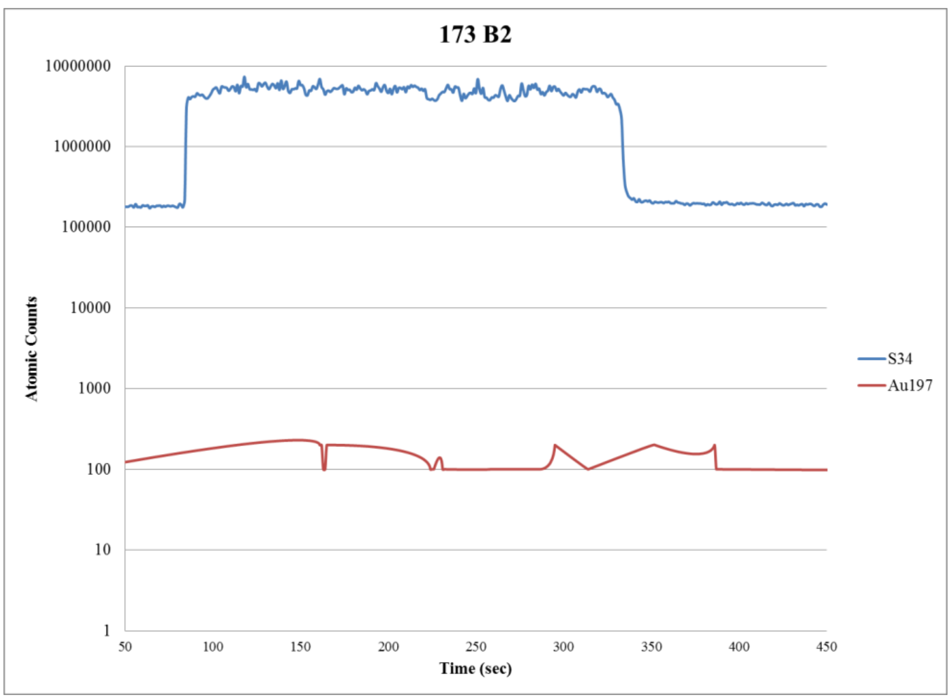

No anomalously high peaks, so no gold inclusions.

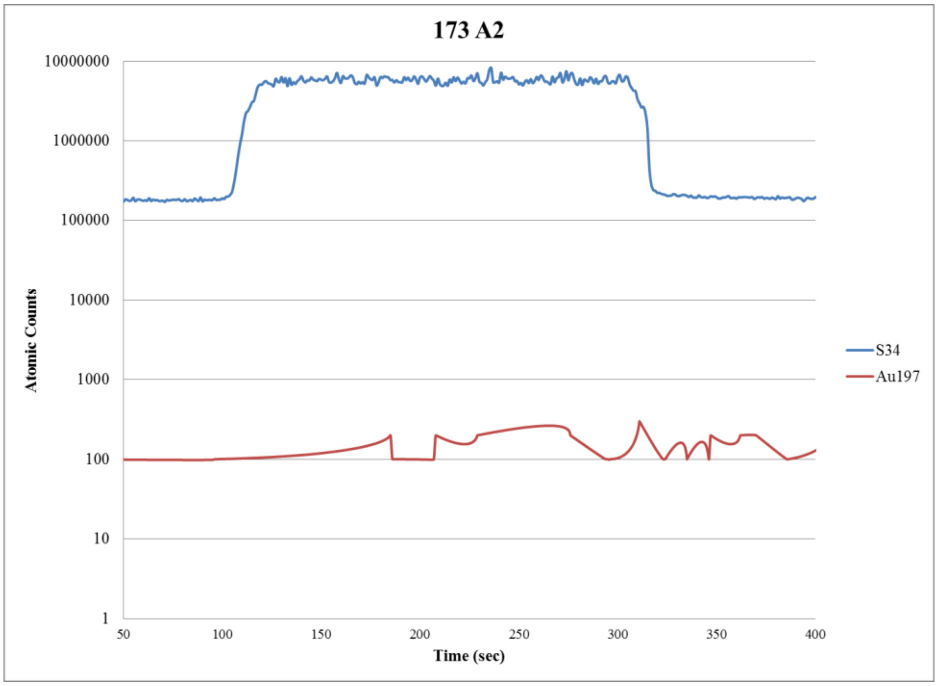

No anomalously high peaks, so no gold inclusions.

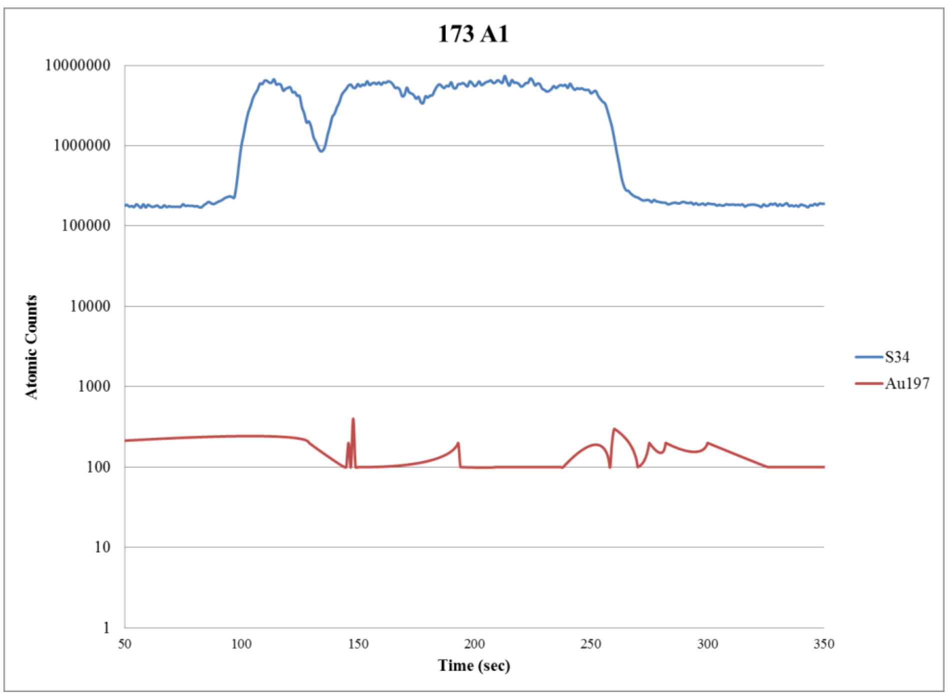

No anomalously high peaks, so no gold inclusions.

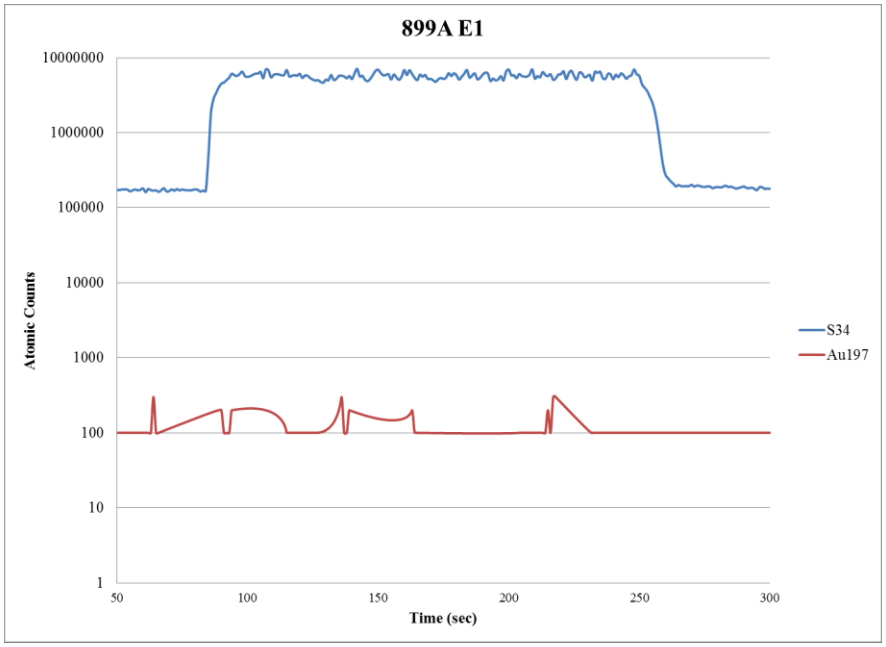

No anomalously high peaks, so no gold inclusions.

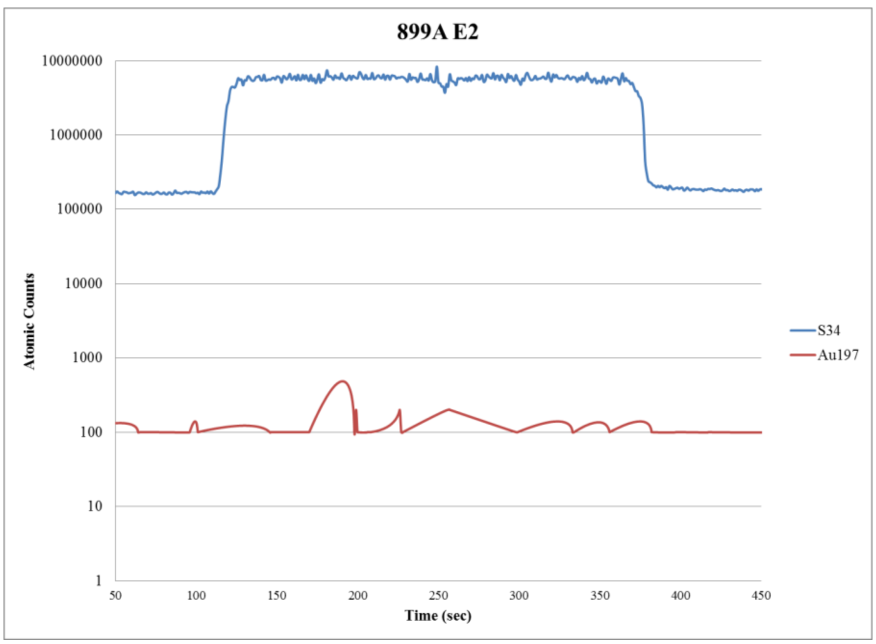

No anomalously high peaks, so no gold inclusions.

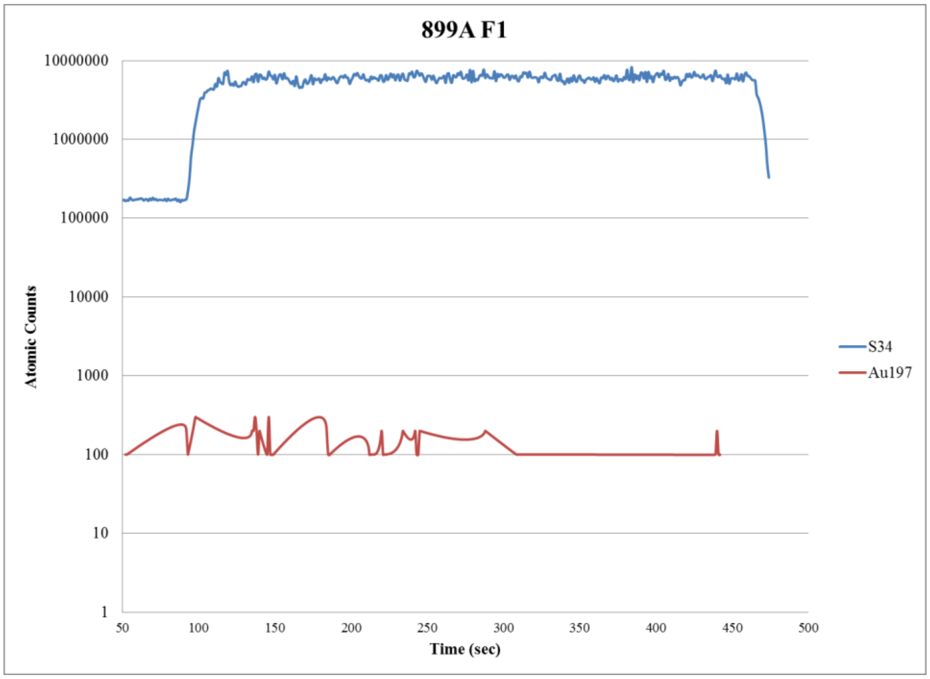

No anomalously high peaks, so no gold inclusions.

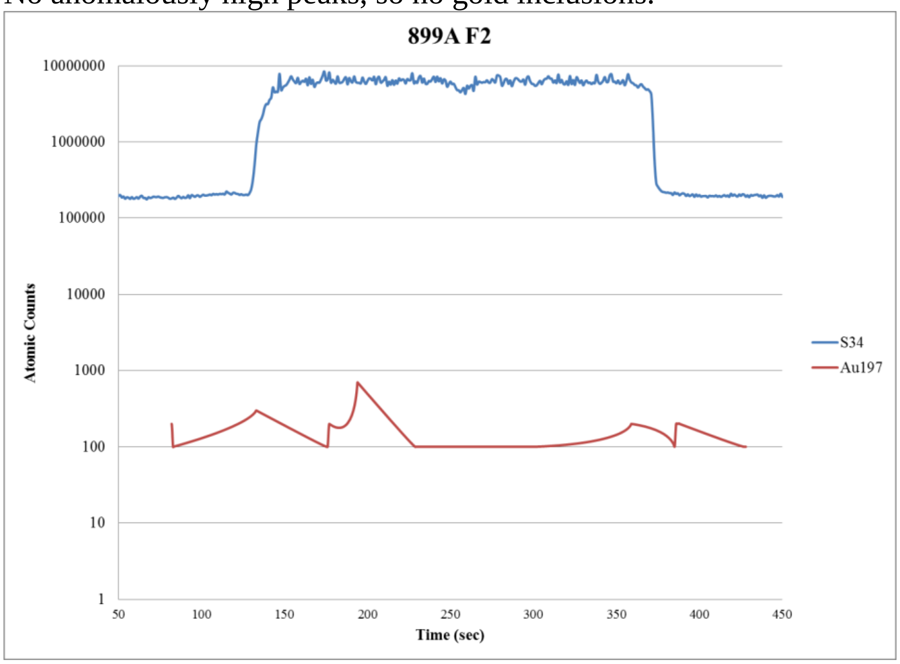

No anomalously high peaks, so no gold inclusions.

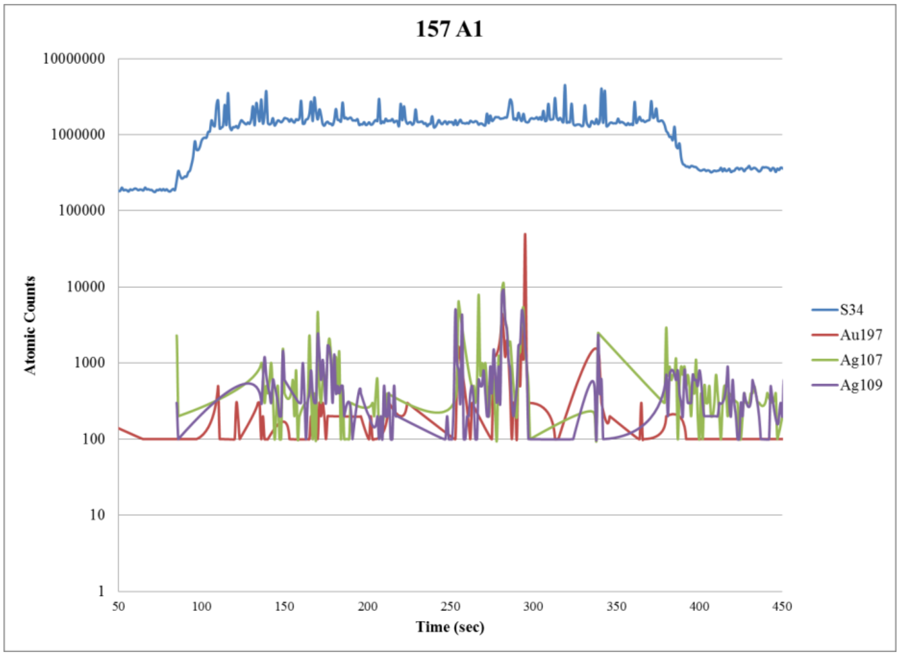

Inclusion found within 157 A1 with the high peak of gold and silver at approximately 300 seconds.

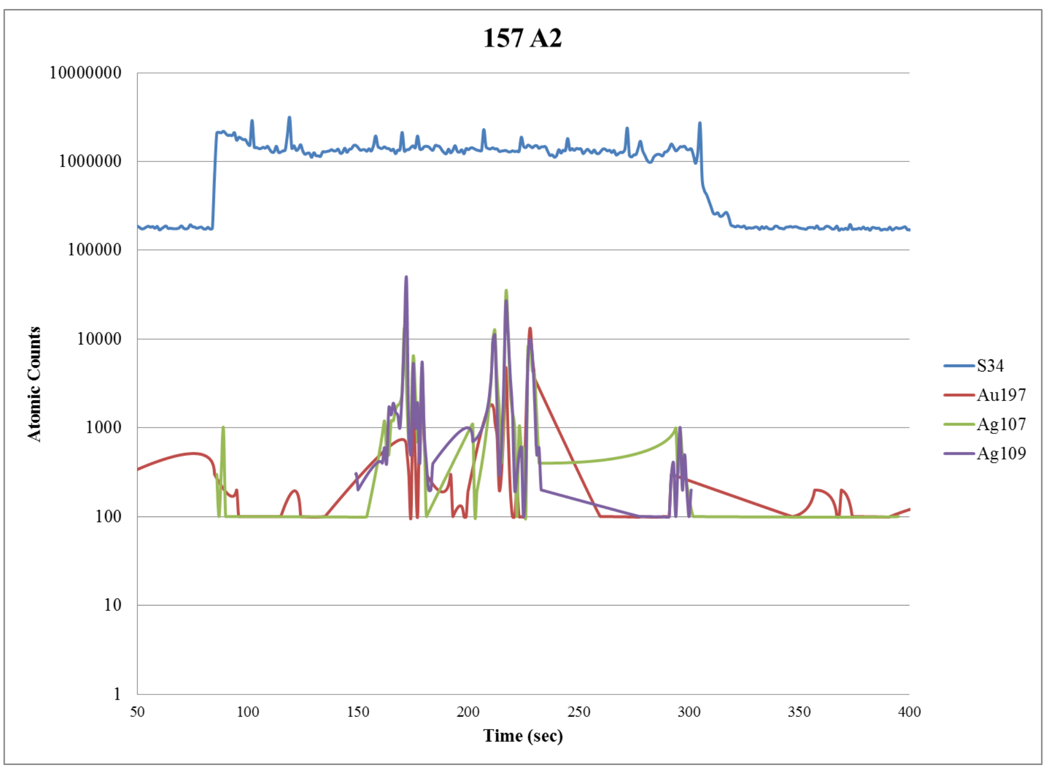

Inclusions found within 157 A1 with the high peaks of gold and silver at approximately 210 seconds and 230 seconds.

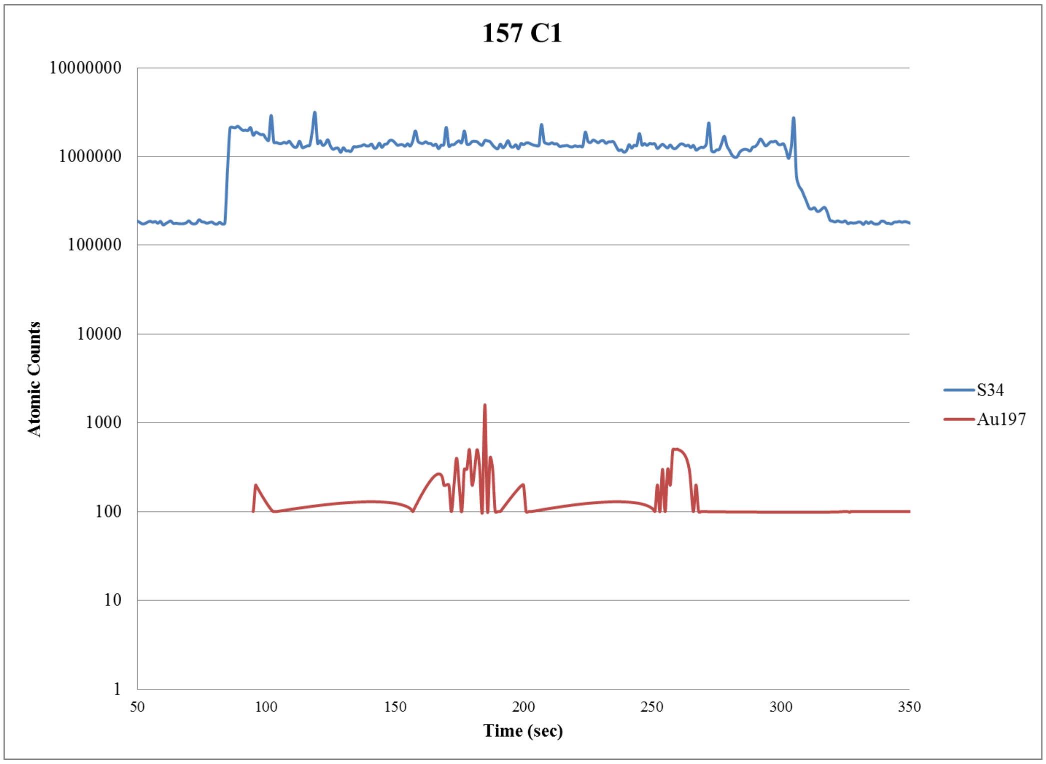

No anomalously high peaks, so no gold inclusions.

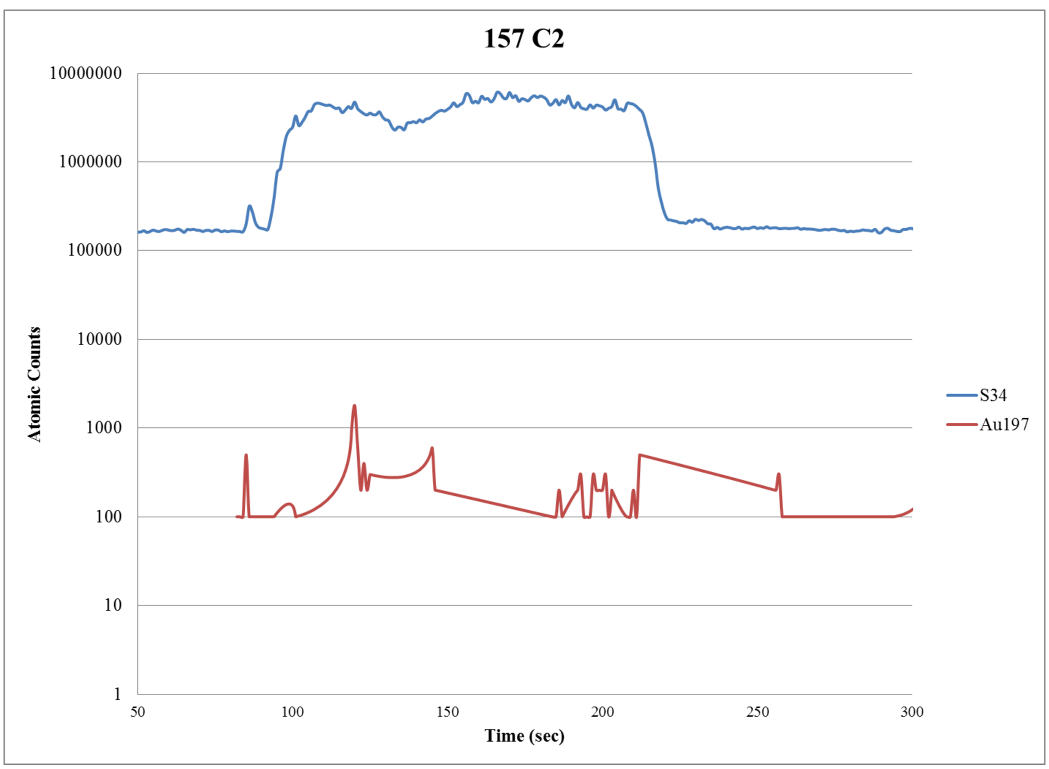

No anomalously high peaks, so no gold inclusions.

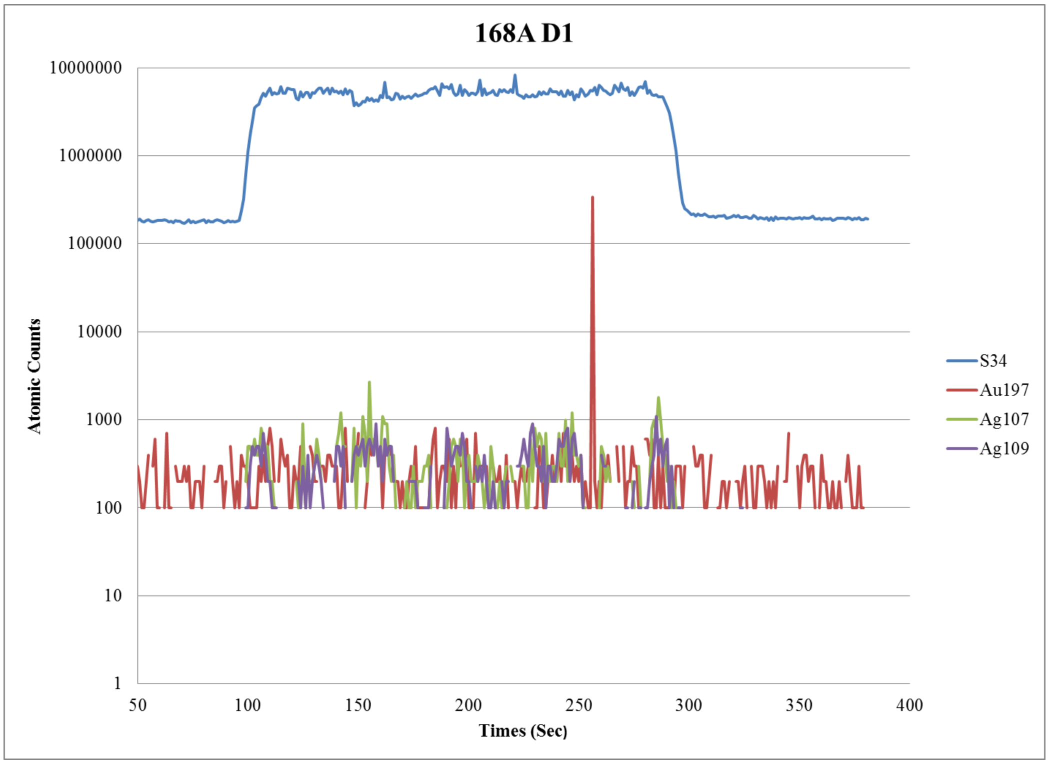

No inclusion within 168A D1 as it is just one anomalously high point that does not show a simultaneously high peak with silver.

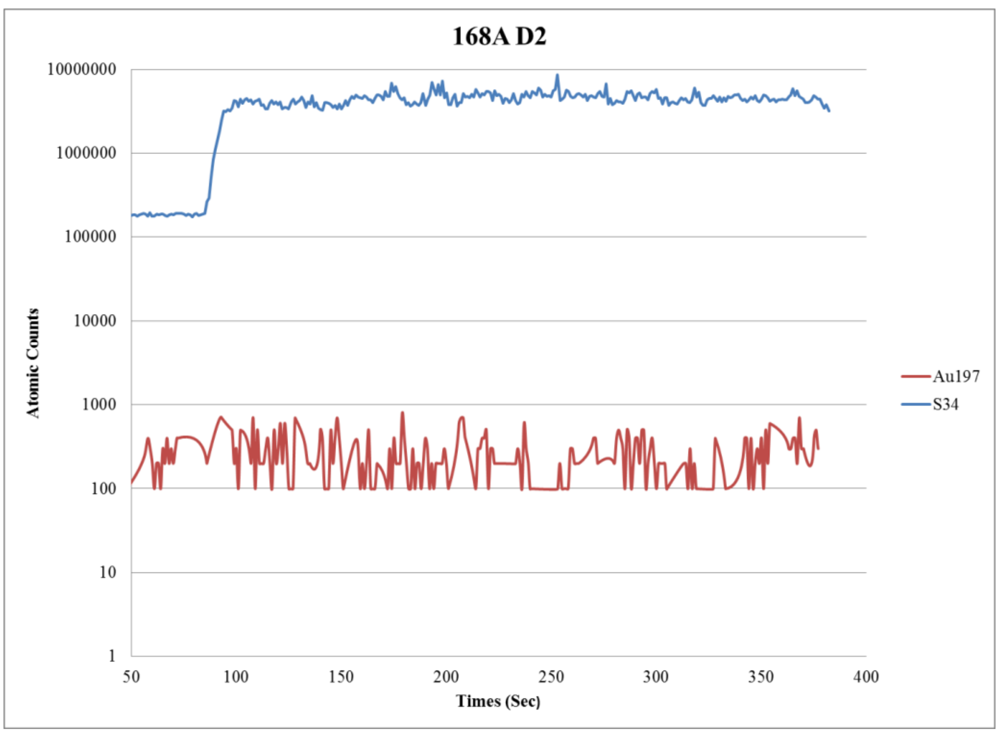

No anomalously high peaks, so no gold inclusions.

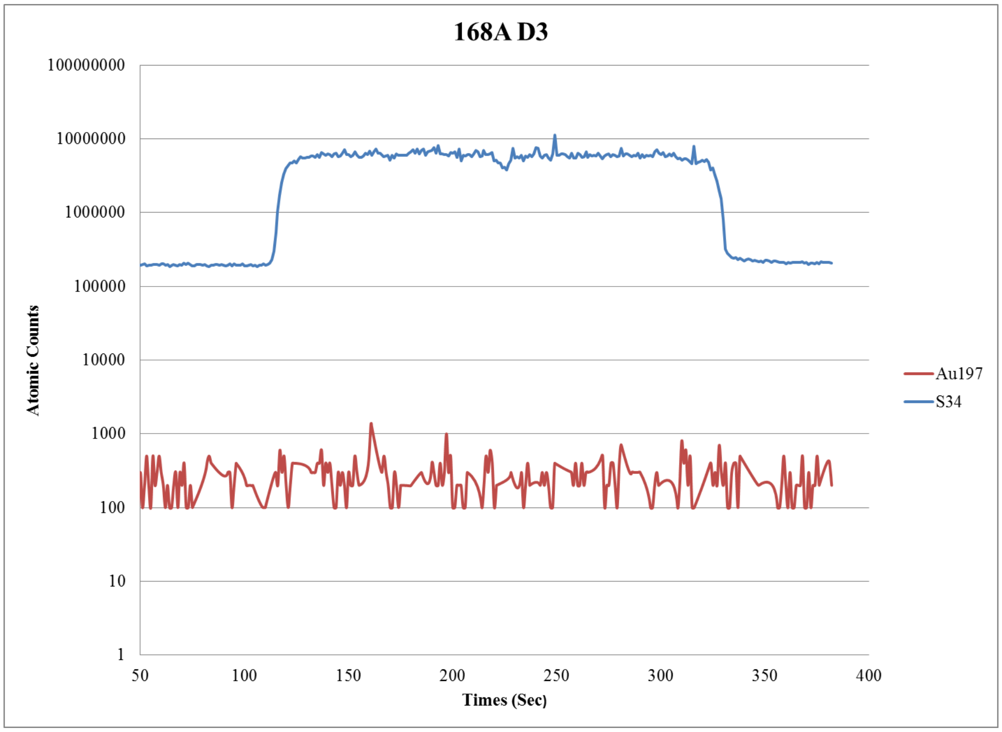

No anomalously high peaks, so no gold inclusions.

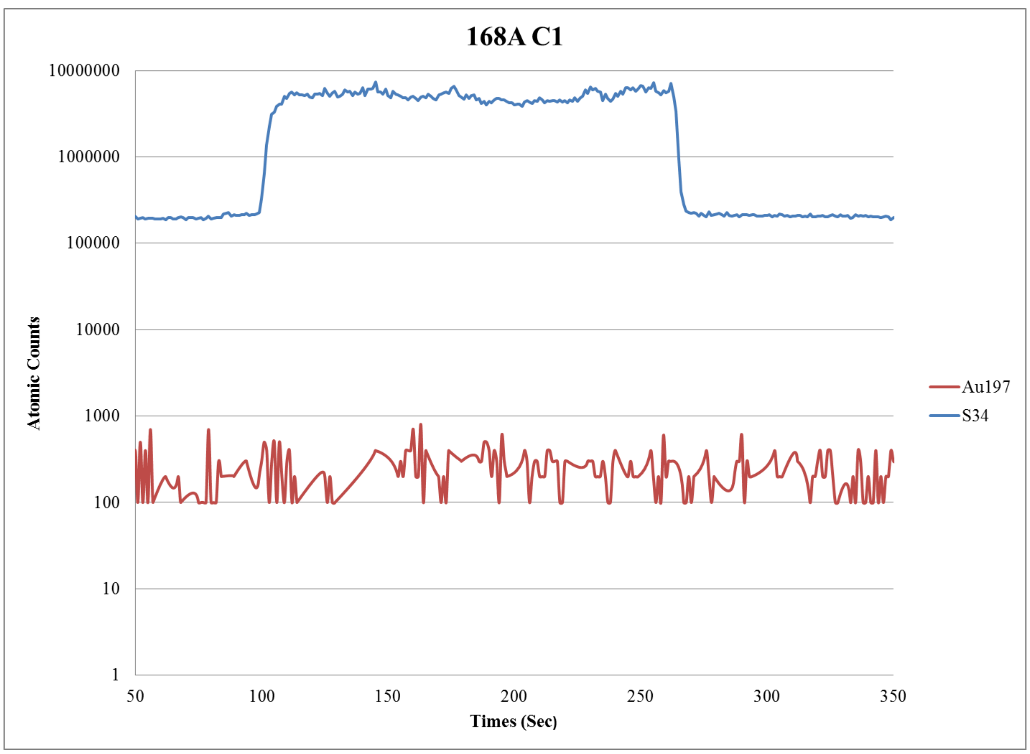

No anomalously high peaks, so no gold inclusions.

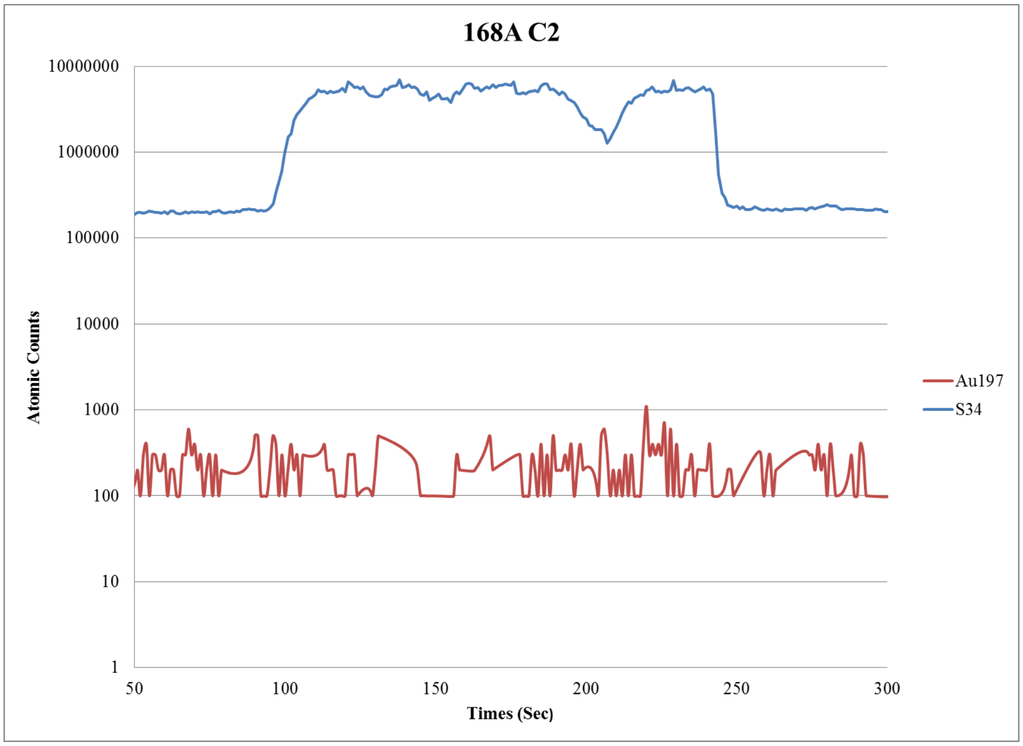

No anomalously high peaks, so no gold inclusions.

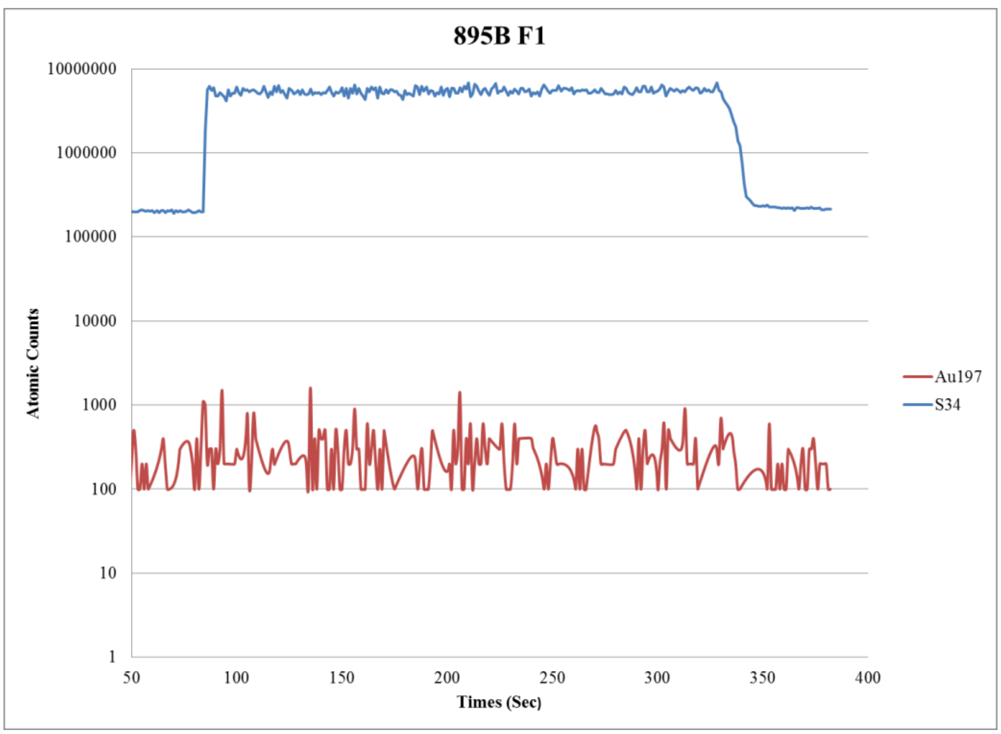

No anomalously high peaks, so no gold inclusions.

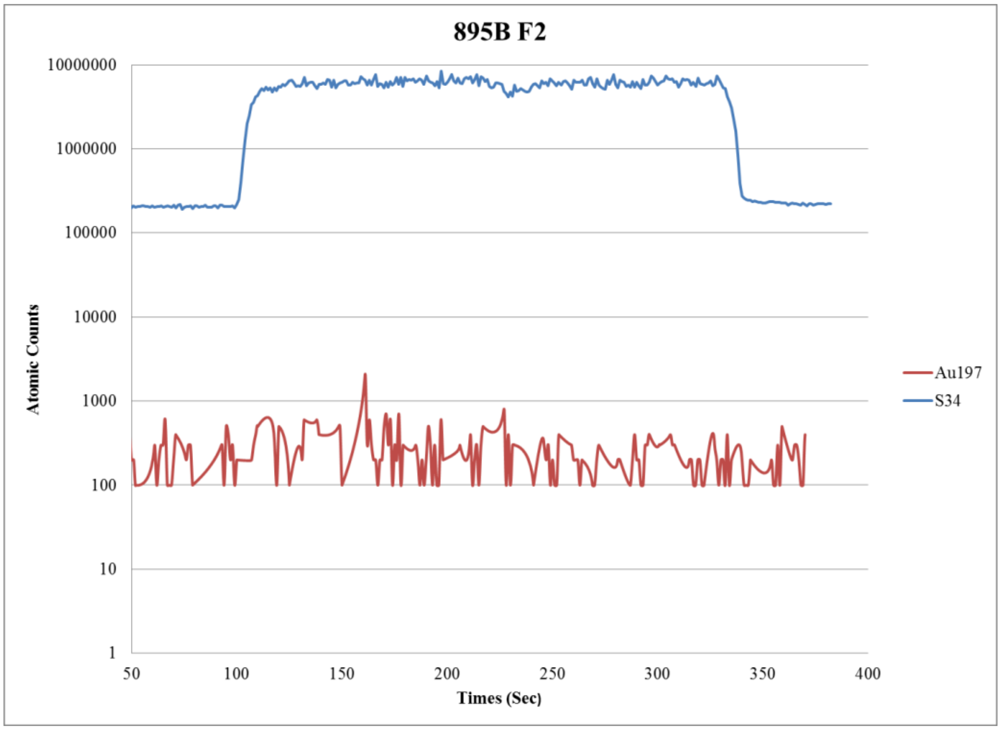

No anomalously high peaks, so no gold inclusions.

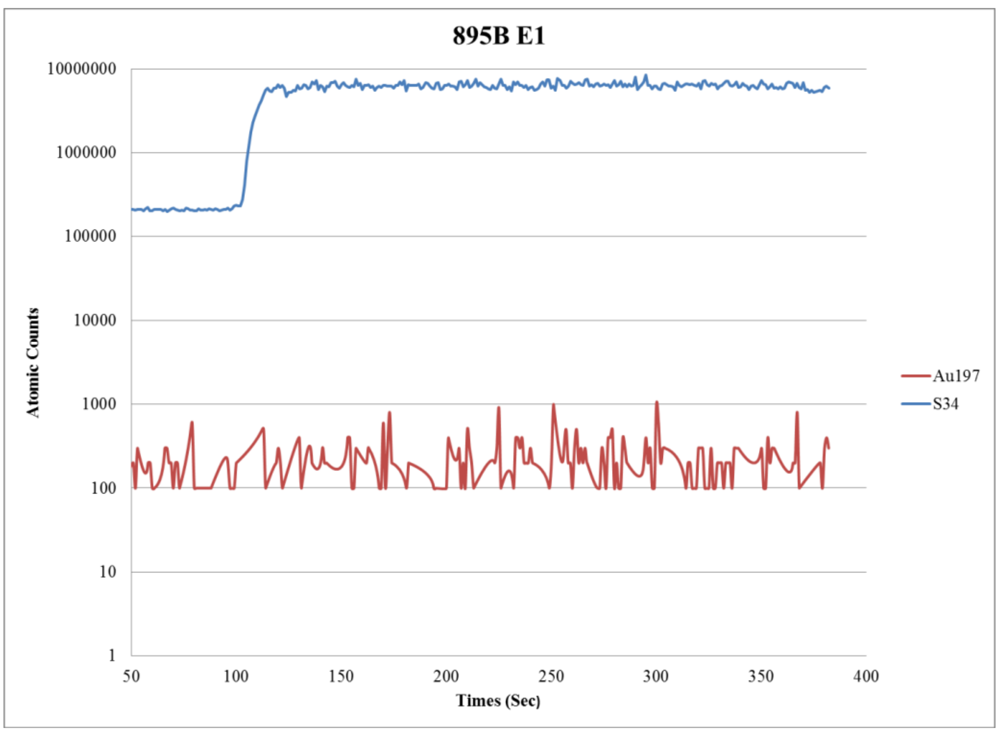

No anomalously high peaks, so no gold inclusions.

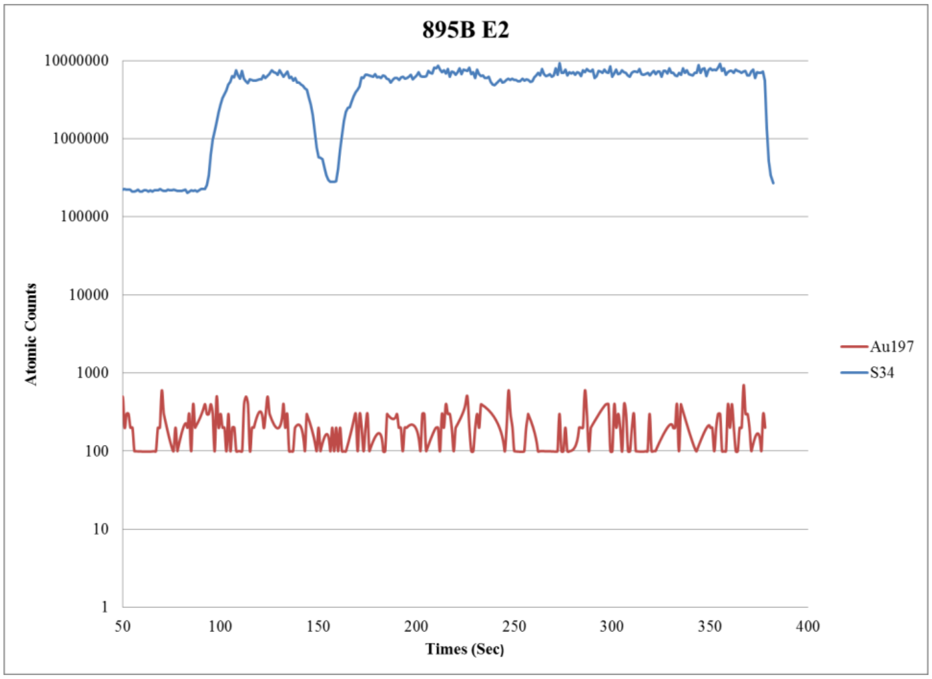

No anomalously high peaks, so no gold inclusions.

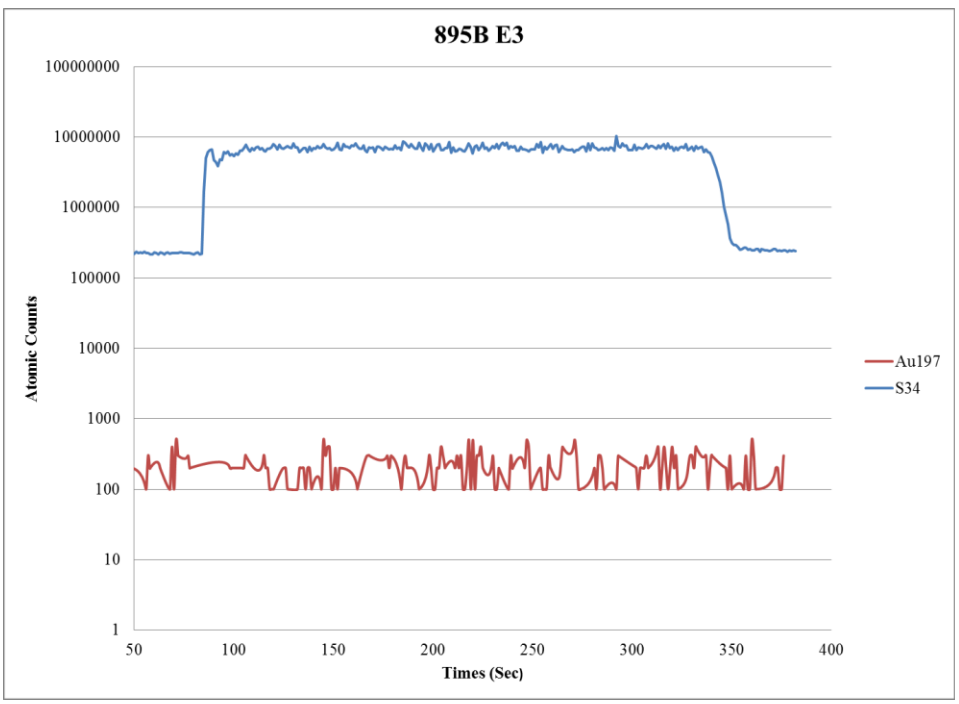

No anomalously high peaks, so no gold inclusions.

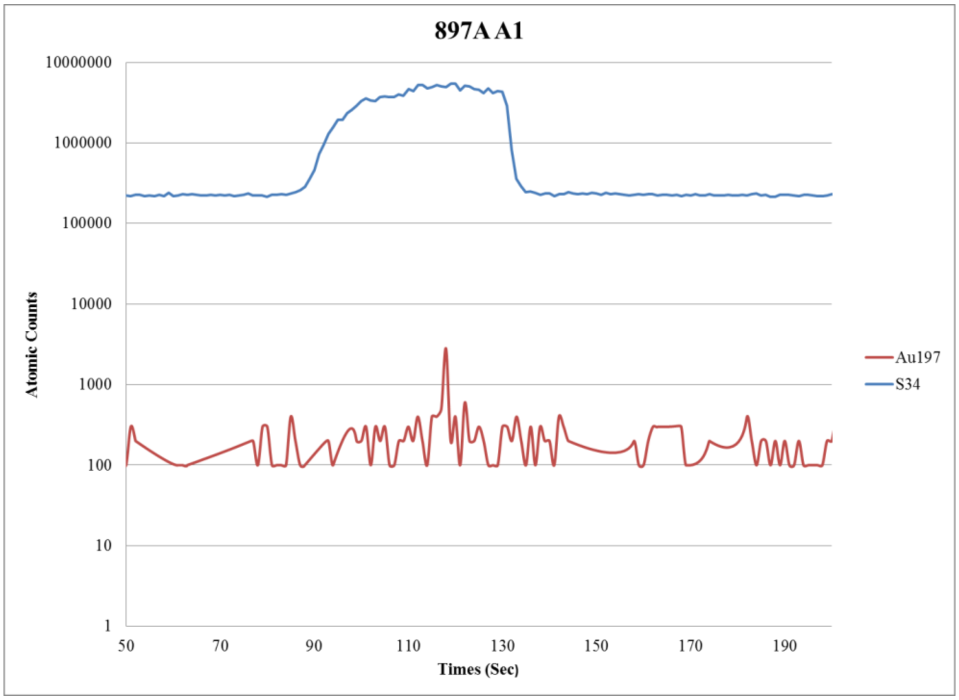

No anomalously high peaks, so no gold inclusions.

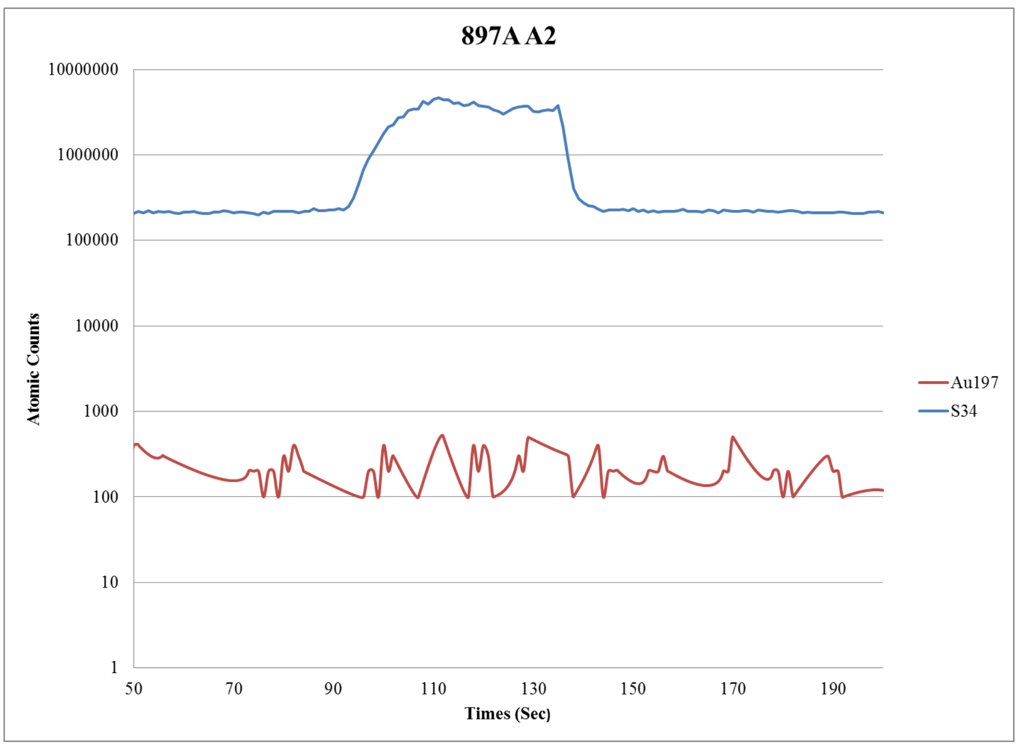

No anomalously high peaks, so no gold inclusions.

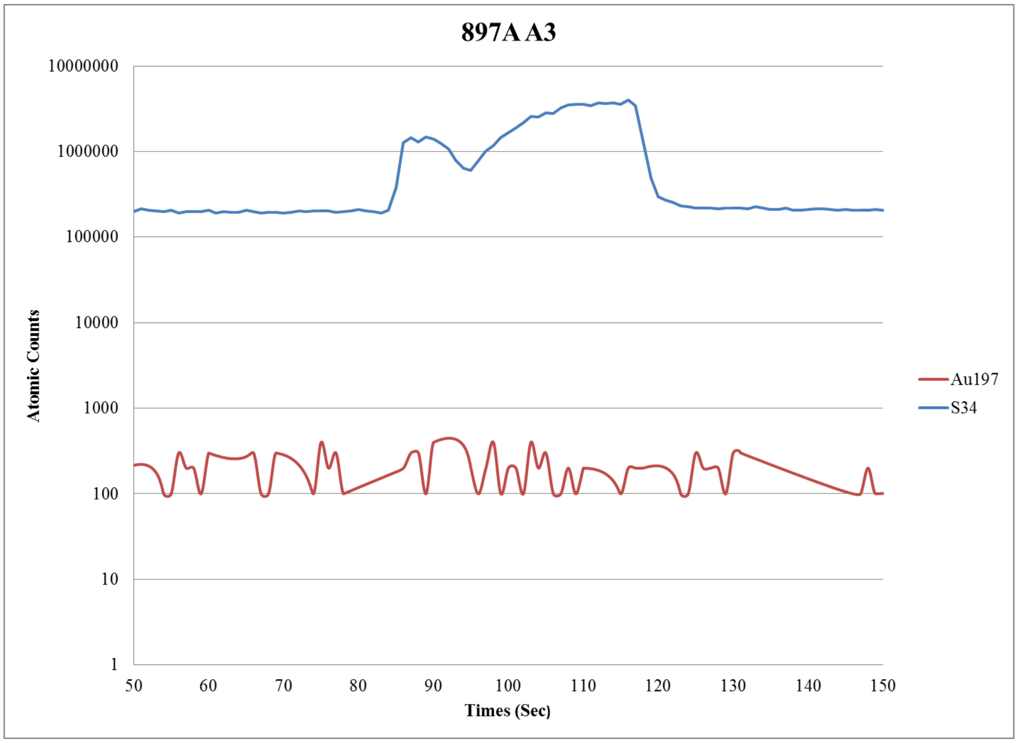

No anomalously high peaks, so no gold inclusions

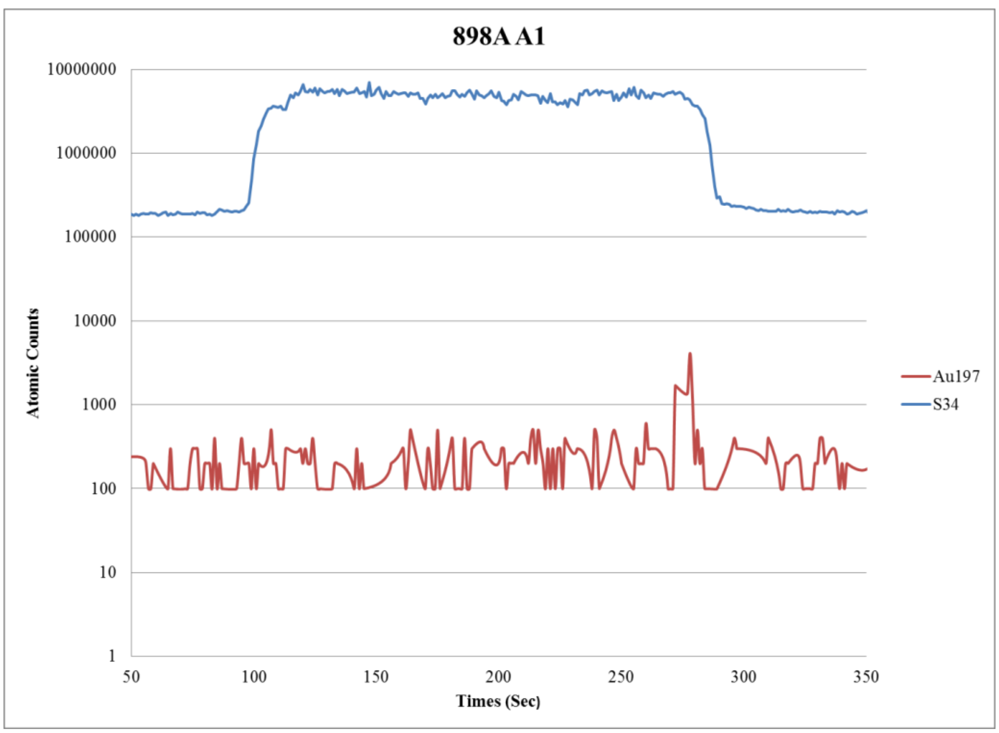

No anomalously high peaks, so no gold inclusions

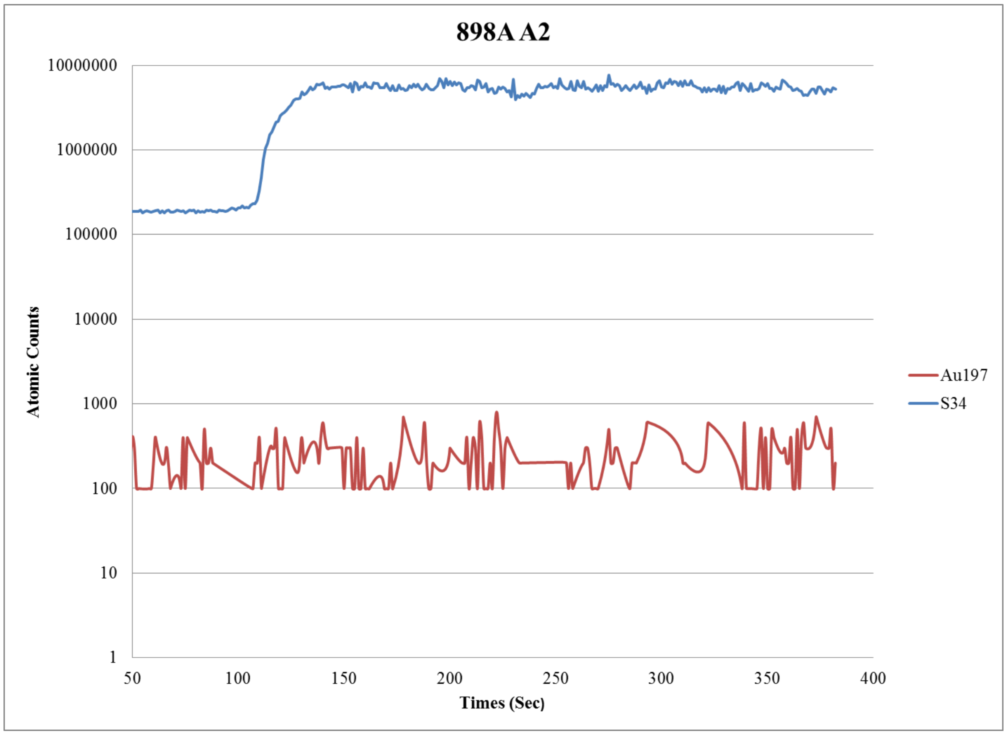

No anomalously high peaks, so no gold inclusions

Inclusion found within 898A B1 with the high peak of gold and silver at approximately 275 seconds.

No anomalously high peaks, so no gold inclusions

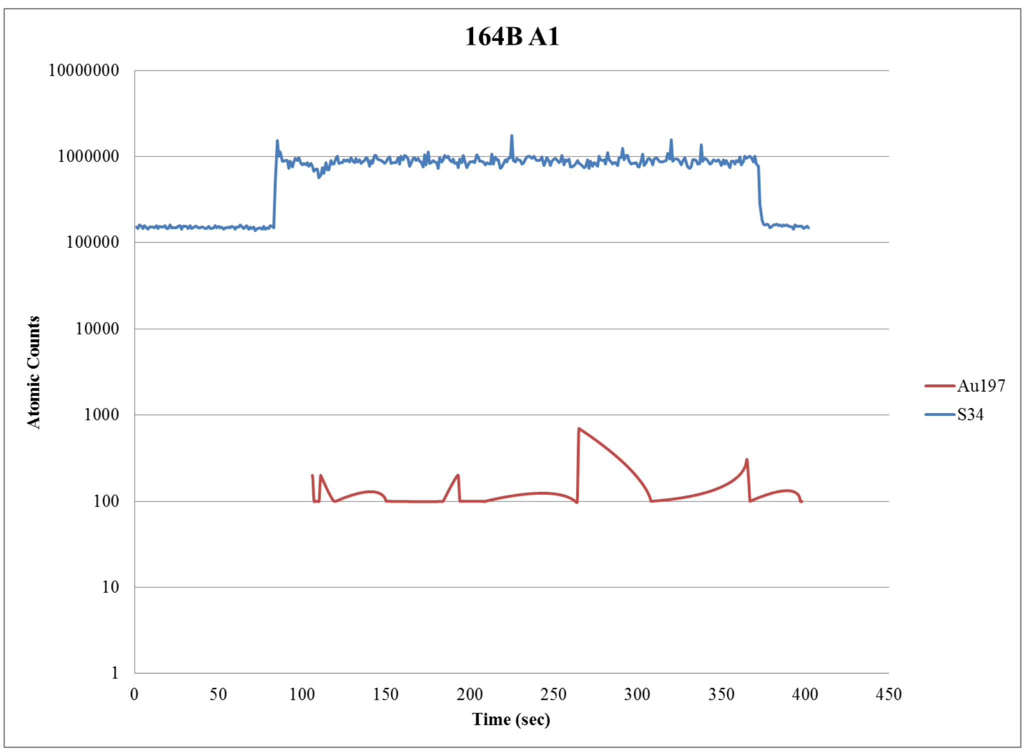

No anomalously high peaks, so no gold inclusions

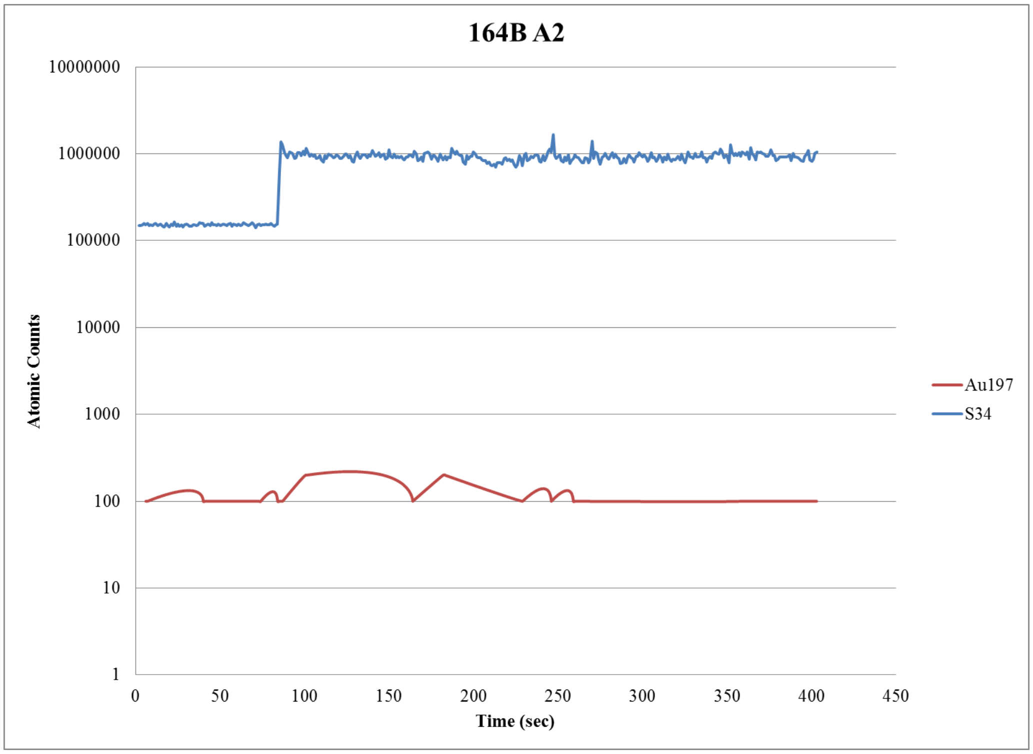

No anomalously high peaks, so no gold inclusions

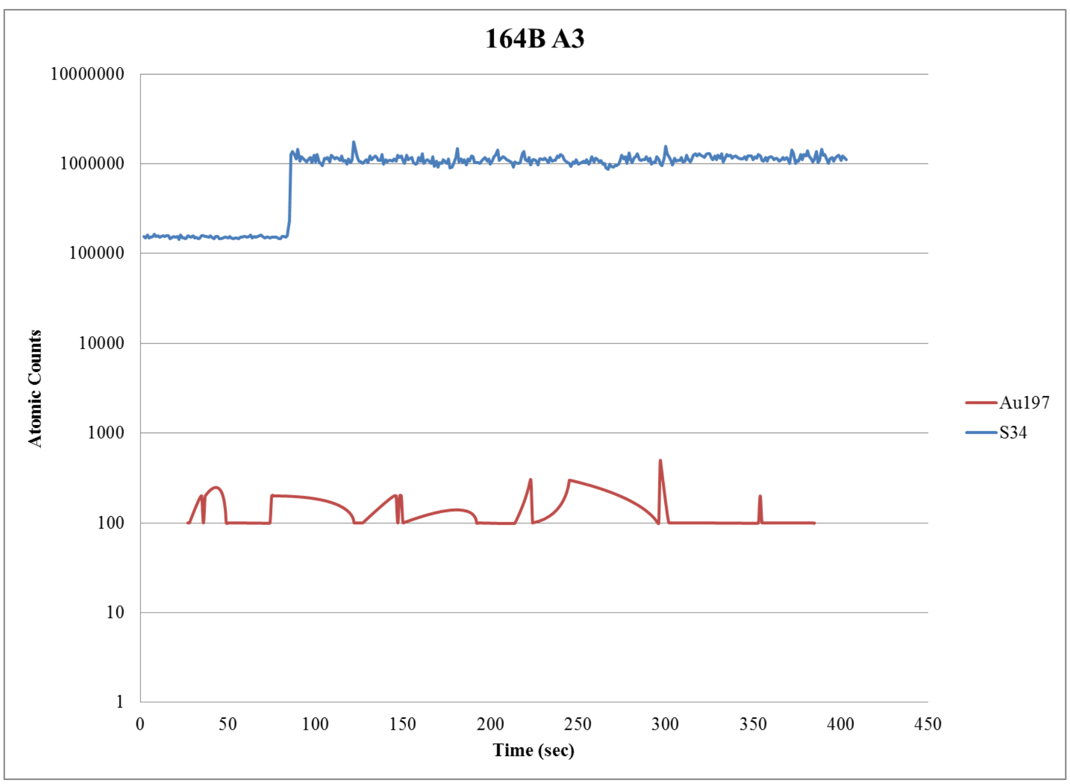

No anomalously high peaks, so no gold inclusions

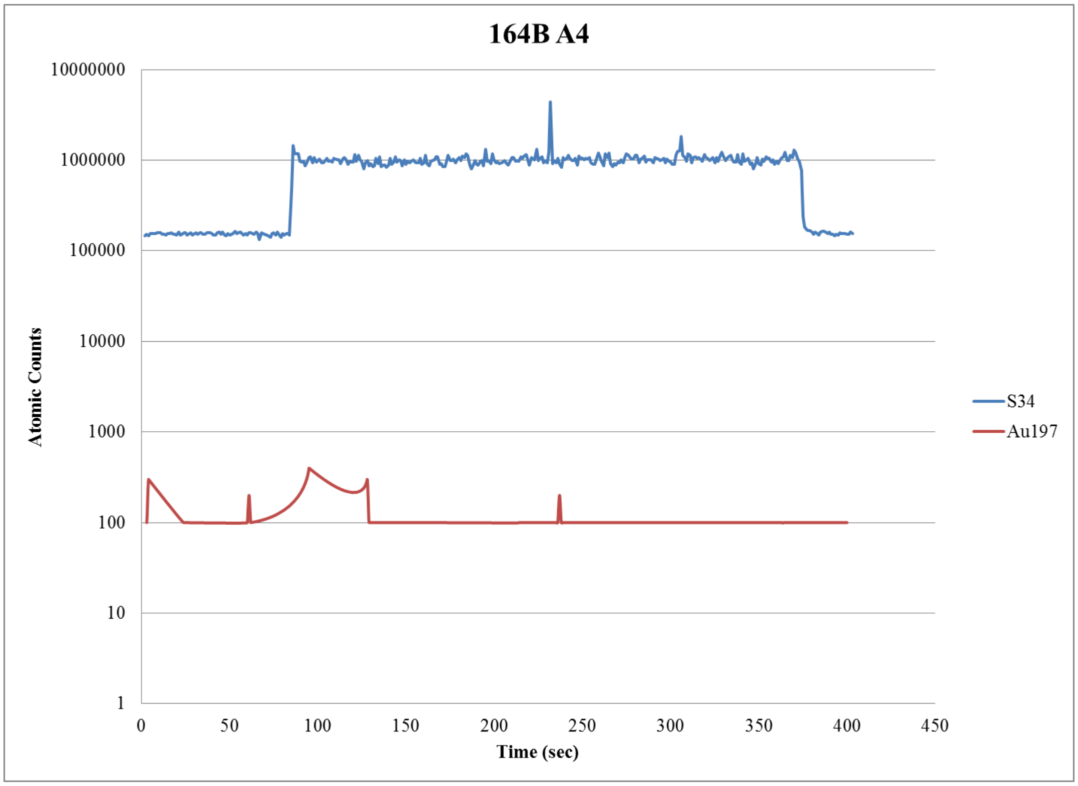

No anomalously high peaks, so no gold inclusions

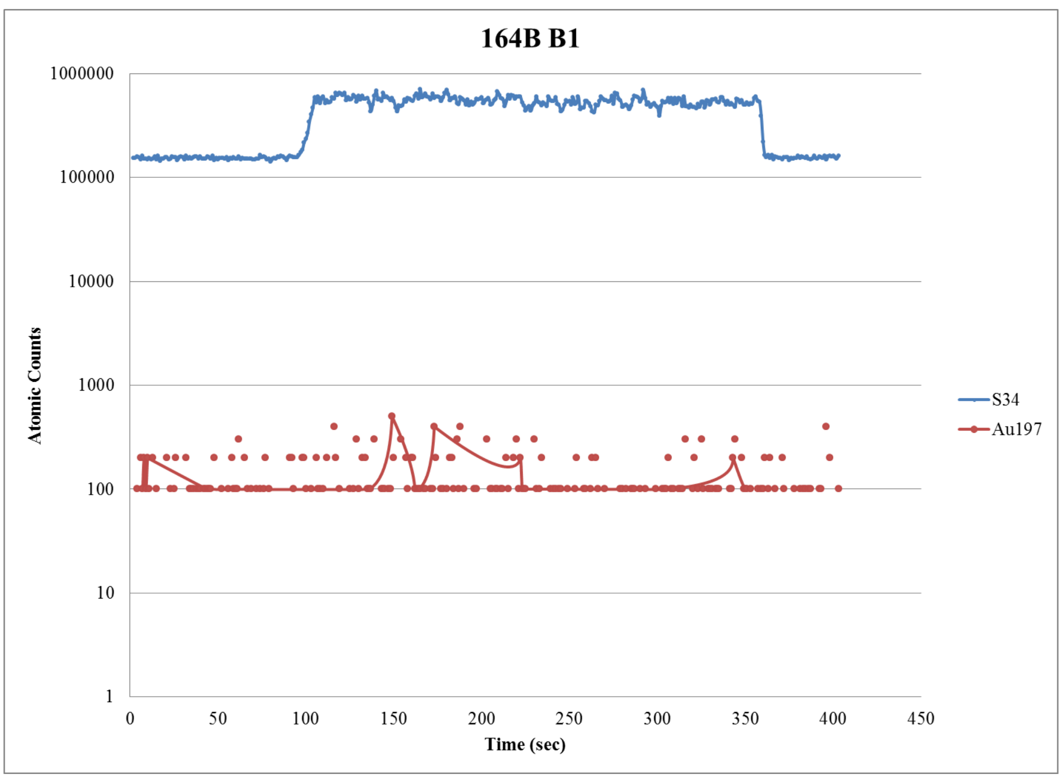

No anomalously high peaks, so no gold inclusions

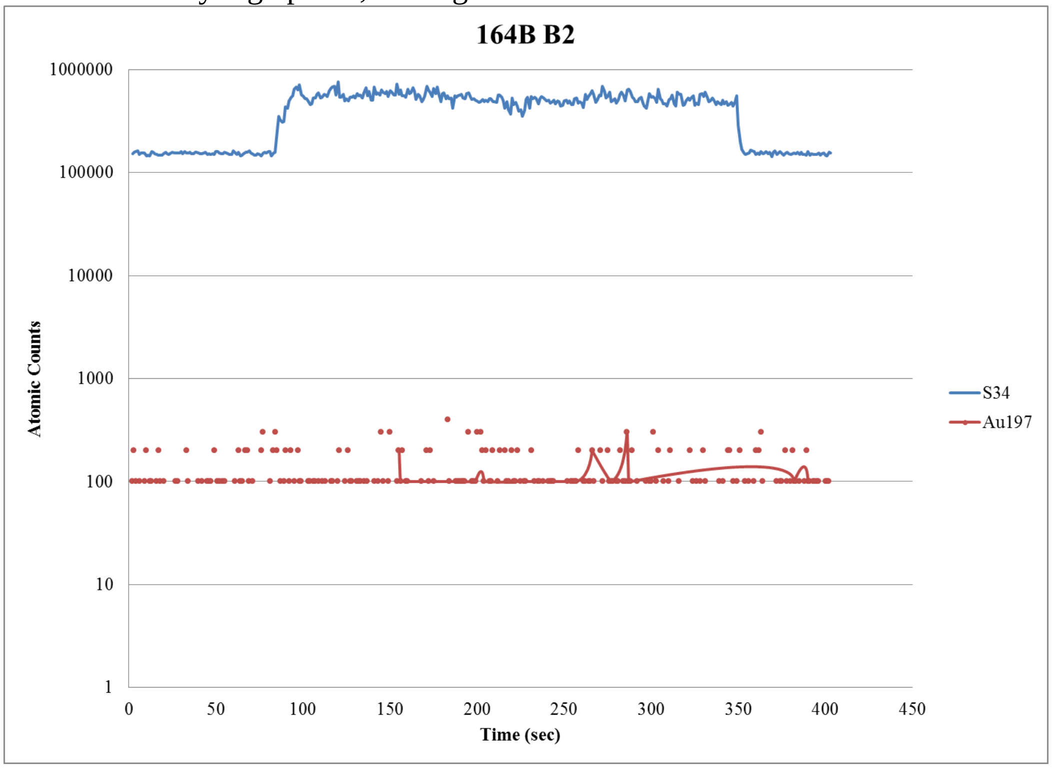

No anomalously high peaks, so no gold inclusions

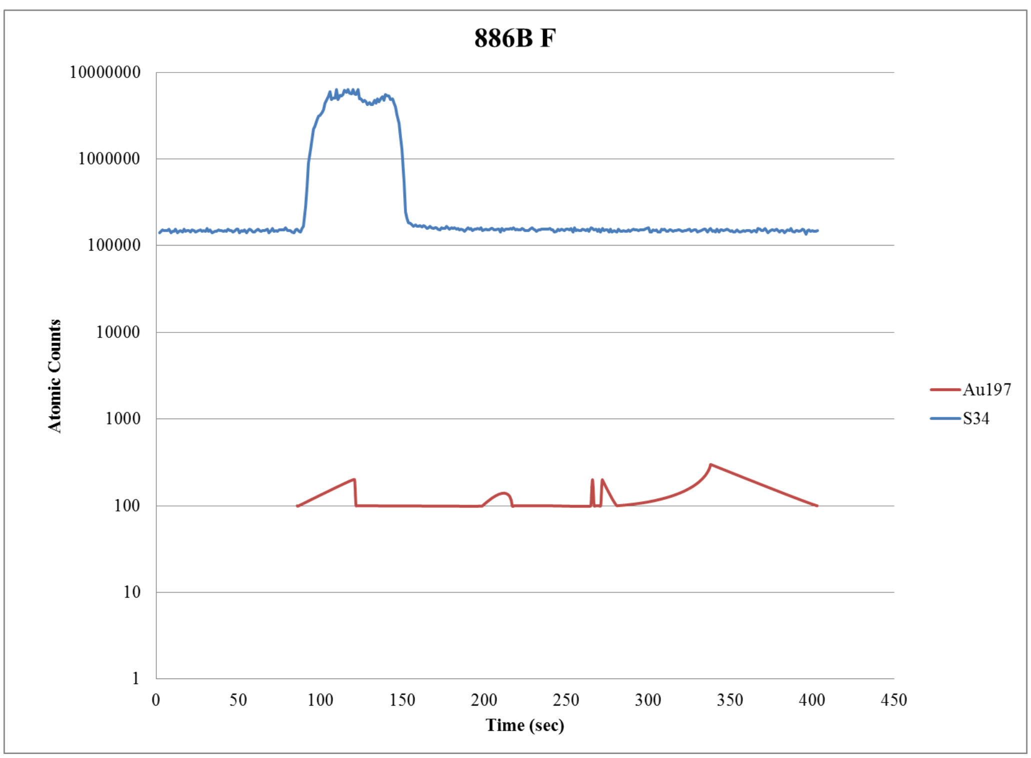

No anomalously high peaks, so no gold inclusions

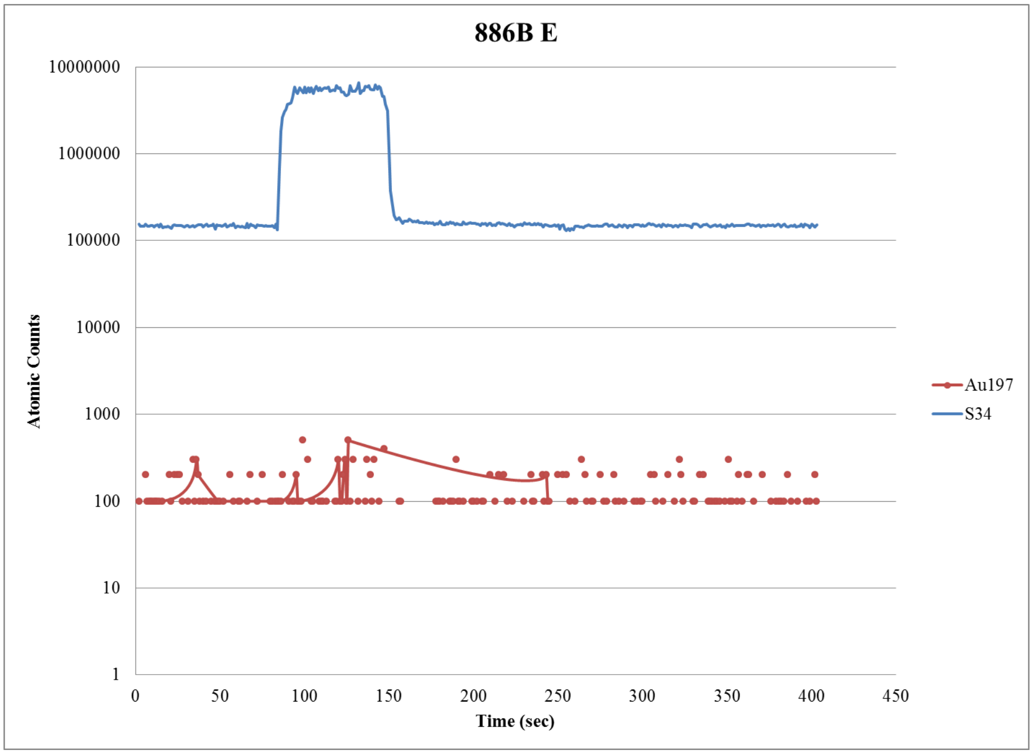

No anomalously high peaks, so no gold inclusions

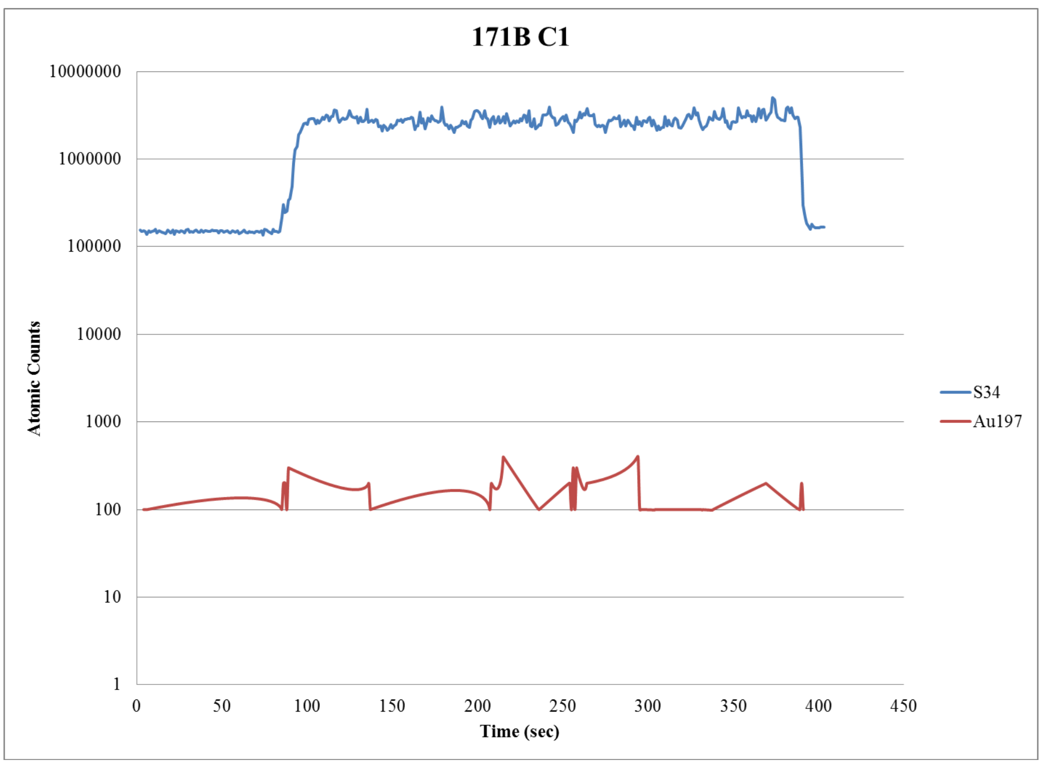

No anomalously high peaks, so no gold inclusions

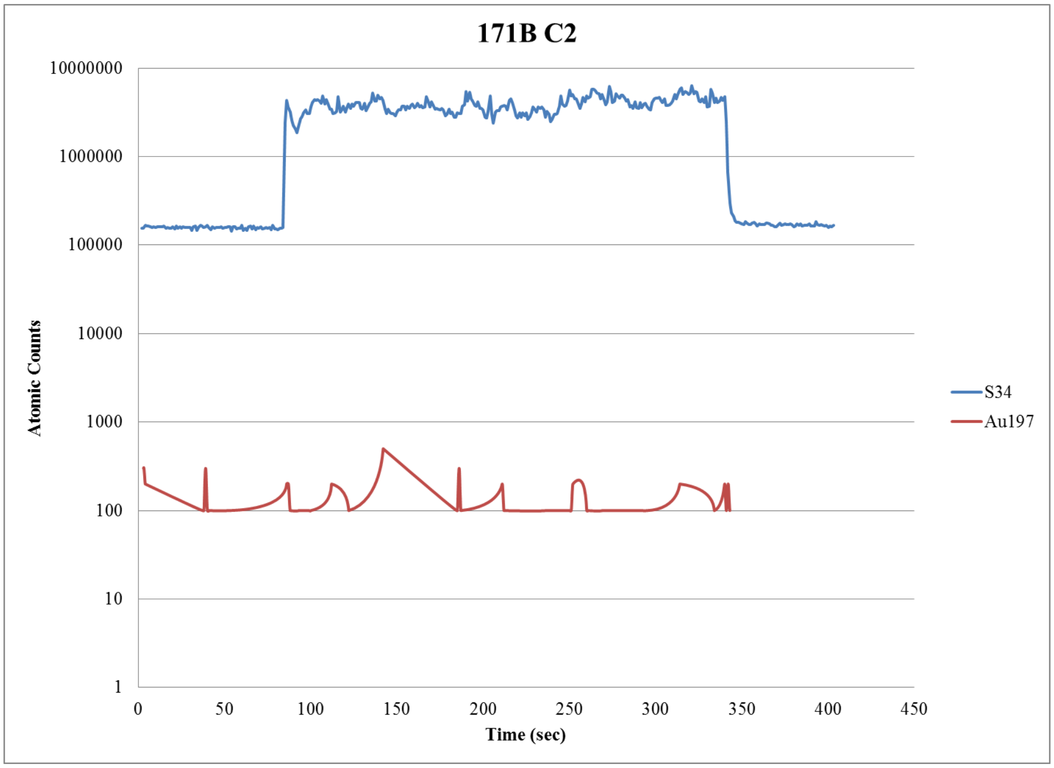

No anomalously high peaks, so no gold inclusions

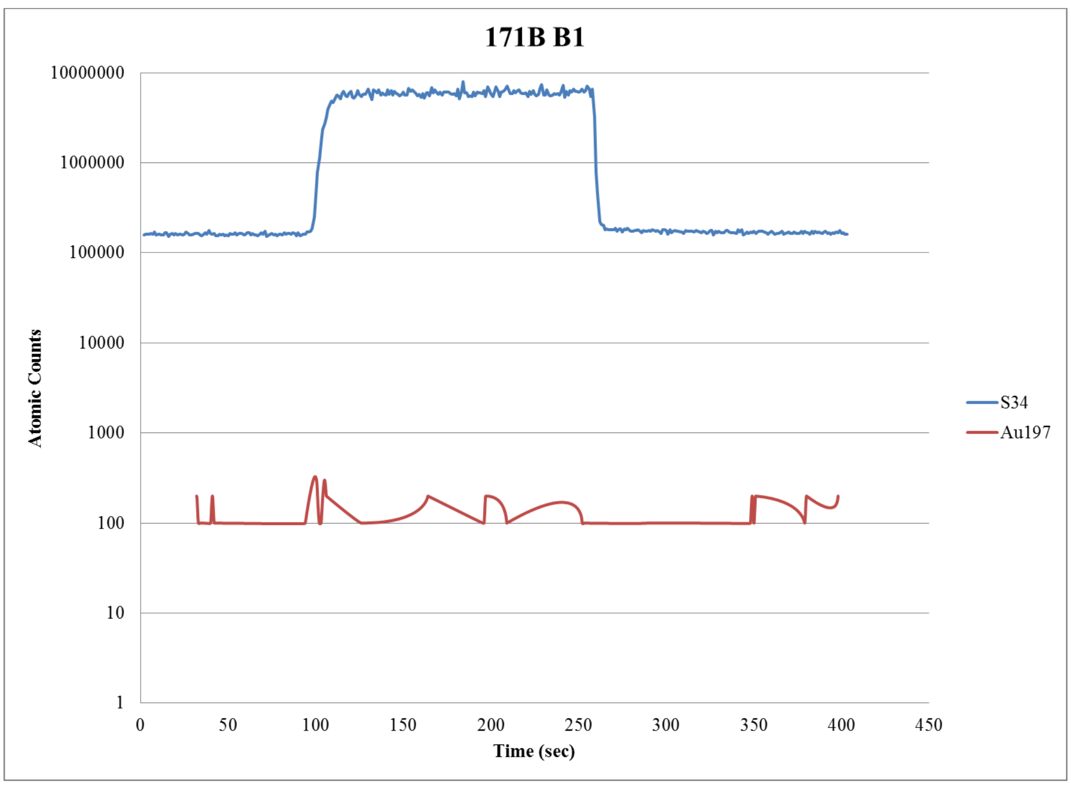

No anomalously high peaks, so no gold inclusions

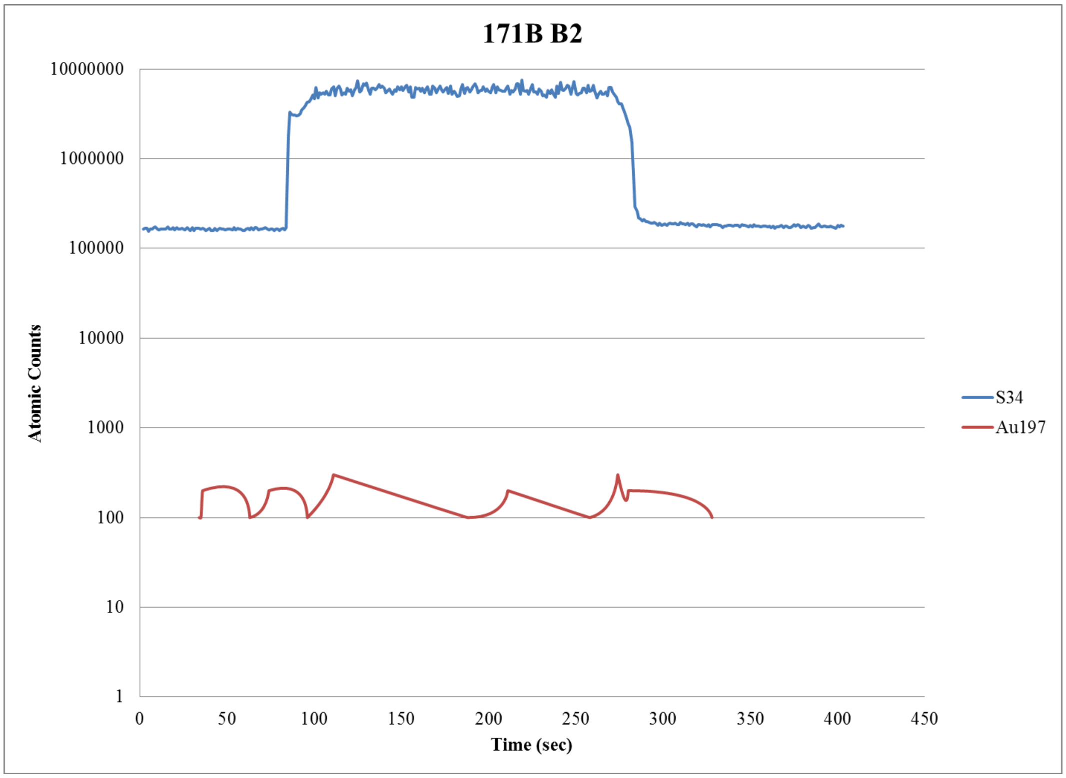

No anomalously high peaks, so no gold inclusions

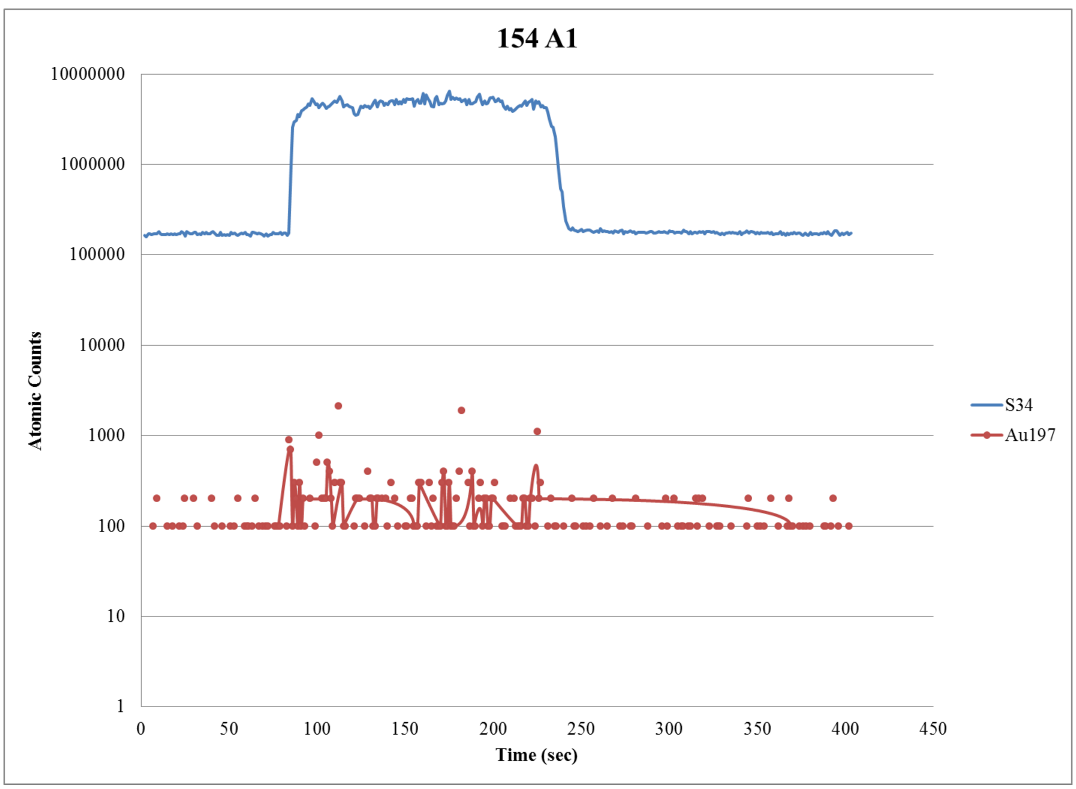

No anomalously high peaks, so no gold inclusions

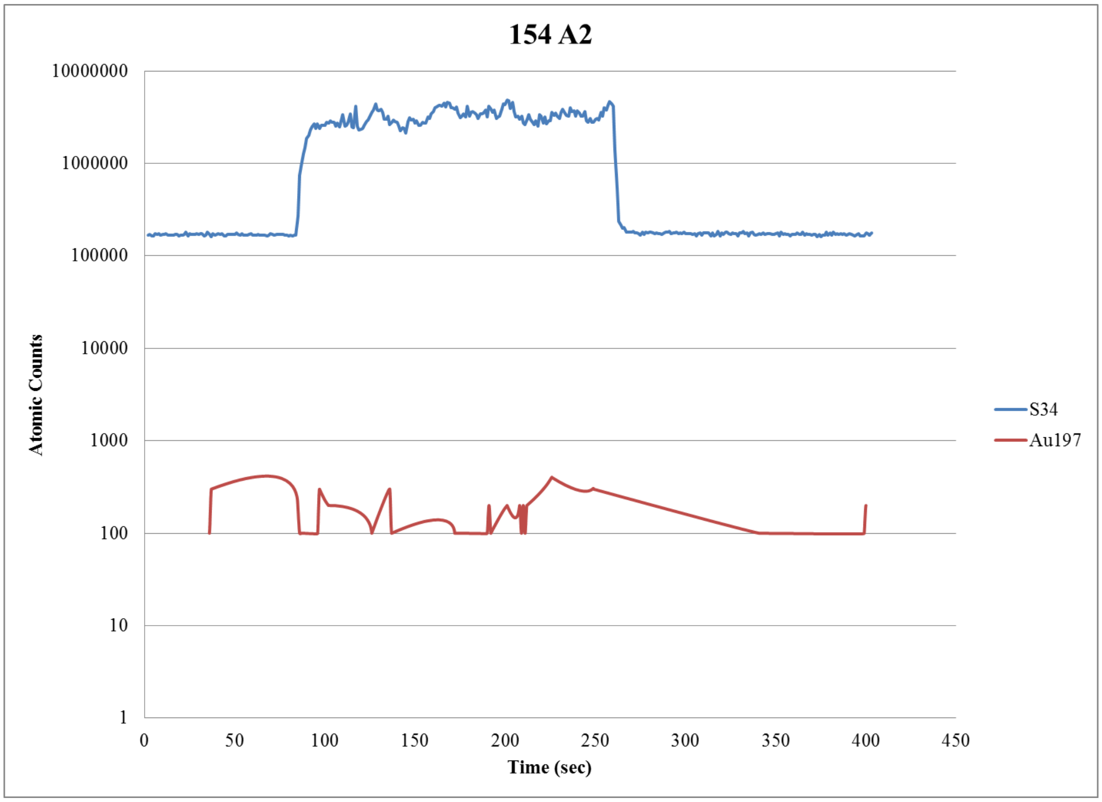

No anomalously high peaks, so no gold inclusions

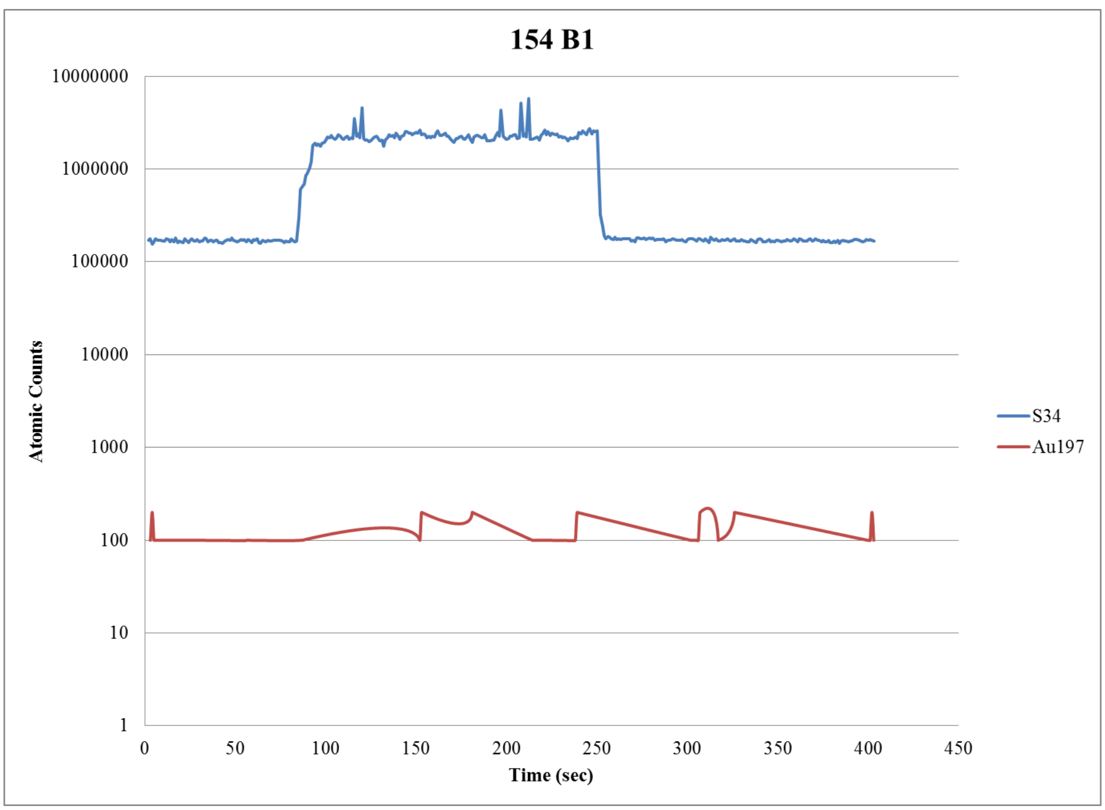

No anomalously high peaks, so no gold inclusions

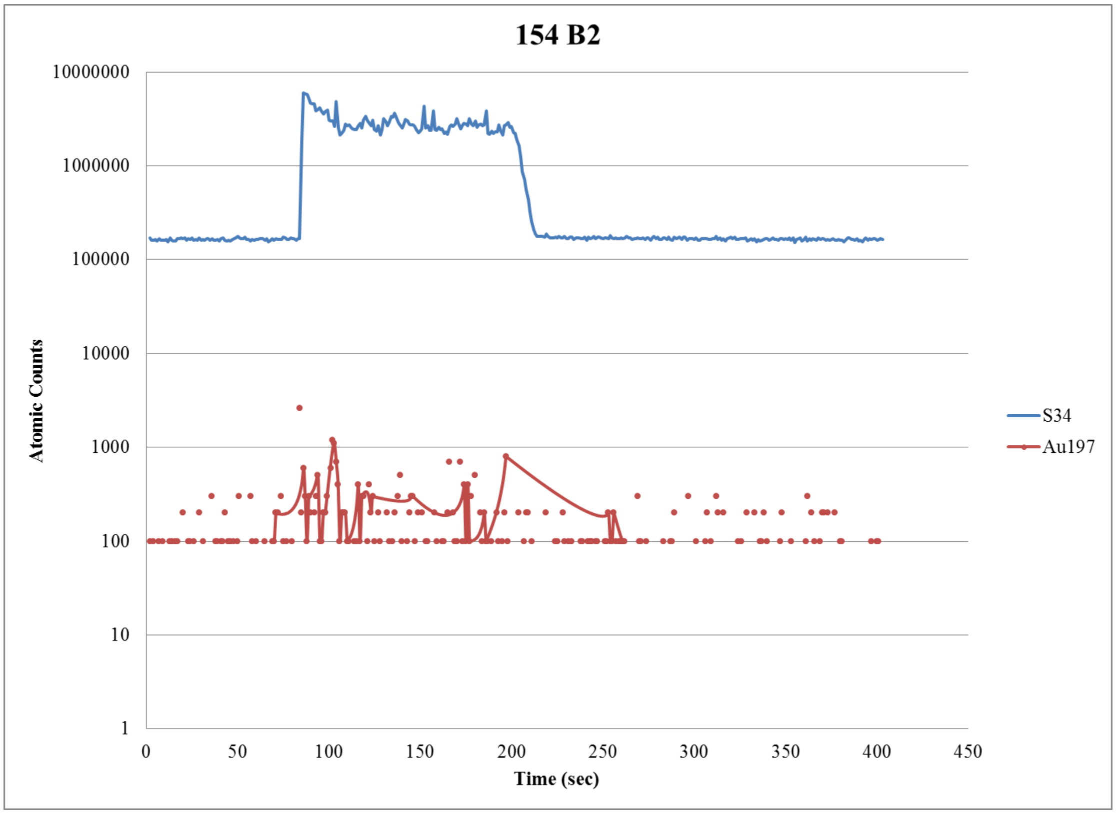

No anomalously high peaks, so no gold inclusions

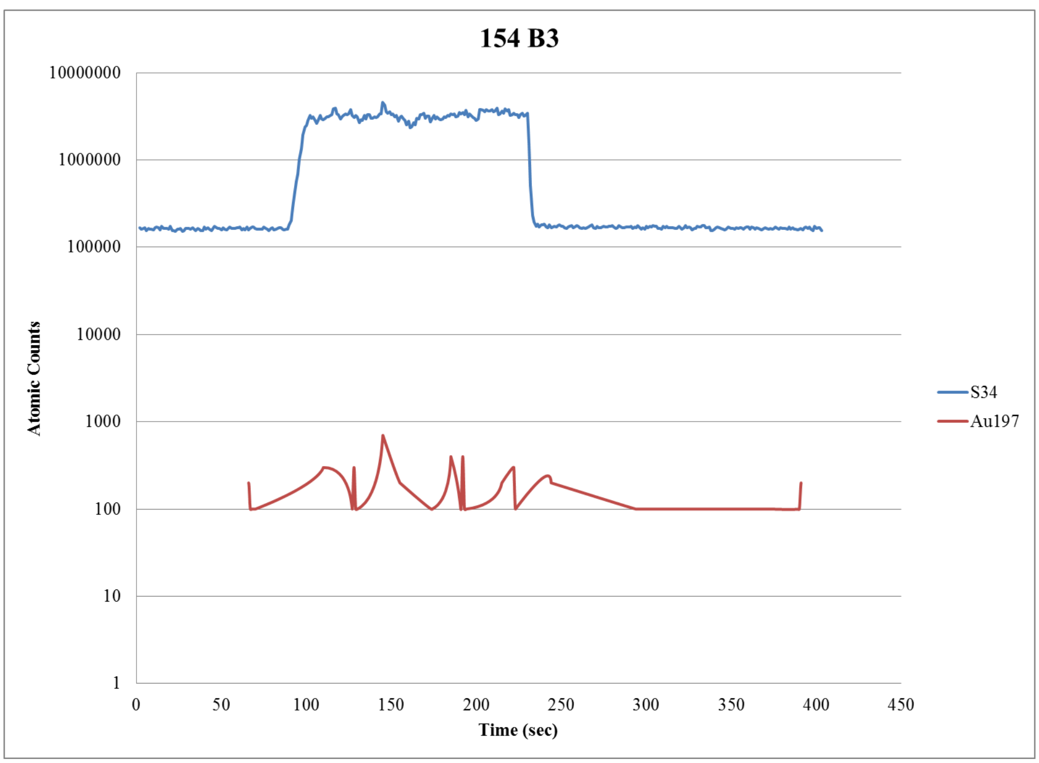

No anomalously high peaks, so no gold inclusions

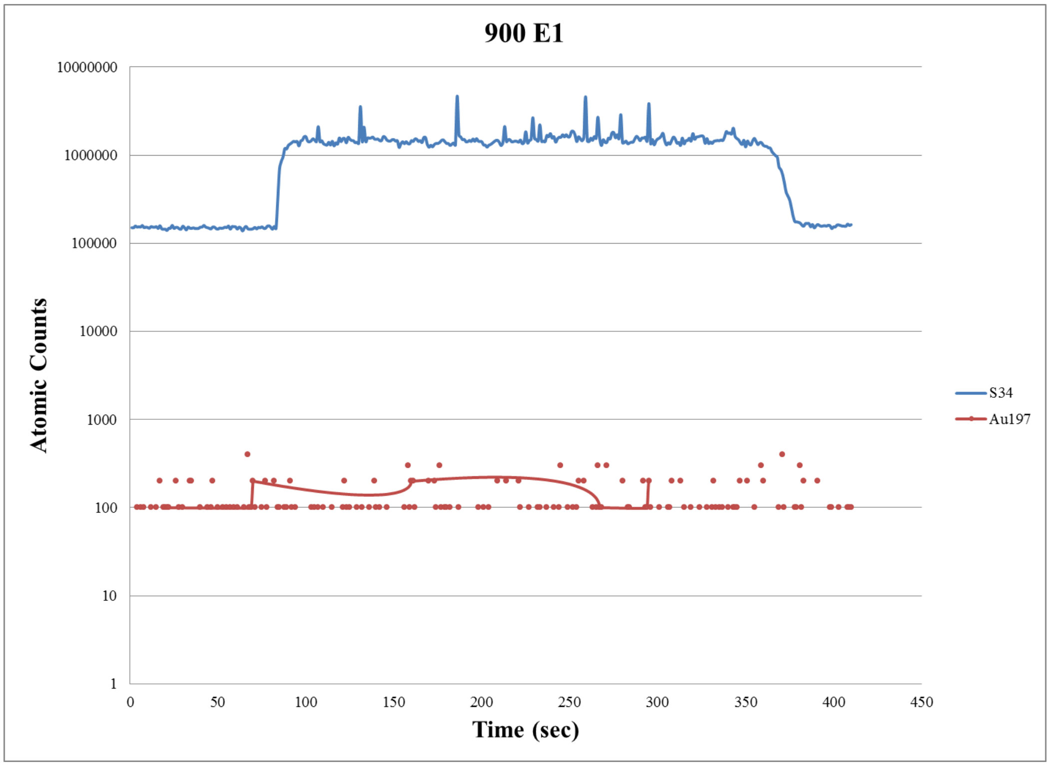

No anomalously high peaks, so no gold inclusions

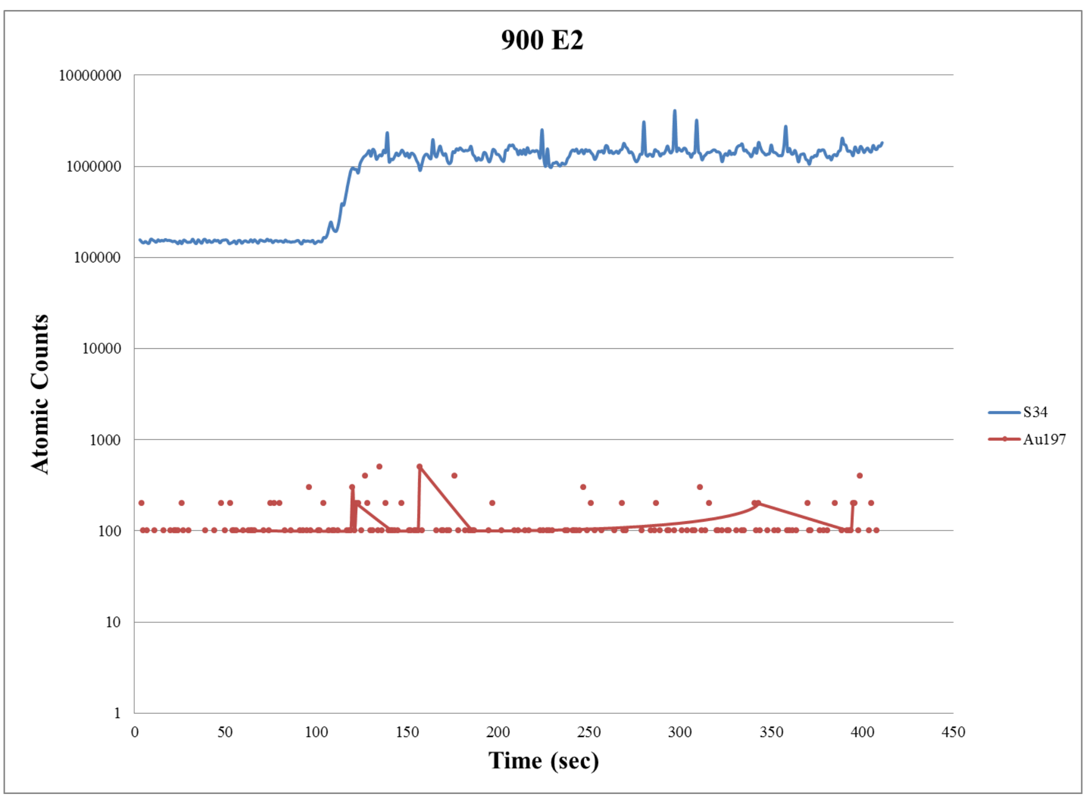

No anomalously high peaks, so no gold inclusions

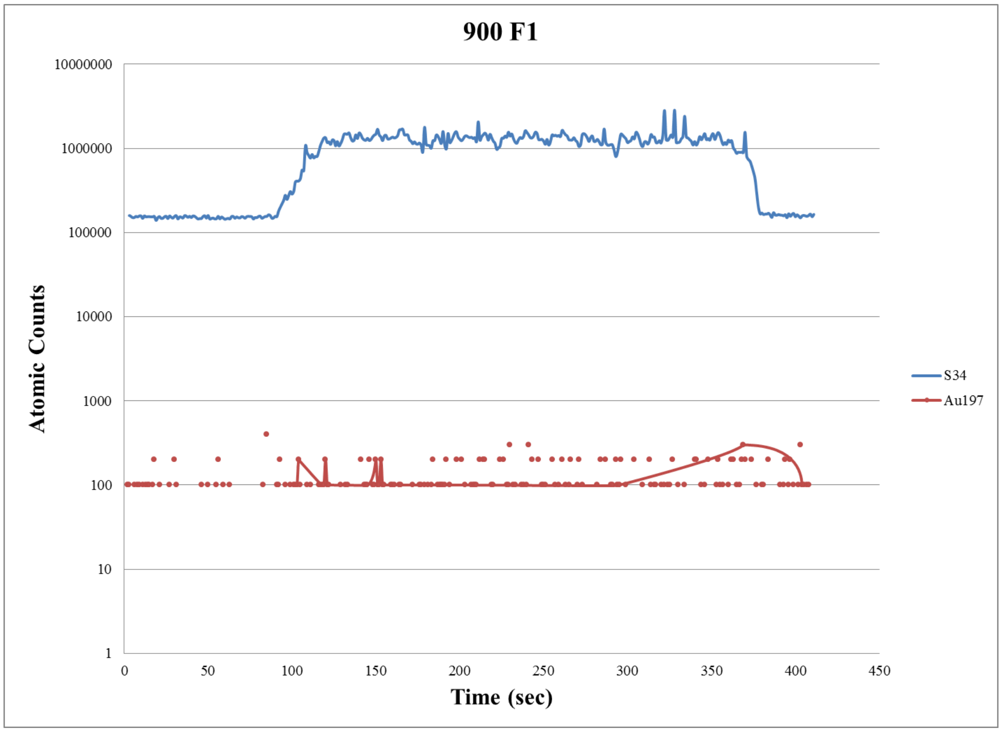

No anomalously high peaks, so no gold inclusions

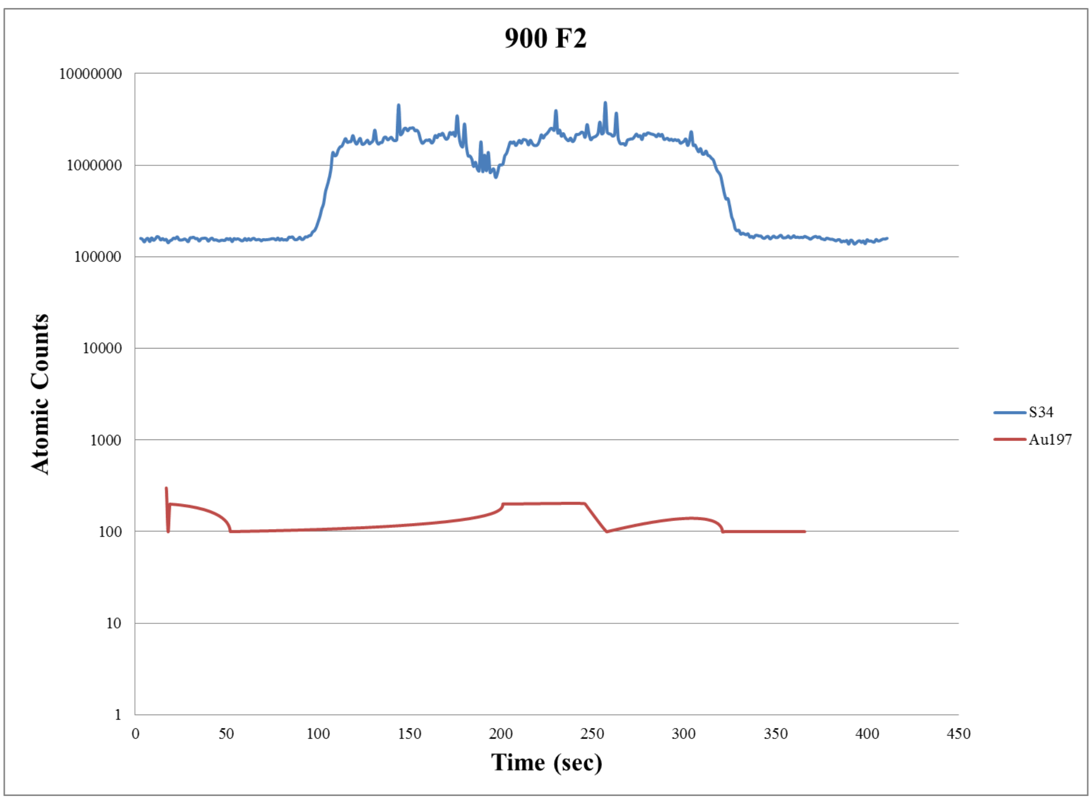

No anomalously high peaks, so no gold inclusions

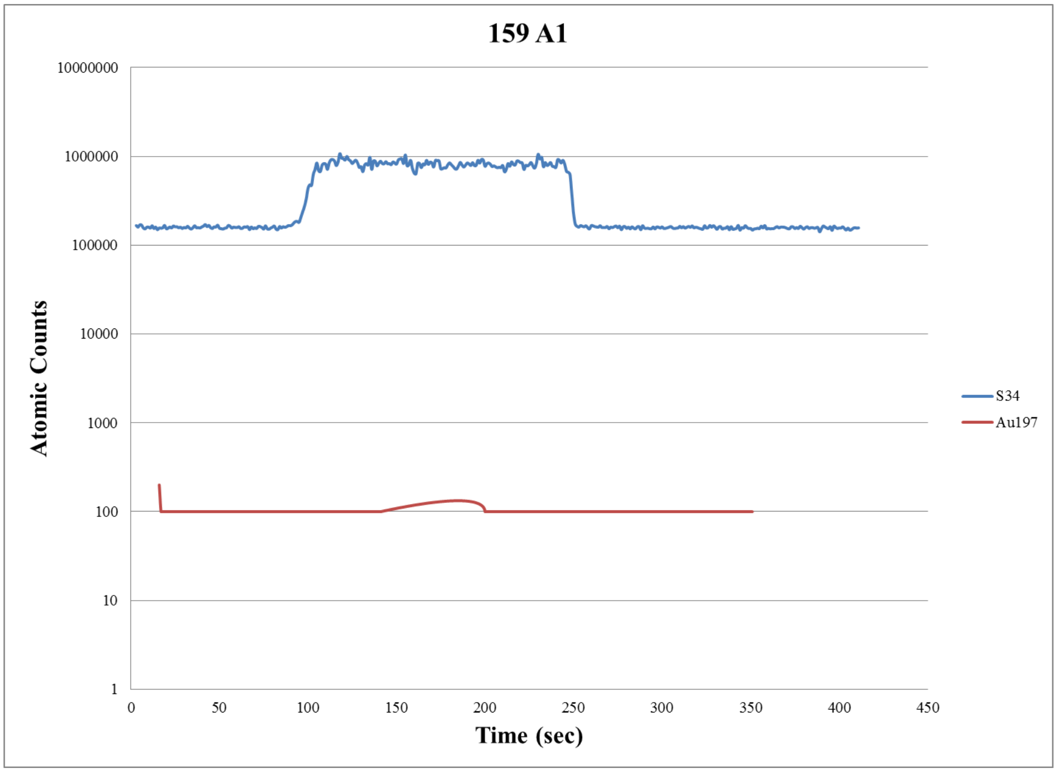

No anomalously high peaks, so no gold inclusions

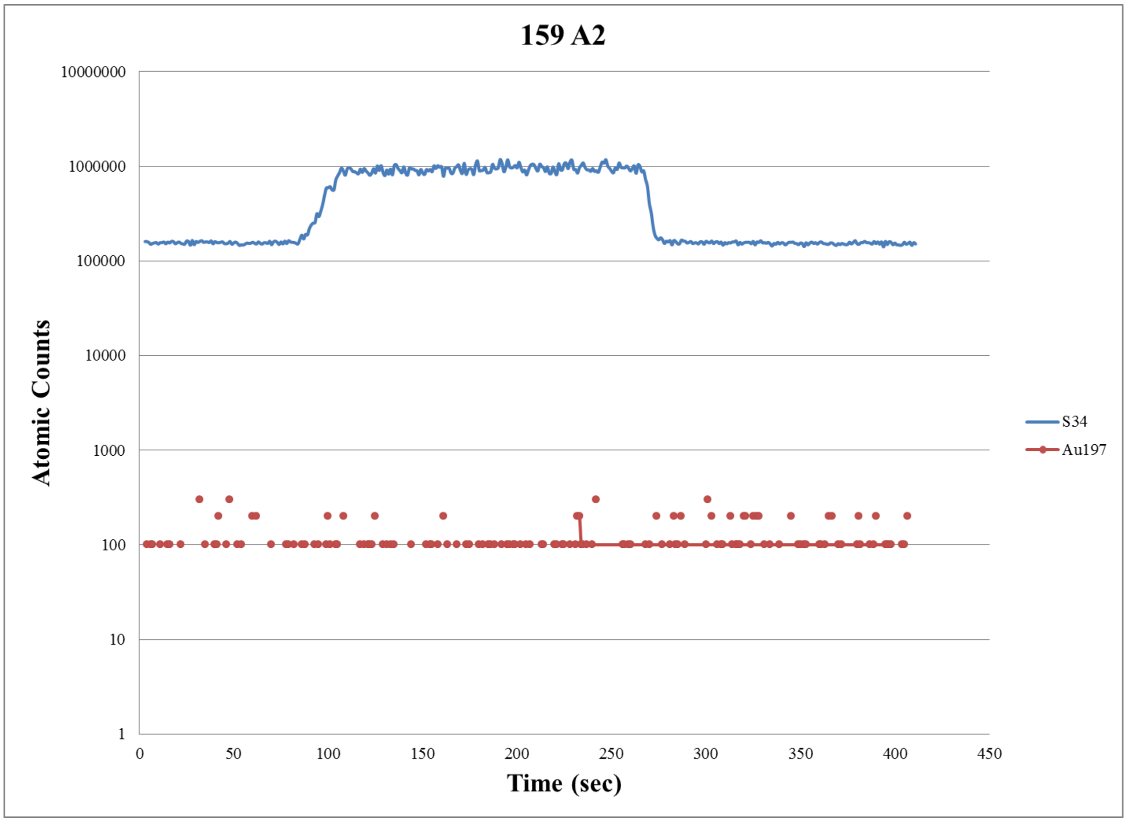

No anomalously high peaks, so no gold inclusions

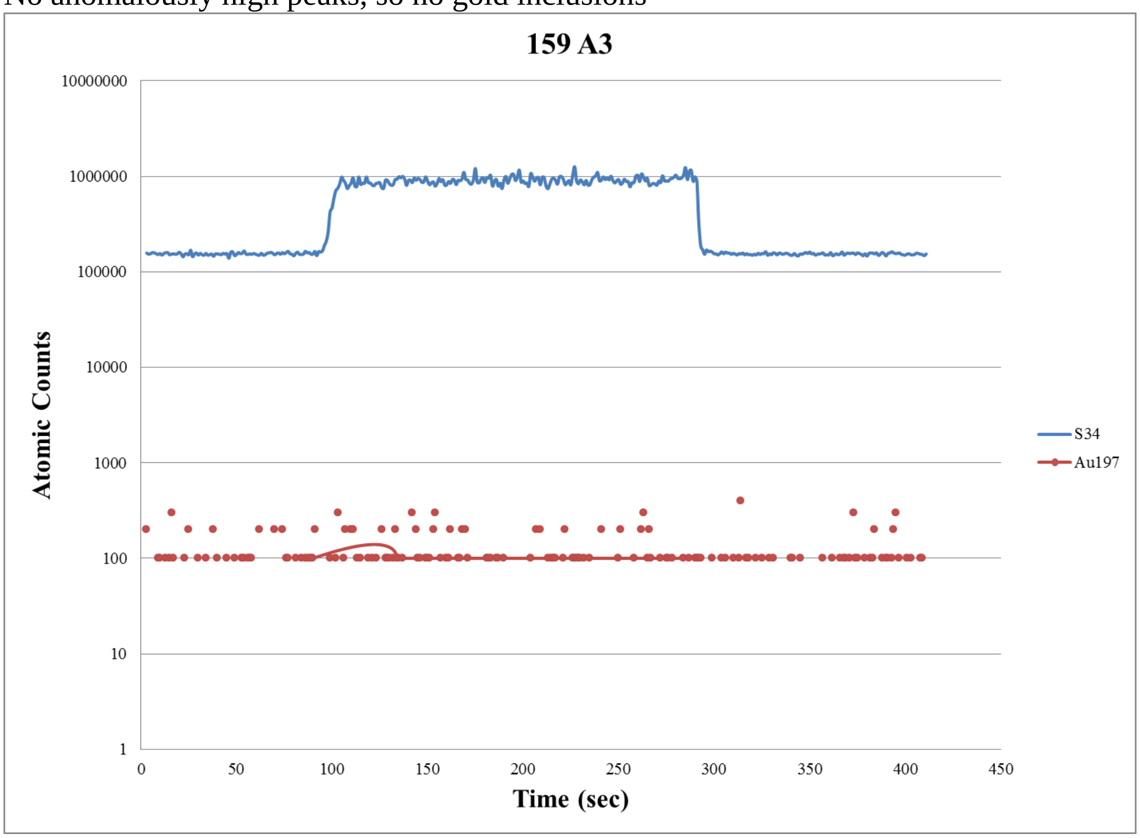

No anomalously high peaks, so no gold inclusions

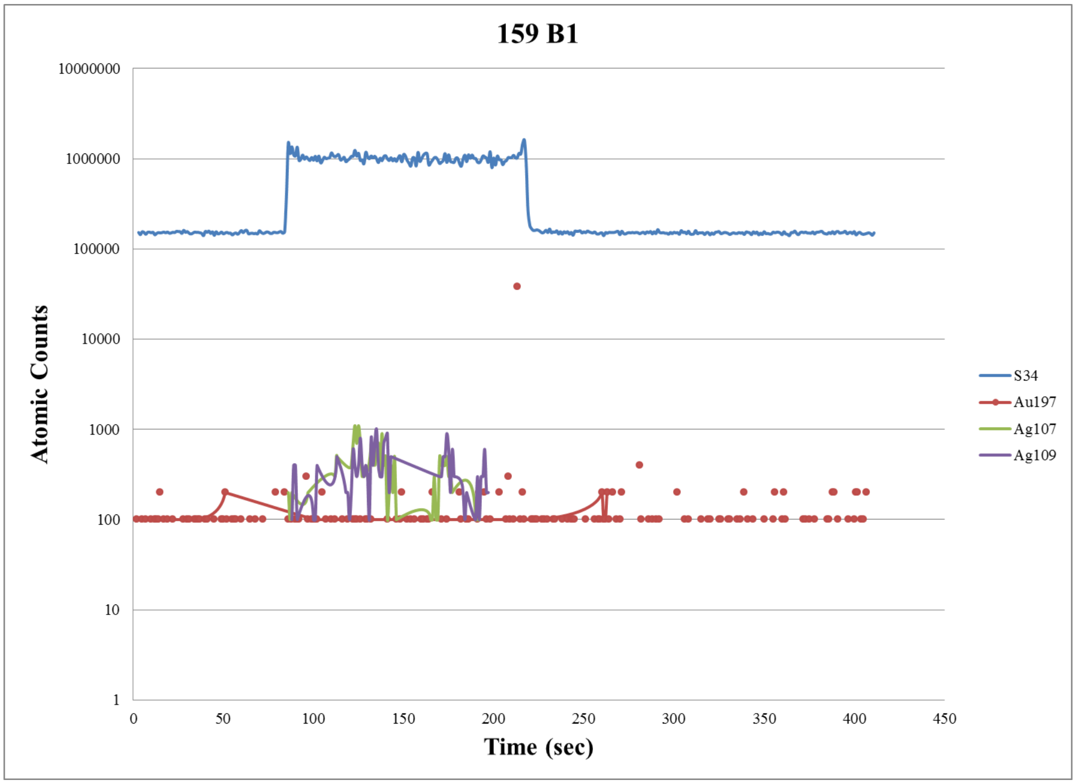

No inclusion within 159 B1 as it is just one anomalously high point that does not show a simultaneously high peak with silver.

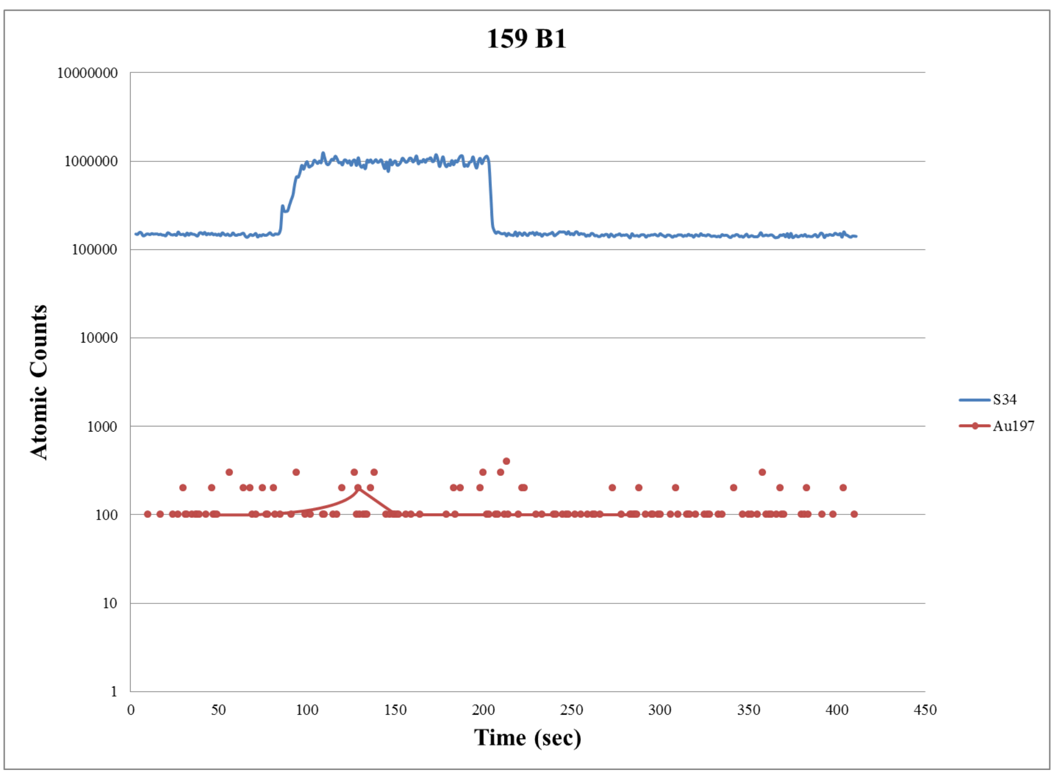

No anomalously high peaks, so no gold inclusions

E3. Trace element intensity peaks and segments analysed during Igor Pro and Iolite processing. Pink represents sulphur atomic counts, red represents gold atomic counts, blue represents nickel and green represents cobalt.

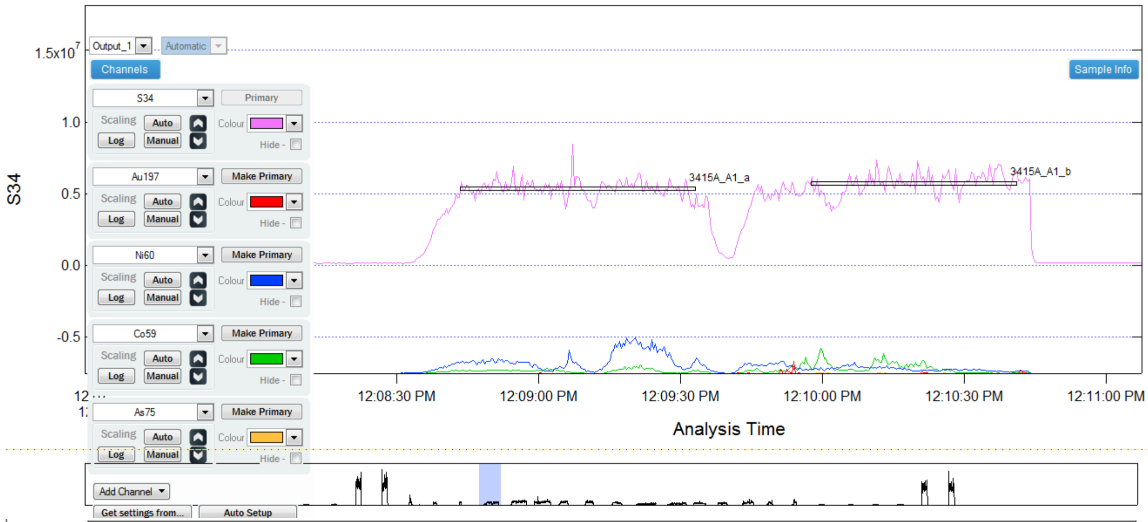

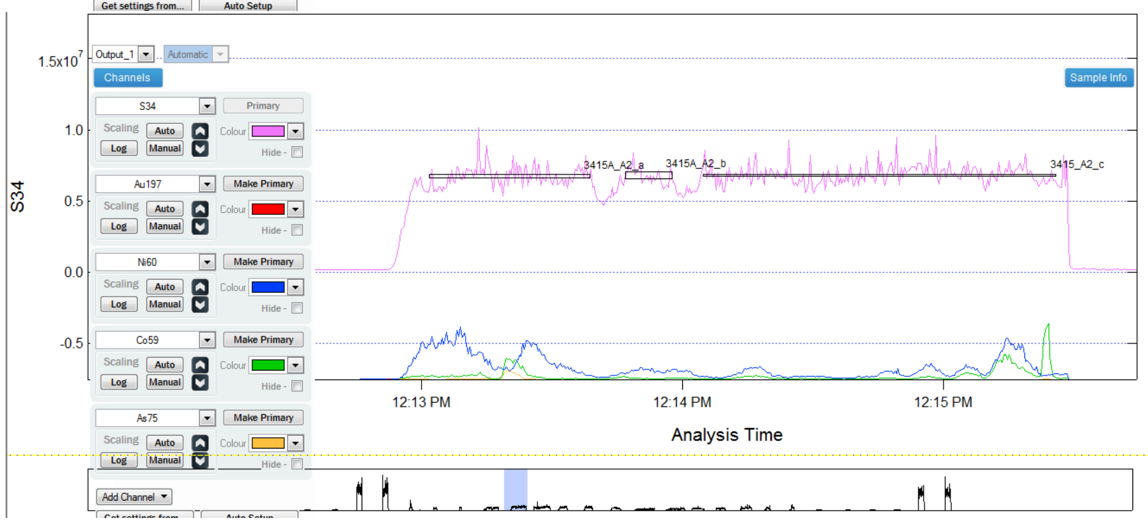

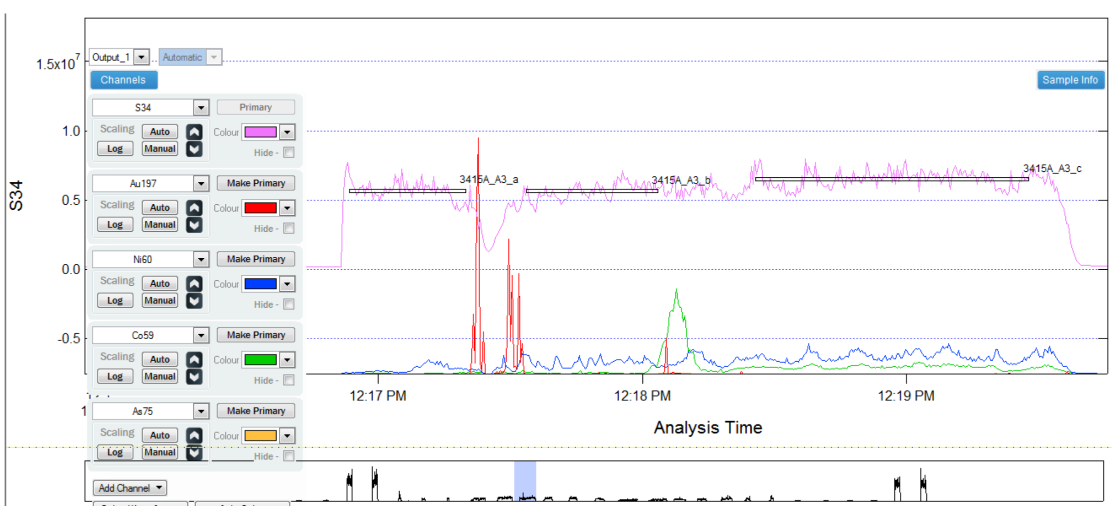

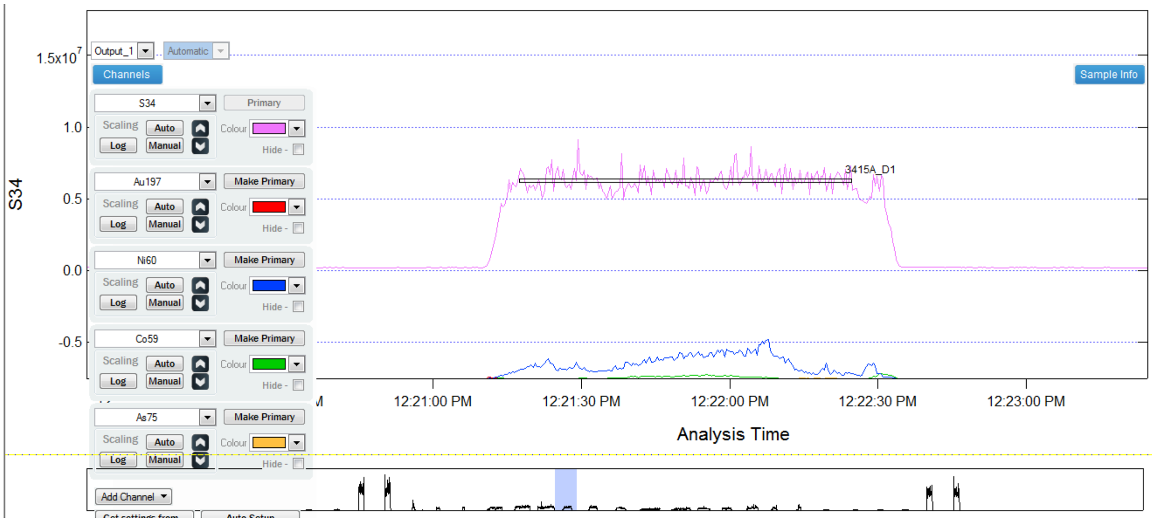
S34
1.5x10^7
1.0
0.5
0.0
-0.5
Output_1
Automatic
Channels
Sample Info
S34
Au197
Ni60
Co59
As75
Add Channel
3415A_D1
12:21:00 PM
12:21:30 PM
12:22:00 PM
12:22:30 PM
12:23:00 PM
Analysis Time

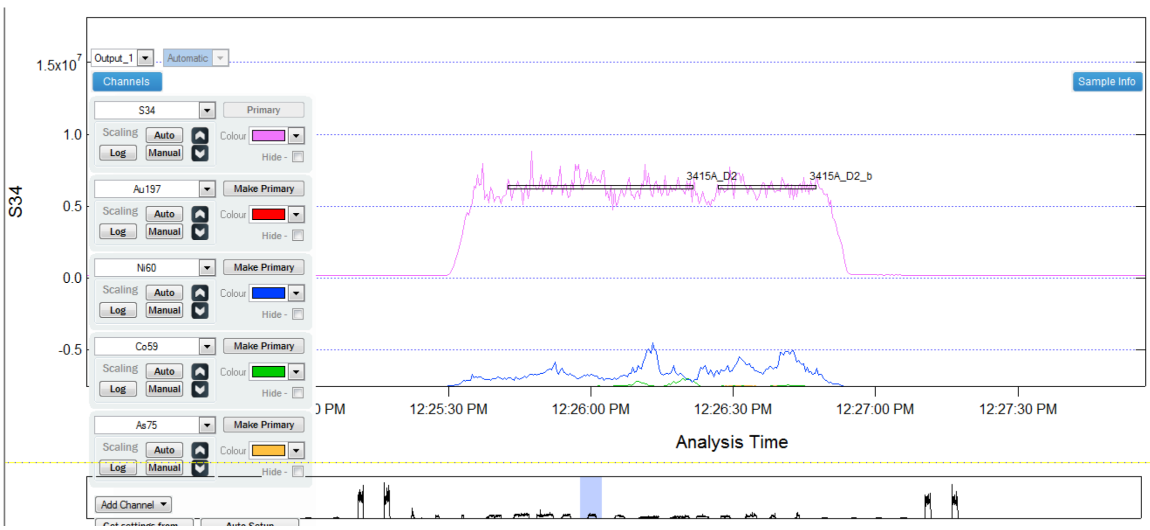
S34
1.5x10^7
1.0
0.5
0.0
-0.5
Output_1
Automatic
Channels
Sample Info
S34
Au197
Ni60
Co59
As75
Add Channel
3415A_D2
3415A_D2_b
12:25:30 PM
12:26:00 PM
12:26:30 PM
12:27:00 PM
12:27:30 PM
Analysis Time

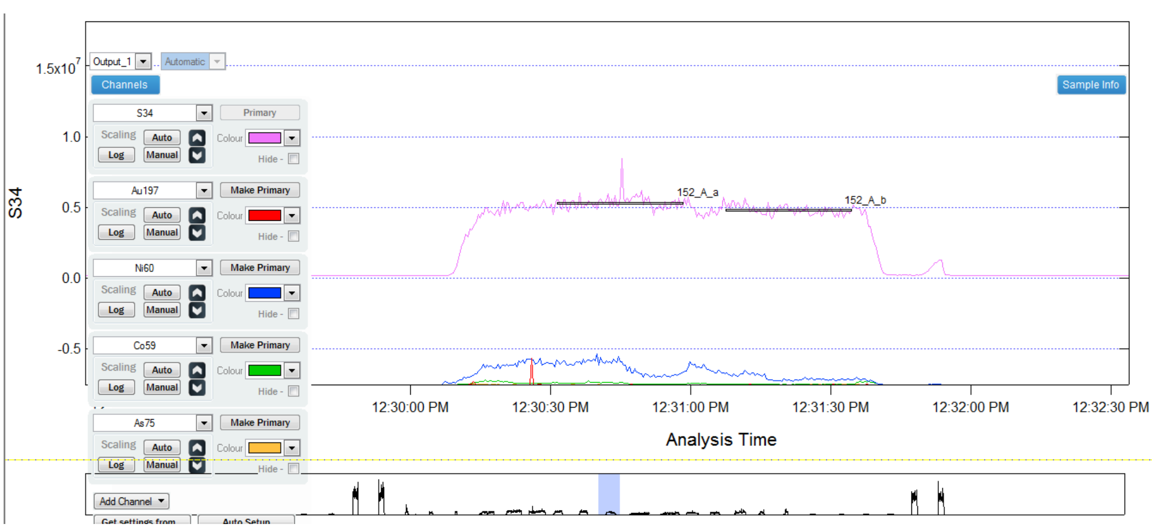
S34
1.5x10^7
1.0
0.5
0.0
-0.5
Output_1
Automatic
Channels
Sample Info
S34
Au197
Ni60
Co59
As75
Add Channel
152_A_a
152_A_b
12:30:00 PM
12:30:30 PM
12:31:00 PM
12:31:30 PM
12:32:00 PM
12:32:30 PM
Analysis Time

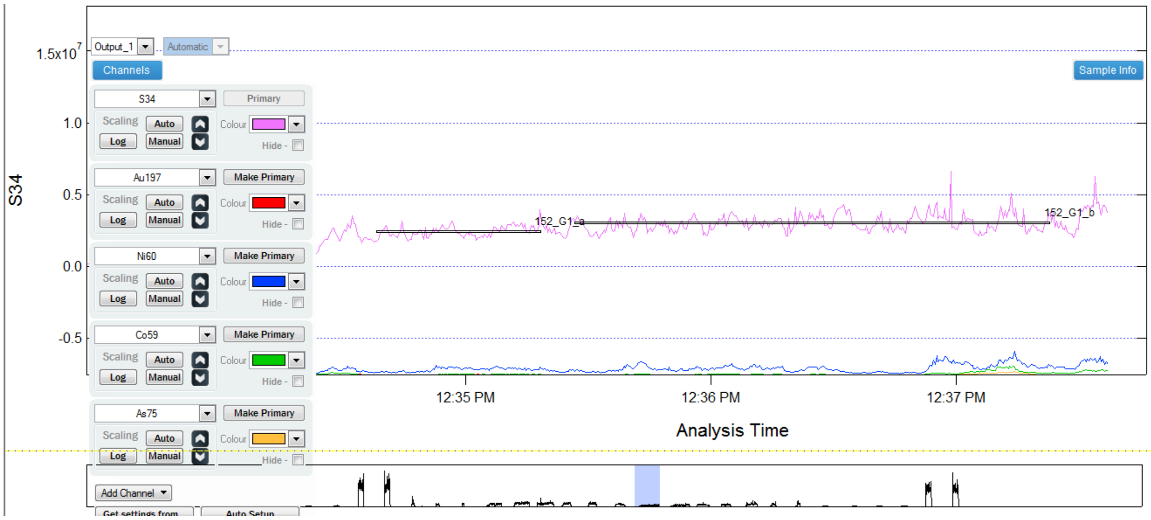
1.5x10^7
1.0
0.5
0.0
-0.5
S34
Output_1
Automatic
Channels
Sample Info
S34
Au197
Ni60
Co59
As75
152_G1_a
152_G1_b
12:35 PM
12:36 PM
12:37 PM
Analysis Time
Add Channel

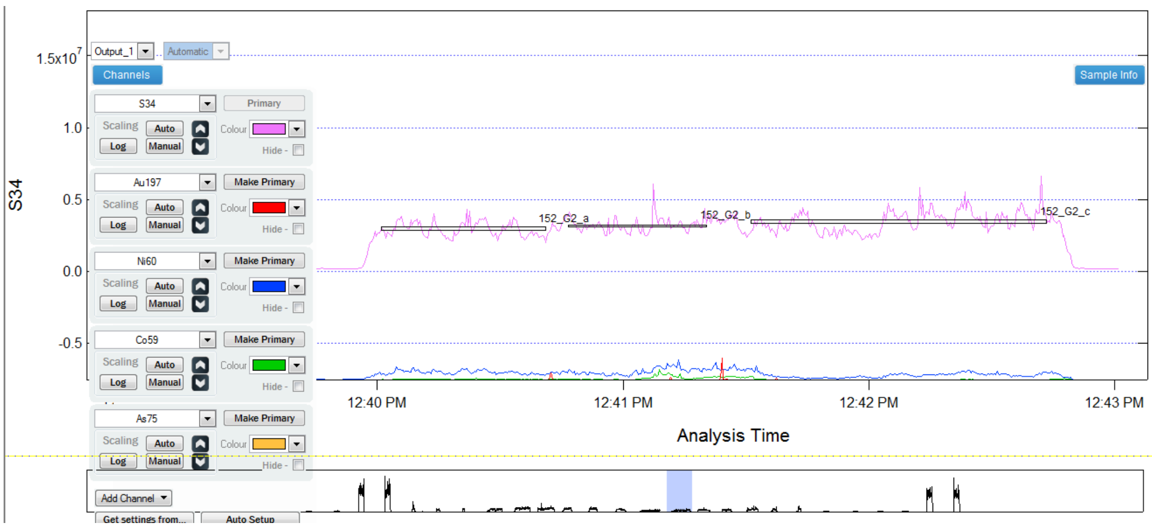
1.5x10^7
1.0
0.5
0.0
-0.5
S34
Output_1
Automatic
Channels
Sample Info
S34
Au197
Ni60
Co59
As75
152_G2_a
152_G2_b
152_G2_c
12:40 PM
12:41 PM
12:42 PM
12:43 PM
Analysis Time
Add Channel
Get settings from...
Auto Setup

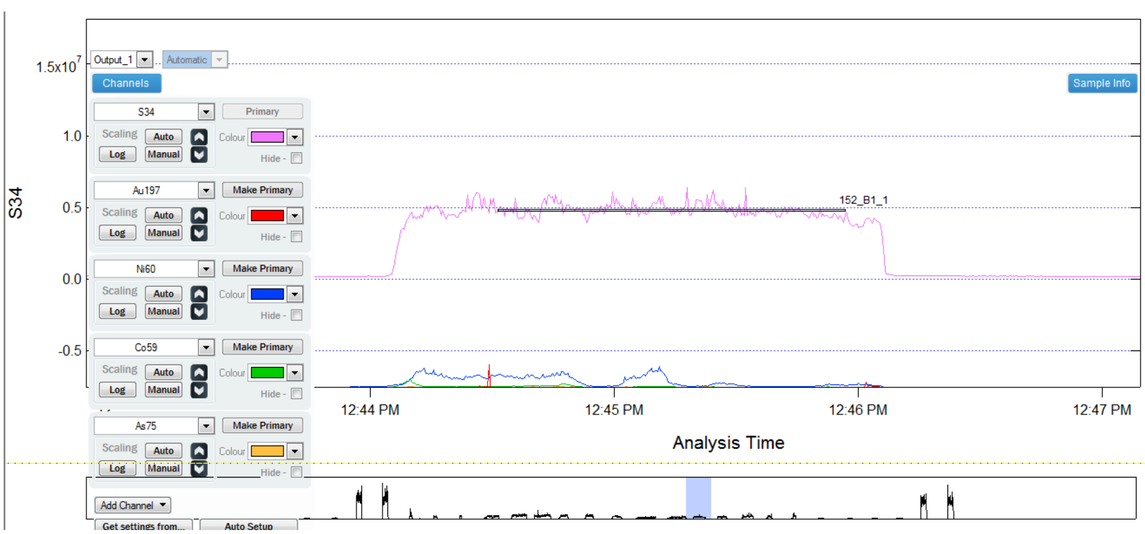
1.5x10^7
1.0
0.5
0.0
-0.5
S34
Output_1
Automatic
Channels
Sample Info
S34
Au197
Ni60
Co59
As75
152_B1_1
12:44 PM
12:45 PM
12:46 PM
12:47 PM
Analysis Time
Add Channel
Get settings from...
Auto Setup

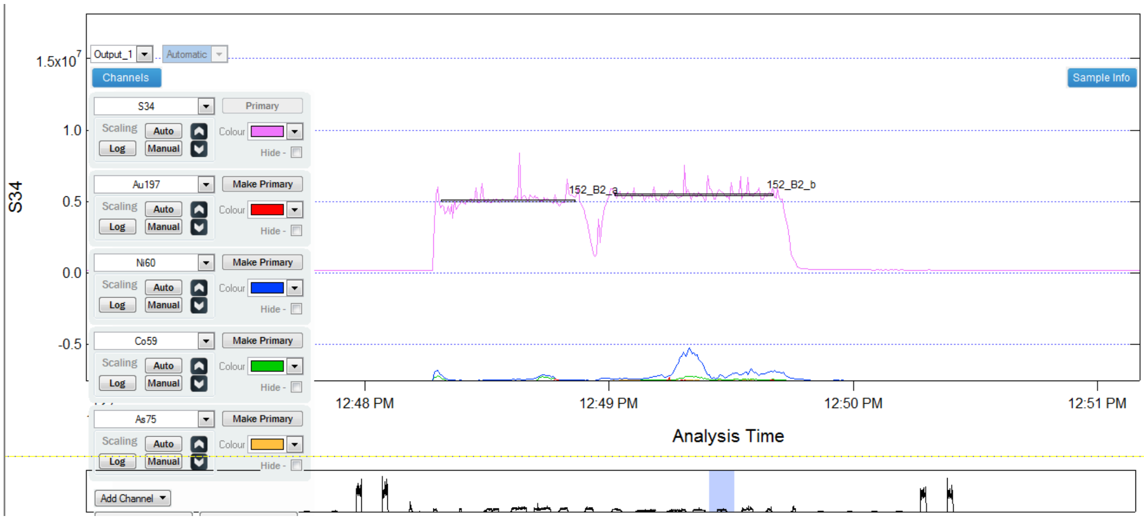
S34
Analysis Time
152_B2_a
152_B2_b
12:48 PM
12:49 PM
12:50 PM
12:51 PM
Sample Info

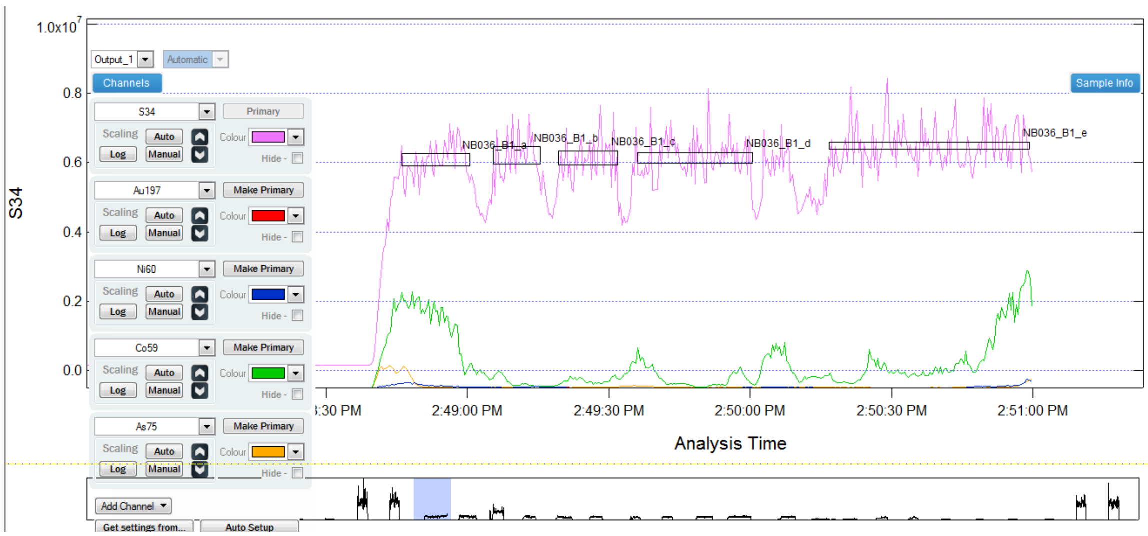
S34
Analysis Time
NB036_B1_a
NB036_B1_b
NB036_B1_c
NB036_B1_d
NB036_B1_e
2:49:00 PM
2:49:30 PM
2:50:00 PM
2:50:30 PM
2:51:00 PM
Sample Info

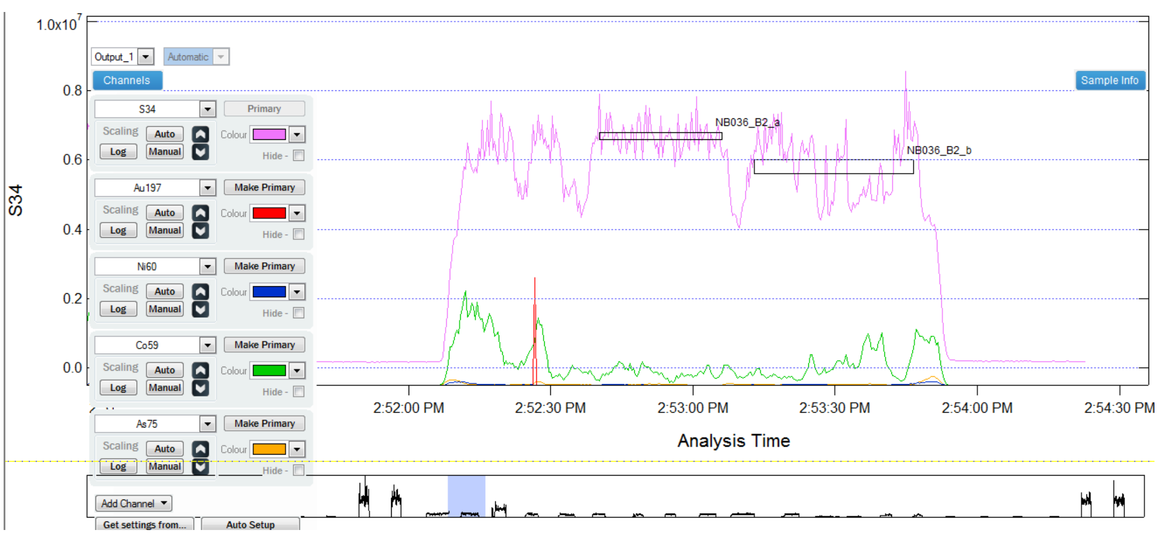
S34
Analysis Time
NB036_B2_a
NB036_B2_b
2:52:00 PM
2:52:30 PM
2:53:00 PM
2:53:30 PM
2:54:00 PM
2:54:30 PM
Sample Info

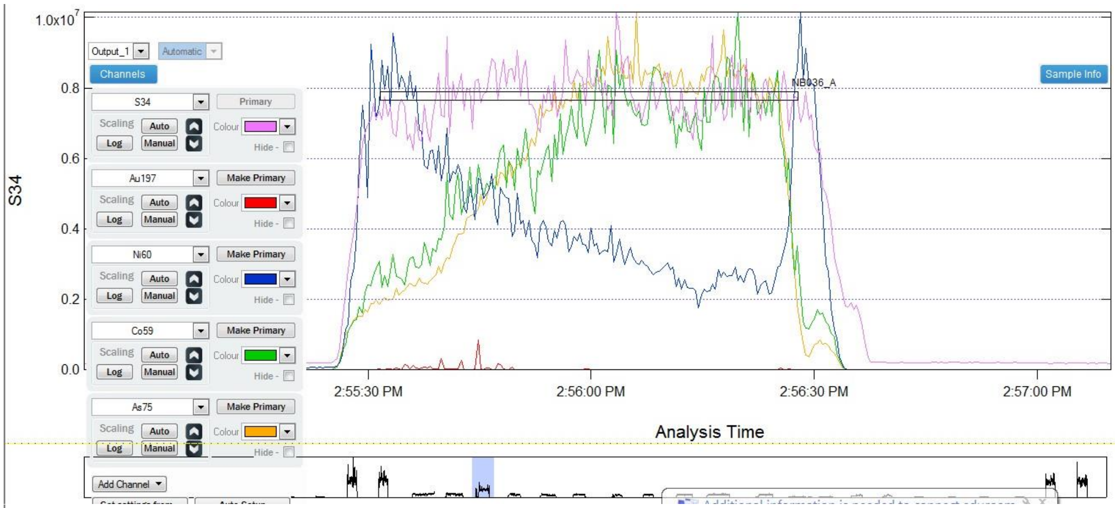
S34
1.0x10^7
0.8
0.6
0.4
0.2
0.0
NB936_A
2:55:30 PM
2:56:00 PM
2:56:30 PM
2:57:00 PM
Analysis Time
Channels
Sample Info
S34
Au197
Ni60
Co59
As75

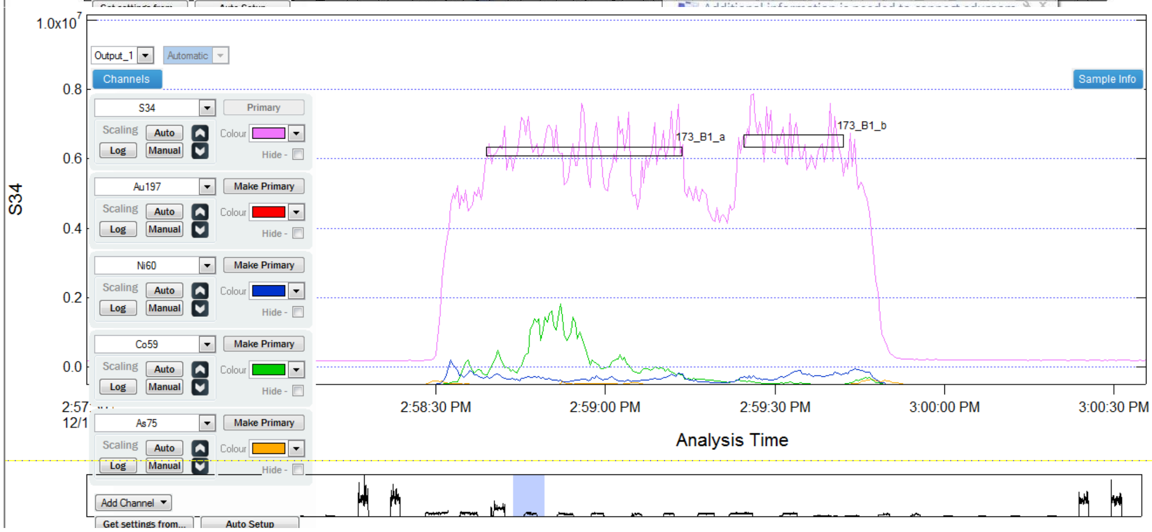
S34
1.0x10^7
0.8
0.6
0.4
0.2
0.0
173_B1_a
173_B1_b
2:58:30 PM
2:59:00 PM
2:59:30 PM
3:00:00 PM
3:00:30 PM
Analysis Time
Channels
Sample Info
S34
Au197
Ni60
Co59
As75

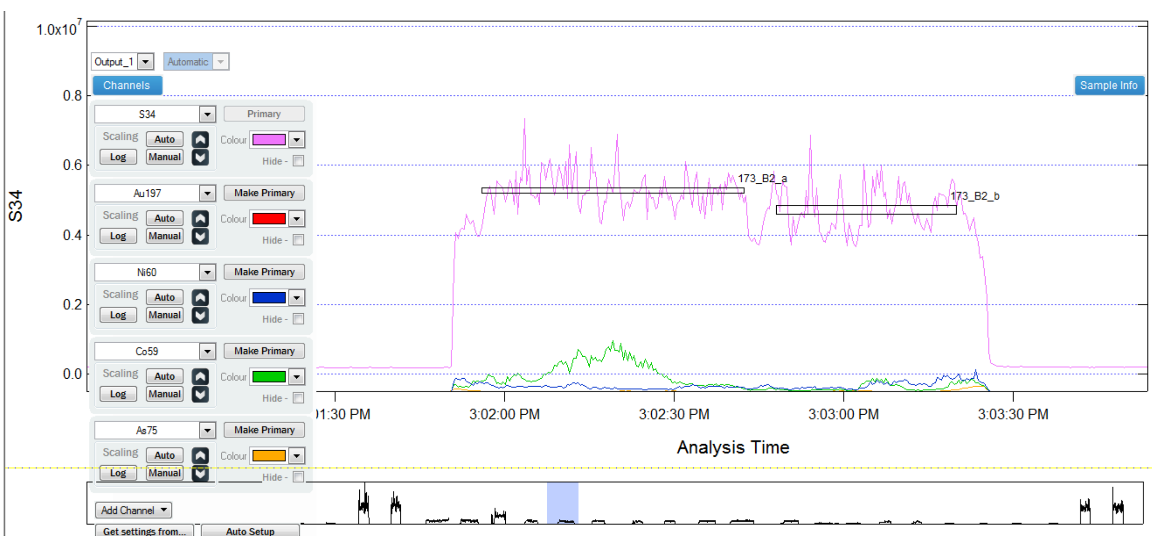
S34
1.0x10^7
0.8
0.6
0.4
0.2
0.0
173_B2_a
173_B2_b
3:02:00 PM
3:02:30 PM
3:03:00 PM
3:03:30 PM
Analysis Time
Channels
Sample Info
S34
Au197
Ni60
Co59
As75

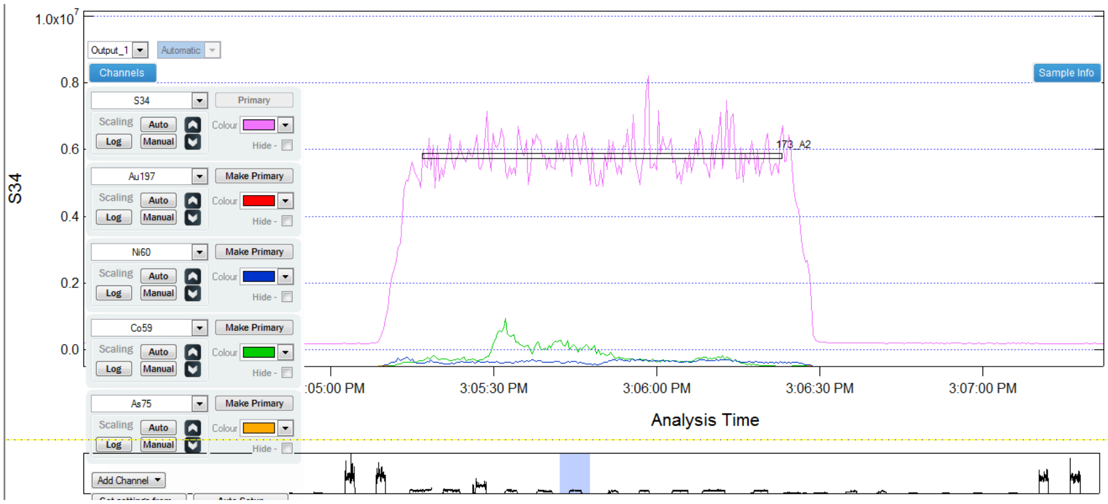
S34
173_A2
Analysis Time
3:05:30 PM
3:06:00 PM
3:06:30 PM
3:07:00 PM

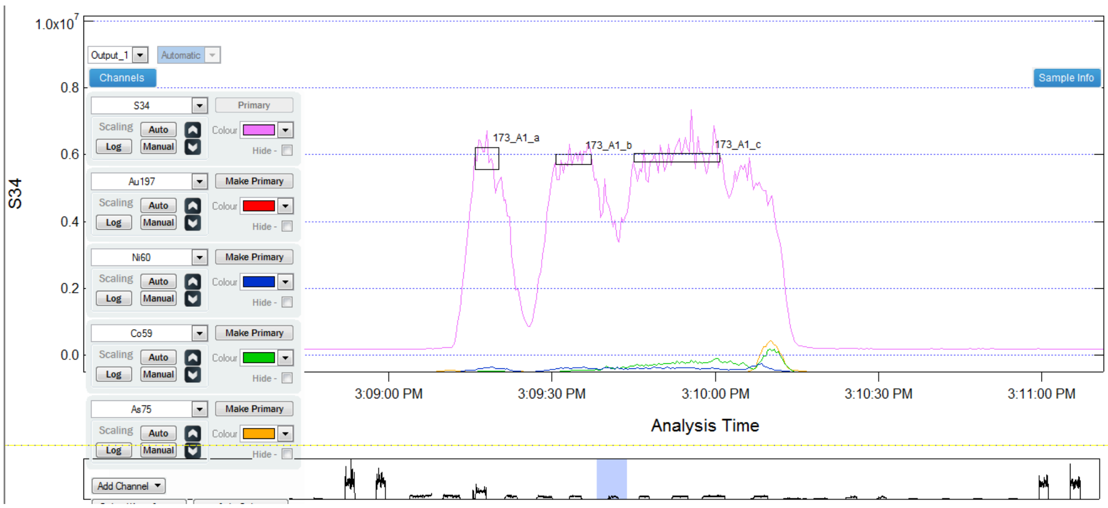
S34
173_A1_a
173_A1_b
173_A1_c
Analysis Time
3:09:00 PM
3:09:30 PM
3:10:00 PM
3:10:30 PM
3:11:00 PM

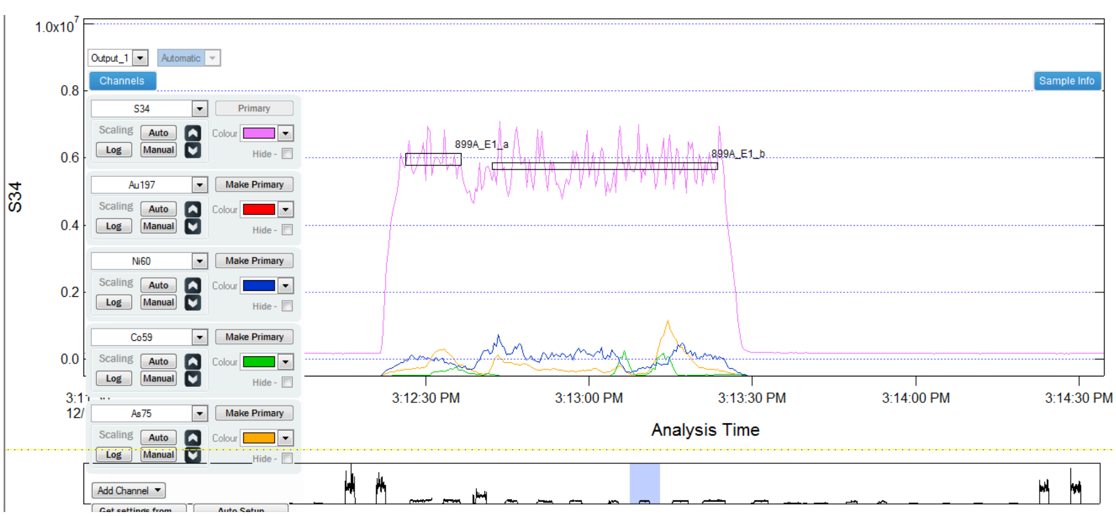
S34
899A_E1_a
899A_E1_b
Analysis Time
3:12:30 PM
3:13:00 PM
3:13:30 PM
3:14:00 PM
3:14:30 PM

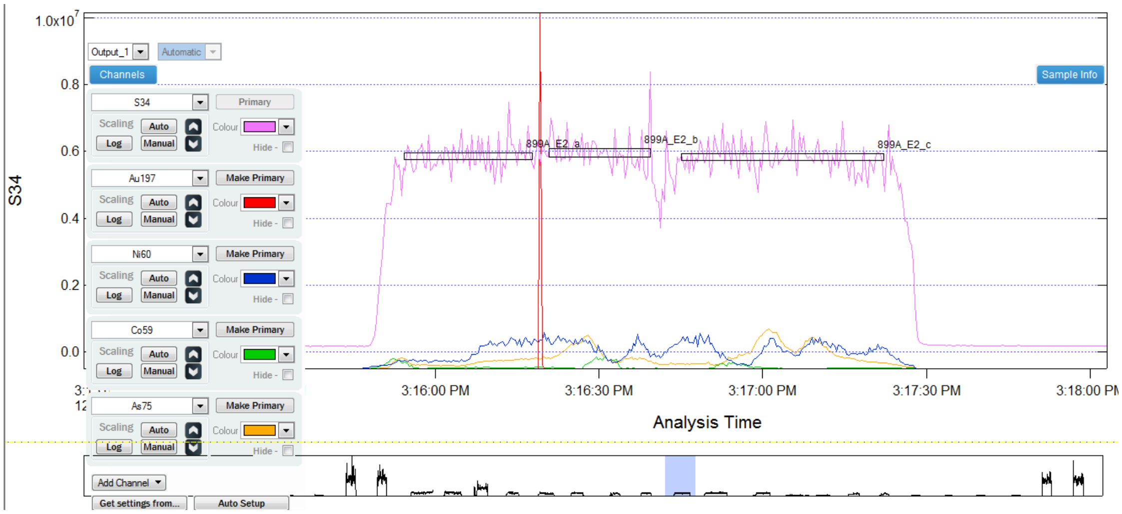
S34
1.0x10^7
0.8
0.6
0.4
0.2
0.0
Output_1
Automatic
Channels
Sample Info
S34
Au197
Ni60
Co59
As75
Primary
Make Primary
Scaling
Auto
Log
Manual
Colour
Hide
899A_E2_a
899A_E2_b
899A_E2_c
3:16:00 PM
3:16:30 PM
3:17:00 PM
3:17:30 PM
3:18:00 PM
Analysis Time
Add Channel
Get settings from...
Auto Setup

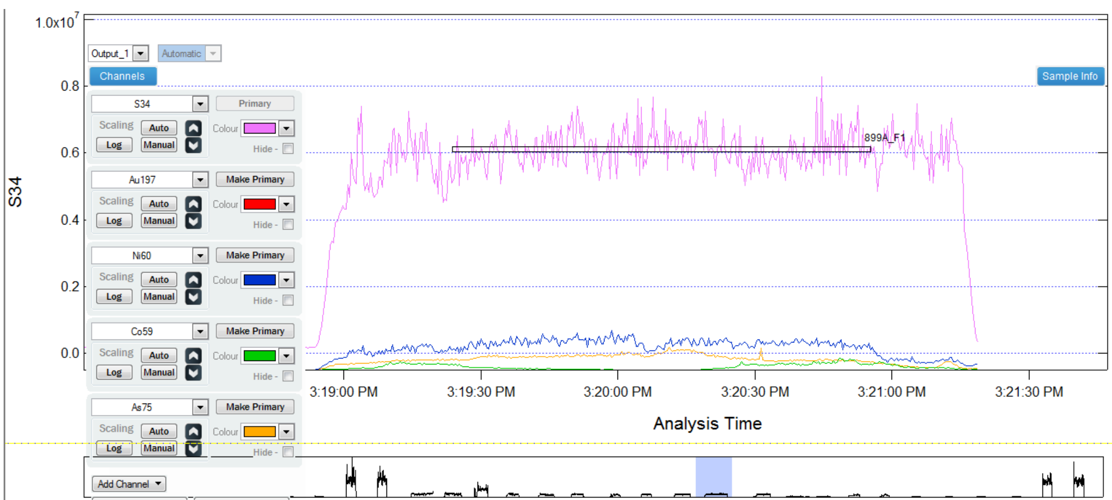
S34
1.0x10^7
0.8
0.6
0.4
0.2
0.0
Output_1
Automatic
Channels
Sample Info
S34
Au197
Ni60
Co59
As75
899A_F1
3:19:00 PM
3:19:30 PM
3:20:00 PM
3:20:30 PM
3:21:00 PM
3:21:30 PM
Analysis Time
Add Channel

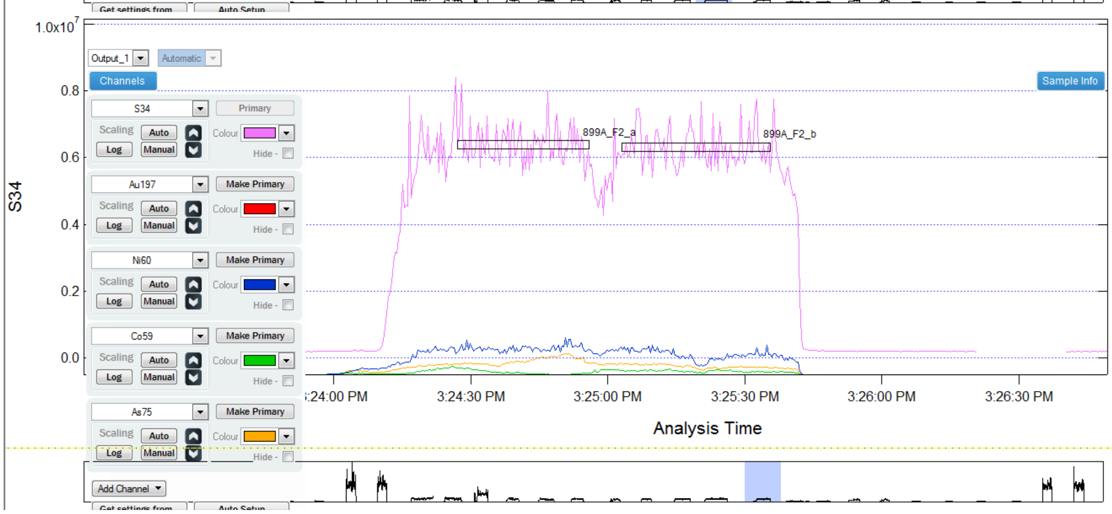
S34
1.0x10^7
0.8
0.6
0.4
0.2
0.0
Output_1
Automatic
Channels
Sample Info
S34
Au197
Ni60
Co59
As75
899A_F2_a
899A_F2_b
3:24:30 PM
3:25:00 PM
3:25:30 PM
3:26:00 PM
3:26:30 PM
Analysis Time
Add Channel

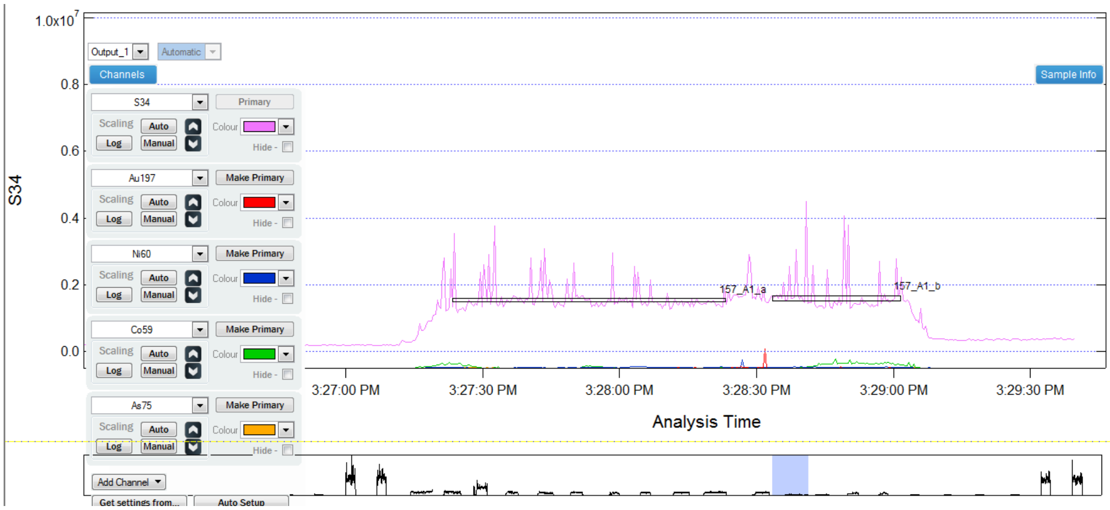
1.0x10^7
0.8
0.6
0.4
0.2
0.0
S34
157_A1_a
157_A1_b
3:27:00 PM
3:27:30 PM
3:28:00 PM
3:28:30 PM
3:29:00 PM
3:29:30 PM
Analysis Time

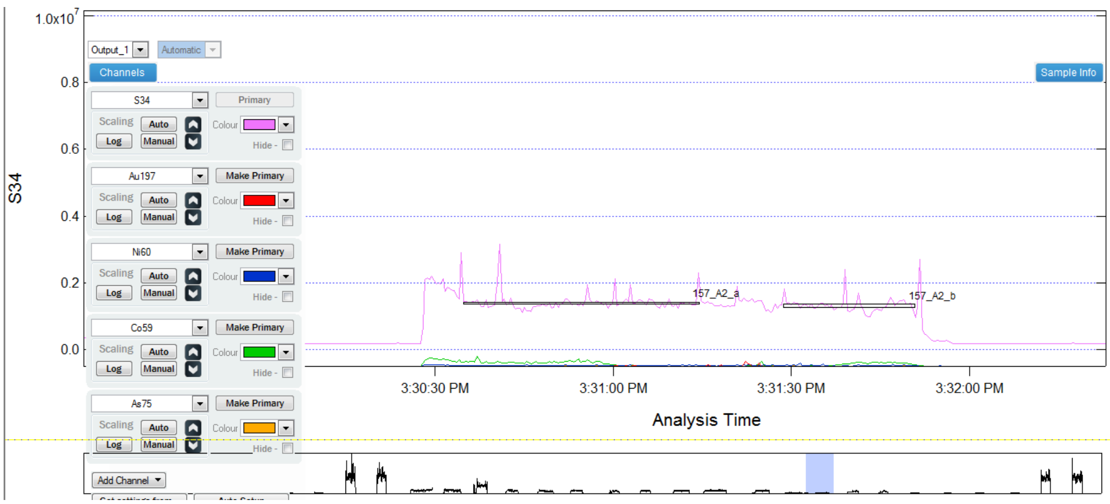
1.0x10^7
0.8
0.6
0.4
0.2
0.0
S34
157_A2_a
157_A2_b
3:30:30 PM
3:31:00 PM
3:31:30 PM
3:32:00 PM
Analysis Time

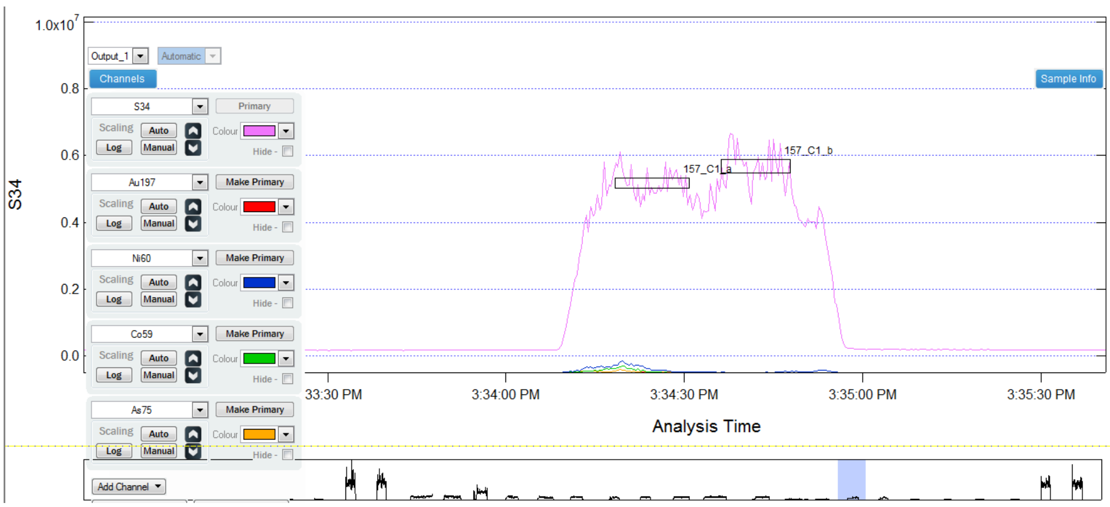
1.0x10^7
0.8
0.6
0.4
0.2
0.0
S34
157_C1_a
157_C1_b
33:30 PM
3:34:00 PM
3:34:30 PM
3:35:00 PM
3:35:30 PM
Analysis Time

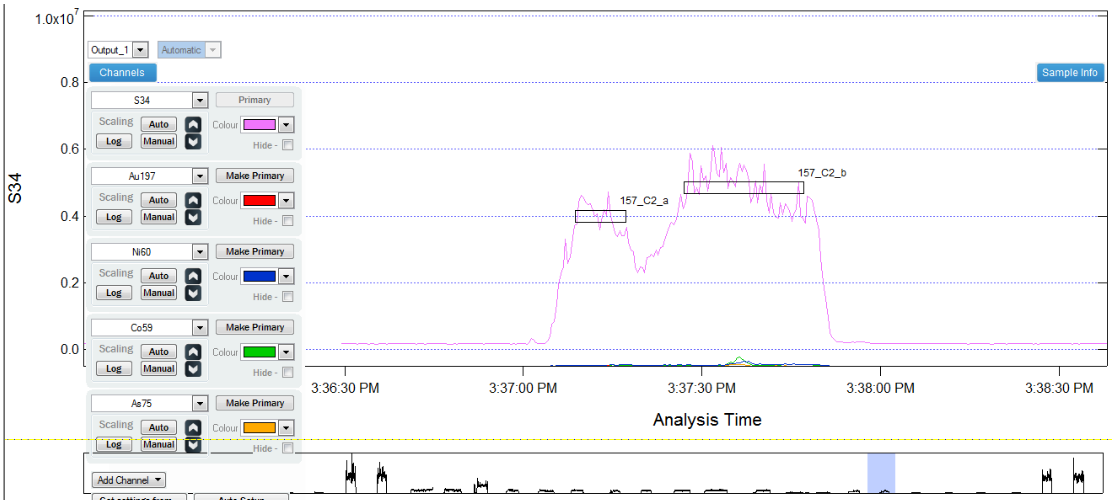
S34
1.0x10^7
0.8
0.6
0.4
0.2
0.0
157_C2_a
157_C2_b
3:36:30 PM
3:37:00 PM
3:37:30 PM
3:38:00 PM
3:38:30 PM
Analysis Time
Channels
Sample Info
S34
Au197
Ni60
Co59
As75
Add Channel

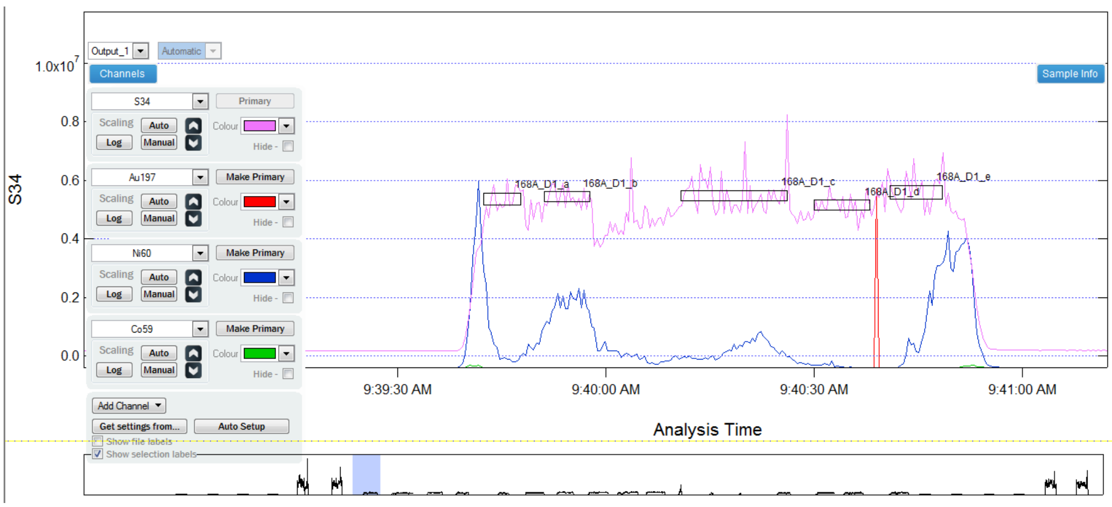
S34
1.0x10^7
0.8
0.6
0.4
0.2
0.0
168A_D1_a
168A_D1_b
168A_D1_c
168A_D1_d
168A_D1_e
9:39:30 AM
9:40:00 AM
9:40:30 AM
9:41:00 AM
Analysis Time
Channels
Sample Info
S34
Au197
Ni60
Co59
Add Channel
Get settings from...
Auto Setup
Show file labels
Show selection labels

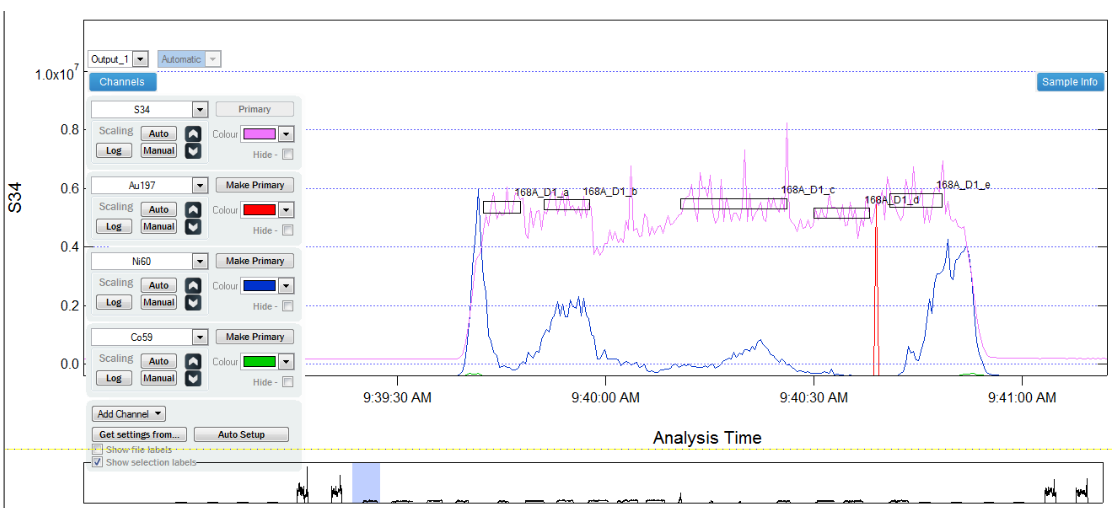
S34
1.0x10^7
0.8
0.6
0.4
0.2
0.0
168A_D1_a
168A_D1_b
168A_D1_c
168A_D1_d
168A_D1_e
9:39:30 AM
9:40:00 AM
9:40:30 AM
9:41:00 AM
Analysis Time
Channels
Sample Info
S34
Au197
Ni60
Co59
Add Channel
Get settings from...
Auto Setup
Show file labels
Show selection labels

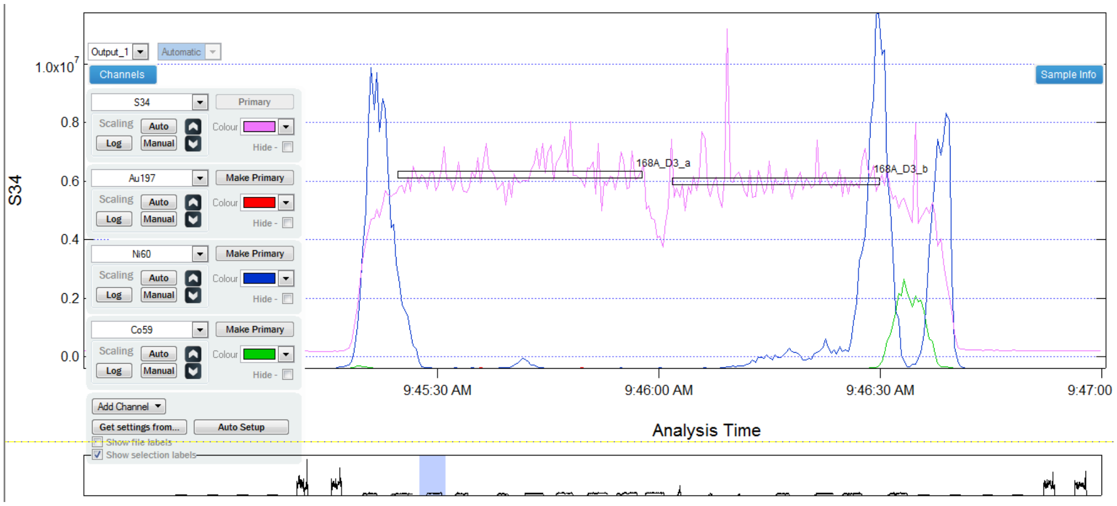

S34
1.0x10^7
0.8
0.6
0.4
0.2
0.0
168A_D3_a
168A_D3_b
9:45:30 AM
9:46:00 AM
9:46:30 AM
9:47:00
Analysis Time

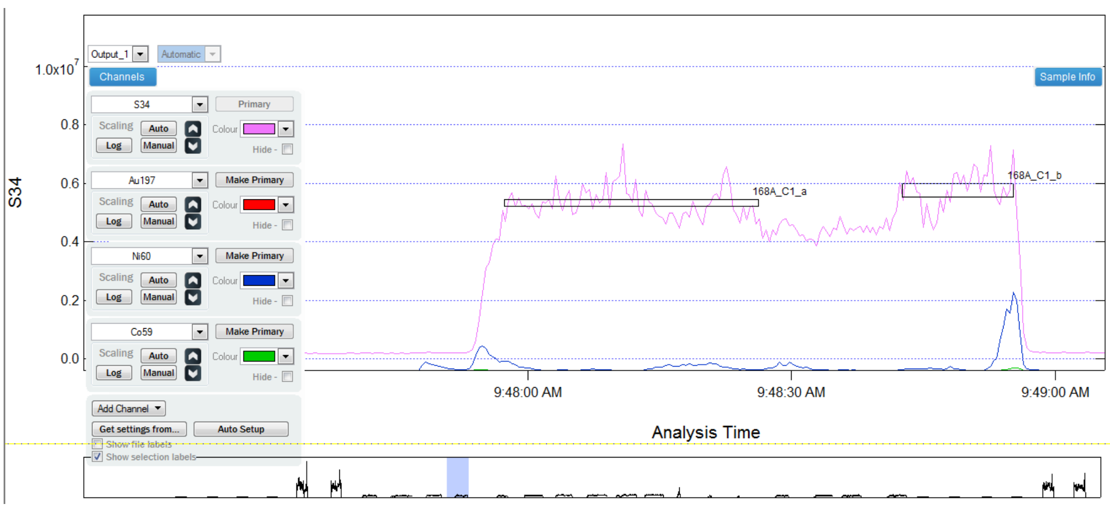

S34
1.0x10^7
0.8
0.6
0.4
0.2
0.0
168A_C1_a
168A_C1_b
9:48:00 AM
9:48:30 AM
9:49:00 AM
Analysis Time

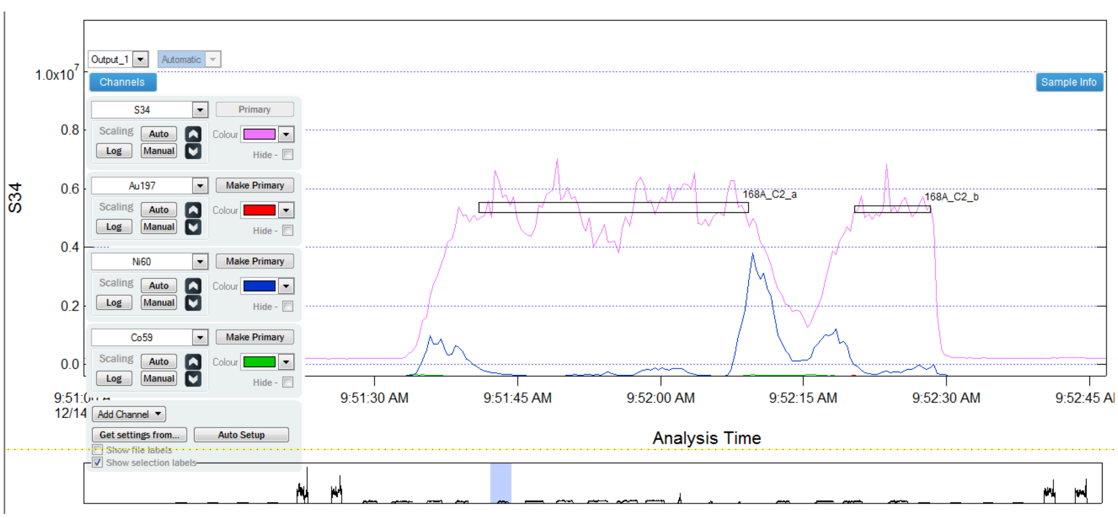

S34
1.0x10^7
0.8
0.6
0.4
0.2
0.0
168A_C2_a
168A_C2_b
9:51:30 AM
9:51:45 AM
9:52:00 AM
9:52:15 AM
9:52:30 AM
Analysis Time

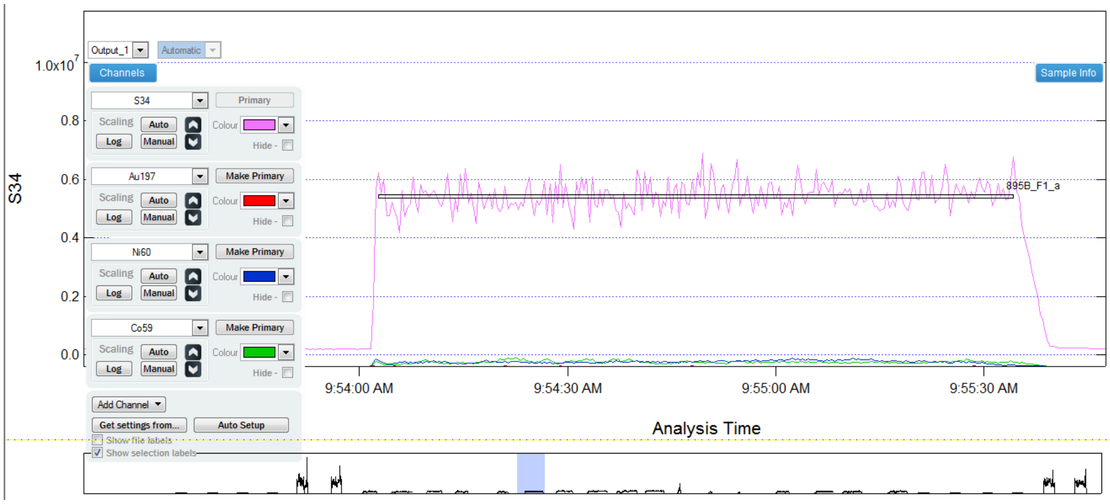
Output_1
Automatic
Channels
Sample Info
S34
Primary
Scaling
Auto
Log
Manual
Colour
Hide -
Au197
Make Primary
Ni60
Co59
Add Channel
Get settings from...
Auto Setup
Show file labels
Show selection labels
1.0x10^7
0.8
0.6
0.4
0.2
0.0
S34
895B_F1_a
9:54:00 AM
9:54:30 AM
9:55:00 AM
9:55:30 AM
Analysis Time

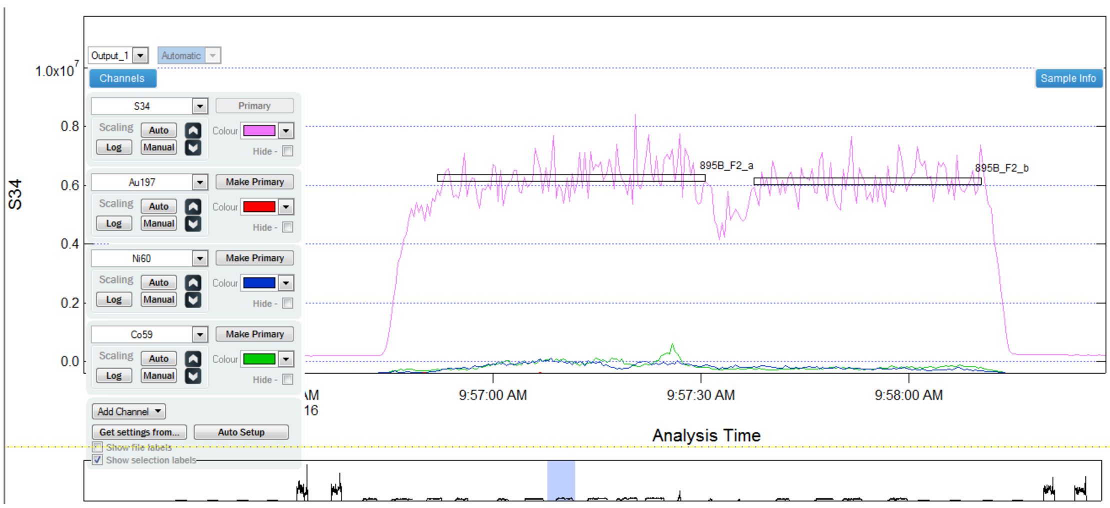
Output_1
Automatic
Channels
Sample Info
S34
Primary
Scaling
Auto
Log
Manual
Colour
Hide -
Au197
Make Primary
Ni60
Co59
Add Channel
Get settings from...
Auto Setup
Show file labels
Show selection labels
1.0x10^7
0.8
0.6
0.4
0.2
0.0
S34
895B_F2_a
895B_F2_b
AM
16
9:57:00 AM
9:57:30 AM
9:58:00 AM
Analysis Time

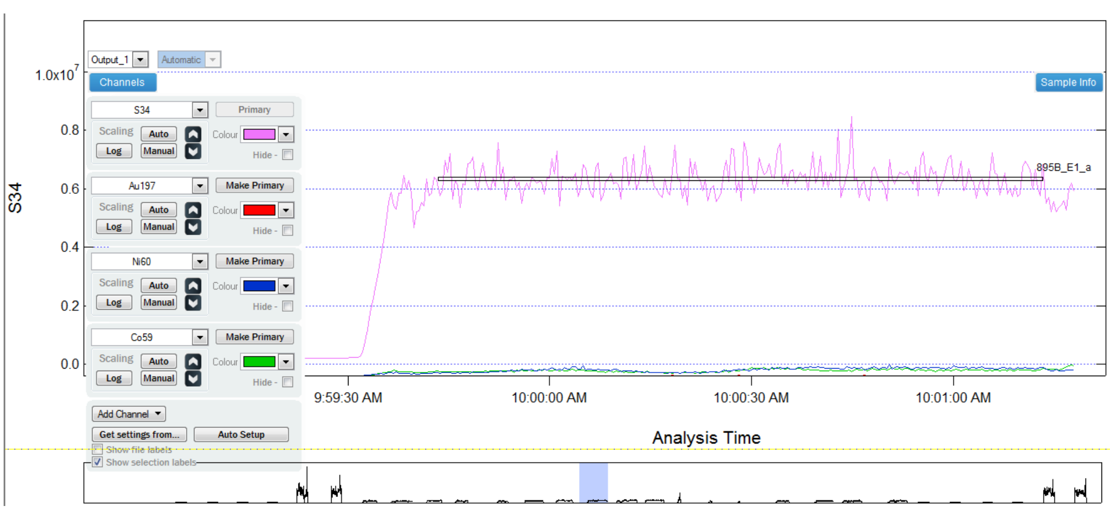
Output_1
Automatic
Channels
Sample Info
S34
Primary
Scaling
Auto
Log
Manual
Colour
Hide -
Au197
Make Primary
Ni60
Co59
Add Channel
Get settings from...
Auto Setup
Show file labels
Show selection labels
1.0x10^7
0.8
0.6
0.4
0.2
0.0
S34
895B_E1_a
9:59:30 AM
10:00:00 AM
10:00:30 AM
10:01:00 AM
Analysis Time

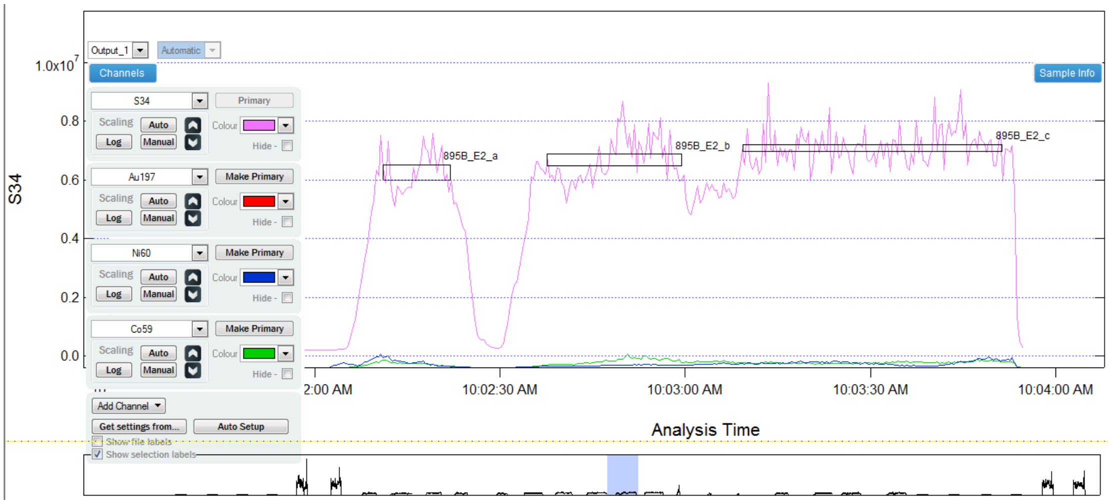
S34
1.0x10^7
0.8
0.6
0.4
0.2
0.0
895B_E2_a
895B_E2_b
895B_E2_c
2:00 AM
10:02:30 AM
10:03:00 AM
10:03:30 AM
10:04:00 AM
Analysis Time

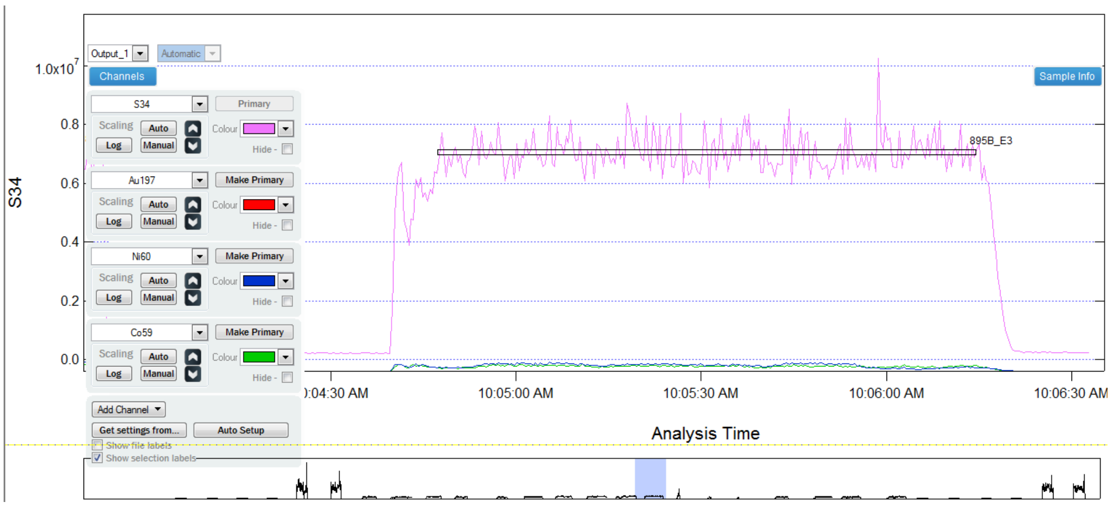
S34
1.0x10^7
0.8
0.6
0.4
0.2
0.0
895B_E3
):04:30 AM
10:05:00 AM
10:05:30 AM
10:06:00 AM
10:06:30 AM
Analysis Time

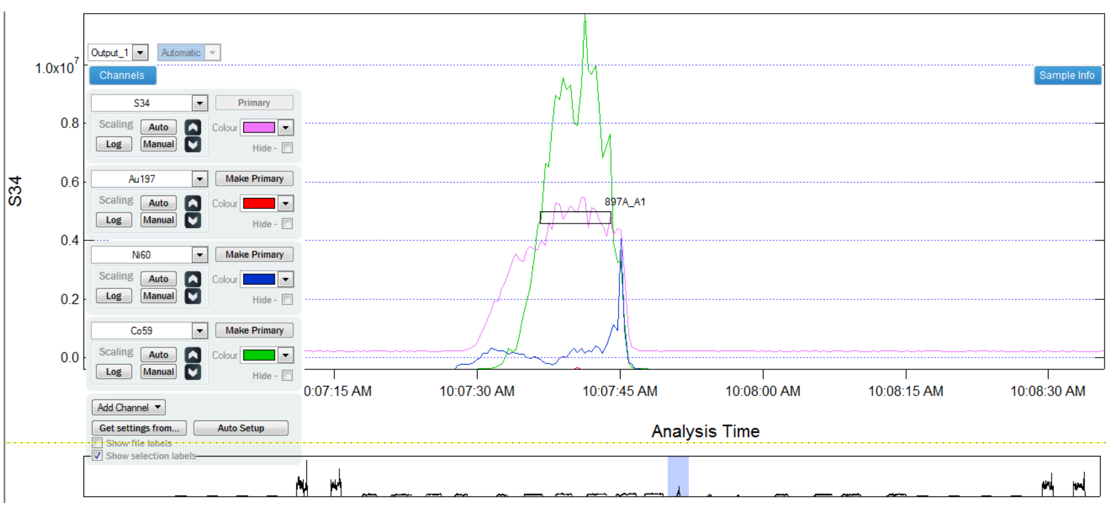
S34
1.0x10^7
0.8
0.6
0.4
0.2
0.0
897A_A1
0:07:15 AM
10:07:30 AM
10:07:45 AM
10:08:00 AM
10:08:15 AM
10:08:30 AM
Analysis Time

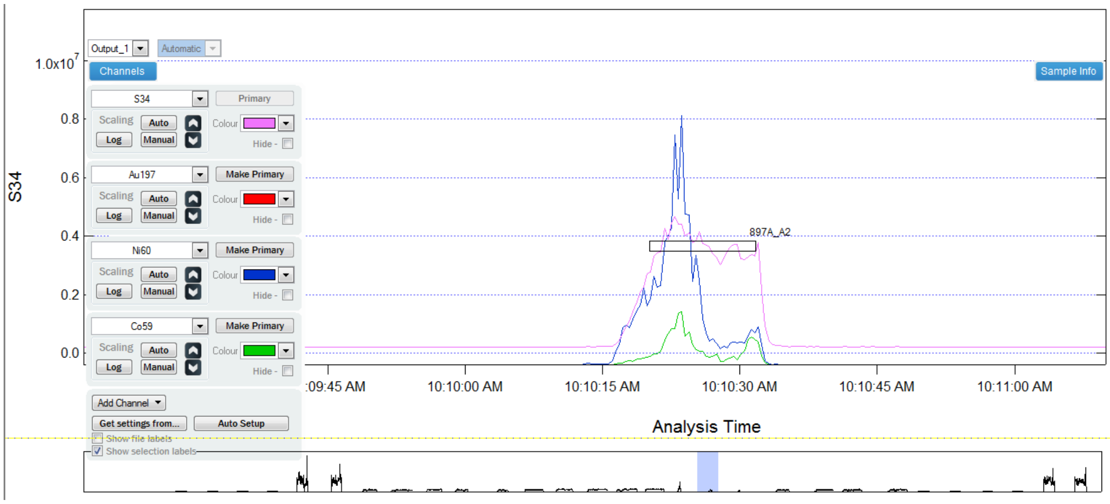
S34
1.0x10^7
0.8
0.6
0.4
0.2
0.0
Output_1
Automatic
Channels
Sample Info
S34
Primary
Au197
Ni60
Co59
Make Primary
Scaling
Auto
Log
Manual
Colour
Hide -
Add Channel
Get settings from...
Auto Setup
Show file labels
Show selection labels
897A_A2
:09:45 AM
10:10:00 AM
10:10:15 AM
10:10:30 AM
10:10:45 AM
10:11:00 AM
Analysis Time

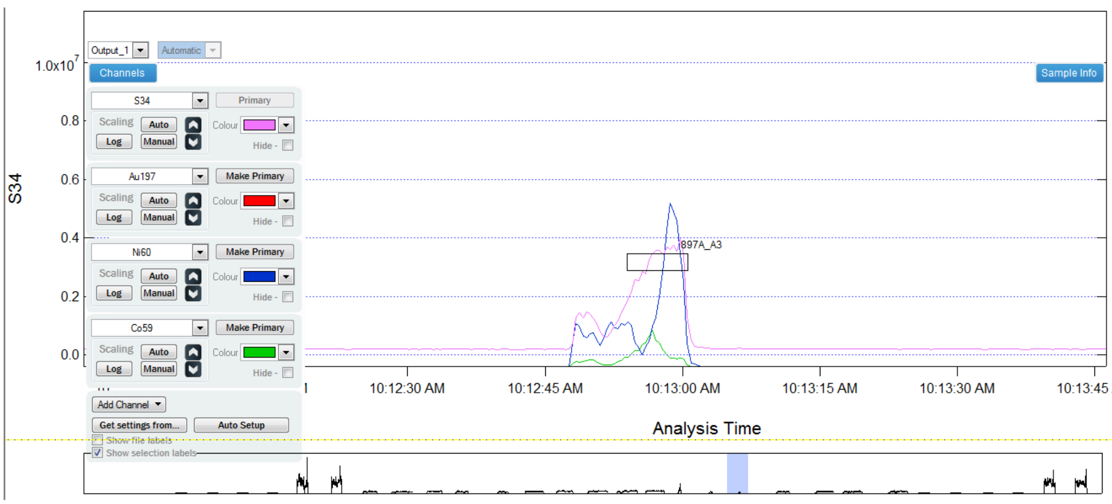
S34
1.0x10^7
0.8
0.6
0.4
0.2
0.0
Output_1
Automatic
Channels
Sample Info
S34
Primary
Au197
Ni60
Co59
Make Primary
Scaling
Auto
Log
Manual
Colour
Hide -
Add Channel
Get settings from...
Auto Setup
Show file labels
Show selection labels
897A_A3
10:12:30 AM
10:12:45 AM
10:13:00 AM
10:13:15 AM
10:13:30 AM
10:13:45
Analysis Time

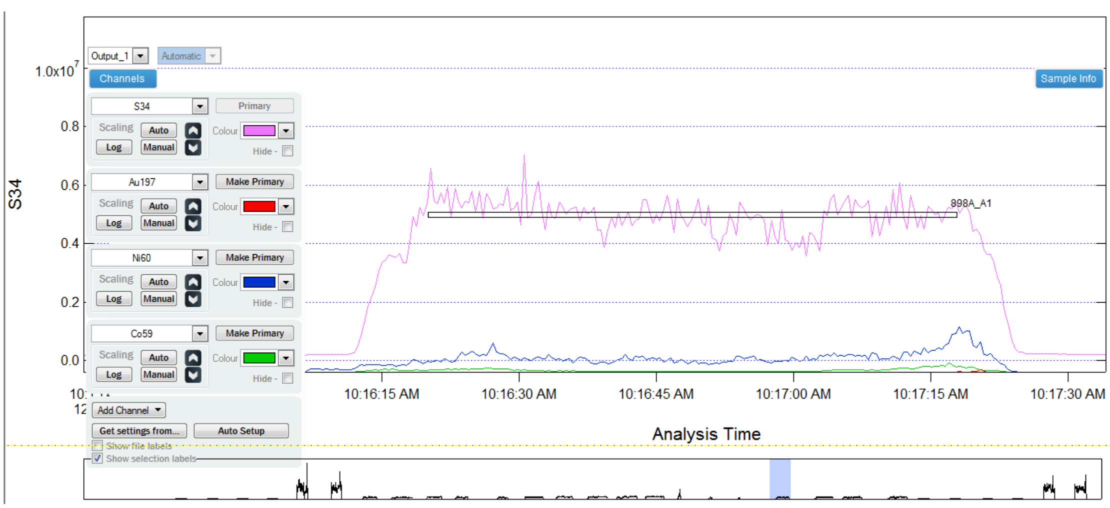
S34
1.0x10^7
0.8
0.6
0.4
0.2
0.0
Output_1
Automatic
Channels
Sample Info
S34
Primary
Au197
Ni60
Co59
Make Primary
Scaling
Auto
Log
Manual
Colour
Hide -
Add Channel
Get settings from...
Auto Setup
Show file labels
Show selection labels
898A_A1
10:16:15 AM
10:16:30 AM
10:16:45 AM
10:17:00 AM
10:17:15 AM
10:17:30 AM
Analysis Time

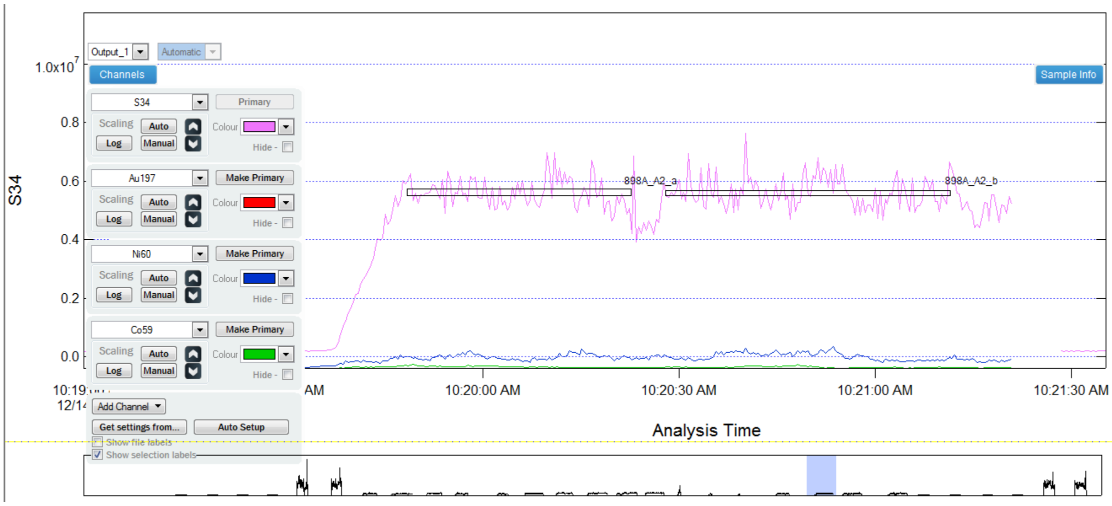
S34
1.0x10^7
0.8
0.6
0.4
0.2
0.0
898A_A2_a
898A_A2_b
10:20:00 AM
10:20:30 AM
10:21:00 AM
10:21:30 AM
Analysis Time
Output_1
Channels
Sample Info
S34
Au197
Ni60
Co59
Add Channel
Get settings from...
Auto Setup

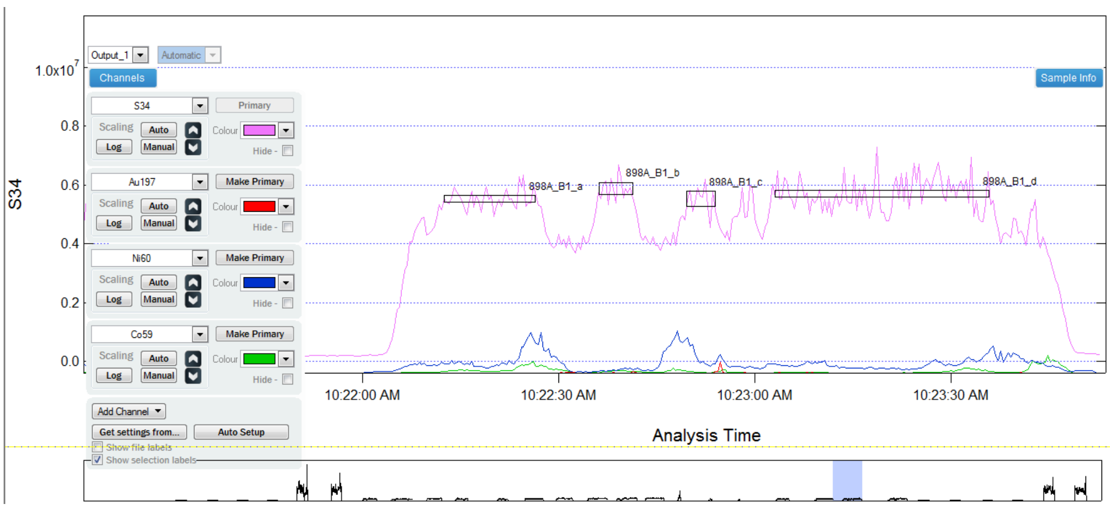
S34
1.0x10^7
0.8
0.6
0.4
0.2
0.0
898A_B1_a
898A_B1_b
898A_B1_c
898A_B1_d
10:22:00 AM
10:22:30 AM
10:23:00 AM
10:23:30 AM
Analysis Time
Output_1
Channels
Sample Info
S34
Au197
Ni60
Co59
Add Channel
Get settings from...
Auto Setup

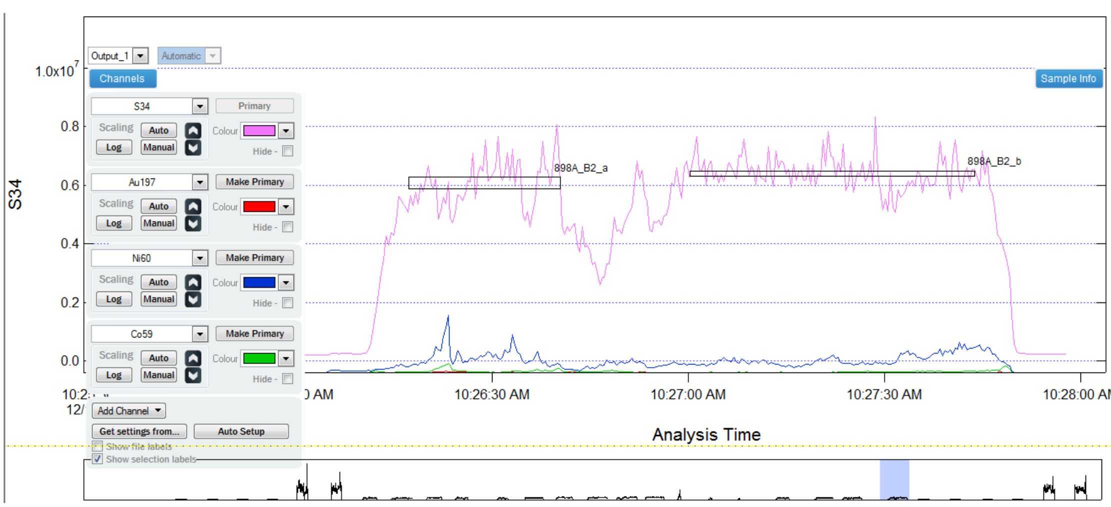
S34
1.0x10^7
0.8
0.6
0.4
0.2
0.0
898A_B2_a
898A_B2_b
10:26:30 AM
10:27:00 AM
10:27:30 AM
10:28:00 AM
Analysis Time
Output_1
Channels
Sample Info
S34
Au197
Ni60
Co59
Add Channel
Get settings from...
Auto Setup

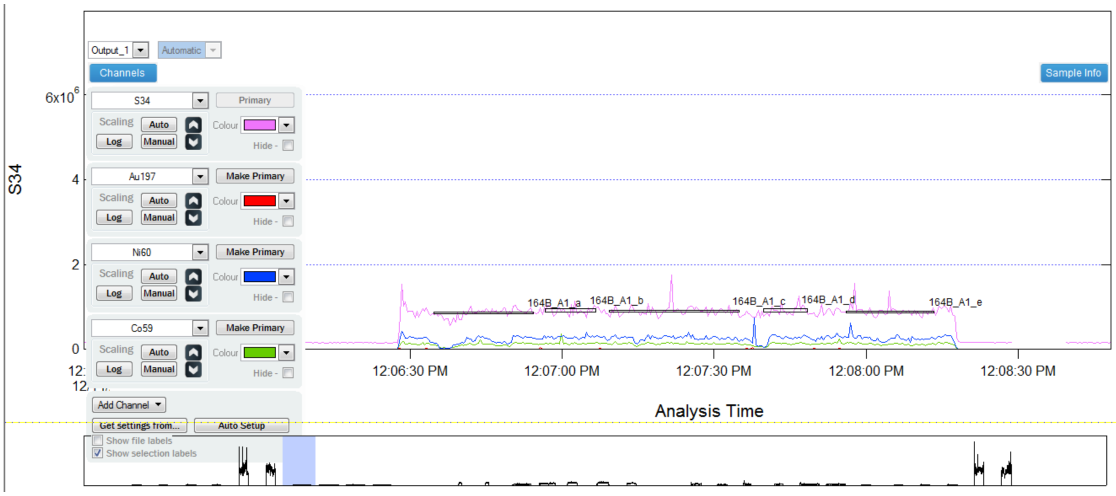

Output_1
Automatic
Channels
Sample Info
S34
Au197
Ni60
Co59
Primary
Make Primary
Scaling
Auto
Log
Manual
Colour
Hide -
Add Channel
Get settings from...
Auto Setup
Show file labels
Show selection labels
6x10^6
4
2
0
164B_A1_a
164B_A1_b
164B_A1_c
164B_A1_d
164B_A1_e
12:06:30 PM
12:07:00 PM
12:07:30 PM
12:08:00 PM
12:08:30 PM
Analysis Time

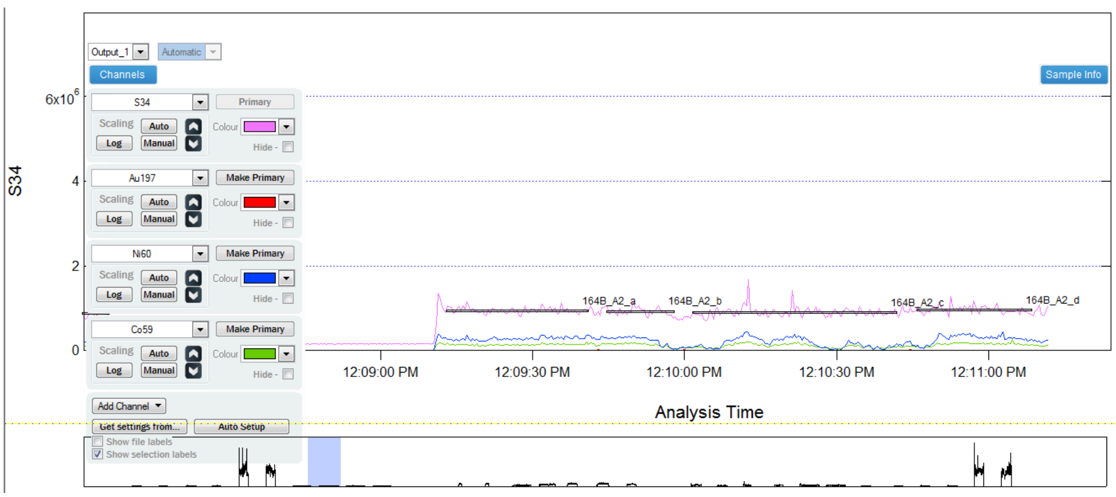

Output_1
Automatic
Channels
Sample Info
S34
Au197
Ni60
Co59
Primary
Make Primary
Scaling
Auto
Log
Manual
Colour
Hide -
Add Channel
Get settings from...
Auto Setup
Show file labels
Show selection labels
6x10^6
4
2
0
164B_A2_a
164B_A2_b
164B_A2_c
164B_A2_d
12:09:00 PM
12:09:30 PM
12:10:00 PM
12:10:30 PM
12:11:00 PM
Analysis Time

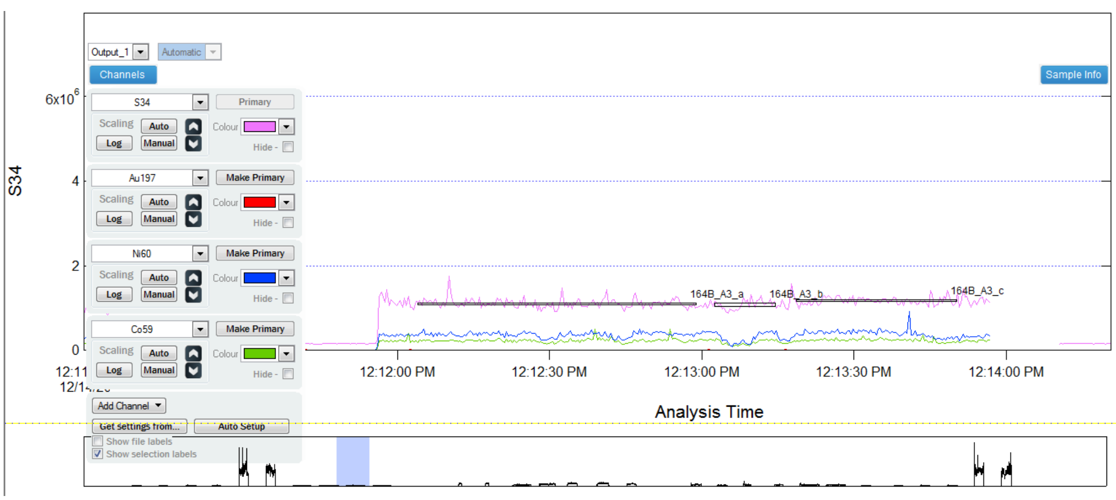

Output_1
Automatic
Channels
Sample Info
S34
Au197
Ni60
Co59
Primary
Make Primary
Scaling
Auto
Log
Manual
Colour
Hide -
Add Channel
Get settings from...
Auto Setup
Show file labels
Show selection labels
6x10^6
4
2
0
164B_A3_a
164B_A3_b
164B_A3_c
12:12:00 PM
12:12:30 PM
12:13:00 PM
12:13:30 PM
12:14:00 PM
Analysis Time

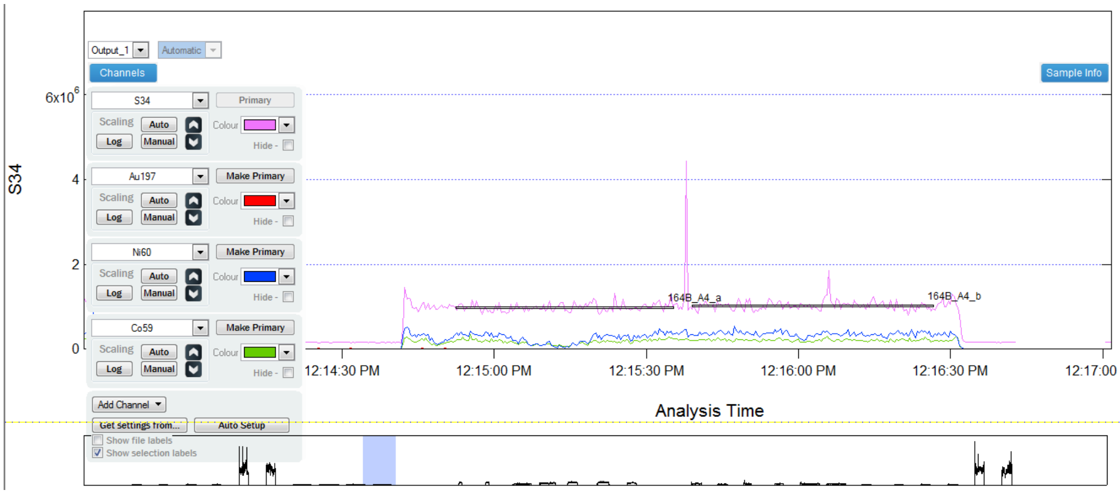
Output_1
Automatic
Channels
Sample Info
S34
Primary
Au197
Ni60
Co59
Make Primary
Scaling
Auto
Log
Manual
Colour
Hide -
Add Channel
Get settings from...
Auto Setup
Show file labels
Show selection labels
6x10^6
4
2
0
164B_A4_a
164B_A4_b
12:14:30 PM
12:15:00 PM
12:15:30 PM
12:16:00 PM
12:16:30 PM
12:17:00
Analysis Time

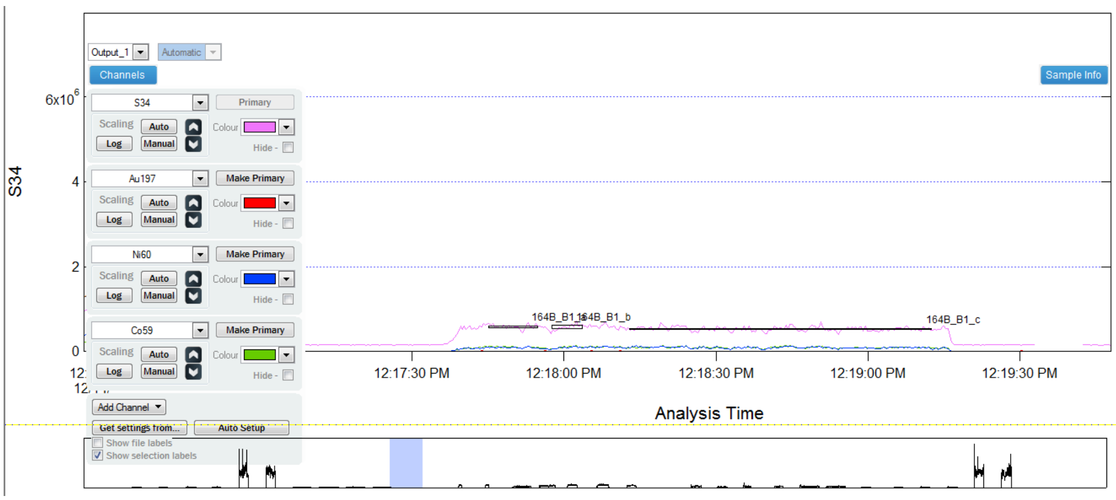
Output_1
Automatic
Channels
Sample Info
S34
Primary
Au197
Ni60
Co59
Make Primary
Scaling
Auto
Log
Manual
Colour
Hide -
Add Channel
Get settings from...
Auto Setup
Show file labels
Show selection labels
6x10^6
4
2
0
164B_B1_a
164B_B1_b
164B_B1_c
12:17:30 PM
12:18:00 PM
12:18:30 PM
12:19:00 PM
12:19:30 PM
Analysis Time

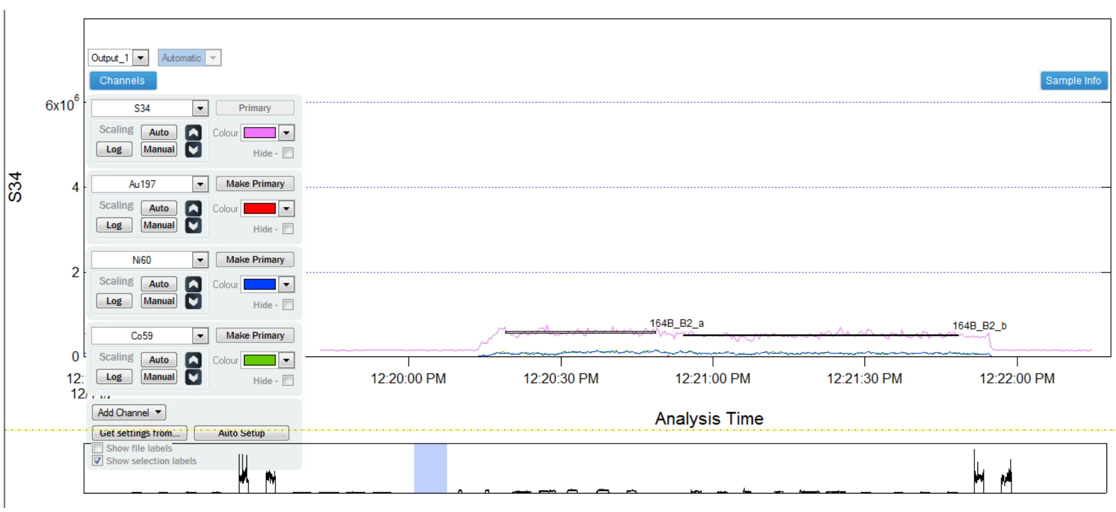
Output_1
Automatic
Channels
Sample Info
S34
Primary
Au197
Ni60
Co59
Make Primary
Scaling
Auto
Log
Manual
Colour
Hide -
Add Channel
Get settings from...
Auto Setup
Show file labels
Show selection labels
6x10^6
4
2
0
164B_B2_a
164B_B2_b
12:20:00 PM
12:20:30 PM
12:21:00 PM
12:21:30 PM
12:22:00 PM
Analysis Time

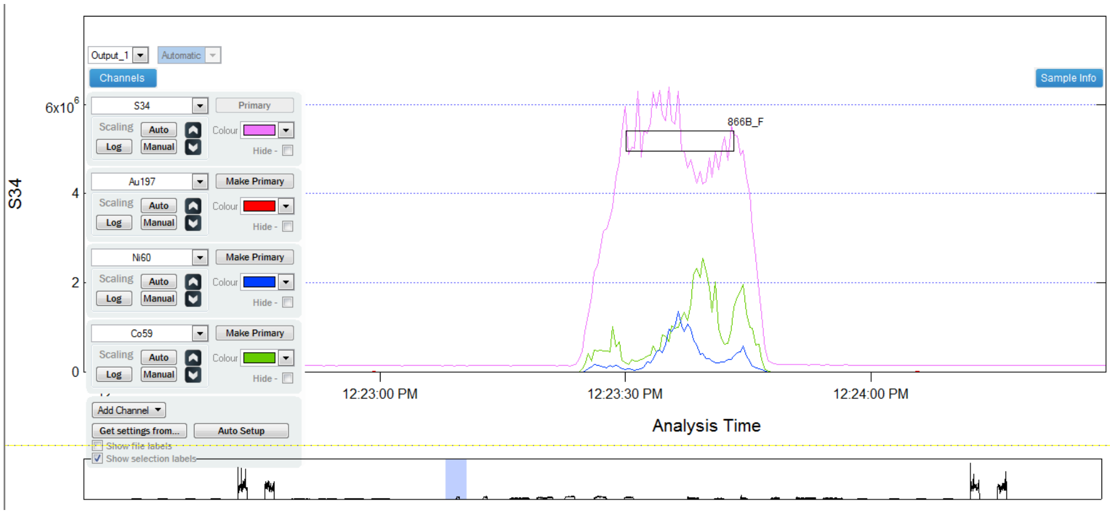
S34
6x10^6
4
2
0
866B_F
12:23:00 PM
12:23:30 PM
12:24:00 PM
Analysis Time
Output_1
Automatic
Channels
Sample Info
S34
Au197
Ni60
Co59
Add Channel
Get settings from...
Auto Setup
Show file labels
Show selection labels

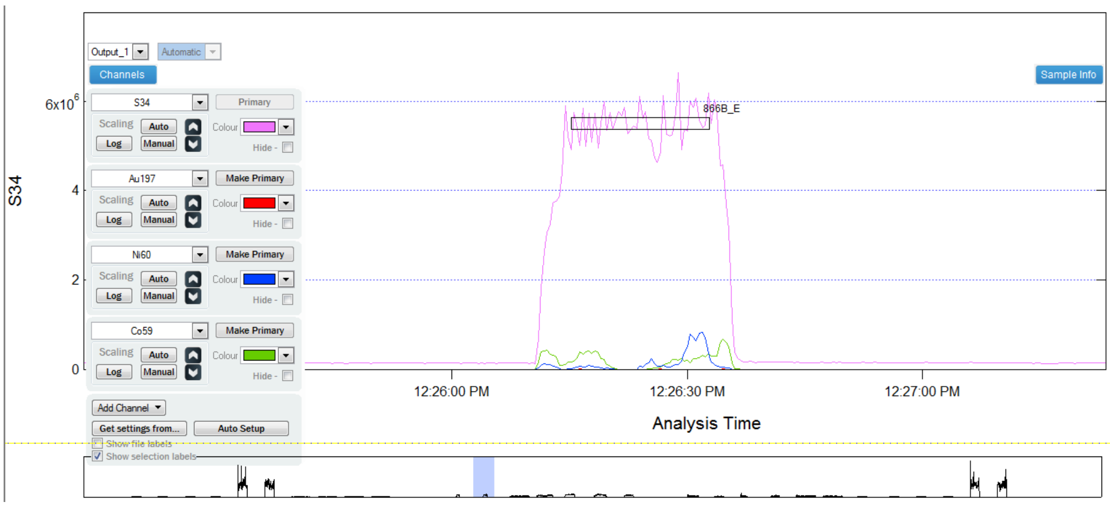
S34
6x10^6
4
2
0
866B_E
12:26:00 PM
12:26:30 PM
12:27:00 PM
Analysis Time
Output_1
Automatic
Channels
Sample Info
S34
Au197
Ni60
Co59
Add Channel
Get settings from...
Auto Setup
Show file labels
Show selection labels

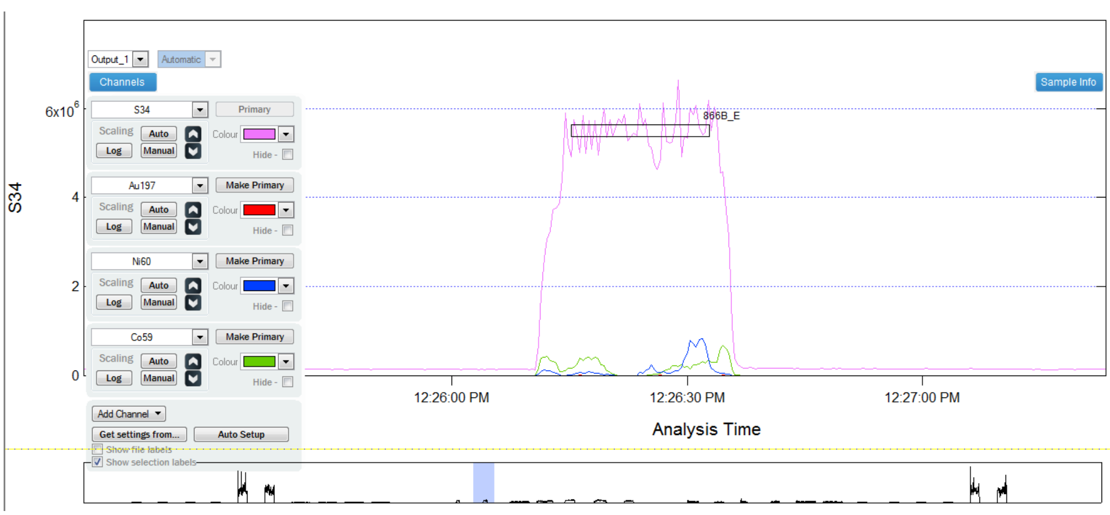
S34
6x10^6
4
2
0
866B_E
12:26:00 PM
12:26:30 PM
12:27:00 PM
Analysis Time
Output_1
Automatic
Channels
Sample Info
S34
Au197
Ni60
Co59
Add Channel
Get settings from...
Auto Setup
Show file labels
Show selection labels

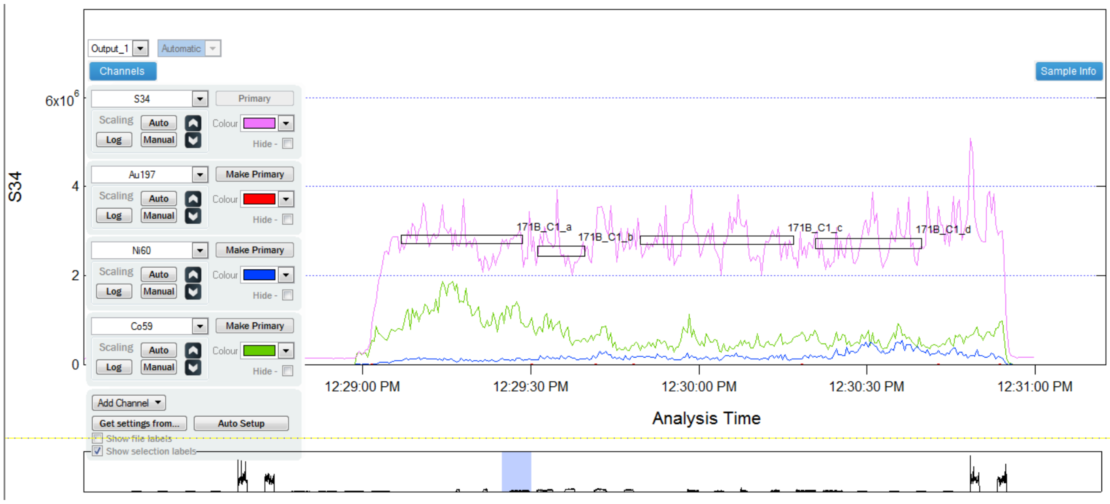
S34
Analysis Time
12:29:00 PM
12:29:30 PM
12:30:00 PM
12:30:30 PM
12:31:00 PM
171B_C1_a
171B_C1_b
171B_C1_c
171B_C1_d

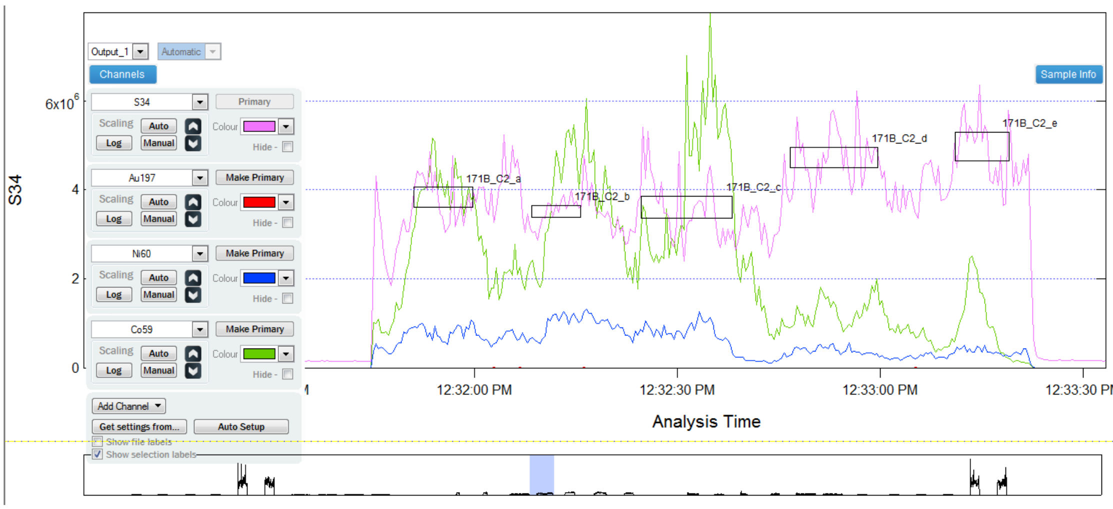
S34
Analysis Time
12:32:00 PM
12:32:30 PM
12:33:00 PM
12:33:30 PM
171B_C2_a
171B_C2_b
171B_C2_c
171B_C2_d
171B_C2_e

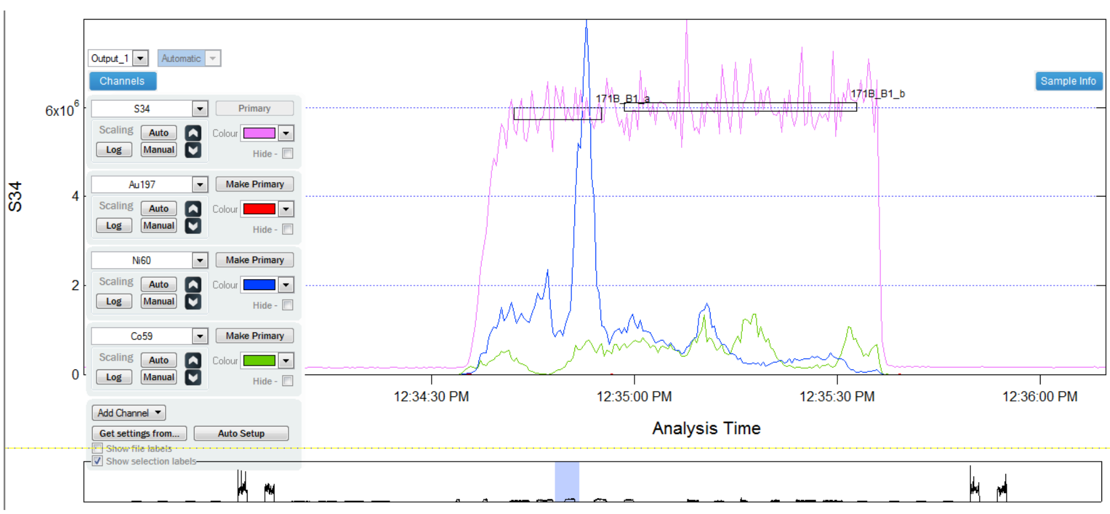
S34
Analysis Time
12:34:30 PM
12:35:00 PM
12:35:30 PM
12:36:00 PM
171B_B1_a
171B_B1_b

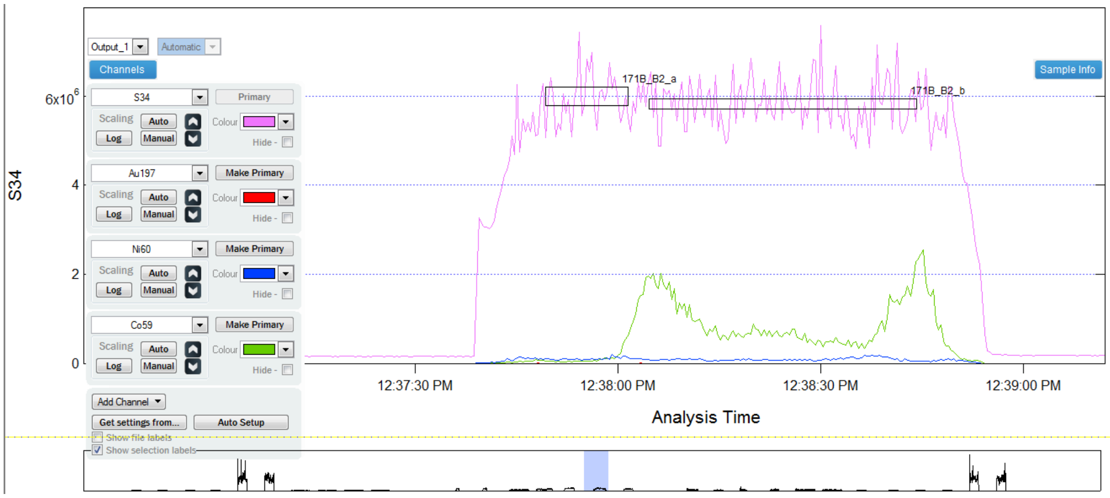
S34
6x10^6
4
2
0
171B_B2_a
171B_B2_b
12:37:30 PM
12:38:00 PM
12:38:30 PM
12:39:00 PM
Analysis Time
Channels
S34
Au197
Ni60
Co59
Sample Info

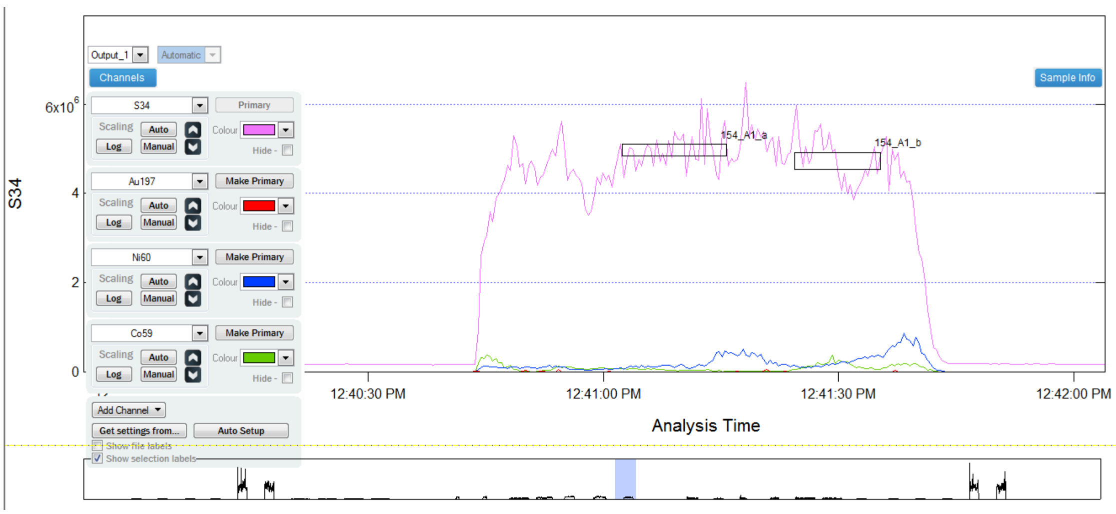
S34
6x10^6
4
2
0
154_A1_a
154_A1_b
12:40:30 PM
12:41:00 PM
12:41:30 PM
12:42:00 PM
Analysis Time
Channels
S34
Au197
Ni60
Co59
Sample Info

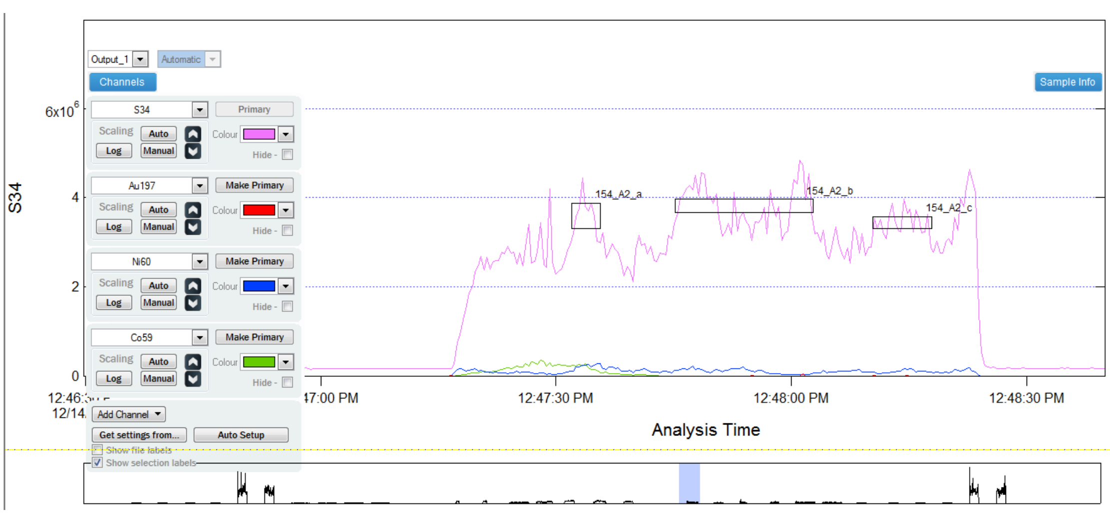
S34
6x10^6
4
2
0
154_A2_a
154_A2_b
154_A2_c
12:47:30 PM
12:48:00 PM
12:48:30 PM
Analysis Time
Channels
S34
Au197
Ni60
Co59
Sample Info

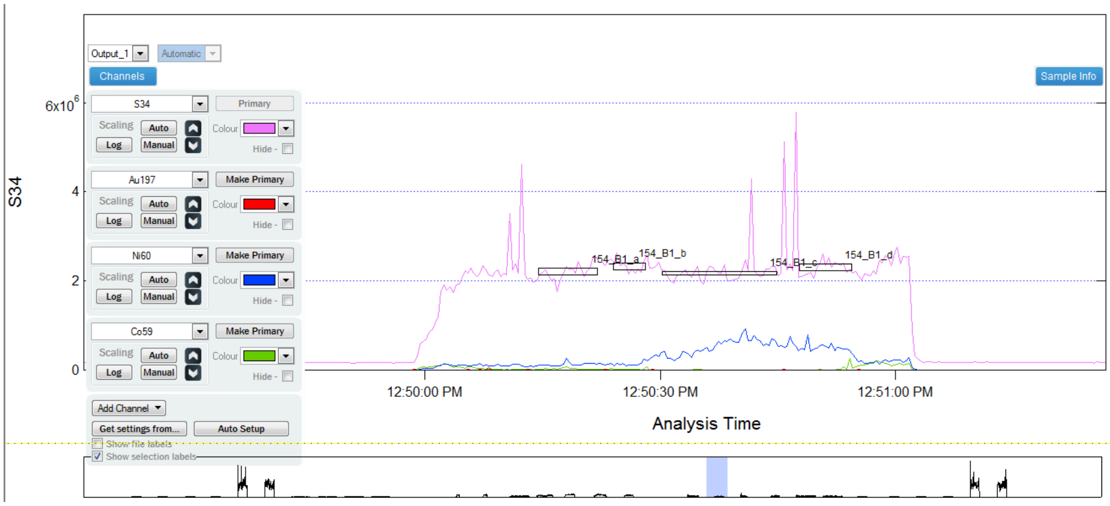
S34
6x10^6
4
2
0
12:50:00 PM
12:50:30 PM
12:51:00 PM
Analysis Time
154_B1_a
154_B1_b
154_B1_c
154_B1_d

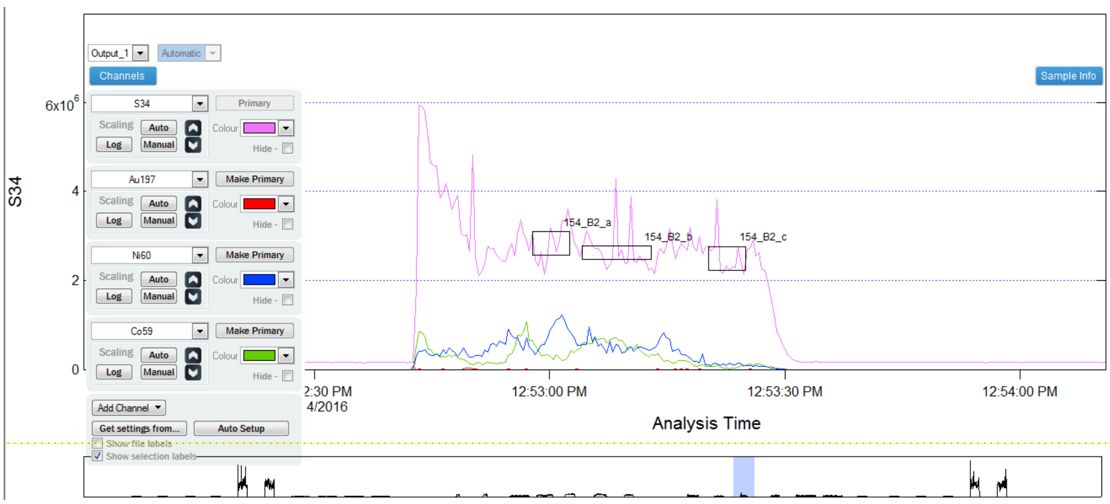
S34
6x10^6
4
2
0
12:53:00 PM
12:53:30 PM
12:54:00 PM
Analysis Time
154_B2_a
154_B2_b
154_B2_c

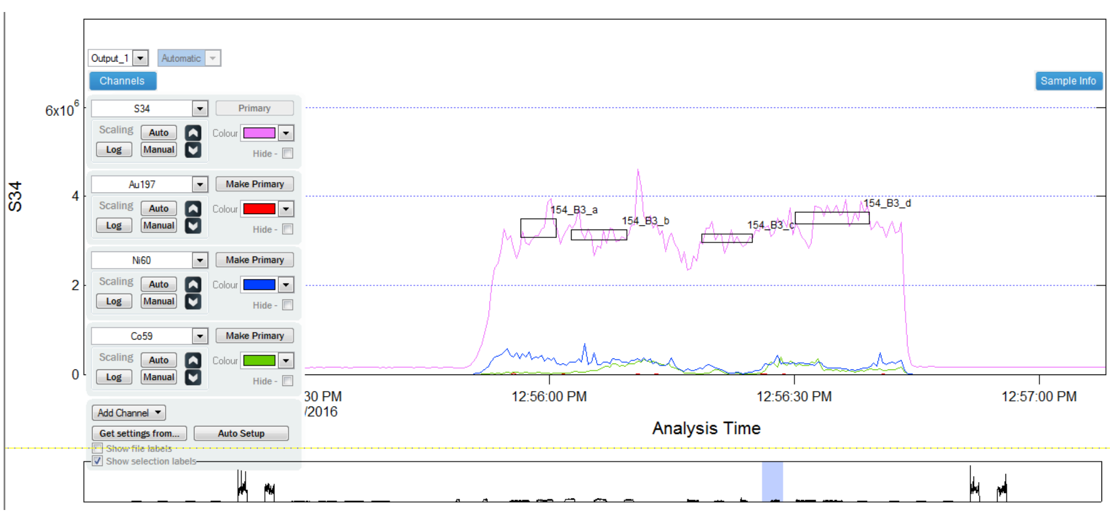
S34
6x10^6
4
2
0
12:56:00 PM
12:56:30 PM
12:57:00 PM
Analysis Time
154_B3_a
154_B3_b
154_B3_c
154_B3_d

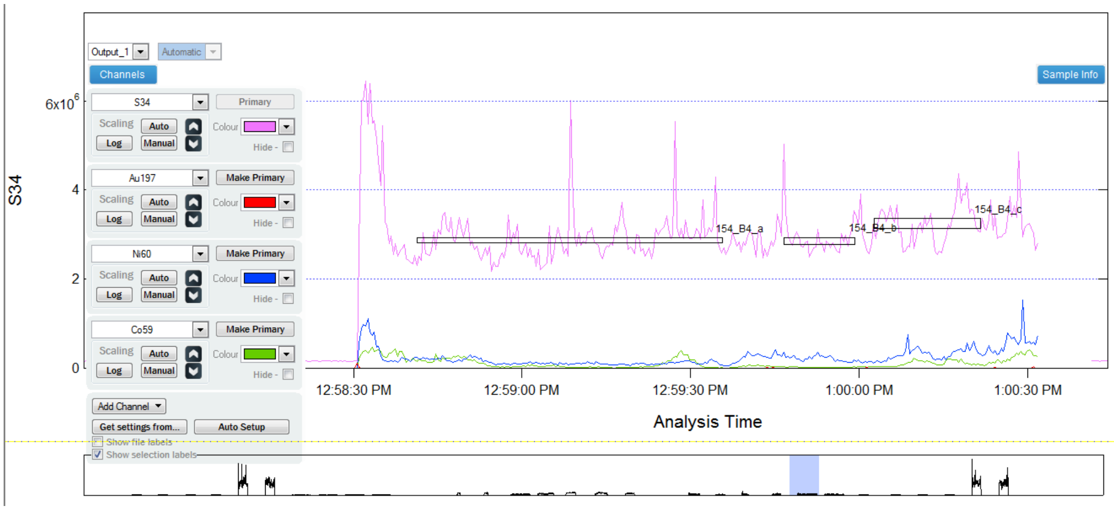
Output_1
Automatic
Channels
Sample Info
S34
Primary
Au197
Ni60
Co59
Make Primary
Scaling
Auto
Log
Manual
Colour
Hide -
Add Channel
Get settings from...
Auto Setup
Show file labels
Show selection labels
S34
6x10^6
4
2
0
154_B4_a
154_B4_b
154_B4_c
12:58:30 PM
12:59:00 PM
12:59:30 PM
1:00:00 PM
1:00:30 PM
Analysis Time

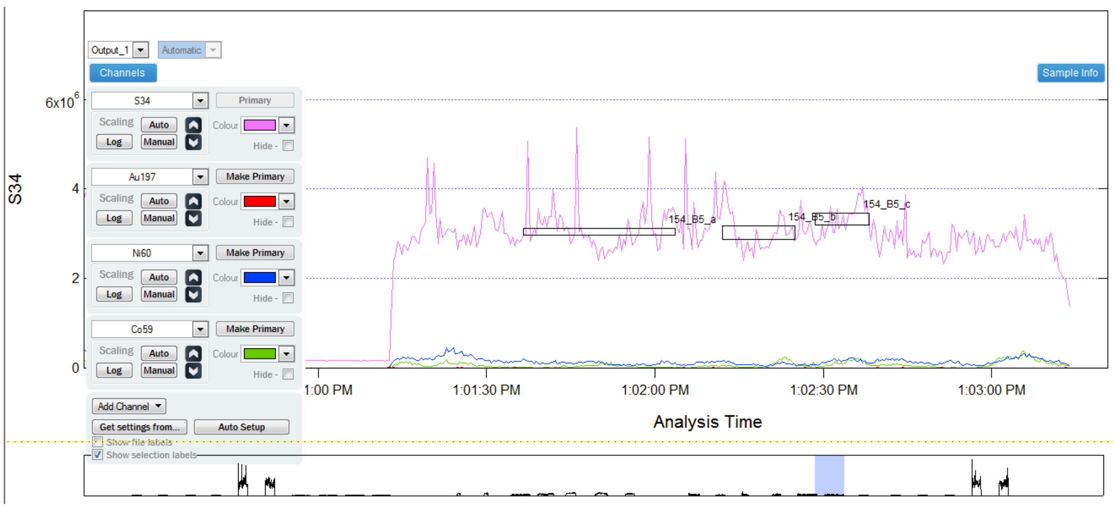
Output_1
Automatic
Channels
Sample Info
S34
Primary
Au197
Ni60
Co59
Make Primary
Scaling
Auto
Log
Manual
Colour
Hide -
Add Channel
Get settings from...
Auto Setup
Show file labels
Show selection labels
S34
6x10^6
4
2
0
154_B5_a
154_B5_b
154_B5_c
1:00 PM
1:01:30 PM
1:02:00 PM
1:02:30 PM
1:03:00 PM
Analysis Time

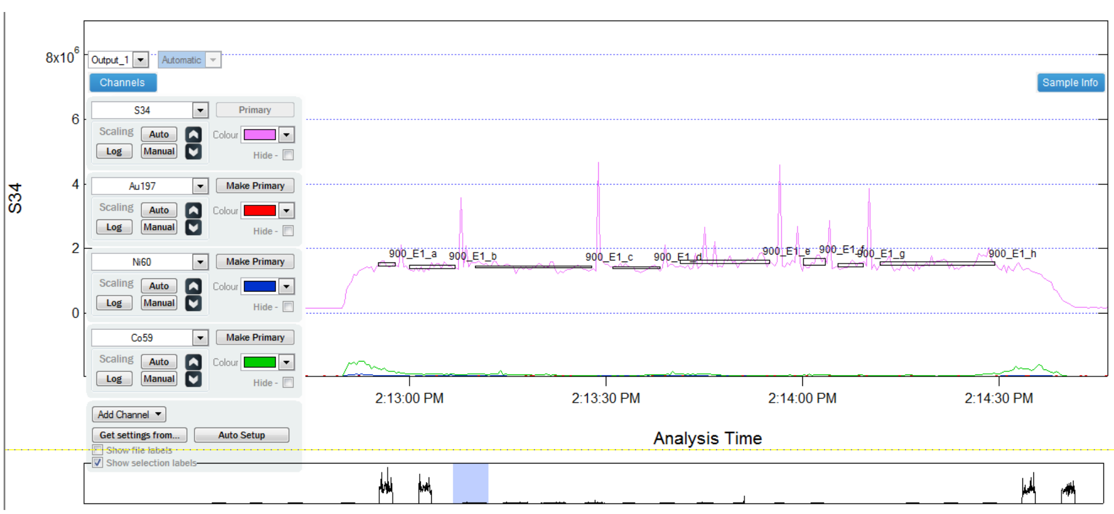
Output_1
Automatic
Channels
Sample Info
S34
Primary
Au197
Ni60
Co59
Make Primary
Scaling
Auto
Log
Manual
Colour
Hide -
Add Channel
Get settings from...
Auto Setup
Show file labels
Show selection labels
S34
8x10^6
6
4
2
0
900_E1_a
900_E1_b
900_E1_c
900_E1_d
900_E1_e
900_E1_f
900_E1_g
900_E1_h
2:13:00 PM
2:13:30 PM
2:14:00 PM
2:14:30 PM
Analysis Time

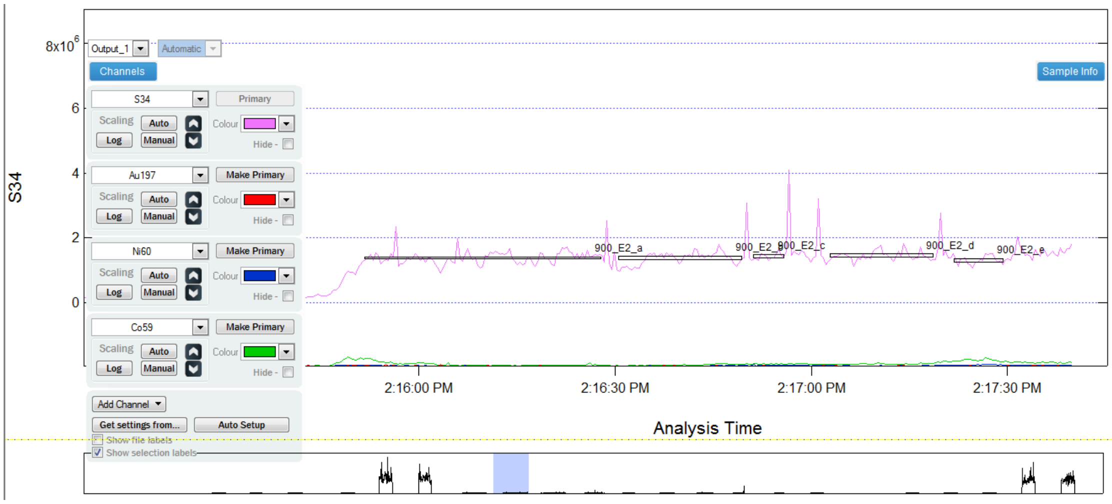
S34
8x10^6
6
4
2
0
Output_1
Automatic
Channels
Sample Info
S34
Primary
Au197
Ni60
Co59
Make Primary
Scaling
Auto
Log
Manual
Colour
Hide -
Add Channel
Get settings from...
Auto Setup
Show file labels
Show selection labels
900_E2_a
900_E2_b
900_E2_c
900_E2_d
900_E2_e
2:16:00 PM
2:16:30 PM
2:17:00 PM
2:17:30 PM
Analysis Time

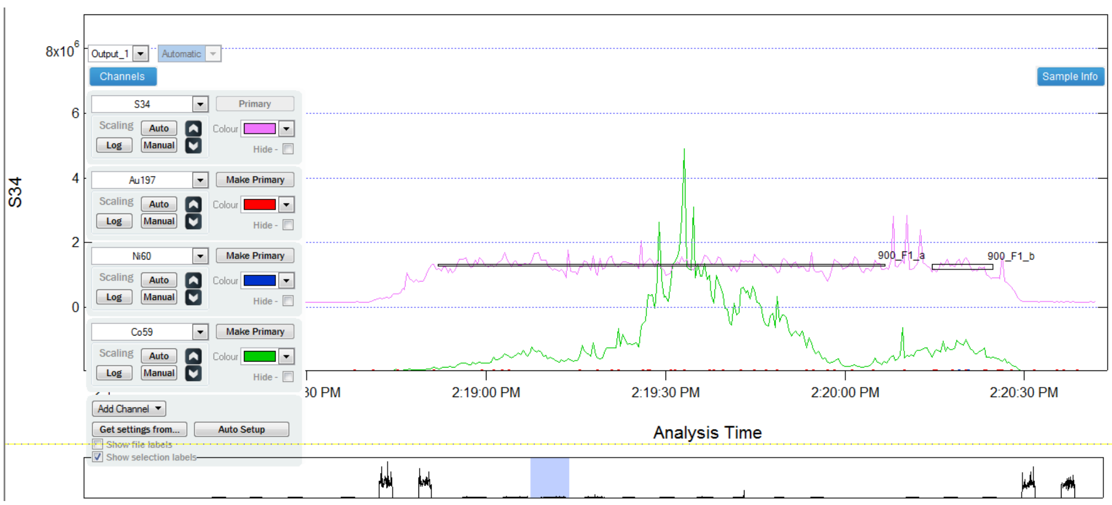
S34
8x10^6
6
4
2
0
Output_1
Automatic
Channels
Sample Info
S34
Primary
Au197
Ni60
Co59
Make Primary
Scaling
Auto
Log
Manual
Colour
Hide -
Add Channel
Get settings from...
Auto Setup
Show file labels
Show selection labels
900_F1_a
900_F1_b
2:19:00 PM
2:19:30 PM
2:20:00 PM
2:20:30 PM
Analysis Time

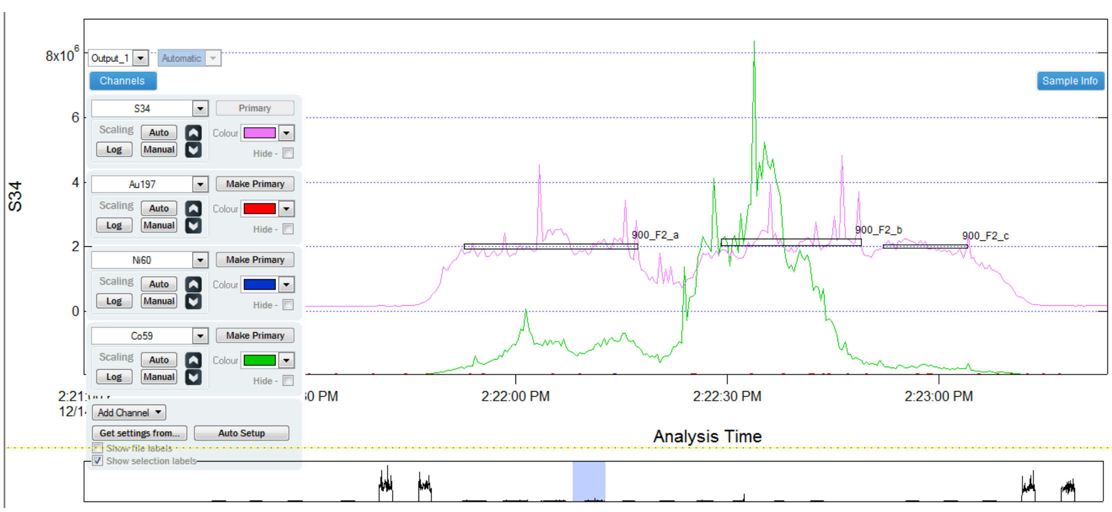
S34
8x10^6
6
4
2
0
Output_1
Automatic
Channels
Sample Info
S34
Primary
Au197
Ni60
Co59
Make Primary
Scaling
Auto
Log
Manual
Colour
Hide -
Add Channel
Get settings from...
Auto Setup
Show file labels
Show selection labels
900_F2_a
900_F2_b
900_F2_c
2:22:00 PM
2:22:30 PM
2:23:00 PM
Analysis Time

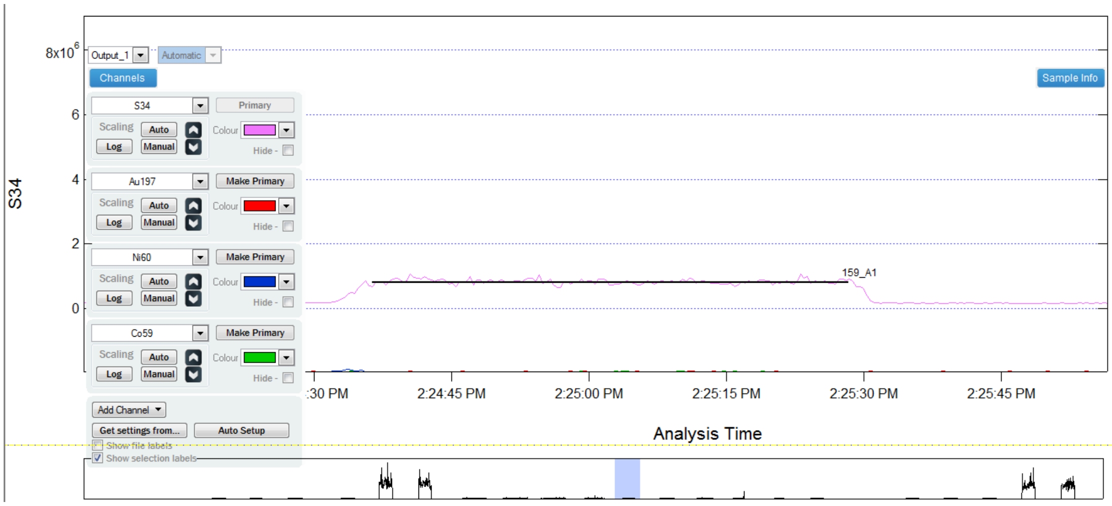
S34
8x10^6
6
4
2
0
Output_1
Automatic
Channels
Sample Info
S34
Primary
Au197
Ni60
Co59
Make Primary
Scaling
Auto
Log
Manual
Colour
Hide -
Add Channel
Get settings from...
Auto Setup
Show file labels
Show selection labels
159_A1
:30 PM
2:24:45 PM
2:25:00 PM
2:25:15 PM
2:25:30 PM
2:25:45 PM
Analysis Time

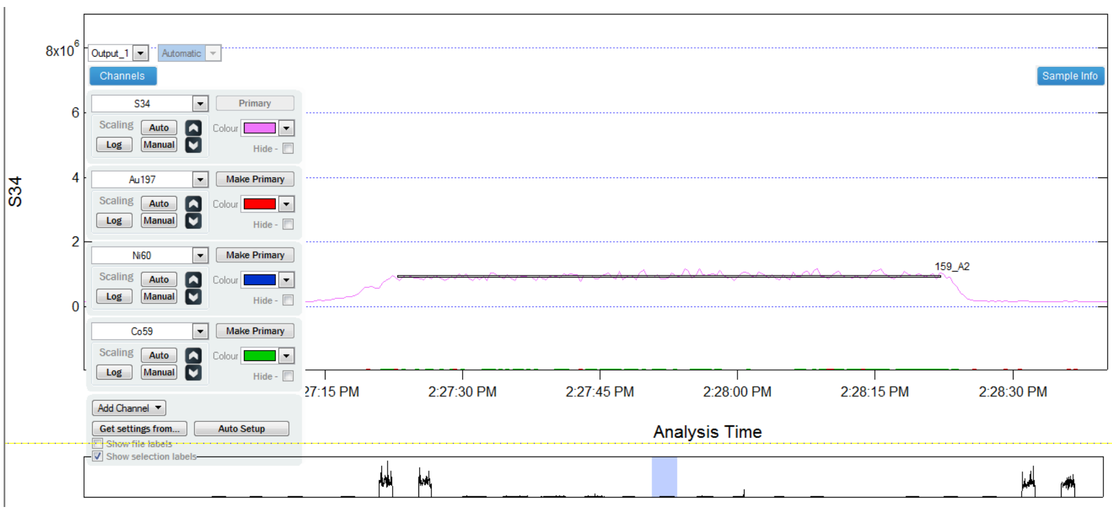
S34
8x10^6
6
4
2
0
Output_1
Automatic
Channels
Sample Info
S34
Primary
Au197
Ni60
Co59
Make Primary
Scaling
Auto
Log
Manual
Colour
Hide -
Add Channel
Get settings from...
Auto Setup
Show file labels
Show selection labels
159_A2
27:15 PM
2:27:30 PM
2:27:45 PM
2:28:00 PM
2:28:15 PM
2:28:30 PM
Analysis Time

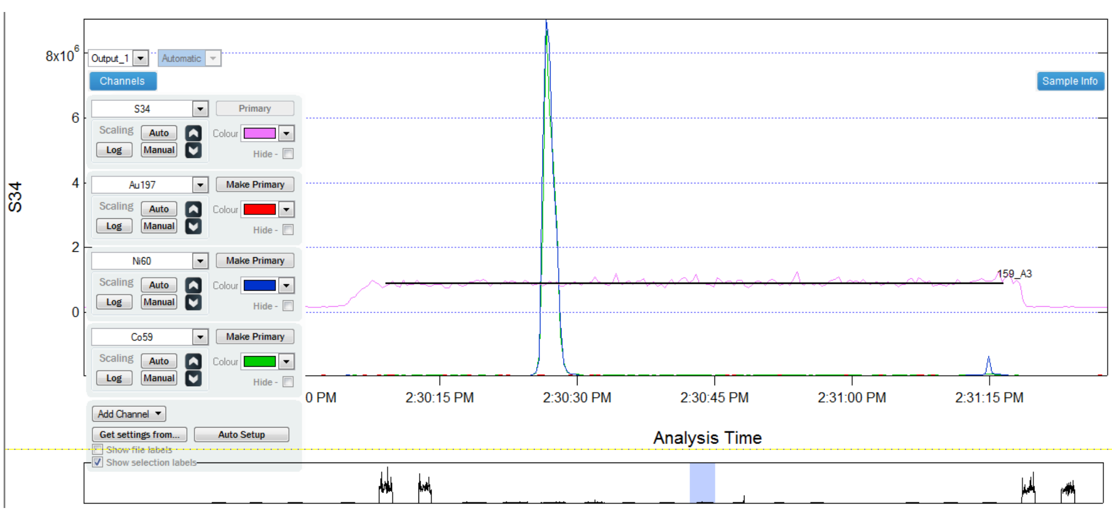
S34
8x10^6
6
4
2
0
Output_1
Automatic
Channels
Sample Info
S34
Primary
Au197
Ni60
Co59
Make Primary
Scaling
Auto
Log
Manual
Colour
Hide -
Add Channel
Get settings from...
Auto Setup
Show file labels
Show selection labels
159_A3
0 PM
2:30:15 PM
2:30:30 PM
2:30:45 PM
2:31:00 PM
2:31:15 PM
Analysis Time

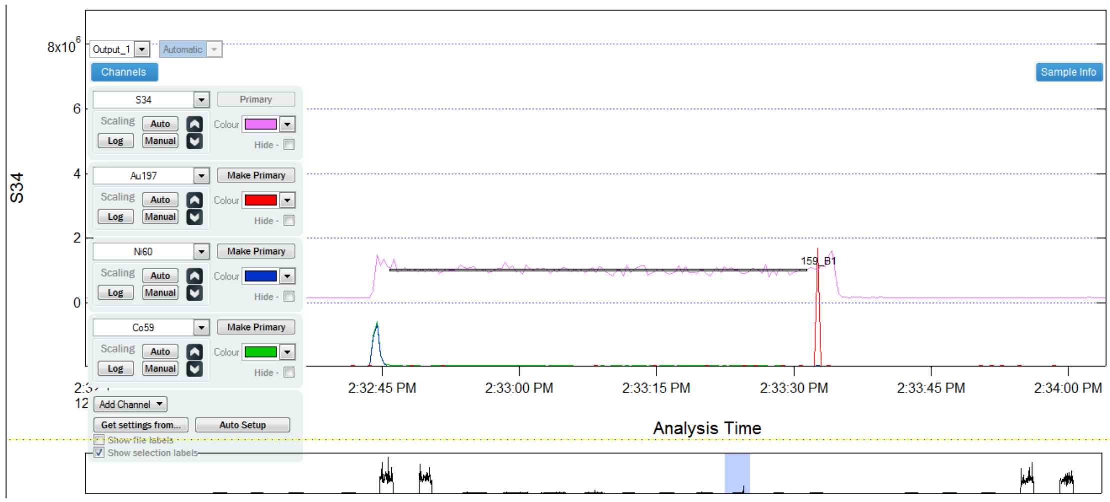
S34
8x10^6
Output_1
Automatic
Channels
Sample Info
S34
Primary
Scaling
Auto
Log
Manual
Colour
Hide -
Au197
Make Primary
Ni60
Co59
Add Channel
Get settings from...
Auto Setup
Show file labels
Show selection labels
159_B1
2:32:45 PM
2:33:00 PM
2:33:15 PM
2:33:30 PM
2:33:45 PM
2:34:00 PM
Analysis Time

Appendix F: Element Concentrations

F.1 Duration (s), total points, beam seconds for each sample, traverse and segment measured for LA ICP-MS for one component and normal type analysis.

Duration(s)	Sample ID, Traverse and Segment	Total points	Beam Seconds
18.58	153_C	49	35.4
11.773	153_B1_a	31	7.9
4.415	153_B1_b	11	23.89
16.74	153_B2	44	29
49.669	3415A_A1_a	131	73.7
53.9	3415A_A1_b	142	139.7
36.976	3415A_A2_a	97	23.2
10.854	3415A_A2_b	29	55.1
81.125	3415_A2_c	213	108.4
26.49	3415A_A3_a	70	14.4
29.801	3415A_A3_b	79	56.4
62.178	3415A_A3_c	163	124.4
66.961	3415A_D1	176	38
38.815	3415A_D2	102	27.7
20.603	3415A_D2_b	54	62.6
39.183	152_Ghost1_a	103	45
26.674	152_Ghost1_b	70	87
40.265	152_G1_a	106	63.4
116.29	152_G1_b	306	59.7
40	152_G2_a	105	40.6
58.013	152_G2_b	152	95.1
37.881	152_G2_c	100	20.7
85.563	152_B1_1	225	65.5
32.848	152_B2_a	86	17.9
38.675	152_B2_b	102	22.9
14.265	NB036_B1_a	36.1	1.4
9.8449	NB036_B1_b	53.4	1.1
12.658	NB036_B1_c	68.4	1.3
24.311	NIST610_B1_d	91	1.8
42.393	NIST610_B1_f	140.8	2.3
25.918	NIST610_B2_a	58.1	1.8
33.449	NIST610_B2_b	94.9	2.1

33.743	NB036_A	43.2	2.1
34.622	173_B1_a	41.2	2.1
17.681	173_B1_b	78.2	1.5
46.412	173_B2_a	28.4	2.4
31.856	173_B2_b	73.3	2
66.211	173_A2	63.2	2.9
4.2193	173_A1_a	2.27	0.76
6.6303	173_A1_b	18.23	0.93
15.872	173_A1_c	37.4	1.4
10.046	899A_E1_a	37	1.1
41.379	899A_E1_b	68.8	2.3
23.507	899A_E2_a	43.1	1.7
18.685	899A_E2_b	67.2	1.6
37.222	899A_E2_c	100.4	2.2
91.594	899A_F1	92.6	3.4
28.932	899A_F2_a	66.8	1.9
32.395	899A_F2_b	104.6	2
59.894	157_A1_a	28	2.5
27.895	157_A1_b	52.1	1.9
39.581	157_A2_a	15	1.7
22.101	157_A2_b	21.4	5.3
12.56	157_C1_a	39	1.3
11.586	157_C1_b	56.5	1.2
8.4385	157_C2_a	41.6	1.1
20.092	157_C2_b	65.7	1.6
5.3421	168A_D1_a	4.46	0.85
6.4753	168A_D1_b	13.77	0.93
15.217	168A_D1_c	37.7	1.4
8.0942	168A_D1_d	53.3	1
7.6085	168A_D1_e	63.7	1
13.598	168A_D2_a	10.3	1.3
8.7417	168A_D2_b	28.4	1.1
67.505	168A_D2_c	71.5	2.9
33.186	168A_D3_a	209.4	2.1
28.006	168A_D3_b	244.2	1.9
28.815	168A_C1_a	360	1.9
12.627	168A_C1_b	397	1.3
28.33	168A_C2_a	583.2	1.9
7.9323	168A_C2_b	612.5	1

91.442	895B_F1_a	46.2	3.4
38.653	895B_F2_a	189.1	2.2
32.899	895B_F2_b	231.6	2.1
89.816	895B_E1_a	385.9	3.4
10.825	895B_E2_a	7.4	1.2
21.802	895B_E2_b	39.5	1.7
41.927	895B_E2_c	81.3	2.3
87.208	895B_E3	50.8	3.3
7.4706	897A_A1	29	28
11.587	897A_A2	16	15
6.5559	897A_A3	156.11	0.93
57.783	898A_A1	388	2.7
34.151	898A_A2_a	584.4	2.1
43.604	898A_A2_b	628.7	2.4
13.874	898A_B1_a	718.4	1.4
5.0312	898A_B1_b	737.75	0.82
4.2689	898A_B1_c	750.67	0.76
32.779	898A_B1_d	778.6	2
23.174	898A_B2_a	967.9	1.7
43.452	898A_B2_b	1020.9	2.4
19.558	166B_A1_a	52	16.2
9.8575	166B_A1_b	26	33.3
25.504	166B_A1_c	67	53.7
8.7622	166B_A1_d	23	75.7
17.368	166B_A1_e	46	96.4
28.008	166B_A2_a	74	15.9
13.456	166B_A2_b	35	40.1
40.212	166B_A2_c	106	70.7
22.688	166B_A2_d	60	106
54.92	166B_A3_a	144	35
11.892	166B_A3_b	31	72.1
31.763	166B_A3_c	83	97.9
43.029	166B_A4_a	113	31.7
47.566	166B_A4_b	126	80.5
9.701	166B_B1_a	26	11.3
5.9458	166B_B1_b	16	21.9
59.614	166B_B1_c	157	63.9
29.572	166B_B2_a	78	17.6
54.138	166B_B2_b	143	64.9

13.186	866B_F	34	7.6
17.599	866B_E	46	10.8
21.633	171B_C1_a	57	18.7
8.2628	171B_C1_b	22	36.4
27.342	171B_C1_c	71	64.3
18.929	171B_C1_d	50	91.5
8.589	171B_C2_a	23	10.3
7.3442	171B_C2_b	19	27
13.444	171B_C2_c	35	46.4
12.946	171B_C2_d	34	68.2
7.8421	171B_C2_e	21	90.1
12.946	171B_B1_a	34	183.4
34.356	171B_B1_b	91	210.6
12.074	171B_B2_a	31	17.1
39.584	171B_B2_b	104	46.1
13.306	154_A1_a	35	24.7
10.946	154_A1_b	29	45.6
3.6827	154_A2_a	10	409.56
17.491	154_A2_b	46	429.7
7.5116	154_A2_c	20	449.8
7.6189	154_B1_a	20	573.8
3.9704	154_B1_b	11	581.63
14.487	154_B1_c	38	593.2
6.5458	154_B1_d	17	606.71
4.7216	154_B2_a	12	16.97
8.692	154_B2_b	23	25.1
4.7216	154_B2_c	12	39.39
4.3997	154_B3_a	11	5.86
6.8678	154_B3_b	18	13.27
6.2239	154_B3_c	17	29.04
9.0139	154_B3_d	24	41.8
54.234	154_B4_a	142	36.9
12.62	154_B4_b	33	81.6
18.929	154_B4_c	50	100.8
26.892	154_B5_a	70	37
12.77	154_B5_b	33	65.3
9.6149	154_B5_c	26	80.3
2.6501	900_E1_a	7	5.89
6.8591	900_E1_b	18	12.92

17.771	900_E1_c	47	28.3
7.1709	900_E1_d	18	44.09
13.562	900_E1_e	35	57.6
3.2737	900_E1_f	9	71.26
3.7413	900_E1_g	10	76.77
17.46	900_E1_h	46	90.1
36.01	900_E2_a	95	22
18.707	900_E2_b	50	52.2
4.6767	900_E2_c	12	65.48
15.589	900_E2_d	41	82.8
7.4827	900_E2_e	20	97.8
74.671	900_F1_a	197	37
10.289	900_F1_b	27	87.2
24.63	900_F2_a	64	192.5
19.798	900_F2_b	52	226.7
12.003	900_F2_c	31	245.5
51.911	159_A1	137	27.8
59.238	159_A2	156	198.1
67.344	159_A3	178	36.4
45.675	159_B1	120	24
36.946	159_B2	98	22.1

F.2 Concentrations of Au and LOD for each of the three standards, NIST610, Po 725 and Mass 1

Sample ID	Au NIST610	Au NIST610 LOD	Au Po725	Au Po725 LOD	Au Mass 1	Au Mass LOD
153_C	0.106	0.049	0.078	0.036	0.067	0.031
153_B1_a	0.125	0.078	0.092	0.057	0.079	0.049
153_B1_b	Below LOD	0.11	Below LOD	0.077	Below LOD	0.066
153_B2	0.064	0.055	0.047	0.04	0.041	0.035
3415A_A1_a	0.056	0.039	0.042	0.029	0.036	0.025
3415A_A1_b	0.28	0.044	0.21	0.032	0.18	0.028
3415A_A2_a	0.094	0.038	0.07	0.028	0.06	0.024
3415A_A2_b	Below LOD	0.053	Below LOD	0.039	Below LOD	0.034
3415_A2_c	Below LOD	0.031	Below LOD	0.023	Below LOD	0.02
3415A_A3_a	0.049	0.046	0.037	0.034	0.032	0.029
3415A_A3_b	0.112	0.048	0.084	0.036	0.072	0.031

3415A_A3_c	0.117	0.029	0.088	0.021	0.076	0.019
3415A_D1	Below LOD	0.029	Below LOD	0.022	Below LOD	0.019
3415A_D2	Below LOD	0.044	Below LOD	0.033	Below LOD	0.029
3415A_D2_b	Below LOD	0.05	Below LOD	0.038	Below LOD	0.033
152_A_a	0.32	0.048	0.241	0.036	0.209	0.032
152_A_b	0.225	0.063	0.171	0.047	0.148	0.041
152_G1_a	0.19	0.11	0.143	0.086	0.124	0.075
152_G1_b	Below LOD	0.076	Below LOD	0.057	Below LOD	0.05
152_G2_a	0.104	0.072	0.079	0.055	0.069	0.047
152_G2_b	0.64	0.06	0.49	0.045	0.43	0.039
152_G2_c	Below LOD	0.057	Below LOD	0.044	Below LOD	0.038
152_B1_1	0.138	0.053	0.106	0.041	0.092	0.035
152_B2_a	0.075	0.07	0.058	0.054	0.051	0.047
152_B2_b	0.47	0.057	0.36	0.044	0.31	0.038
NB036_B1_a	Below LOD	0.038	Below LOD	0.028	Below LOD	0.024
NB036_B1_b	Below LOD	0.043	Below LOD	0.031	Below LOD	0.027
NB036_B1_c	Below LOD	0.039	Below LOD	0.028	Below LOD	0.025
NB036_B1_d	Below LOD	0.032	Below LOD	0.023	Below LOD	0.02
NB036_B1_f	Below LOD	0.026	Below LOD	0.019	Below LOD	0.016
NB036_B2_a	Below LOD	0.029	Below LOD	0.021	Below LOD	0.018
NB036_B2_b	Below LOD	0.04	Below LOD	0.028	Below LOD	0.025
NB036_A	0.63	0.03	0.49	0.021	0.46	0.019
173_B1_a	Below LOD	0.03	Below LOD	0.021	Below LOD	0.019
173_B1_b	Below LOD	0.037	Below LOD	0.026	Below LOD	0.023
173_B2_a	Below LOD	0.028	Below LOD	0.019	Below LOD	0.018
173_B2_b	Below LOD	0.036	Below LOD	0.025	Below LOD	0.023
173_A2	Below LOD	0.021	Below LOD	0.014	Below LOD	0.013

173_A1_a	Below LOD	0.073	Below LOD	0.049	Below LOD	0.046
173_A1_b	Below LOD	0.058	Below LOD	0.039	Below LOD	0.037
173_A1_c	Below LOD	0.042	Below LOD	0.028	Below LOD	0.026
899A_E1_a	Below LOD	0.045	Below LOD	0.03	Below LOD	0.029
899A_E1_b	Below LOD	0.03	Below LOD	0.02	Below LOD	0.019
899A_E2_a	Below LOD	0.033	Below LOD	0.022	Below LOD	0.021
899A_E2_b	Below LOD	0.036	Below LOD	0.024	Below LOD	0.023
899A_E2_c	Below LOD	0.026	Below LOD	0.017	Below LOD	0.017
899A_F1	Below LOD	0.021	Below LOD	0.014	Below LOD	0.014
899A_F2_a	Below LOD	0.029	Below LOD	0.019	Below LOD	0.019
899A_F2_b	Below LOD	0.026	Below LOD	0.016	Below LOD	0.017
157_A1_a	0.262	0.12	0.186	0.075	0.196	0.079
157_A1_b	0.33	0.13	0.24	0.083	0.25	0.087
157_A2_a	0.34	0.14	0.24	0.088	0.25	0.092
157_A2_b	Below LOD	0.14	Below LOD	0.092	Below LOD	0.097
157_C1_a	0.11	0.039	0.078	0.026	0.083	0.027
157_C1_b	Below LOD	0.037	Below LOD	0.024	Below LOD	0.025
157_C2_a	0.16	0.072	0.113	0.048	0.119	0.051
157_C2_b	0.062	0.039	0.044	0.026	0.047	0.027
168A_D1_a	0.07	0.066	0.078	0.074	0.07	0.066
168A_D1_b	Below LOD	0.057	Below LOD	0.065	Below LOD	0.057
168A_D1_c	Below LOD	0.043	Below LOD	0.049	Below LOD	0.043
168A_D1_d	Below LOD	0.061	Below LOD	0.069	Below LOD	0.061
168A_D1_e	Below LOD	0.042	Below LOD	0.048	Below LOD	0.042
168A_D2_a	0.054	0.052	0.062	0.059	0.054	0.052
168A_D2_b	Below LOD	0.049	Below LOD	0.056	Below LOD	0.049

168A_D2_c	Below LOD	0.029	Below LOD	0.034	Below LOD	0.029
168A_D3_a	Below LOD	0.028	Below LOD	0.033	Below LOD	0.028
168A_D3_b	Below LOD	0.03	Below LOD	0.035	Below LOD	0.03
168A_C1_a	Below LOD	0.033	Below LOD	0.04	Below LOD	0.033
168A_C1_b	Below LOD	0.037	Below LOD	0.045	Below LOD	0.037
168A_C2_a	Below LOD	0.039	Below LOD	0.048	Below LOD	0.039
168A_C2_b	Below LOD	0.063	Below LOD	0.077	Below LOD	0.063
895B_F1_a	0.027	0.022	0.032	0.027	0.027	0.022
895B_F2_a	Below LOD	0.024	Below LOD	0.03	Below LOD	0.024
895B_F2_b	Below LOD	0.023	Below LOD	0.029	Below LOD	0.023
895B_E1_a	Below LOD	0.019	Below LOD	0.024	Below LOD	0.019
895B_E2_a	Below LOD	0.039	Below LOD	0.051	Below LOD	0.039
895B_E2_b	Below LOD	0.028	Below LOD	0.037	Below LOD	0.028
895B_E2_c	Below LOD	0.024	Below LOD	0.031	Below LOD	0.024
895B_E3	Below LOD	0.021	Below LOD	0.028	Below LOD	0.021
897A_A1	0.069	0.06	0.087	0.082	0.069	0.06
897A_A2	Below LOD	0.061	Below LOD	0.084	Below LOD	0.061
897A_A3	Below LOD	0.11	Below LOD	0.16	Below LOD	0.11
898A_A1	0.031	0.024	0.041	0.034	0.031	0.024
898A_A2_a	0.031	0.029	Below LOD	0.042	0.031	0.029
898A_A2_b	Below LOD	0.023	Below LOD	0.034	Below LOD	0.023
898A_B1_a	0.049	0.032	0.067	0.047	0.049	0.032
898A_B1_b	0.195	0.042	0.266	0.062	0.195	0.042
898A_B1_c	0.111	0.053	0.152	0.078	0.111	0.053
898A_B1_d	0.037	0.025	0.051	0.036	0.037	0.025
898A_B2_a	0.238	0.025	0.33	0.038	0.238	0.025
898A_B2_b	0.033	0.019	0.046	0.029	0.033	0.019

164B_A1_a	Below LOD	0.26	Below LOD	0.3	Below LOD	0.26
164B_A1_b	Below LOD	0.31	Below LOD	0.35	Below LOD	0.31
164B_A1_c	Below LOD	0.22	Below LOD	0.25	Below LOD	0.22
164B_A1_d	Below LOD	0.28	Below LOD	0.32	Below LOD	0.28
164B_A1_e	Below LOD	0.23	Below LOD	0.25	Below LOD	0.23
164B_A2_a	Below LOD	0.18	Below LOD	0.21	Below LOD	0.18
164B_A2_b	Below LOD	0.23	Below LOD	0.26	Below LOD	0.23
164B_A2_c	Below LOD	0.21	Below LOD	0.24	Below LOD	0.21
164B_A2_d	Below LOD	0.23	Below LOD	0.25	Below LOD	0.23
164B_A3_a	Below LOD	0.16	Below LOD	0.17	Below LOD	0.16
164B_A3_b	Below LOD	0.23	Below LOD	0.26	Below LOD	0.23
164B_A3_c	Below LOD	0.16	Below LOD	0.18	Below LOD	0.16
164B_A4_a	Below LOD	0.17	Below LOD	0.19	Below LOD	0.17
164B_A4_b	Below LOD	0.15	Below LOD	0.17	Below LOD	0.15
164B_B1_a	Below LOD	0.55	Below LOD	0.61	Below LOD	0.55
164B_B1_b	Below LOD	0.74	Below LOD	0.82	Below LOD	0.74
164B_B1_c	Below LOD	0.39	Below LOD	0.43	Below LOD	0.39
164B_B2_a	Below LOD	0.39	Below LOD	0.43	Below LOD	0.39
164B_B2_b	Below LOD	0.42	Below LOD	0.47	Below LOD	0.42
886B_F	Below LOD	0.039	Below LOD	0.043	Below LOD	0.039
886B_E	Below LOD	0.026	Below LOD	0.028	Below LOD	0.026
171B_C1_a	Below LOD	0.05	Below LOD	0.055	Below LOD	0.05
171B_C1_b	Below LOD	0.075	Below LOD	0.082	Below LOD	0.075

171B_C1_c	Below LOD	0.048	Below LOD	0.053	Below LOD	0.048
171B_C1_d	Below LOD	0.055	Below LOD	0.061	Below LOD	0.055
171B_C2_a	Below LOD	0.055	Below LOD	0.06	Below LOD	0.055
171B_C2_b	Below LOD	0.057	Below LOD	0.063	Below LOD	0.057
171B_C2_c	Below LOD	0.05	Below LOD	0.055	Below LOD	0.05
171B_C2_d	Below LOD	0.039	Below LOD	0.042	Below LOD	0.039
171B_C2_e	Below LOD	0.044	Below LOD	0.048	Below LOD	0.044
171B_B1_a	Below LOD	0.027	Below LOD	0.03	Below LOD	0.027
171B_B1_b	Below LOD	0.02	Below LOD	0.022	Below LOD	0.02
171B_B2_a	Below LOD	0.031	Below LOD	0.034	Below LOD	0.031
171B_B2_b	Below LOD	0.022	Below LOD	0.024	Below LOD	0.022
154_A1_a	0.036	0.028	0.037	0.031	0.036	0.028
154_A1_b	0.047	0.032	0.048	0.035	0.047	0.032
154_A2_a	Below LOD	0.091	Below LOD	0.1	Below LOD	0.091
154_A2_b	Below LOD	0.051	Below LOD	0.056	Below LOD	0.051
154_A2_c	Below LOD	0.076	Below LOD	0.084	Below LOD	0.076
154_B1_a	Below LOD	0.098	Below LOD	0.11	Below LOD	0.098
154_B1_b	0.11	0.093	0.11	0.1	0.11	0.093
154_B1_c	Below LOD	0.076	Below LOD	0.084	Below LOD	0.076
154_B1_d	Below LOD	0.092	Below LOD	0.1	Below LOD	0.092
154_B2_a	Below LOD	0.11	Below LOD	0.12	Below LOD	0.11
154_B2_b	Below LOD	0.094	Below LOD	0.1	Below LOD	0.094
154_B2_c	Below LOD	0.14	Below LOD	0.16	Below LOD	0.14
154_B3_a	0.124	0.072	0.133	0.08	0.124	0.072

154_B3_b	Below LOD	0.064	Below LOD	0.071	Below LOD	0.064
154_B3_c	Below LOD	0.063	Below LOD	0.07	Below LOD	0.063
154_B3_d	Below LOD	0.046	Below LOD	0.051	Below LOD	0.046
154_B4_a	Below LOD	0.057	Below LOD	0.063	Below LOD	0.057
154_B4_b	Below LOD	0.082	Below LOD	0.091	Below LOD	0.082
154_B4_c	Below LOD	0.061	Below LOD	0.068	Below LOD	0.061
154_B5_a	Below LOD	0.063	Below LOD	0.07	Below LOD	0.063
154_B5_b	Below LOD	0.077	Below LOD	0.086	Below LOD	0.077
154_B5_c	Below LOD	0.073	Below LOD	0.082	Below LOD	0.073
900_E1_a	Below LOD	0.25	Below LOD	0.29	Below LOD	0.25
900_E1_b	Below LOD	0.15	Below LOD	0.18	Below LOD	0.15
900_E1_c	Below LOD	0.12	Below LOD	0.14	Below LOD	0.12
900_E1_d	Below LOD	0.16	Below LOD	0.19	Below LOD	0.16
900_E1_e	Below LOD	0.12	Below LOD	0.14	Below LOD	0.12
900_E1_f	Below LOD	0.14	Below LOD	0.16	Below LOD	0.14
900_E1_g	Below LOD	0.16	Below LOD	0.19	Below LOD	0.16
900_E1_h	Below LOD	0.092	Below LOD	0.11	Below LOD	0.092
900_E2_a	Below LOD	0.088	Below LOD	0.11	Below LOD	0.088
900_E2_b	Below LOD	0.11	Below LOD	0.13	Below LOD	0.11
900_E2_c	Below LOD	0.14	Below LOD	0.16	Below LOD	0.14
900_E2_d	Below LOD	0.088	Below LOD	0.11	Below LOD	0.088
900_E2_e	Below LOD	0.13	Below LOD	0.16	Below LOD	0.13
900_F1_a	Below LOD	0.07	Below LOD	0.088	Below LOD	0.07

900_F1_b	Below LOD	0.16	Below LOD	0.2	Below LOD	0.16
900_F2_a	Below LOD	0.075	Below LOD	0.096	Below LOD	0.075
900_F2_b	Below LOD	0.069	Below LOD	0.089	Below LOD	0.069
900_F2_c	Below LOD	0.073	Below LOD	0.094	Below LOD	0.073
159_A1	Below LOD	0.14	Below LOD	0.18	Below LOD	0.14
159_A2	Below LOD	0.12	Below LOD	0.16	Below LOD	0.12
159_A3	Below LOD	0.12	Below LOD	0.16	Below LOD	0.12
159_B1	Below LOD	0.086	Below LOD	0.12	Below LOD	0.086
159_B2	Below LOD	0.11	Below LOD	0.15	Below LOD	0.11

F.3 Concentrations of Co, Ni, Se77, and Se78 in ppm in the samples under the standard NIST610

Sample ID	Co ppm	Co5 ppm LOD	Ni ppm	Ni ppm LOD	Se77 ppm	Se77 ppm LOD	Se77 ppm LOD	Se78 ppm LOD
153_C	8.00E+03	0.016	4390	0.19	26.9	0.51	35.9	13
153_B1_a	41	0.02	27	0.32	5.7	0.76	Below LOD	17
153_B1_b	41	0.027	15.5	0.43	1.3	1	Below LOD	23
153_B2	11	0.024	30	0.21	14.5	0.54	18.5	11
3415A_A1_a	302	0.011	480	0.16	14	0.48	24.8	10
3415A_A1_b	566	0.031	186	0.23	14.87	0.56	29.4	11
3415A_A2_a	361	0.027	691	0.2	4.44	0.49	Below LOD	9.5
3415A_A2_b	122	0.037	256	0.28	11.3	0.68	21.3	13
3415_A2_c	309	0.016	201	0.12	14.42	0.45	21.3	8.1

3415A_A3_a	55	0.024	177	0.19	14.6	0.66	20.3	12
3415A_A3_b	125	0.025	419	0.19	10.5	0.69	14.4	13
3415A_A3_c	639	0.018	514	0.14	14.69	0.38	21.3	8.4
3415A_D1	110	0.018	483	0.14	5.73	0.38	14.2	8.4
3415A_D2	96	0.016	375	0.17	3.94	0.44	Below LOD	11
3415A_D2_b	43	0.018	622	0.2	19.3	0.5	28.6	12
152_A_a	211	0.02	765	0.19	23.4	0.58	24.8	13
152_A_b	91	0.025	335	0.25	24	0.75	41.7	16
152_G1_a	112.9	0.039	505	0.51	27.5	1.5	38	32
152_G1_b	212	0.026	496	0.34	21.4	1	40.8	21
152_G2_a	131.2	0.048	567	0.39	24.3	1.2	25.2	23
152_G2_b	312	0.04	519	0.32	18.4	0.96	27	19
152_G2_c	41.8	0.028	300	0.29	20.2	0.78	17.6	16
152_B1_1	92	0.026	285	0.27	28.1	0.72	30.1	15
152_B2_a	81	0.032	84	0.33	27.3	0.83	41.8	20
152_B2_b	205	0.026	432	0.27	26.6	0.67	45.5	16
NB036_B1_a	5130	0.015	134	0.17	22.4	0.46	34.1	14
NB036_B1_b	450	0.016	38	0.2	38.4	0.52	50	16
NB036_B1_c	546	0.015	11.5	0.18	40.8	0.47	58	15
NB036_B1_d	660	0.012	3.6	0.14	35.6	0.38	53.5	12
NB036_B1_f	1990	0.013	28.8	0.11	50	0.32	80.3	10
NB036_B2_a	840	0.015	14.6	0.13	31.4	0.35	48.9	11
NB036_B2_b	1720	0.016	25.8	0.12	29.4	0.59	46.5	13
NB036_A	14150	0.012	4830	0.092	32.9	0.44	51.6	9.6
173_B1_a	2220	0.015	301	0.15	9.3	0.39	13	11
173_B1_b	74	0.018	461	0.18	7.7	0.48	23.1	14
173_B2_a	1780	0.012	277	0.13	8.89	0.5	Below LOD	14
173_B2_b	376	0.015	478	0.17	12.8	0.64	25.4	18
173_A2	910	0.014	271	0.11	7.71	0.37	12.6	10

173_A1_a	62.9	0.03	234	0.33	6.6	0.81	Below LOD	29
173_A1_b	103	0.024	226	0.26	5.8	0.64	Below LOD	23
173_A1_c	707	0.017	215	0.19	6.45	0.46	Below LOD	16
899A_E1_a	282	0.013	915	0.19	7.1	0.58	Below LOD	20
899A_E1_b	237	0.009	1178	0.13	13	0.39	18	14
899A_E2_a	88	0.022	880	0.14	8.64	0.37	Below LOD	12
899A_E2_b	259	0.024	1180	0.16	9.2	0.4	Below LOD	13
899A_E2_c	82	0.015	1130	0.18	9.8	0.44	Below LOD	11
899A_F1	229	0.012	1518	0.14	8.56	0.36	12.8	9.1
899A_F2_a	168	0.016	1482	0.12	8.1	0.51	17.2	12
899A_F2_b	280	0.016	1120	0.14	9	0.37	13.8	12
157_A1_a	196	0.071	181	0.65	9	1.7	Below LOD	54
157_A1_b	1580	0.089	264	0.63	16.4	2.2	Below LOD	67
157_A2_a	1390	0.095	291	0.67	19.8	2.3	Below LOD	69
157_A2_b	1040	0.099	310	0.71	9.2	2.4	Below LOD	72
157_C1_a	189	0.028	318	0.2	16.9	0.63	20	15
157_C1_b	5.3	0.026	24.4	0.19	7	0.59	Below LOD	14
157_C2_a	66	0.032	110	0.46	12.6	1.1	Below LOD	26
157_C2_b	105	0.017	144	0.25	20.6	0.56	33.9	14

168A_D1_a	0.46	0.027	960	0.31	10.6	0.89	Below LOD	18
168A_D1_b	0.05	0.024	2760	0.27	10.3	0.78	22	16
168A_D1_c	2.79	0.018	820	0.2	32.2	0.58	54	12
168A_D1_d	0.25	0.025	53	0.29	29.8	0.82	53	17
168A_D1_e	0.19	0.015	1390	0.21	15.3	0.86	22.4	17
168A_D2_a	8	0.018	2230	0.26	20.1	1.1	41	21
168A_D2_b	0.067	0.017	270	0.25	43.9	1	69	20
168A_D2_c	0.068	0.011	112	0.15	28.5	0.61	46.7	12
168A_D3_a	0.336	0.0086	95	0.12	20.9	0.36	33.2	12
168A_D3_b	4	0.0097	950	0.14	29.2	0.38	43.9	11
168A_C1_a	1.69	0.011	113	0.16	39.1	0.42	65.1	13
168A_C1_b	7.4	0.012	180	0.18	50.4	0.47	82.7	14
168A_C2_a	2.8	0.016	127	0.15	42	0.57	70.2	15
168A_C2_b	1.25	0.026	278	0.24	23.1	0.92	48	23
895B_F1_a	512	0.0097	209.6	0.13	6.05	0.4	Below LOD	10
895B_F2_a	973	0.0062	334	0.15	5.53	0.38	14.7	10
895B_F2_b	505	0.012	181	0.15	5.19	0.44	Below LOD	10
895B_E1_a	507	0.01	234.6	0.13	5.69	0.36	9.5	8.5
895B_E2_a	451	0.023	230	0.33	6.1	0.71	Below LOD	15
895B_E2_b	650	0.017	87	0.24	5.58	0.52	Below LOD	11
895B_E2_c	451	0.0097	158	0.11	5.69	0.34	11.6	9.5
895B_E3	431	0.0085	199.1	0.093	5.37	0.3	10.5	8.3
897A_A1	3.76E+04	0.022	870	0.34	66	1	95	26
897A_A2	3440	0.031	5.40E+03	0.46	52.2	1.4	64	35
897A_A3	5.40E+03	0.053	7.70E+03	0.64	102	2.3	161	48
898A_A1	225	0.01	700	0.15	27.9	0.54	36.4	12

898A_A2_a	184	0.0097	514	0.14	27.1	0.41	42.5	11
898A_A2_b	142	0.011	545	0.13	28.9	0.49	44.3	12
898A_B1_a	405	0.015	590	0.18	31.2	0.68	49.3	16
898A_B1_b	213	0.02	138	0.24	35.6	0.9	56	21
898A_B1_c	96	0.024	770	0.3	30.2	1.1	48	26
898A_B1_d	107	0.011	353	0.14	29.7	0.52	48.2	12
898A_B2_a	188	0.013	646	0.16	30.2	0.49	47.7	14
898A_B2_b	67.8	0.0079	481	0.12	32.2	0.49	48.8	11
164B_A1_a	334	0.14	940	1.7	34.7	4.1	Below LOD	120
164B _A1_b	442	0.17	1392	2	38	4.9	Below LOD	150
164B _A1_c	418	0.12	1292	1.4	34.5	3.5	Below LOD	100
164B _A1_d	425	0.18	1340	2.5	33.2	5.4	Below LOD	150
164B _A1_e	421	0.15	1309	2	31.1	4.3	Below LOD	120
164B _A2_a	443	0.12	1344	1.7	33.7	3.5	Below LOD	97
164B _A2_b	451	0.15	1220	2.1	33.3	4.4	Below LOD	120
164B _A2_c	325	0.037	780	1.6	32.7	3.4	Below LOD	97
164B _A2_d	435	0.039	1260	1.8	36.5	3.7	Below LOD	100
164B _A3_a	554	0.027	1374	1.2	32.6	2.5	Below LOD	71
164B _A3_b	449	0.17	1030	1.5	25.9	3.9	Below LOD	97

164B _A3_c	543	0.12	1367	1	30.4	2.7	Below LOD	67
164B _A4_a	442	0.13	1015	1.1	30.1	2.9	Below LOD	73
164B _A4_b	560	0.058	1430	1.2	32.9	3.1	Below LOD	82
164B _B1_a	685	0.22	868	4.4	35.8	11	Below LOD	300
164B _B1_b	692	0.29	903	5.9	49	15	Below LOD	410
164B _B1_c	747	0.25	1066	3.1	43.7	10	Below LOD	220
164B _B2_a	709	0.25	975	3.1	44	10	Below LOD	220
164B _B2_b	735	0.27	1042	3.4	42.5	11	Below LOD	240
886B_F	440	0.025	272	0.2	12.6	0.46	17.3	15
886B_E	57	0.014	92	0.22	5.76	0.41	Below LOD	13
171B_C1_a	1072	0.033	145.6	0.46	5.6	1	Below LOD	29
171B_C1_b	715	0.049	212	0.69	8.8	1.5	Below LOD	43
171B_C1_c	422	0.032	210	0.44	8.6	0.98	Below LOD	28
171B_C1_d	491	0.027	421	0.52	11	0.97	Below LOD	30
171B_C2_a	2740	0.027	811	0.51	18.6	0.96	32	30
171B_C2_b	2310	0.028	897	0.53	20.5	1	Below LOD	32

171B_C2_c	3220	0.025	889	0.47	22.5	0.88	Below LOD	28
171B_C2_d	627	0.025	292	0.25	7.2	0.67	Below LOD	19
171B_C2_e	540	0.029	266	0.28	9.7	0.75	Below LOD	21
171B_B1_a	99	0.018	1120	0.18	13.5	0.47	15.8	13
171B_B1_b	207	0.013	287	0.13	11.03	0.35	17.9	10
171B_B2_a	27.2	0.011	60	0.19	19.5	0.51	25.1	15
171B_B2_b	293	0.008	48.2	0.14	18.4	0.36	31.8	11
154_A1_a	19.4	0.019	97	0.27	14.9	0.66	25.4	15
154_A1_b	67	0.021	148	0.31	13.7	0.74	18	18
154_A2_a	112	0.039	205	0.53	22.8	1.1	Below LOD	40
154_A2_b	0.273	0.021	99	0.29	12.1	0.59	Below LOD	22
154_A2_c	1.98	0.032	107	0.44	13.4	0.88	39	33
154_B1_a	35.4	0.07	211	0.78	4.2	1.7	Below LOD	56
154_B1_b	16.9	0.066	182	0.75	5.8	1.6	Below LOD	54
154_B1_c	2.4	0.054	903	0.61	24	1.3	Below LOD	44
154_B1_d	12	0.066	746	0.74	21.9	1.6	63	53
154_B2_a	277	0.062	1020	0.6	7.2	1.8	Below LOD	49
154_B2_b	560	0.053	754	0.52	17.1	1.6	Below LOD	42
154_B2_c	67	0.08	201	0.78	9	2.3	Below LOD	64
154_B3_a	30.6	0.034	429	0.71	6.4	1.6	Below LOD	52

154_B3_b	110	0.029	381	0.63	5.7	1.4	Below LOD	46
154_B3_c	33	0.029	105	0.62	5.8	1.4	Below LOD	46
154_B3_d	98	0.021	178	0.45	4	1	Below LOD	33
154_B4_a	74	0.036	168	0.29	6.32	0.77	Below LOD	22
154_B4_b	18.1	0.053	293	0.42	15.9	1.1	Below LOD	32
154_B4_c	86	0.039	356	0.32	7.3	0.84	Below LOD	24
154_B5_a	29.3	0.04	132.8	0.32	8.4	0.85	Below LOD	24
154_B5_b	59	0.049	107	0.4	4.3	1.1	Below LOD	30
154_B5_c	76	0.047	165	0.38	6.9	1	Below LOD	28
900_E1_a	207	0.13	145	1.5	47	4.1	Below LOD	130
900_E1_b	79	0.08	98	0.94	10	2.5	Below LOD	78
900_E1_c	57.5	0.062	67.6	0.73	6.6	2	Below LOD	60
900_E1_d	34.5	0.087	71.6	1	9.2	2.7	Below LOD	84
900_E1_e	48	0.066	72	0.77	3.6	2.1	Below LOD	64
900_E1_f	44	0.077	47.7	1.3	3.3	2.7	Below LOD	94

900_E1_g	31.4	0.09	28.2	1.6	7	3.2	Below LOD	110
900_E1_h	34.7	0.052	42.8	0.9	5.7	1.8	Below LOD	63
900_E2_a	63	0.051	57.7	0.88	7.6	1.8	Below LOD	61
900_E2_b	46.6	0.062	65	1.1	5	2.2	Below LOD	75
900_E2_c	76	0.12	125	1.6	7.3	3.5	Below LOD	110
900_E2_d	74.8	0.078	76	1	6.2	2.3	Below LOD	71
900_E2_e	254	0.12	293	1.6	13	3.4	Below LOD	110
900_F1_a	1480	0.065	16.6	0.86	5.5	1.8	Below LOD	58
900_F1_b	970	0.061	80	0.82	6.5	2.9	Below LOD	88
900_F2_a	651	0.029	27.3	0.39	3.4	1.4	Below LOD	42
900_F2_b	2650	0.027	13	0.36	5.3	1.3	Below LOD	38
900_F2_c	171	0.042	18.3	0.8	4.5	2.1	Below LOD	48
159_A1	20.13	0.081	3.14	1.5	35.3	4	Below LOD	91
159_A2	23.76	0.084	9.1	1.2	33.6	3.3	Below LOD	76
159_A3	57	0.087	530	1.1	33.8	3	Below LOD	76
159_B1	23.7	0.1	7.11	1	31.8	2.7	86	68

159_B2	25.1	0.081	5.87	1.1	32.3	2.2	Below LOD	69

F.4 Concentrations of Ag 107, Ag 109, As, and Sb in ppm in the samples under the standard NIST610

Sample ID	Ag107 ppm	Ag107 ppm LOD	Ag109 ppm	Ag109 ppm LOD	As ppm	As ppm LOD	Sb ppm	Sb ppm LOD
153_C	4.9	0.016	4.7	0.02	2700	0.37	0.277	0.063
153_B1_a	3.65	0.042	3.82	0.032	78	0.58	3.41	0.092
153_B1_b	1.38	0.057	1.56	0.043	10.2	0.78	0.97	0.12
153_B2	0.062	0.033	0.063	0.028	4.5	0.43	Below LOD	0.068
3415A_A1_a	0.3	0.016	0.31	0.012	7.74	0.27	Below LOD	0.061
3415A_A1_b	1.07	0.037	1.6	0.039	10.45	0.41	Below LOD	0.064
3415A_A2_a	0.205	0.032	0.32	0.034	33	0.35	Below LOD	0.056
3415A_A2_b	0.069	0.045	0.066	0.047	6.6	0.49	Below LOD	0.077
3415_A2_c	0.038	0.018	0.036	0.023	2.11	0.27	Below LOD	0.041
3415A_A3_a	0.29	0.027	0.39	0.033	10	0.39	Below LOD	0.061
3415A_A3_b	0.94	0.028	0.69	0.035	5.77	0.41	Below LOD	0.064
3415A_A3_c	0.317	0.015	0.335	0.022	6.73	0.28	Below LOD	0.055
3415A_D1	Below LOD	0.015	Below LOD	0.022	4.86	0.28	Below LOD	0.055
3415A_D2	Below LOD	0.024	Below LOD	0.024	2.8	0.28	Below LOD	0.051
3415A_D2_b	Below LOD	0.027	Below LOD	0.027	10.7	0.32	Below LOD	0.058
152_A_a	0.7	0.022	0.64	0.028	12.62	0.42	0.102	0.063
152_A_b	1.16	0.028	1.2	0.036	18	0.55	0.196	0.082
152_G1_a	0.38	0.062	0.31	0.051	12.13	0.91	Below LOD	0.15
152_G1_b	0.146	0.041	0.138	0.034	27.6	0.6	Below LOD	0.1

152_G2_a	0.194	0.051	0.156	0.034	9.01	0.68	Below LOD	0.12
152_G2_b	2	0.042	1.14	0.028	9.53	0.57	Below LOD	0.1
152_G2_c	0.066	0.034	0.05	0.032	5.36	0.49	Below LOD	0.075
152_B1_1	0.645	0.031	0.691	0.03	17.5	0.45	0.076	0.07
152_B2_a	0.284	0.031	0.258	0.033	11.63	0.7	Below LOD	0.094
152_B2_b	3.9	0.025	3.4	0.027	25	0.57	0.095	0.076
NB036_B1_a	Below LOD	0.016	Below LOD	0.02	75	0.36	Below LOD	0.06
NB036_B1_b	0.21	0.018	0.153	0.022	10.4	0.41	Below LOD	0.067
NB036_B1_c	0.02	0.016	0.027	0.02	10.5	0.37	Below LOD	0.062
NB036_B1_d	Below LOD	0.013	Below LOD	0.016	15.3	0.3	Below LOD	0.05
NB036_B1_f	4	0.02	5.7	0.011	11.9	0.22	Below LOD	0.044
NB036_B2_a	Below LOD	0.022	0.024	0.013	10.8	0.24	Below LOD	0.049
NB036_B2_b	1.06	0.017	1.14	0.02	16.6	0.32	Below LOD	0.04
NB036_A	79	0.013	61	0.015	5920	0.24	Below LOD	0.03
173_B1_a	0.35	0.018	0.39	0.012	10.7	0.24	Below LOD	0.048
173_B1_b	Below LOD	0.021	Below LOD	0.014	2.1	0.29	Below LOD	0.058
173_B2_a	0.107	0.014	0.114	0.014	4.69	0.29	Below LOD	0.058
173_B2_b	0.086	0.018	0.13	0.018	10	0.37	Below LOD	0.074
173_A2	Below LOD	0.015	Below LOD	0.012	2.23	0.25	Below LOD	0.035
173_A1_a	Below LOD	0.029	Below LOD	0.035	2.59	0.55	Below LOD	0.086
173_A1_b	Below LOD	0.023	Below LOD	0.028	1.91	0.44	Below LOD	0.068
173_A1_c	Below LOD	0.016	Below LOD	0.02	1.66	0.31	Below LOD	0.049
899A_E1_a	Below LOD	0.024	Below LOD	0.021	404	0.34	Below LOD	0.064

899A_E1_b	Below LOD	0.016	Below LOD	0.014	296	0.23	Below LOD	0.043
899A_E2_a	Below LOD	0.013	Below LOD	0.013	150	0.23	Below LOD	0.044
899A_E2_b	Below LOD	0.014	Below LOD	0.014	403	0.25	Below LOD	0.048
899A_E2_c	Below LOD	0.011	Below LOD	0.014	411	0.24	Below LOD	0.038
899A_F1	Below LOD	0.0089	Below LOD	0.011	330	0.19	Below LOD	0.03
899A_F2_a	Below LOD	0.016	Below LOD	0.013	356	0.26	Below LOD	0.043
899A_F2_b	Below LOD	0.015	Below LOD	0.0094	212	0.25	Below LOD	0.037
157_A1_a	1.2	0.067	1.35	0.043	29.4	1.2	Below LOD	0.17
157_A1_b	0.23	0.075	0.28	0.086	29.2	1.5	Below LOD	0.23
157_A2_a	1.7	0.079	2.4	0.092	33.3	1.6	Below LOD	0.25
157_A2_b	0.26	0.083	0.33	0.097	26.3	1.6	Below LOD	0.26
157_C1_a	2.83	0.021	2.89	0.025	30.8	0.31	Below LOD	0.059
157_C1_b	0.041	0.02	Below LOD	0.024	1.07	0.29	Below LOD	0.056
157_C2_a	6.5	0.031	6.5	0.034	11.6	0.91	Below LOD	0.12
157_C2_b	0.97	0.016	0.87	0.018	14.7	0.49	0.072	0.067
168A_D1_a	0.104	0.012	0.109	0.022	1.43	0.64	1.17	0.1
168A_D1_b	0.26	0.011	0.188	0.019	1.11	0.56	1.85	0.091
168A_D1_c	0.205	0.0081	0.202	0.014	1.15	0.42	2.73	0.069
168A_D1_d	0.4	0.011	0.38	0.02	0.72	0.59	9	0.097
168A_D1_e	0.085	0.017	0.066	0.015	1.24	0.49	1.6	0.077
168A_D2_a	0.6	0.021	0.6	0.018	2.68	0.6	11.1	0.095
168A_D2_b	0.226	0.02	0.26	0.017	2.18	0.56	6.7	0.09
168A_D2_c	0.561	0.012	0.544	0.01	1.93	0.34	18.4	0.054
168A_D3_a	0.432	0.0091	0.45	0.013	1.5	0.29	14.9	0.042
168A_D3_b	0.379	0.0098	0.347	0.0089	2.46	0.34	5.5	0.056
168A_C1_a	0.328	0.011	0.33	0.0099	0.53	0.38	6.7	0.063
168A_C1_b	0.126	0.012	0.148	0.011	Below LOD	0.43	0.83	0.07
168A_C2_a	0.263	0.015	0.255	0.011	0.57	0.46	2.13	0.053
168A_C2_b	0.617	0.025	0.76	0.017	2.5	0.74	0.67	0.085

895B_F1_a	Below LOD	0.0088	Below LOD	0.012	2.13	0.29	Below LOD	0.038
895B_F2_a	0.0056	NaN	Below LOD	0.01	1.9	0.27	Below LOD	0.037
895B_F2_b	Below LOD	0.0097	0.0075	0.0073	1.64	0.33	Below LOD	0.041
895B_E1_a	Below LOD	0.0081	Below LOD	0.0061	1.14	0.27	Below LOD	0.034
895B_E2_a	Below LOD	0.013	Below LOD	0.01	0.95	0.52	Below LOD	0.065
895B_E2_b	Below LOD	0.0097	Below LOD	0.0073	1.26	0.38	Below LOD	0.047
895B_E2_c	Below LOD	0.0083	Below LOD	0.0055	1.35	0.27	Below LOD	0.033
895B_E3	Below LOD	0.0073	Below LOD	0.0048	1.076	0.24	Below LOD	0.029
897A_A1	81	0.025	110	0.019	47.1	0.77	1.28	0.091
897A_A2	6.6	0.012	6.2	0.031	66	0.69	5.6	0.11
897A_A3	24.7	0.045	23.5	0.041	274	1.4	3.2	0.16
898A_A1	0.0109	0.007	0.0143	0.011	543	0.29	0.093	0.046
898A_A2_a	0.073	0.0085	0.095	0.0073	262	0.35	0.096	0.044
898A_A2_b	0.0229	0.0085	0.0202	0.0052	622	0.29	0.134	0.041
898A_B1_a	0.067	0.012	0.101	0.0071	920	0.4	0.209	0.056
898A_B1_b	1.04	0.015	1.16	0.0094	199	0.52	Below LOD	0.074
898A_B1_c	0.294	0.019	0.39	0.012	840	0.65	Below LOD	0.092
898A_B1_d	0.165	0.0089	0.169	0.0055	370	0.3	0.063	0.043
898A_B2_a	0.66	0.0076	0.83	0.012	828	0.33	0.057	0.044
898A_B2_b	0.04	0.0043	0.0292	NaN	326	0.24	Below LOD	0.038
164B_A1_a	0.83	0.083	0.94	NaN	3.7	3.7	Below LOD	0.5
164B _A1_b	0.63	0.099	0.53	NaN	Below LOD	4.4	Below LOD	0.6
164B _A1_c	10.4	0.071	6	NaN	Below LOD	3.1	Below LOD	0.42
164B _A1_d	1.75	NaN	1.25	0.15	Below LOD	4.4	Below LOD	0.74
164B A1_e	0.62	NaN	0.57	0.12	Below LOD	3.5	Below LOD	0.59
164B _A2_a	0.65	NaN	0.68	0.098	Below LOD	2.8	Below LOD	0.48
164B _A2_b	0.5	NaN	0.54	0.12	Below LOD	3.6	Below LOD	0.6

164B _A2_c	1.36	0.08	1.15	0.066	Below LOD	2.6	Below LOD	0.45
164B _A2_d	0.79	0.086	0.73	0.071	Below LOD	2.9	Below LOD	0.49
164B _A3_a	0.479	0.059	0.53	0.048	Below LOD	1.9	Below LOD	0.33
164B _A3_b	0.61	0.072	0.31	0.071	Below LOD	3.3	Below LOD	0.44
164B _A3_c	0.49	0.049	0.3	0.049	Below LOD	2.3	Below LOD	0.3
164B _A4_a	0.35	0.053	0.251	0.053	Below LOD	2.5	Below LOD	0.33
164B A4_b	0.177	0.075	0.284	0.053	Below LOD	2.1	Below LOD	0.29
164B _B1_a	0.42	0.28	0.48	0.2	Below LOD	7.7	Below LOD	1.1
164B B1_b	Below LOD	0.37	Below LOD	0.26	Below LOD	10	Below LOD	1.4
164B _B1_c	0.37	0.15	0.26	0.11	Below LOD	5.8	Below LOD	0.9
164B _B2_a	0.42	0.15	0.48	0.11	Below LOD	5.8	Below LOD	0.9
164B _B2_b	0.43	0.17	0.54	0.12	Below LOD	6.3	Below LOD	0.98
886B_F	0.13	0.012	0.153	0.01	100	0.42	2.9	0.051
886B_E	Below LOD	0.012	Below LOD	0.016	10.9	0.4	0.17	0.048
171B_C1_a	Below LOD	0.019	Below LOD	0.029	104.6	0.77	Below LOD	0.12
171B_C1_b	0.031	0.029	Below LOD	0.044	115	1.1	Below LOD	0.17
171B_C1_c	Below LOD	0.018	Below LOD	0.028	82.8	0.73	Below LOD	0.11
171B_C1_d	Below LOD	0.025	Below LOD	0.02	99	0.82	Below LOD	0.12
171B_C2_a	0.029	0.025	0.038	0.02	82	0.81	Below LOD	0.12
171B_C2_b	Below LOD	0.026	Below LOD	0.021	9.7	0.84	Below LOD	0.13
171B_C2_c	Below LOD	0.023	Below LOD	0.019	11.8	0.74	Below LOD	0.11
171B_C2_d	Below LOD	0.009	Below LOD	0.0089	83.8	0.51	Below LOD	0.066
171B_C2_e	0.023	0.01	Below LOD	0.01	52.7	0.57	Below LOD	0.075

171B_B1_a	Below LOD	0.0064	Below LOD	0.0063	10.6	0.36	Below LOD	0.047
171B_B1_b	0.0051	0.0048	0.0096	0.0047	4.02	0.27	Below LOD	0.035
171B_B2_a	Below LOD	0.013	Below LOD	0.0074	6.14	0.45	Below LOD	0.064
171B_B2_b	Below LOD	0.0089	Below LOD	0.0052	3.96	0.32	Below LOD	0.045
154_A1_a	0.031	0.012	0.065	NaN	77	0.48	Below LOD	0.071
154_A1_b	Below LOD	0.014	Below LOD	NaN	232	0.55	Below LOD	0.081
154_A2_a	Below LOD	0.034	Below LOD	0.034	4.1	0.99	Below LOD	0.15
154_A2_b	Below LOD	0.019	Below LOD	0.019	5.71	0.55	Below LOD	0.083
154_A2_c	Below LOD	0.028	Below LOD	0.028	4.29	0.82	Below LOD	0.13
154_B1_a	Below LOD	0.048	Below LOD	0.049	1.6	1.4	Below LOD	0.21
154_B1_b	Below LOD	0.046	Below LOD	0.047	3.6	1.4	Below LOD	0.2
154_B1_c	0.45	0.038	0.32	0.038	23.1	1.1	Below LOD	0.16
154_B1_d	Below LOD	0.046	Below LOD	0.046	14.6	1.4	Below LOD	0.19
154_B2_a	0.12	0.061	0.12	0.044	7.8	1.2	Below LOD	0.19
154_B2_b	0.091	0.053	0.13	0.038	8.7	1	Below LOD	0.16
154_B2_c	Below LOD	0.079	Below LOD	0.057	2.5	1.5	Below LOD	0.25
154_B3_a	Below LOD	0.022	Below LOD	0.032	1.42	1.1	Below LOD	0.16
154_B3_b	Below LOD	0.02	Below LOD	0.028	1.53	0.98	Below LOD	0.14
154_B3_c	0.032	0.019	Below LOD	0.028	3.35	0.97	Below LOD	0.14
154_B3_d	0.037	0.014	0.14	0.02	1.28	0.71	Below LOD	0.1
154_B4_a	Below LOD	0.013	Below LOD	0.018	2.58	0.64	Below LOD	0.099
154_B4_b	0.159	0.018	0.028	0.027	5.7	0.93	Below LOD	0.14
154_B4_c	0.15	0.014	0.26	0.02	3.89	0.7	Below LOD	0.11

154_B5_a	Below LOD	0.014	Below LOD	0.021	2.16	0.71	Below LOD	0.11
154_B5_b	Below LOD	0.017	Below LOD	0.025	1.48	0.87	Below LOD	0.14
154_B5_c	Below LOD	0.016	Below LOD	0.024	2.16	0.83	Below LOD	0.13
900_E1_a	Below LOD	0.059	Below LOD	0.062	4.9	2.9	Below LOD	0.56
900_E1_b	Below LOD	0.036	Below LOD	0.038	2.6	1.8	Below LOD	0.34
900_E1_c	Below LOD	0.028	Below LOD	0.029	3.5	1.4	Below LOD	0.26
900_E1_d	Below LOD	0.039	Below LOD	0.041	Below LOD	1.9	Below LOD	0.37
900_E1_e	Below LOD	0.03	Below LOD	0.031	4.6	1.4	Below LOD	0.28
900_E1_f	Below LOD	0.066	Below LOD	0.079	Below LOD	1.9	Below LOD	0.3
900_E1_g	Below LOD	0.076	Below LOD	0.092	Below LOD	2.2	Below LOD	0.35
900_E1_h	Below LOD	0.044	Below LOD	0.053	3.4	1.3	Below LOD	0.2
900_E2_a	Below LOD	0.043	Below LOD	0.052	3.21	1.2	Below LOD	0.2
900_E2_b	Below LOD	0.052	Below LOD	0.063	4.6	1.5	Below LOD	0.24
900_E2_c	Below LOD	0.12	Below LOD	0.051	3.2	2.5	Below LOD	0.35
900_E2_d	Below LOD	0.075	Below LOD	0.033	4.6	1.6	Below LOD	0.23
900_E2_e	Below LOD	0.11	Below LOD	0.05	6	2.4	Below LOD	0.35
900_F1_a	Below LOD	0.062	0.037	0.027	10.67	1.3	Below LOD	0.19
900_F1_b	0.48	0.076	0.48	NaN	8.4	2	Below LOD	0.31
900_F2_a	Below LOD	0.037	0.004	NaN	7.5	0.96	Below LOD	0.15
900_F2_b	Below LOD	0.034	0.02	NaN	10	0.89	Below LOD	0.14
900_F2_c	Below LOD	0.032	Below LOD	0.023	5.9	1.2	Below LOD	0.16
159_A1	1.28	0.061	1.28	0.045	3.4	2.4	Below LOD	0.32
159_A2	1.2	NaN	1.37	0.075	4.29	1.9	Below LOD	0.26

159_A3	1.8	0.063	1.69	NaN	4.38	2.1	Below LOD	0.29
159_B1	1.14	0.033	1.11	0.067	Below LOD	2	Below LOD	0.29
159_B2	1.5	0.051	1.57	NaN	Below LOD	2	Below LOD	0.29

Table F5. Concentrations of Pb and Bi in ppm in the samples under the standard NIST610

Comments	Pb ppm	Pb ppm LOD	Bi ppm	Bi ppm LOD
153_C	28	0.017	57	0.011
153_B1_a	118	0.029	50	0.017
153_B1_b	46	0.04	14.4	0.022
153_B2	0.48	0.026	0.044	0.014
3415A_A1_a	2.55	0.011	0.49	0.0079
3415A_A1_b	1.34	0.025	0.37	0.014
3415A_A2_a	0.82	0.022	0.282	0.013
3415A_A2_b	3.6	0.03	0.23	0.017
3415_A2_c	0.73	0.018	0.149	0.0075
3415A_A3_a	1.94	0.026	0.48	0.011
3415A_A3_b	2.23	0.027	0.52	0.012
3415A_A3_c	0.9	0.015	0.454	0.0081
3415A_D1	0.059	0.015	Below LOD	0.0081
3415A_D2	0.039	0.017	Below LOD	0.01
3415A_D2_b	0.038	0.019	Below LOD	0.012
152_A_a	9.1	0.024	3.93	0.013
152_A_b	18	0.03	9.3	0.017
152_G1_a	2.08	0.042	1.56	0.032
152_G1_b	1.19	0.027	0.911	0.021
152_G2_a	1.1	0.042	1.08	0.019
152_G2_b	4.63	0.035	5.73	0.016
152_G2_c	0.314	0.027	0.336	0.017
152_B1_1	10.02	0.025	5.83	0.016
152_B2_a	5.46	0.029	2.95	0.011
152_B2_b	63	0.023	9.1	0.0091
NB036_B1_a	0.063	0.021	0.023	0.0084
NB036_B1_b	1.04	0.023	2	0.0094

NB036_B1_c	0.27	0.021	0.3	0.0086
NB036_B1_d	0.082	0.017	0.071	0.0069
NB036_B1_f	17	0.012	11	0.006
NB036_B2_a	0.234	0.014	0.34	0.0066
NB036_B2_b	41	0.012	5.9	0.0079
NB036_A	62	0.0086	220	0.0058
173_B1_a	5.4	0.013	4.4	0.0072
173_B1_b	0.162	0.015	0.411	0.0088
173_B2_a	4.7	0.017	1.83	0.0072
173_B2_b	6.4	0.022	1.7	0.0093
173_A2	0.183	0.011	0.214	0.0063
173_A1_a	0.202	0.036	0.055	0.013
173_A1_b	0.192	0.029	0.028	0.01
173_A1_c	0.15	0.021	0.047	0.0075
899A_E1_a	0.039	0.019	Below LOD	0.0095
899A_E1_b	0.54	0.013	0.142	0.0064
899A_E2_a	Below LOD	0.043	Below LOD	0.035
899A_E2_b	0.102	0.047	0.04	0.038
899A_E2_c	0.2	0.013	0.057	0.0064
899A_F1	0.0311	0.011	0.0054	0.0052
899A_F2_a	0.0196	0.014	Below LOD	0.0061
899A_F2_b	0.0227	0.011	0.0098	0.0046
157_A1_a	2.66	0.053	13.9	0.021
157_A1_b	0.8	0.066	1.28	0.035
157_A2_a	3.3	0.071	5.2	0.037
157_A2_b	1.72	0.074	5.8	0.039
157_C1_a	2.99	0.02	23.4	0.012
157_C1_b	0.18	0.019	1.38	0.011
157_C2_a	7.3	0.046	38	0.019
157_C2_b	3.5	0.025	16.8	0.01
168A_D1_a	28	0.029	0.28	0.017
168A_D1_b	48	0.026	0.34	0.015
168A_D1_c	43	0.019	0.284	0.011
168A_D1_d	118	0.027	0.36	0.016
168A_D1_e	28	0.02	0.114	0.016
168A_D2_a	150	0.025	3.7	0.019
168A_D2_b	128	0.023	5.2	0.018
168A_D2_c	270	0.014	1.55	0.011
168A_D3_a	217	0.014	0.26	0.0057

168A_D3_b	151	0.016	10.8	0.0078
168A_C1_a	86	0.018	0.074	0.0087
168A_C1_b	6.4	0.02	0.144	0.0097
168A_C2_a	29.3	0.015	0.064	0.01
168A_C2_b	11.9	0.025	0.052	0.017
895B_F1_a	0.0303	0.011	Below LOD	0.0062
895B_F2_a	0.018	0.0096	0.0095	0.0052
895B_F2_b	0.015	0.012	Below LOD	0.0044
895B_E1_a	0.0192	0.0096	0.0044	0.0037
895B_E2_a	0.067	0.019	0.033	0.01
895B_E2_b	0.02	0.014	0.019	0.0073
895B_E2_c	0.0167	0.0087	Below LOD	0.0058
895B_E3	0.0194	0.0076	Below LOD	0.0051
897A_A1	7.10E+03	0.037	30	0.014
897A_A2	167	0.037	77	0.018
897A_A3	430	0.067	61	0.034
898A_A1	2.95	0.013	2.14	0.0073
898A_A2_a	3.3	0.0098	3.78	0.0048
898A_A2_b	3.59	0.016	1.82	0.0048
898A_B1_a	4.55	0.021	7.1	0.0066
898A_B1_b	3.83	0.028	18.1	0.0087
898A_B1_c	7.9	0.035	20.8	0.011
898A_B1_d	2.5	0.016	3.81	0.005
898A_B2_a	5.2	0.015	33	0.007
898A_B2_b	1.2	0.01	3.29	0.0036
164B_A1_a	3.54	0.14	3	0.084
164B _A1_b	1.73	0.17	0.84	0.1
164B _A1_c	4.1	0.12	1.53	0.071
164B _A1_d	7.1	0.22	6.9	0.057
164B _A1_e	17.6	0.18	2.65	0.046
164B _A2_a	2.54	0.14	0.86	0.037
164B _A2_b	4.13	0.18	0.36	0.047
164B _A2_c	5.07	0.1	4.6	0.056
164B _A2_d	2.88	0.11	1.57	0.06
164B _A3_a	1.86	0.076	0.59	0.041
164B _A3_b	1.85	0.12	0.88	0.069
164B A3_c	2.68	0.08	1.39	0.047
164B _A4_a	1.27	0.087	0.57	0.051

164B _A4_b	2.62	0.082	0.421	0.039
164B _B1_a	4.4	0.3	1.3	0.14
164B _B1_b	8.7	0.41	0.41	0.19
164B _B1_c	7.27	0.27	0.95	0.1
164B _B2_a	4.41	0.27	0.5	0.1
164B _B2_b	6.63	0.29	0.68	0.11
886B_F	37	0.013	0.68	0.011
886B_E	2.2	0.012	0.104	0.0045
171B_C1_a	0.19	0.037	0.07	0.014
171B_C1_b	0.265	0.055	0.79	0.021
171B_C1_c	0.149	0.035	0.042	0.014
171B_C1_d	0.169	0.033	0.033	0.017
171B_C2_a	1.2	0.033	2.1	0.017
171B_C2_b	0.169	0.034	0.165	0.018
171B_C2_c	0.161	0.03	0.214	0.015
171B_C2_d	0.081	0.018	0.151	0.012
171B_C2_e	0.08	0.021	0.052	0.014
171B_B1_a	0.039	0.013	0.081	0.0085
171B_B1_b	0.078	0.0097	0.102	0.0063
171B_B2_a	0.046	0.013	0.326	0.0076
171B_B2_b	0.034	0.0093	0.0601	0.0053
154_A1_a	1.26	0.017	2.23	0.012
154_A1_b	0.088	0.019	Below LOD	0.014
154_A2_a	0.129	0.04	Below LOD	0.026
154_A2_b	0.143	0.022	Below LOD	0.014
154_A2_c	0.065	0.033	Below LOD	0.022
154_B1_a	0.25	0.055	Below LOD	0.029
154_B1_b	0.17	0.052	0.12	0.028
154_B1_c	3.4	0.043	1.93	0.023
154_B1_d	0.72	0.052	0.28	0.027
154_B2_a	0.99	0.076	0.57	0.019
154_B2_b	1.89	0.065	0.83	0.016
154_B2_c	0.27	0.098	0.032	0.024
154_B3_a	0.22	0.053	0.063	0.02
154_B3_b	0.3	0.047	0.201	0.018
154_B3_c	0.065	0.046	0.035	0.017
154_B3_d	2.1	0.034	1.77	0.013

154_B4_a	0.137	0.027	0.0122	0.011
154_B4_b	2.8	0.039	1.36	0.015
154_B4_c	3.7	0.029	2.6	0.011
154_B5_a	0.12	0.03	0.032	0.012
154_B5_b	0.146	0.037	Below LOD	0.014
154_B5_c	0.068	0.035	Below LOD	0.014
900_E1_a	9.6	0.097	1.5	0.079
900_E1_b	Below LOD	0.059	Below LOD	0.048
900_E1_c	0.077	0.046	Below LOD	0.037
900_E1_d	Below LOD	0.064	Below LOD	0.052
900_E1_e	Below LOD	0.048	Below LOD	0.04
900_E1_f	Below LOD	4.8	Below LOD	0.065
900_E1_g	Below LOD	5.6	Below LOD	0.076
900_E1_h	Below LOD	3.2	Below LOD	0.044
900_E2_a	Below LOD	3.2	Below LOD	0.043
900_E2_b	Below LOD	3.8	Below LOD	0.052
900_E2_c	Below LOD	0.071	Below LOD	0.045
900_E2_d	0.135	0.046	Below LOD	0.029
900_E2_e	0.32	0.07	Below LOD	0.044
900_F1_a	0.168	0.038	Below LOD	0.024
900_F1_b	39	0.094	17.9	0.045
900_F2_a	0.107	0.045	Below LOD	0.022
900_F2_b	0.069	0.042	Below LOD	0.02
900_F2_c	1.34	0.05	1.6	0.018
159_A1	1.35	0.098	0.96	0.035
159_A2	4	0.072	4.6	0.03
159_A3	22	0.063	4.9	0.042

159_B1	3.6	0.064	1.94	0.024
159_B2	2.44	0.068	28	0.04

F.6 Concentrations of Co, As, Se 77 and Se 78 in ppm in the samples under the standard Mass 1

Sample	Co ppm	Co ppm LOD	As ppm	As ppm LOD	Se 77 ppm	Se 77 ppm LOD	Se 78 ppm	Se 78 ppm LOD
153_C	8900	0.018	1890	0.25	20.4	0.39	17.5	6
153_B1_a	46	0.022	54	0.4	4.4	0.58	8	8
153_B1_b	46	0.03	7	0.54	0.96	0.79	11	11
153_B2	12	0.027	3.09	0.3	11.1	0.42	9	5.4
3415A_A1_a	343	0.012	5.39	0.19	10.74	0.37	12	4.9
3415A_A1_b	643	0.035	7.28	0.28	11.42	0.44	14.2	5.1
3415A_A2_a	412	0.031	22.9	0.25	3.42	0.38	4.5	4.5
3415A_A2_b	140	0.043	4.61	0.34	8.7	0.53	10.3	6.2
3415_A2_c	353	0.019	1.48	0.18	11.12	0.35	10.3	3.8
3415A_A3_a	63	0.028	6.97	0.27	11.3	0.52	9.8	5.6
3415A_A3_b	144	0.029	4.04	0.29	8.15	0.54	6.9	5.9
3415A_A3_c	735	0.021	4.72	0.2	11.36	0.3	10.2	3.9
3415A_D1	127	0.021	3.42	0.2	4.44	0.3	6.8	3.9
3415A_D2	111	0.019	1.97	0.2	3.07	0.35	5.1	5.1
3415A_D2_b	50	0.021	7.55	0.23	15	0.4	13.7	5.8
152_Ghost1_a	246	0.023	8.92	0.3	18.2	0.46	11.9	5.8
152_Ghost1_b	106	0.03	12.7	0.39	18.7	0.59	19.9	7.5
152_G1_a	133	0.046	8.6	0.64	21.5	1.2	18.1	15
152_G1_b	251	0.031	19.6	0.43	16.75	0.82	19.5	10
152_G2_a	155.5	0.058	6.41	0.48	19.1	0.92	12	11
152_G2_b	370	0.048	6.79	0.4	14.5	0.77	12.9	8.9
152_G2_c	49.7	0.034	3.82	0.35	15.9	0.62	8.4	7.5
152_B1_1	109	0.031	12.5	0.32	22.1	0.57	14.3	6.9
152_B2_a	97	0.039	8.33	0.5	21.6	0.66	19.8	9.1
152_B2_b	246	0.031	17.9	0.41	21	0.53	21.6	7.3
NB036_B1_a	6280	0.018	60	0.29	18.8	0.35	18.9	6.4
NB036_B1_b	550	0.02	8.3	0.32	32.2	0.39	27.5	7.1
NB036_B1_c	668	0.018	8.3	0.3	34.2	0.36	32.3	6.6
NB036_B1_d	800	0.015	12.2	0.24	29.9	0.29	29.6	5.3

NB036_B1_f	2430	0.016	9.4	0.18	41.9	0.24	44.5	4.5
NB036_B2_a	1030	0.018	8.6	0.2	26.3	0.27	27	5
NB036_B2_b	2100	0.019	13.2	0.26	24.7	0.45	25.7	5.6
NB036_A	20350	0.014	4680	0.2	27.6	0.33	28.5	4.1
173_B1_a	2710	0.019	8.4	0.2	7.79	0.3	7.2	4.8
173_B1_b	90	0.023	1.66	0.24	6.49	0.36	12.7	5.9
173_B2_a	2170	0.015	3.7	0.24	7.46	0.38	6.2	5.9
173_B2_b	458	0.019	7.9	0.31	10.8	0.49	14	7.6
173_A2	1110	0.018	1.76	0.21	6.46	0.28	6.9	4.2
173_A1_a	77	0.038	2.04	0.48	5.5	0.62	Below LOD	12
173_A1_b	125	0.03	1.5	0.38	4.87	0.49	Below LOD	9.5
173_A1_c	859	0.022	1.31	0.27	5.41	0.36	7.4	6.9
899A_E1_a	340	0.017	317	0.3	5.9	0.45	8.6	8.5
899A_E1_b	290	0.011	232	0.2	10.9	0.3	9.8	5.8
899A_E2_a	107	0.027	117	0.21	7.25	0.29	Below LOD	4.9
899A_E2_b	310	0.03	316	0.23	7.7	0.31	6	5.4
899A_E2_c	99	0.019	322	0.21	8.2	0.34	5.1	4.8
899A_F1	278	0.015	257.9	0.17	7.18	0.28	6.9	3.9
899A_F2_a	204	0.021	278	0.23	6.79	0.4	9.3	5.5
899A_F2_b	338	0.02	165.7	0.23	7.54	0.29	7.5	5.2
157_A1_a	237	0.09	22.9	1	7.5	1.3	Below LOD	24
157_A1_b	1910	0.11	22.7	1.3	13.8	1.7	Below LOD	30
157_A2_a	1680	0.12	25.9	1.4	16.6	1.8	Below LOD	32
157_A2_b	1260	0.12	20.5	1.4	7.7	1.9	Below LOD	33
157_C1_a	228	0.034	23.9	0.26	14.2	0.51	10.8	7.3
157_C1_b	6.39	0.032	0.83	0.25	5.91	0.47	Below LOD	6.8
157_C2_a	80	0.039	9	0.75	10.6	0.85	Below LOD	13
157_C2_b	127	0.021	11.4	0.4	17.3	0.45	18.2	6.8
168A_D1_a	0.52	0.032	0.93	0.41	8.1	0.67	Below LOD	8.6
168A_D1_b	0.057	0.028	0.72	0.36	7.9	0.58	10.2	7.5
168A_D1_c	3.14	0.021	0.74	0.27	24.6	0.44	25.1	5.6
168A_D1_d	0.27	0.03	0.47	0.38	22.7	0.62	24.5	7.9
168A_D1_e	0.22	0.018	0.8	0.31	11.7	0.65	10.4	8.1

168A_D2_a	8.7	0.022	1.74	0.38	15.3	0.79	19	9.9
168A_D2_b	0.072	0.02	1.42	0.36	33.5	0.75	31.7	9.3
168A_D2_c	0.073	0.012	1.25	0.22	21.69	0.45	21.6	5.6
168A_D3_a	0.344	0.0099	0.98	0.18	15.9	0.26	15.3	5.3
168A_D3_b	4	0.011	1.6	0.21	22.2	0.28	20.3	5.3
168A_C1_a	1.66	0.012	0.35	0.24	29.7	0.31	30	5.9
168A_C1_b	7.2	0.014	Below LOD	0.27	38.2	0.34	38.2	6.5
168A_C2_a	2.6	0.018	0.37	0.28	31.7	0.41	32.3	6.6
168A_C2_b	1.17	0.028	1.64	0.46	17.5	0.66	21.9	11
895B_F1_a	464	0.011	1.4	0.18	4.56	0.28	Below LOD	4.7
895B_F2_a	867	0.0068	1.26	0.17	4.16	0.27	6.7	4.6
895B_F2_b	447	0.013	1.08	0.2	3.91	0.31	4.5	4.5
895B_E1_a	441	0.011	0.753	0.17	4.27	0.25	4.4	3.7
895B_E2_a	389	0.025	0.63	0.32	4.61	0.49	Below LOD	6.8
895B_E2_b	559	0.018	0.84	0.23	4.19	0.36	Below LOD	4.9
895B_E2_c	386	0.01	0.9	0.16	4.27	0.23	5.3	4.1
895B_E3	366.5	0.0091	0.718	0.14	4.02	0.2	4.8	3.6
897A_A1	3.18E+04	0.023	31.5	0.47	49.4	0.7	43.6	11
897A_A2	2900	0.032	44	0.42	38.9	0.94	29.5	15
897A_A3	4.50E+03	0.056	185	0.88	75.6	1.6	73	21
898A_A1	192	0.011	367	0.18	20.71	0.36	16.6	5.2
898A_A2_a	160	0.01	178	0.22	20	0.28	19.4	4.8
898A_A2_b	124	0.012	423	0.18	21.3	0.33	20.2	4.9
898A_B1_a	359	0.016	630	0.24	23.1	0.46	22.5	6.8
898A_B1_b	189	0.021	135	0.32	26.2	0.61	25.6	9
898A_B1_c	86	0.027	580	0.4	22.3	0.76	22.1	11
898A_B1_d	96	0.012	252	0.19	21.9	0.35	22	5.2
898A_B2_a	174	0.014	566	0.21	22.3	0.33	21.7	5.8
898A_B2_b	63.8	0.0088	223	0.15	23.7	0.33	22.2	4.8
164B_A1_a	528	0.23	2.6	2.5	27.6	3.3	Below LOD	68
164B _A1_b	698	0.27	Below LOD	3	30	3.9	Below LOD	81

164B _A1_c	659	0.19	Below LOD	2.1	27.5	2.8	Below LOD	58
164B A1_d	670	0.29	Below LOD	3	26.5	4.3	Below LOD	83
164B _A1_e	664	0.23	Below LOD	2.4	24.8	3.4	Below LOD	67
164B _A2_a	697	0.19	Below LOD	1.9	26.9	2.8	Below LOD	54
164B _A2_b	709	0.24	Below LOD	2.4	26.6	3.5	Below LOD	68
164B _A2_c	511	0.058	Below LOD	1.8	26.1	2.7	Below LOD	54
164B _A2_d	683	0.062	Below LOD	1.9	29.2	2.9	Below LOD	59
164B _A3_a	868	0.042	Below LOD	1.3	26	2	Below LOD	40
164B _A3_b	704	0.27	Below LOD	2.2	20.7	3.1	Below LOD	54
164B _A3_c	849	0.18	Below LOD	1.5	24.3	2.1	Below LOD	37
164B _A4_a	690	0.2	Below LOD	1.6	24.1	2.3	Below LOD	40
164B _A4_b	873	0.092	Below LOD	1.4	26.4	2.4	Below LOD	45
164B _B1_a	1066	0.34	Below LOD	4.9	28.7	9	Below LOD	170
164B B1_b	1077	0.45	Below LOD	6.6	39	12	Below LOD	230
164B _B1_c	1161	0.39	Below LOD	3.7	35	8	Below LOD	120
164B _B2_a	1100	0.39	Below LOD	3.7	35.3	8	Below LOD	120
164B _B2_b	1139	0.42	Below LOD	4	34.1	8.7	Below LOD	130
886B_F	680	0.039	67	0.27	10.1	0.36	9.5	8.2
886B_E	88	0.021	7.38	0.25	4.64	0.33	Below LOD	7.2
171B_C1_a	1640	0.05	70.9	0.48	4.48	0.82	Below LOD	16
171B_C1_b	1090	0.074	78.1	0.7	7.1	1.2	Below LOD	24
171B_C1_c	645	0.048	56.2	0.45	6.96	0.78	Below LOD	15
171B_C1_d	751	0.041	67.2	0.51	8.9	0.77	Below LOD	17

171B_C2_a	4190	0.041	56	0.5	15	0.77	18	16
171B_C2_b	3520	0.042	6.63	0.52	16.5	0.8	Below LOD	17
171B_C2_c	4910	0.037	8.1	0.46	18.2	0.7	Below LOD	15
171B_C2_d	957	0.038	57	0.31	5.8	0.53	Below LOD	10
171B_C2_e	820	0.043	35.9	0.35	7.8	0.6	Below LOD	12
171B_B1_a	151	0.027	7.25	0.22	10.9	0.38	8.5	7.3
171B_B1_b	315	0.02	2.74	0.16	8.91	0.28	9.7	5.4
171B_B2_a	41.2	0.017	4.21	0.28	15.8	0.41	13.5	8.1
171B_B2_b	444	0.012	2.72	0.19	14.9	0.29	17.1	5.7
154_A1_a	29.3	0.028	54	0.3	12.1	0.52	13.6	8.3
154_A1_b	102	0.031	161	0.34	11.1	0.59	9.6	9.4
154_A2_a	168	0.056	2.85	0.62	18.5	0.85	Below LOD	21
154_A2_b	0.41	0.031	4.01	0.34	9.8	0.47	Below LOD	12
154_A2_c	3	0.046	3.02	0.51	10.9	0.7	20.8	17
154_B1_a	53	0.1	1.12	0.9	3.5	1.3	Below LOD	30
154_B1_b	25.2	0.096	2.6	0.86	4.7	1.3	Below LOD	28
154_B1_c	3.5	0.078	16.3	0.7	19.5	1	Below LOD	23
154_B1_d	18	0.095	10.3	0.85	17.8	1.3	33	28
154_B2_a	412	0.089	5.5	0.74	5.9	1.4	Below LOD	26
154_B2_b	830	0.076	6.2	0.63	14	1.2	Below LOD	22
154_B2_c	99	0.11	1.77	0.95	7.4	1.9	Below LOD	33
154_B3_a	45.4	0.048	1.02	0.71	5.2	1.3	Below LOD	27
154_B3_b	162	0.042	1.09	0.62	4.7	1.1	Below LOD	24
154_B3_c	49	0.042	2.4	0.61	4.7	1.1	Below LOD	24
154_B3_d	145	0.03	0.92	0.45	3.26	0.82	Below LOD	17
154_B4_a	110	0.052	1.86	0.41	5.16	0.61	Below LOD	11
154_B4_b	26.7	0.075	4.12	0.6	13	0.89	Below LOD	16

154_B4_c	127	0.056	2.81	0.45	5.9	0.67	Below LOD	12
154_B5_a	43.1	0.057	1.56	0.46	6.9	0.68	Below LOD	12
154_B5_b	87	0.07	1.08	0.57	3.5	0.84	Below LOD	15
154_B5_c	112	0.066	1.57	0.54	5.6	0.79	Below LOD	15
900_E1_a	346	0.23	3.7	2.4	39	3.4	Below LOD	64
900_E1_b	134	0.14	1.9	1.5	8.2	2.1	Below LOD	39
900_E1_c	98	0.11	2.63	1.1	5.4	1.6	Below LOD	30
900_E1_d	60	0.16	Below LOD	1.6	7.6	2.2	Below LOD	42
900_E1_e	84	0.12	3.41	1.2	3	1.7	Below LOD	32
900_E1_f	78	0.14	Below LOD	1.6	2.7	2.2	Below LOD	48
900_E1_g	55.4	0.16	Below LOD	1.8	5.8	2.6	Below LOD	56
900_E1_h	61.8	0.094	2.55	1.1	4.7	1.5	Below LOD	32
900_E2_a	121	0.095	2.39	1	6.3	1.5	Below LOD	31
900_E2_b	91	0.12	3.4	1.3	4.1	1.8	Below LOD	38
900_E2_c	151	0.23	2.4	2	6	2.9	Below LOD	55
900_E2_d	149	0.15	3.41	1.3	5.2	1.9	Below LOD	36
900_E2_e	511	0.23	4.5	2	10.8	2.8	Below LOD	55
900_F1_a	3190	0.13	7.95	1.1	4.55	1.5	Below LOD	29
900_F1_b	2130	0.12	6.2	1.6	5.4	2.4	Below LOD	44
900_F2_a	1500	0.057	5.59	0.76	2.8	1.1	Below LOD	21
900_F2_b	6.20E+03	0.053	7.47	0.7	4.4	1	Below LOD	19
900_F2_c	400	0.08	4.4	0.97	3.7	1.7	Below LOD	24
159_A1	48.7	0.16	2.54	1.9	29.4	3.3	Below LOD	46

159_A2	58.8	0.16	3.21	1.4	28	2.7	Below LOD	38
159_A3	142	0.16	3.29	1.5	28.3	2.5	Below LOD	38
159_B1	57.3	0.18	Below LOD	1.5	26.7	2.2	43	34
159_B2	58.1	0.14	Below LOD	1.4	27.2	1.8	Below LOD	34

F.7 Concentrations of Ag 107, Ag 108, Sb and Bi in ppm in the samples under the standard Mass 1.

Comments	Ag 107 ppm	Ag 107 ppm	Ag 108 ppm LOD	Ag 108 ppm LOD	Sb ppm	Sb ppm LOD	Bi ppm	Bi ppm LOD
153_C	3.4	0.011	3.4	0.014	0.169	0.038	4.1	0.0008
153_B1_a	2.63	0.03	2.73	0.023	2.09	0.056	3.55	0.0012
153_B1_b	0.99	0.041	1.11	0.03	0.6	0.075	1.03	0.0016
153_B2	0.045	0.025	0.045	0.02	0.042	0.042	0.0031	0.00096
3415A_A1_a	0.218	0.012	0.223	0.0089	0.037	0.037	0.035	0.00056
3415A_A1_b	0.8	0.028	1.16	0.028	0.039	0.039	0.0266	0.001
3415A_A2_a	0.153	0.025	0.234	0.025	0.034	0.034	0.0203	0.00089
3415A_A2_b	0.052	0.034	0.048	0.034	0.047	0.047	0.0166	0.0012
3415_A2_c	0.0287	0.014	0.0259	0.016	0.025	0.025	0.0107	0.00053
3415A_A3_a	0.22	0.021	0.28	0.024	0.038	0.038	0.035	0.00079
3415A_A3_b	0.71	0.021	0.5	0.025	0.039	0.039	0.0376	0.00083
3415A_A3_c	0.238	0.012	0.243	0.016	0.034	0.034	0.0329	0.00058
3415A_D1	0.012	0.012	0.016	0.016	0.034	0.034	Below LOD	0.00058
3415A_D2	0.018	0.018	0.018	0.018	0.031	0.031	Below LOD	0.00073
3415A_D2_b	0.021	0.021	0.02	0.02	0.036	0.036	Below LOD	0.00083

152_A_a	0.52	0.017	0.46	0.021	0.064	0.039	0.288	0.00094
152_A_b	0.87	0.022	0.86	0.026	0.123	0.051	0.68	0.0012
152_G1_a	0.28	0.049	0.222	0.038	Below LOD	0.096	0.115	0.0023
152_G1_b	0.109	0.032	0.098	0.025	Below LOD	0.064	0.0673	0.0015
152_G2_a	0.145	0.04	0.111	0.025	Below LOD	0.076	0.08	0.0014
152_G2_b	1.5	0.033	0.82	0.021	Below LOD	0.063	0.425	0.0012
152_G2_c	0.049	0.026	0.035	0.024	Below LOD	0.047	0.0249	0.0013
152_B1_1	0.479	0.024	0.493	0.022	0.048	0.044	0.434	0.0012
152_B2_a	0.21	0.024	0.184	0.025	Below LOD	0.059	0.22	0.00083
152_B2_b	2.9	0.019	2.4	0.02	0.061	0.048	0.68	0.00067
NB036_B1_a	Below LOD	0.012	Below LOD	0.015	Below LOD	0.039	0.0018	0.00068
NB036_B1_b	0.16	0.014	0.121	0.017	Below LOD	0.044	0.16	0.00076
NB036_B1_c	0.016	0.012	0.022	0.015	Below LOD	0.04	0.024	0.0007
NB036_B1_d	Below LOD	0.01	Below LOD	0.012	Below LOD	0.032	0.0057	0.00057
NB036_B1_f	3.1	0.015	4.5	0.0085	Below LOD	0.029	0.88	0.00049
NB036_B2_a	Below LOD	0.017	0.019	0.0094	Below LOD	0.032	0.027	0.00055
NB036_B2_b	0.83	0.013	0.91	0.015	Below LOD	0.026	0.47	0.00066
NB036_A	62	0.0098	49	0.011	Below LOD	0.019	17	0.00049
173_B1_a	0.27	0.014	0.3	0.0088	0.032	0.03	0.35	0.00063
173_B1_b	Below LOD	0.017	Below LOD	0.011	Below LOD	0.037	0.0326	0.00077
173_B2_a	0.084	0.011	0.09	0.011	Below LOD	0.037	0.145	0.00064
173_B2_b	0.067	0.014	0.104	0.014	Below LOD	0.048	0.135	0.00083
173_A2	Below LOD	0.012	Below LOD	0.0088	Below LOD	0.023	0.0169	0.00057

173_A1_a	Below LOD	0.023	Below LOD	0.026	Below LOD	0.055	0.0043	0.0012
173_A1_b	Below LOD	0.018	Below LOD	0.021	Below LOD	0.044	0.0022	0.00096
173_A1_c	Below LOD	0.013	Below LOD	0.015	Below LOD	0.031	0.0037	0.00069
899A_E1_a	Below LOD	0.019	Below LOD	0.016	Below LOD	0.041	Below LOD	0.00089
899A_E1_b	Below LOD	0.013	Below LOD	0.011	Below LOD	0.028	0.0112	0.0006
899A_E2_a	Below LOD	0.01	Below LOD	0.0096	Below LOD	0.028	Below LOD	0.0033
899A_E2_b	Below LOD	0.011	Below LOD	0.011	Below LOD	0.031	Below LOD	0.0036
899A_E2_c	Below LOD	0.0087	Below LOD	0.01	Below LOD	0.024	0.0045	0.00061
899A_F1	Below LOD	0.0071	Below LOD	0.0084	Below LOD	0.02	Below LOD	0.0005
899A_F2_a	Below LOD	0.013	Below LOD	0.0097	Below LOD	0.028	Below LOD	0.00058
899A_F2_b	Below LOD	0.012	Below LOD	0.0072	Below LOD	0.024	0.00077	0.00043
157_A1_a	0.95	0.054	1.05	0.033	Below LOD	0.11	1.09	0.002
157_A1_b	0.18	0.06	0.22	0.066	Below LOD	0.15	0.1	0.0032
157_A2_a	1.34	0.064	1.9	0.071	Below LOD	0.16	0.41	0.0034
157_A2_b	0.21	0.066	0.26	0.074	Below LOD	0.17	0.45	0.0036
157_C1_a	2.25	0.017	2.24	0.019	Below LOD	0.039	1.83	0.0011
157_C1_b	0.033	0.015	Below LOD	0.018	Below LOD	0.036	0.108	0.001
157_C2_a	5.2	0.024	5	0.025	Below LOD	0.08	2.9	0.0016
157_C2_b	0.77	0.013	0.67	0.014	0.049	0.043	1.31	0.00087
168A_D1_a	0.073	0.0084	0.075	0.015	0.68	0.061	0.019	0.0012
168A_D1_b	0.18	0.0073	0.129	0.013	1.08	0.054	0.023	0.001
168A_D1_c	0.143	0.0055	0.139	0.0097	1.59	0.04	0.0192	0.00077
168A_D1_d	0.279	0.0078	0.261	0.014	5.2	0.057	0.0242	0.0011

168A_D1_e	0.059	0.012	0.046	0.01	0.94	0.046	0.0077	0.001
168A_D2_a	0.418	0.014	0.42	0.012	6.5	0.057	0.25	0.0013
168A_D2_b	0.158	0.014	0.178	0.012	3.9	0.054	0.36	0.0012
168A_D2_c	0.391	0.0082	0.376	0.0071	10.8	0.033	0.106	0.00074
168A_D3_a	0.302	0.0061	0.313	0.0086	8.7	0.025	0.018	0.00038
168A_D3_b	0.265	0.0066	0.241	0.006	3.22	0.035	0.74	0.00052
168A_C1_a	0.23	0.0073	0.229	0.0066	3.96	0.039	0.005	0.00058
168A_C1_b	0.088	0.0082	0.103	0.0074	0.49	0.044	0.0099	0.00065
168A_C2_a	0.185	0.01	0.177	0.007	1.26	0.033	0.0044	0.0007
168A_C2_b	0.434	0.016	0.527	0.011	0.39	0.054	0.0036	0.0011
895B_F1_a	Below LOD	0.0058	Below LOD	0.008	Below LOD	0.025	Below LOD	0.00041
895B_F2_a	0.004	NaN	Below LOD	0.0066	Below LOD	0.024	0.00065	0.00035
895B_F2_b	Below LOD	0.0063	0.0052	0.0048	Below LOD	0.027	Below LOD	0.00029
895B_E1_a	Below LOD	0.0053	Below LOD	0.004	Below LOD	0.023	0.00031	0.00025
895B_E2_a	Below LOD	0.0087	Below LOD	0.0065	Below LOD	0.044	0.0023	0.00068
895B_E2_b	Below LOD	0.0063	Below LOD	0.0047	Below LOD	0.032	0.00132	0.0005
895B_E2_c	Below LOD	0.0054	Below LOD	0.0035	Below LOD	0.022	Below LOD	0.00039
895B_E3	Below LOD	0.0047	Below LOD	0.0031	Below LOD	0.02	Below LOD	0.00034
897A_A1	57	0.016	75	0.012	0.77	0.062	2.11	0.00098
897A_A2	4.7	0.0078	4.4	0.02	3.4	0.075	5.5	0.0012
897A_A3	17.6	0.029	16.5	0.026	1.94	0.11	4.31	0.0023
898A_A1	0.0078	0.0045	0.0101	0.0073	0.056	0.032	0.152	0.0005
898A_A2_a	0.053	0.0055	0.067	0.0047	0.059	0.031	0.269	0.00033
898A_A2_b	0.0164	0.0055	0.0143	0.0033	0.082	0.028	0.13	0.00033
898A_B1_a	0.048	0.0075	0.072	0.0046	0.127	0.039	0.5	0.00045

898A_B1_b	0.75	0.01	0.82	0.0061	Below LOD	0.051	1.29	0.0006
898A_B1_c	0.211	0.012	0.27	0.0076	Below LOD	0.064	1.49	0.00075
898A_B1_d	0.119	0.0058	0.12	0.0035	0.039	0.03	0.272	0.00035
898A_B2_a	0.47	0.005	0.59	0.008	0.035	0.031	2.4	0.00048
898A_B2_b	0.0289	0.0028	0.0208	NaN	Below LOD	0.026	0.236	0.00025
164B_A1_a	0.64	0.066	0.72	NaN	Below LOD	0.32	0.23	0.0066
164B _A1_b	0.49	0.079	0.41	NaN	Below LOD	0.38	0.063	0.0078
164B _A1_c	8	0.056	4.6	NaN	Below LOD	0.27	0.115	0.0056
164B _A1_d	1.35	NaN	0.96	0.12	Below LOD	0.47	0.52	0.0045
164B _A1_e	0.48	NaN	0.43	0.1	Below LOD	0.38	0.199	0.0036
164B _A2_a	0.5	NaN	0.52	0.08	Below LOD	0.31	0.065	0.0029
164B _A2_b	0.38	NaN	0.41	0.1	Below LOD	0.39	0.027	0.0037
164B _A2_c	1.05	0.064	0.88	0.054	Below LOD	0.29	0.34	0.0044
164B _A2_d	0.61	0.069	0.56	0.058	Below LOD	0.31	0.118	0.0048
164B _A3_a	0.371	0.047	0.408	0.039	Below LOD	0.21	0.044	0.0032
164B _A3_b	0.47	0.057	0.24	0.058	Below LOD	0.28	0.067	0.0054
164B _A3_c	0.38	0.039	0.227	0.04	Below LOD	0.19	0.105	0.0037
164B _A4_a	0.27	0.042	0.192	0.043	Below LOD	0.21	0.0426	0.004
164B_A4_b	0.137	0.06	0.218	0.043	Below LOD	0.19	0.0317	0.003
164B _B1_a	0.33	0.22	0.37	0.16	Below LOD	0.69	0.098	0.011
164B _B1_b	Below LOD	0.29	Below LOD	0.21	Below LOD	0.93	0.031	0.015
164B _B1_c	0.29	0.12	0.203	0.087	Below LOD	0.58	0.072	0.0082
164B _B2_a	0.33	0.12	0.37	0.087	Below LOD	0.58	0.038	0.0082

164B _B2_b	0.34	0.13	0.41	0.094	Below LOD	0.63	0.051	0.0089
886B_F	0.101	0.0098	0.117	0.008	1.9	0.033	0.051	0.00084
886B_E	Below LOD	0.0095	Below LOD	0.012	0.111	0.031	0.0078	0.00035
171B_C1_a	Below LOD	0.015	Below LOD	0.023	Below LOD	0.076	0.0053	0.0011
171B_C1_b	0.024	0.022	Below LOD	0.034	Below LOD	0.11	0.059	0.0017
171B_C1_c	Below LOD	0.015	Below LOD	0.022	Below LOD	0.073	0.0032	0.0011
171B_C1_d	Below LOD	0.02	Below LOD	0.016	Below LOD	0.079	0.0025	0.0013
171B_C2_a	0.023	0.02	0.029	0.016	Below LOD	0.079	0.16	0.0013
171B_C2_b	Below LOD	0.02	Below LOD	0.016	Below LOD	0.082	0.0125	0.0014
171B_C2_c	Below LOD	0.018	Below LOD	0.014	Below LOD	0.072	0.0162	0.0012
171B_C2_d	Below LOD	0.0071	Below LOD	0.0069	Below LOD	0.043	0.0115	0.00093
171B_C2_e	0.018	0.008	Below LOD	0.0078	Below LOD	0.049	0.0039	0.001
171B_B1_a	Below LOD	0.005	Below LOD	0.0049	Below LOD	0.03	0.0062	0.00066
171B_B1_b	0.0039	0.0037	0.0073	0.0037	Below LOD	0.023	0.0078	0.00049
171B_B2_a	Below LOD	0.0099	Below LOD	0.0057	Below LOD	0.041	0.0248	0.00058
171B_B2_b	Below LOD	0.007	Below LOD	0.004	Below LOD	0.029	0.00457	0.00041
154_A1_a	0.024	0.0093	0.05	NaN	Below LOD	0.046	0.17	0.00095
154_A1_b	Below LOD	0.011	Below LOD	NaN	Below LOD	0.052	Below LOD	0.0011
154_A2_a	Below LOD	0.026	Below LOD	0.025	Below LOD	0.097	Below LOD	0.002
154_A2_b	Below LOD	0.014	Below LOD	0.014	Below LOD	0.054	Below LOD	0.0011
154_A2_c	Below LOD	0.021	Below LOD	0.021	Below LOD	0.081	Below LOD	0.0016
154_B1_a	Below LOD	0.037	Below LOD	0.036	Below LOD	0.13	Below LOD	0.0022
154_B1_b	Below LOD	0.035	Below LOD	0.035	Below LOD	0.13	0.0091	0.0021

154_B1_c	0.35	0.029	0.25	0.028	Below LOD	0.1	0.148	0.0017
154_B1_d	Below LOD	0.035	Below LOD	0.034	Below LOD	0.13	0.022	0.0021
154_B2_a	0.093	0.047	0.091	0.032	Below LOD	0.12	0.044	0.0014
154_B2_b	0.071	0.04	0.102	0.028	Below LOD	0.11	0.063	0.0012
154_B2_c	Below LOD	0.06	Below LOD	0.042	Below LOD	0.16	0.0025	0.0018
154_B3_a	Below LOD	0.017	Below LOD	0.023	Below LOD	0.1	0.0049	0.0015
154_B3_b	Below LOD	0.015	Below LOD	0.021	Below LOD	0.091	0.0154	0.0013
154_B3_c	0.025	0.015	Below LOD	0.02	Below LOD	0.09	0.0027	0.0013
154_B3_d	0.029	0.011	0.11	0.015	Below LOD	0.066	0.135	0.00095
154_B4_a	Below LOD	0.0096	Below LOD	0.013	Below LOD	0.064	0.00094	0.00078
154_B4_b	0.123	0.014	0.022	0.019	Below LOD	0.092	0.104	0.0011
154_B4_c	0.116	0.01	0.2	0.015	Below LOD	0.069	0.197	0.00085
154_B5_a	Below LOD	0.011	Below LOD	0.015	Below LOD	0.07	0.0025	0.00087
154_B5_b	Below LOD	0.013	Below LOD	0.018	Below LOD	0.087	Below LOD	0.0011
154_B5_c	Below LOD	0.012	Below LOD	0.017	Below LOD	0.082	Below LOD	0.001
900_E1_a	Below LOD	0.05	Below LOD	0.051	Below LOD	0.41	0.114	0.007
900_E1_b	Below LOD	0.031	Below LOD	0.031	Below LOD	0.25	Below LOD	0.0043
900_E1_c	Below LOD	0.024	Below LOD	0.024	Below LOD	0.2	Below LOD	0.0033
900_E1_d	Below LOD	0.033	Below LOD	0.034	Below LOD	0.27	Below LOD	0.0046
900_E1_e	Below LOD	0.025	Below LOD	0.026	Below LOD	0.21	Below LOD	0.0035
900_E1_f	Below LOD	0.056	Below LOD	0.065	Below LOD	0.22	Below LOD	0.0058
900_E1_g	Below LOD	0.065	Below LOD	0.076	Below LOD	0.26	Below LOD	0.0067
900_E1_h	Below LOD	0.037	Below LOD	0.043	Below LOD	0.15	Below LOD	0.0038

900_E2_a	Below LOD	0.036	Below LOD	0.042	Below LOD	0.15	Below LOD	0.0038
900_E2_b	Below LOD	0.044	Below LOD	0.051	Below LOD	0.18	Below LOD	0.0046
900_E2_c	Below LOD	0.097	Below LOD	0.041	Below LOD	0.26	Below LOD	0.0039
900_E2_d	Below LOD	0.063	Below LOD	0.027	Below LOD	0.17	Below LOD	0.0026
900_E2_e	Below LOD	0.096	Below LOD	0.041	Below LOD	0.26	Below LOD	0.0039
900_F1_a	Below LOD	0.052	0.029	0.022	Below LOD	0.14	Below LOD	0.0021
900_F1_b	0.39	0.064	0.38	NaN	Below LOD	0.22	1.41	0.0039
900_F2_a	Below LOD	0.03	0.002 8	NaN	Below LOD	0.11	Below LOD	0.0019
900_F2_b	Below LOD	0.028	0.016	NaN	Below LOD	0.097	Below LOD	0.0017
900_F2_c	Below LOD	0.026	Below LOD	0.018	Below LOD	0.12	0.13	0.0015
159_A1	1.05	0.05	1.03	0.035	Below LOD	0.22	0.076	0.0029
159_A2	0.98	NaN	1.11	0.058	Below LOD	0.18	0.36	0.0025
159_A3	1.48	0.051	1.36	NaN	Below LOD	0.19	0.39	0.0035
159_B1	0.94	0.027	0.9	0.051	Below LOD	0.19	0.155	0.0019
159_B2	1.24	0.041	1.28	NaN	Below LOD	0.19	2.2	0.0032

Appendix H: Pyrite Saturation Calculation

H.1 Convert formula for Reich et al. (2005) from mole percent to ppm

C_{As}	C_{Au} (C_{Au} = 0.02*C_{As} + 4x10^{-5})	C_{Fe}	C_S	wt (g) As (C_{As} x molecular weight $As_)$	wt (g) Au (C_{Au} x molecular weight $Au_)$	wt (g) Fe (C_{Fe} x molecular weight $Fe_)$	wt (g) S (C_S x molecular weight $S_)$	ppm As (Wt_{As}/ (Wt_{As} + Wt_{Au} + Wt_{Fe} + Wt_S))*100*10000	ppm Au (Wt_{Au}/ (Wt_{As} + Wt_{Au} + Wt_{Fe} + Wt_S))*100*10000
1.00E-07	0.000040002	33.33	66.667	7.49216E-06	0.007879	1861.31385	2137.744	0.001873	1.97E+00
1.00E-06	0.00004002	33.33	66.667	7.49216E-05	0.007883	1861.31385	2137.744	0.018735	1.97E+00
0.0000005	0.00004001	33.33	66.667	3.74608E-05	0.007881	1861.31385	2137.744	0.009367	1.97E+00
0.000005	0.0000401	33.33	66.667	0.000374608	0.007898	1861.31385	2137.7439	0.093674	1.98E+00
0.00001	0.0000402	33.33	66.667	0.000749216	0.007918	1861.31385	2137.7437	0.187348	1.98E+00
0.00001	0.0000402	33.33	66.667	0.000749216	0.007918	1861.31385	2137.7437	0.187348	1.98E+00
0.00005	0.000041	33.33	66.667	0.00374608	0.008076	1861.31385	2137.7424	0.936738	2.02E+00
0.0001	0.000042	33.33	66.667	0.00749216	0.008273	1861.31385	2137.7408	1.873475	2.07E+00
0.001	0.00006	33.33	66.666	0.0749216	0.011818	1861.31385	2137.712	18.73456	2.96E+00
0.01	0.00024	33.33	66.657	0.749216	0.047272	1861.31385	2137.4234	187.3258	1.18E+01
0.1	0.00204	33.33	66.567	7.49216	0.401812	1861.31385	2134.5374	1871.288	1.00E+02
1	0.02004	33.33	65.667	74.9216	3.94721	1861.31385	2105.678	18518.09	9.76E+02
10	0.20004	33.33	56.667	749.216	39.40119	1861.31385	1817.084	167721.8	8.82E+03

33	0.66004	33.33	33.667	2472.4128	130.0058	1861.31385	1079.566	446018.3	2.35E+04

H.2 Convert formula for Dedithius et al. (2014) from mole percent to ppm

C_{As}	C_{Au} (C_{Au} = 0.004*C_{As} + 2x10^{-7})	C_{Fe}	C_S	wt (g) As (C_{As} x molecular weight As)	wt (g) Au (C_{Au} x molecular weight Au)	wt (g) Fe (C_{Fe} x molecular weight Fe)	wt (g) S (C_S x molecular weight S	ppm As (Wt_{As}/(Wt_{As} + Wt_{Au} + Wt_{Fe} + Wt_S))*100*10000	ppm Au (Wt_{Au}/(Wt_{As} + Wt_{Au} + Wt_{Fe} + Wt_S))*100*10000
0.0000001	2.004E-07	33.33	66.667	7.49216E-06	3.95E-05	1861.31385	2137.744	0.001873	9.87E-03
0.0000005	0.000000202	33.33	66.667	3.74608E-05	3.98E-05	1861.31385	2137.744	0.009367	9.95E-03
0.000001	0.000000204	33.33	66.667	7.49216E-05	4.02E-05	1861.31385	2137.744	0.018735	1.00E-02
0.000005	0.00000022	33.33	66.667	0.000374608	4.33E-05	1861.31385	2137.7439	0.093674	1.08E-02
0.00001	0.00000024	33.33	66.667	0.000749216	4.73E-05	1861.31385	2137.7437	0.187348	1.18E-02
0.00001	0.00000024	33.33	66.667	0.000749216	4.73E-05	1861.31385	2137.7437	0.187348	1.18E-02
0.00005	0.0000004	33.33	66.667	0.00374608	7.88E-05	1861.31385	2137.7424	0.93674	1.97E-02
0.0001	0.0000006	33.33	66.667	0.00749216	0.000118	1861.31385	2137.7408	1.873479	2.96E-02
0.001	0.0000042	33.33	66.666	0.0749216	0.000827	1861.31385	2137.712	18.73461	2.07E-01
0.01	0.0000402	33.33	66.657	0.749216	0.007918	1861.31385	2137.4234	187.3277	1.98E+00
0.1	0.0004002	33.33	66.567	7.49216	0.078826	1861.31385	2134.5374	1871.439	1.97E+01
1	0.0040002	33.33	65.667	74.9216	0.787906	1861.31385	2105.678	18532.56	1.95E+02
10	0.0400002	33.33	56.667	749.216	7.878701	1861.31385	1817.084	168913.8	1.78E+03
33	0.1320002	33.33	33.667	2472.4128	25.99962	1861.31385	1079.566	454546.8	4.78E+03